UNIVERSITY OF CALIFORNIA, SAN DIEGO

**Development and Potential of HMGB1-Derived Immunostimulatory Peptides as Adjuvants in Cancer Immunotherapy**

A dissertation submitted in partial satisfaction of the requirements for the degree Doctor of Philosophy

in

Biomedical Sciences

by

Rebecca Kathleen Saenz

Committee in charge:

Sadik C. Esener, Chair
Jack D. Bui, Co-Chair
Dennis A. Carson
Michael J. Heller
Davorka Messmer
Victor Nizet

2011

The Dissertation of Rebecca Kathleen Saenz is approved, and it is acceptable in quality and form for publication on microfilm and electronically:

_____

_____

_____

_____

_____

Co-Chair

_____

Chair

University of California, San Diego

2011

**DEDICATION**

For my husband and best friend, Luis, who has provided limitless love, support, and encouragement. For my 3-month old daughter, Alexa, who, while I wrote this dissertation, had to clock more hours in a bounce chair and swing than a child should have to endure. For my mom, who let me pursue my dreams, exposed me to the field of medicine, and for her continued support of my journey. For my dad, who set me on a path to pursue science and engineering, encouraged me to keep doors open, and loved me unconditionally. For my brother, Ben, who was always a few steps ahead of me and was an amazing guide for me to follow in school and in life. And for all my friends who are too numerous to name, and too valuable to ever forget.

**EPIGRAPH**

Hope lies in dreams, in imagination, and in the courage of those
who dare to make dreams into reality.
*Jonas Salk*

**TABLE OF CONTENTS**

## LIST OF FIGURES

**LIST OF TABLES**

**ACKNOWLEDGEMENTS**

I would like to thank Davorka Messmer and Professor Sadik Esener for their continued mentorship and guidance throughout my graduate career. Dr. Messmer's expertise in the fields of dendritic cells and immunotherapy has been invaluable. In addition, she has educated me in the art of scientific writing and presentation. Dr. Esener has been an inspirational example of an interdisciplinary scientist and engineer. I thank Dr. Esener for chairing my committee and being available for advice.

My colleagues in Dr. Messmer's group have been an invaluable asset to my intellectual and scientific development, as well as a huge help with experiments and as great friends. Most credit goes to Diahnn Futalan for her continued and enthusiastic help, especially with the *in vivo* and nanoparticle experiments. I cherish the camaraderie and friendship that Diahnn and I have developed. Dr. Jessie-Farah Fecteau has been a great friend and guide throughout my Ph.D. program. Jessie has listened intently through my lab meeting presentations, has critically read my manuscripts, and has provided invaluable scientific expertise, especially with flow cytometry and Western blots. I owe a lot to Jasmine Chien-Tze Huang, who paved the way for me and taught me many of the experimental protocols that I used throughout my graduate career. I appreciate Ila Bharati's friendship, help with *in vivo* experiments and many scientific protocols, incredible organizational abilities, and how she put up with my unending reagent orders. The contagious smile, uplifting personality, and youthful attitude of Daniel Seible was ever appreciated. Thanks to everybody who helped with weekly blood processing, especially Andrew Hsu-Hsiang Chang, Daniel Seible, and Ila Bharati. Jennifer Marciniac for friendship, for lending a listening ear, and providing advice. I recognize the contributions of Lien Leutenez, Fien Eeckhout, Stig Sundgvist, and Simeon Sundelius for all their hard work on the Westerns and flow

cytometry/uptake experiments. Thanks to Dr. Cacilda da Silva Souza for her expertise in dermatology and help with the *in vivo* work. And thanks to the other students, David Yang Yang Liu, Christine Pai, Chang Park, Niclas Ambrén, and Jonathan Ahlqvist for their optimism and examples of hard work. I thank them all for their contributions to my research and for their friendship.

I want to thank all my colleagues in Professor Esener's group. Corbin Clawson has been a great resource for the manufacture, DLS, release kinetics, and HPLC analysis of our nanoparticles. Also, he quietly put up with our lab's urgent requests for help. Inanç Ortaç for his help with electron microscopy and his example as a innovator and engineer. Marta Sartor for her guidance and friendship. Carolyn Schutt for her friendship and awesome Ghirardelli brownies. Michael Benchimol for his friendship and example as a leader and engineer. Stu Ibsen for his inspiration and his ability to remind me about what is important in life. Jason Steiner for his insights into life and grad school.

Many thanks to Drs. Marie Larsson and Bradley Messmer for their protocols, expertise, guidance, and reagents. Thanks to Dr. Tomoko Hayashi, Christine Grey, and Dr. Dennis Carson for assisting with, breeding, and providing the knockout mice. Thanks to Dr. Kersi Pestonjamasp for putting up with my seemingly endless questions and phone calls about confocal microscopy. Thanks to Mary Noe, Dr. Yitzhak Tor, and Dr. Elizabeth Komives for their help with circular dichroism. Thanks to Daniel Goff and the Jamieson lab for their friendship and for lending reagents when we found ourselves out – especially the cell strainers and MACS columns. Thanks to Dr. Greg Daniels, Dr. Dong-Er Zang, and Dr. Maurizio Zanetti for providing cell lines and other expertise. Thanks to Dr. Wen Ma for helping with the double emulsion NP protocol. Thanks to Morgan O'Hayre who helped with the calcium flux experiment. Thanks to

Shahram Salek-Ardakani at LIAI who helped with and donated reagents for the vaccinia model. And of course, many thanks to Dr. Liangfang Zhang who, along with Corbin Clawson, developed our nanoprecipitation NP protocol.

Many thanks to all others who have helped me with research, made me laugh or smile, gave me ideas for great places to eat, talked with me about favorite TV shows or the perils of buying a house, and/or donated freshly-caught fish to poor graduates students like me: Brad Messmer, Sergio Sandoval, Gen Yang, Manuel Ruidiaz, and many others. Thanks to the immortal Henrietta Lacks who unknowingly donated her cells to my work and to the world.

And finally thanks to Mary Alice Kiisel, Dr. Paul Insel, and the Medical Scientist Training Program. Thanks to Leanne Nordeman and the Biomedical Sciences Graduate Program. Thanks to the staff at the UCSD Medical School and all my professors for providing the foundation and infrastructure that made my interdisciplinary education possible. And, of course, many thanks to my thesis co-chair Dr. Jack Bui, and the rest of my thesis committee; Dr. Dennis Carson, Dr. Michael Heller, and Dr. Victor Nizet, without whom I would not be able to graduate!

Chapter 2, in part, is a reprint of the material as it appears in Vaccine, 2010, Rebecca Saenz, Cacilda da Silva Souza, Chien-Tze Huang, Marie Larsson, Sadik Esener, and Davorka Messmer. The dissertation author was the primary investigator and author of this paper.

Chapter 3, in part, is currently being prepared into a manuscript for future submission for publication. Rebecca Saenz, Diahnn Futalan, Lien Leutenez, Fien Eeckhout, Jessie-Farah Fecteau, Simeon Sundelius, Stig Sundqvist, Marie Larsson, Brad

Messmer, Tomoko Hayashi, Dennis Carson, Sadik Esener, and Davorka Messmer. The dissertation author is the primary investigator and author of the manuscript.

Chapter 4, in part, is currently being prepared into a manuscript for future submission for publication. Rebecca Saenz, Diahnn Futalan, Brad Messmer, Yitzhak Tor, Greg Daniels, Sadik Esener and Davorka Messmer. The dissertation author is the primary investigator and author of the manuscript.

Chapter 5, in part, is a reprint of the material as it appears in Nanomedicine, 2010, Corbin Clawson, Chien-Tze Huang, Diahnn Futalan, Daniel Martin Seible, Rebecca Saenz, Marie Larsson, Wenxue Ma, Boris Minev, Fiona Zhang, Mihri Ozkan, Cengiz Ozkan, Sadik Esener, and Davorka Messmer. The dissertation author was a major contributor to the dendritic cell activation experiments and co-author of this paper. The primary investigator of this paper, Corbin Clawson, acknowledges that the dissertation author is using this journal article, in part.

Chapter 5, in part, is currently being prepared into a manuscript for future submission for publication. Diahnn Futalan, Rebecca Saenz, Ila Bharati, Daniel Seible, Marie Larsson, Liangfang Zhang, Davorka Messmer. The dissertation author was a major contributor to the *in vitro* and *in vivo* experiments.

## VITA

| | |
|---|---|
| 2001 | Bachelor of Science, Yale University |
| 2002 | Master of Science, Yale University |
| 2011 | Doctor of Philosophy, University of California, San Diego |
| 2014 | (Expected) Medical Doctor, University of California, San Diego |

## PUBLICATIONS

1. **Saenz, R.**; Souza, C. da S.; Huang, CT.; Larsson, M; Esener, S.; Messmer, D. HMGB1-derived peptide acts as adjuvant inducing immune responses to peptide and protein antigen. Vaccine. 2010 Nov 3;28(47):7556-62.

2. Clawson, C.; Huang, CT; Futalan, D.; Seible, DM; **Saenz, R.**; Larsson, M.; Ma, W.; Minev, B.; Zhang, F.; Ozkan, M.; Ozkan, C.; Esener, S.; Messmer, D. Delivery of a peptide via poly(D,L-lactic-co-glycolic) acid nanoparticles enhances its dendritic cell-stimulatory capacity. Nanomedicine-Nanotechnology Biology and Medicine. 2010;6(5):651-61.

3. **Saenz, R**.; Futalan, D.; Leutenez, L.; Eeckhout, F.; Fecteau, J.F.; Sundelius, S.; Sundqvist, S.; Larsson, M.; Messmer, B.; Hayashi, T.; Carson, D.; Esener, S.; and Messmer, D. "TLR4-Dependent Activation of Dendritic Cells by an HMGB1-Derived Peptide Adjuvant" 2011, manuscript prepared for submission for publication.

4. **Saenz, R**.; Futalan, D.; Messmer, B.; Tor, Y.; Esener, S.; Messmer, D. "The activity of the HMGB1-derived immunostimulatory peptide Hp91 resides in the helical C-terminal portion and is enhanced by dimerization" 2011, manuscript prepared for submission for publication.

5. Futalan, D.; **Saenz, R**.; Bharati, I.; Seible, D.; Larsson, M.; Zhang, L.; Messmer, D. "Enhanced anti-tumor immune responses and tumor regression in HER2 mice immunized with immunostimulatory peptides in PLGA nanoparticles" 2011, manuscript in preparation for submission for publication.

## FIELDS OF STUDY

Major Field: Cancer Immunotherapy and Adjuvant Development

Studies in Immunology
Davorka Messmer

Studies in NanoEngineering and Cancer Therapeutics
Professor Sadik Esener

**ABSTRACT OF THE DISSERTATION**

**Development and Potential of HMGB1-Derived Immunostimulatory Peptides as Adjuvants in Cancer Immunotherapy**

by

Rebecca Kathleen Saenz

Doctor of Philosophy in Biomedical Sciences

University of California, San Diego, 2011

Professor Sadik C. Esener, Chair
Professor Jack D. Bui, Co-Chair

Vaccine-based immunotherapy holds promise as an effective treatment of metastatic malignancies with potential for long-term remission. The goal is to elicit Th1-type immune responses that utilize cytotoxic T lymphocytes to generate a protective antitumor response. Aluminum salts (alum), which generate predominantly Th2-type immune responses, are the sole adjuvants approved for use in the majority of countries worldwide. Thus, for significant advancement of cancer immunotherapy, there is a great need for the development of new immunostimulatory adjuvants that will induce Th1-type immune responses.

This dissertation documents the research and development of several peptides that act as Th1-type adjuvants. These peptides are derived from, or based upon, an endogenous immunostimulatory protein, HMGB1. Most focus is placed on one particular peptide, named Hp91. The dissertation starts with an evaluation of the Th1 adjuvant properties of Hp91, and is followed by a study of the characteristics and mechanism of action. The remainder of the dissertation focuses on the research to find, as well as engineer, more potent adjuvant derivates based upon Hp91. Examples include shortened and mutated derivates, peptide dimers, and encapsulation within nanoparticles. A summary of the findings are presented here.

The dissertation author shows that Hp91 potentiates *in vivo* cellular immune responses to peptide and protein antigen. Hp91 promotes the *in vivo* production of the Th1 cytokines, as well as antigen-specific activation of CD8+ CTLs. Hp91-induced secretion of IL-6 is MyD88- and TLR4-dependent, is mediated through p38 MAPK and NFκB, and signaling is dependent on clathrin- and dynamin-mediated endocytosis of Hp91. Additionally, Hp91 activates the MyD88-independent signaling pathway.

The author demonstrates that the C-terminal domain of Hp91, named UC1018, is responsible for the adjuvant activity. UC1018 generates significant antitumor responses when used as adjuvant in a prophylactic cancer vaccine. Additionally, several Hp91 mutants showed enhanced immunostimulatory activity.

The findings presented in this dissertation are significant because they identify and characterize novel, Th1-type synthetic peptide adjuvants that may allow development of new prophylactic and potentially therapeutic treatments of cancer. The results warrant continued development of these peptide adjuvants and may serve as a guide for the future engineering of synthetic Th1-type peptide adjuvants.

# 1. Introduction

## 1.1 Immunotherapies

Immunotherapy is becoming increasingly important in modern oncology treatments. FDA-approved immunotherapies include passive approaches such as monoclonal antibody-based treatments (1) and the newly-approved Provenge® autologous cellular immunotherapy for prostate cancer (2). Strategies in development include *in situ* vaccine-based active immunotherapies that aim to stimulate the patient's immune system *in vivo* to recognize tumor cells as targets for killing (3).

Vaccine-based immunotherapy holds promise as an effective treatment of metastatic malignancies with potential for long-term remission. The goal is to elicit a Th1-type immune response that utilizes cytotoxic T lymphocytes (CTLs) to generate a protective antitumor response. The most commonly used vaccine adjuvants are aluminum salts (alum), which are ineffective for cancer because they induce a mostly humoral Th2-type immune response with few or no tumor-specific CTLs (4). Recently, a vaccine adjuvant containing MPL has been approved in the US and Europe, but historical data is lacking to determine its efficacy for a broad spectrum of antigens. Adjuvant research and development for a Th1-type immune response is critical for the advancement of cancer immunotherapy.

### 1.1.1 Moving beyond current cancer treatment options

Current cancer therapies, including surgery/transplantation, chemotherapy, radiation, and targeted therapy (including mAbs or small molecules) have relatively high levels of side effects, and many of the therapies will not have a long-term effect to prevent cancer regression. While passive immunotherapies such as monoclonal treatment have been very successful over the last two decades and will likely be continued for many decades to come, we anticipate active immunotherapies will be the next logical chapter in cancer treatment and may lead to long-term remission with low or reduced side effects.

During the last decade, great progress has been made in cancer immunotherapy and tumor immunology, including identification of many tumor-associated antigens. Great enthusiasm led to hundreds of cancer vaccine trials that have generally shown low objective response rates (5, 6). To improve clinical responses, it is critical to develop alternative vaccine strategies. Clear improvements need to be made in at least two areas: 1) adjuvant research and development for the generation of the appropriate and desired immune response and 2) approaches to combat the local immunosuppressive microenvironment. These two areas are precisely what the work described in this dissertation addresses.

### 1.1.2 Adjuvants

The goal of vaccination or immunotherapy is the generation of a strong immune response to the administered antigen, able to provide long-term protection against the infection or tumor antigen (4). Unfortunately, most proteins and peptides are poorly immunogenic or fail to mount an immune response entirely when

administered alone in a vaccine. To achieve a strong immune response after an immunization, these protein or peptide antigens usually must be co-injected with an adjuvant. The word "adjuvant" is derived from the Latin word *adiuvare*, meaning to help or aid, and is defined as any substance that enhances the immunogenicity of substances mixed with it (7). Examples include aluminum salts (alum), Freund's adjuvant, CpG, and MPL (Table 1.1) (8). Alum is the sole adjuvant approved for human use in the majority of countries worldwide (4).

For successful immunization against tumor antigens, the development of the appropriate type of immune response is essential. Robust cell-mediated immunity, which is associated with a Th1-type immune response, is thought to be required for the control of cancer (Table 1.2) (9). Humoral immunity, characterized by a Th2-type response is useful for vaccination against extracellular pathogens, such as bacteria. By choosing an appropriate adjuvant, the immune response can be selectively modulated to initiate a Th1- or Th2-type (10). Aluminum salts (alum), which with rare exception are the only vaccine adjuvants currently approved by the US Food and Drug Administration for use in humans (11, 12), favor a Th2 response with weak or absent Th1 responses (13-17), and are consequently not ideal adjuvants for cancer therapy.

Although a large variety of adjuvants has been developed, most of them exhibit excess toxicity, making them unsuitable for routine clinical use (18). The recent U.S. approval of the Cervarix HPV vaccine however, formulated with the TLR4-targeted adjuvant MPL, is a landmark event, and will likely usher in renewed interest and investment in the development of new vaccine candidates and adjuvants (19).

**Table 1.1.** Examples of adjuvants and general characteristics*

| **Adjuvant** | **Composition** | **Mechanism of Action** | **Approved Use?** | **Toxicity/ Side Effects** |
|---|---|---|---|---|
| Alum | Aluminum salts | Nalp3 inflammasome activation (20); Delayed release of antigen. | **Yes. Most vaccines use alum.** | Granulomas; sterile abscesses; eosinophilia; myofascitis. |
| Incomplete Freund's Adjuvant (IFA) (e.g. Montanide) | Oil-in-water emulsion | Delayed release of antigen; enhanced uptake by macrophages. | No. Trials have shown side effects. | Mild granulomas. Sterile abscesses. |
| Complete Freund's Adjuvant (CFA) | Oil-in-water emulsion with inactivated mycoplasma. | Delayed release of antigen; enhanced uptake by macrophages. | No. Human use is forbidden. | Skin ulceration; necrosis; muscle lesion; lipid embolism. Use in humans is forbidden. |
| CpG | Bacterial DNA with unmethylated cytosine-guanine motifs. | Immunostimulant via TLR9. | No. Used in trials. | Skin inflammatory reactions. |
| Squalene (e.g. MF59) | Oil-in-water emulsion. | Depot effect and direct stimulation of APCs? | **Yes. Licensed in Europe in influenza vaccines.** | Overall acceptable safety profile. Flu-like symptoms. |
| Monophos-phoryl lipid A (MPL) (e.g. in AS04) | Low toxicity derivative of LPS. | Immunostimulant via TLR4. | **Yes. Cervarix® (US). Fendrix® and Pollinex Quattro® (Europe).** | Overall safe and well-tolerated. Local reactions. Flu-like symptoms. |
| Cytokines (GM-CSF, IL-2) | Self proteins. | Immunostimulant via cytokine receptors. | No. Used in trials, usually as bolus dose with antigen. | Local reactions. Diarrhea. "First dose effect" |
| Imiquimod | Small molecule | Immune modifier or immunostimulant; binds via TLR7/8. | Approved in the US for <u>topical</u> use as an immune modifier. | Local inflammatory reaction. Flu-like symptoms. |

* This table is derived from material found in several texts (4, 7, 19, 21).

**Table 1.2.** *Th1 versus Th2 immune response.*

| | **Th1-type response** | **Th2-type response** |
|---|---|---|
| **Predominant immunity:** | Cell-mediated | Humoral |
| **Cytokine profile:** | IFN-γ, IL-12 | IL-4 |
| **Useful for protection from:** | Cancer, intracellular bacteria, viruses | Extracellular bacteria, parasites, toxins |

One class of adjuvants that may see much new development is the peptide adjuvant class. It is desirable to develop peptide adjuvants for several reasons: 1) peptides are biodegradable by proteases, which ensures that any induced effects are temporary, 2) peptides can be synthesized without LPS and/or DNA contaminants using good manufacturing practices (GMP), thus can be easily transitioned to future human clinical trials, 3) their production is cost effective and yields a standardized product, 4) peptides can be easily modified to enhance (or diminish) activity, and 5) can be lyophilized without a loss in activity, which is desirable for vaccine manufacture, storage, and shelf-life.

Several previously described peptide adjuvants include residues 32-51 of the Limulus polyphemus protein (LALF(32-51)) which can generate antitumor responses in mice (22) and host defensins such as human neutrophil peptides 1-3 (HNP1, HNP2, and HNP3) (23, 24) and the host antimicrobial cathelicidin peptide LL-37 (25), which promote adaptive immunity. These defensin peptides are large and considered impractical for vaccine use, thus shorter synthetic mimics, like the 13-aa peptide IDR-1 (26) and HH2 (27), both conceptually based on LL-37, have been made and also act as adjuvants. All these peptides are high in Arginine and Lysine content and thus cationic in charge. Furthermore, since they interact with cell membranes due to their

hydrophobic regions, their activity might not be cell specific, but act on a broad number of cells.

This dissertation focuses on High Mobility Group Box 1 (HMGB1)-derived peptides, including Hp91 and UC1018, which are shown in the following chapters to serve as adjuvants, inducing antigen-specific immune responses when co-injected with antigen. In contrast to the peptide sequences mentioned in the previous paragraph, Hp91 presents a more defined mechanism of action, such as activating dendritic cells through Toll like receptor 4 (TLR4) and the interferon α/β receptor (IFN-αβR).

## 1.2 Immune Fundamentals

### 1.2.1 Dendritic cells as antigen presenting cells

To induce an adaptive immune response, antigens must be taken up and displayed by antigen presenting cells. Dendritic cells (DCs) are the most potent antigen-presenting cell and central for the initiation of adaptive immune responses (28) (Figure 1.1). However, in order to present antigen, upregulate co-stimulatory and adhesion molecules, and become potent activators of T cells, DCs need to receive a maturation signal. Mature DCs then stimulate T cells that can 1) act as cytotoxic T lymphocytes or 2) provide help for antigen-specific B cells to produce antibodies (Figure 1.2).

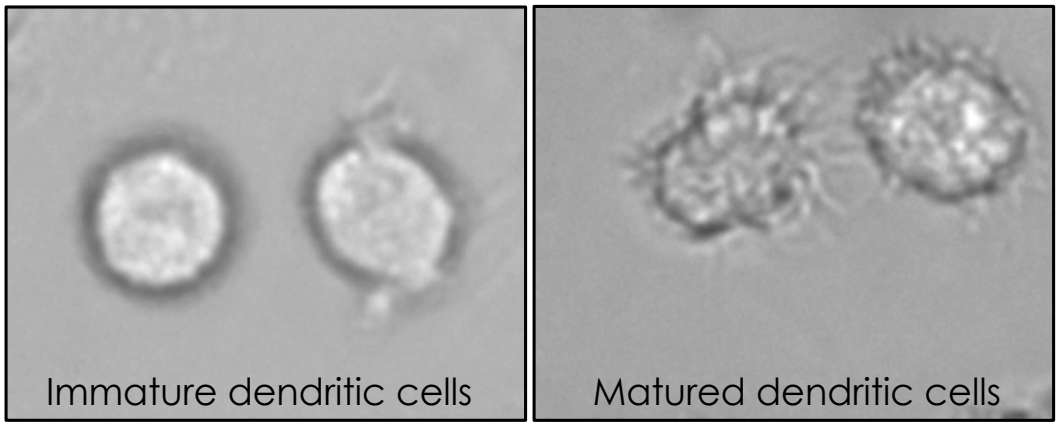


**Figure 1.1.** *Immature and mature dendritic cells*. Human monocyte-derived dendritic cells, immature and mature, in culture were imaged by light microscopy. Immature cells (left) appear round with few dendrites in contrast to mature cells (right), which are covered with many thin dendrites. These cells (right) were matured with an Hp91 tetramer.

DC maturation can be induced by evolutionarily conserved molecular structures unique to foreign pathogens, such as LPS (29) or to DNA molecules containing un-methylated CpG motifs (30) (Figure 1.2). Alternately, DCs can respond to endogenous signals of cellular distress or damage. These can take the form of inflammatory cytokines secreted by cells more proximal to the site of injury (31) or, potentially, the normally sequestered internal components of damaged cells. Evidence for the latter includes reports that necrotic cell lysates and, more specifically, heat shock proteins (HSPs) and HMGB1, can induce DC maturation (32-34). This dissertation focuses on peptides based on HMGB1, such as Hp91, and the immunostimulatory effects these peptides have on dendritic cells.

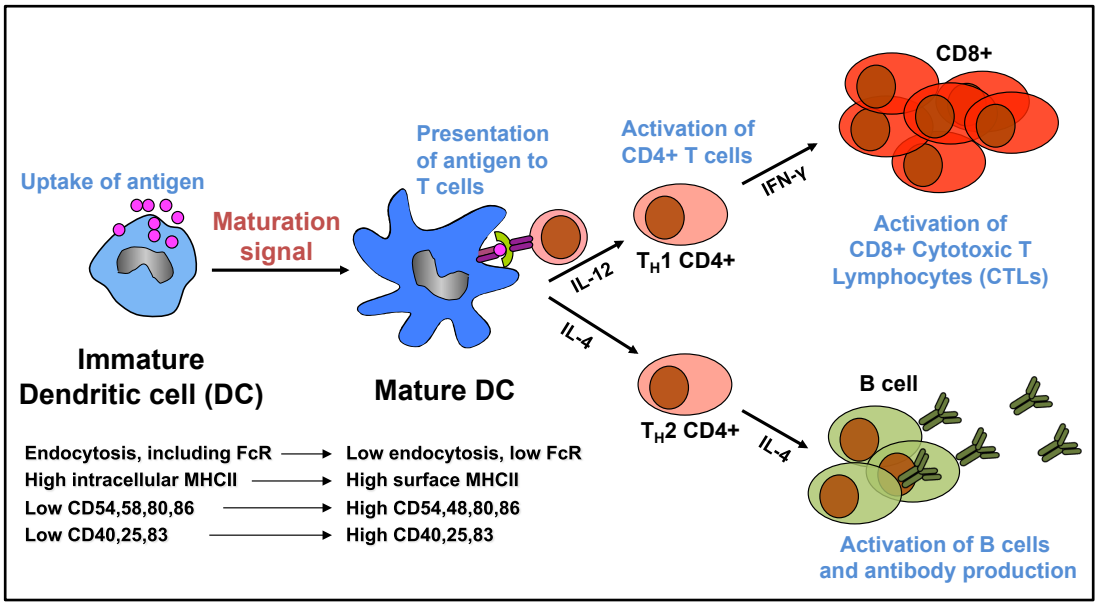


**Figure 1.2**. *DC maturation.* A summary of dendritic cell maturation and the adaptive immune response.

When DCs mature in response to foreign or endogenous danger signals, they can be driven down differing pathways of differentiation (35). Subsequently, these different subsets of DCs can activate distinct immune responses, stimulating CD4+ T cells to become, for example, Th1- or Th2-type helper T cells. While the Th1- versus Th2-type responses are not entirely understood, there are some general differences. Th1-type responses are characterized by the production of interferon-γ and cytotoxic T lymphocytes (CTLs) (cell-mediated immunity) compared to Th2-type responses which are characterized by the production of IL-4 and high levels of neutralizing antibodies (humoral immunity) (Table 1.2, Figure 1.2). Th1 responses are considered valuable for protection against many intracellular pathogens and tumors (35). In fact, in studies of colorectal cancer, the presence of a Th1-type of immune response correlates with a better prognosis. In this dissertation, ELISpot and ELISA experiments are utilized used to determine the Th1 versus Th2 profile of the generated immune responses.

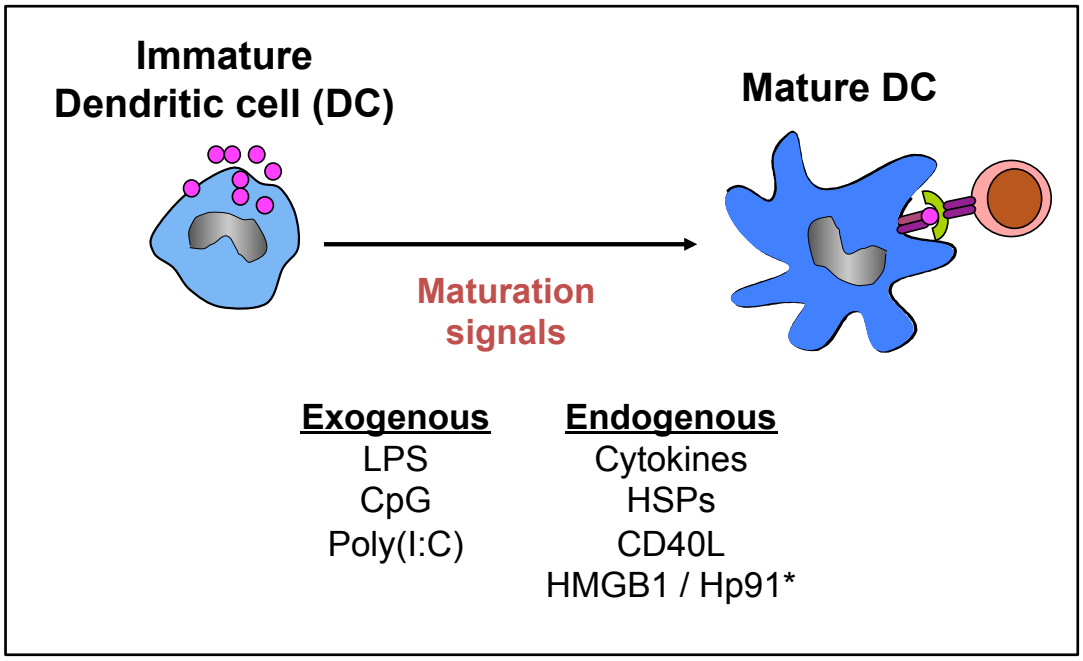


**Figure 1.3.** *DC Maturation Signals.* Examples of exogenous and endogenous DC stimuli. *Hp91 is a synthetic peptide derived from HMGB1 protein.

### 1.2.2 High Mobility Group Box 1 Protein

HMGB1 is an endogenous protein that was originally described as a nuclear protein that facilitates DNA bending and stabilizes nucleosome formation (36). HMGB1 contains three domains, including two homologous DNA binding motifs termed A and B boxes, each approximately 80 aa long, and a negatively charged C-terminus (37, 38) (Figure 1.4).


| Peptide | Sequence | Charge | pI |
|---|---|---|---|
| Hp91 | DPNAPKRPPSAFFLFCSE | -0.12 | 6.20 |

**Figure 1.4.** *High Mobility Group Box 1 Protein structure.* HMGB1 contains three domains, including two DNA binding motifs and an acidic, negatively charged C-terminus. Hp91 peptide is derived from the N-terminal portion of the B box.

In addition to the nuclear functions, HMGB1 is secreted from both macrophages and monocytes after exposure to LPS, TNF-α or IL-1β (39) and acts back on monocytes by stimulating the synthesis of additional pro-inflammatory cytokines (40). The pro-inflammatory domain of HMGB1 maps to the B box, which alone is sufficient to recapitulate the cytokine-stimulating effect of full length HMGB1 (41, 42). Meanwhile, the A box acts as an antagonist of HMGB1 both *in vitro* and *in vivo (43)*. More recently, HMGB1 was identified as a damage-associated molecular pattern (DAMP) (44, 45); HMGB1 serum levels are high in septic and lupus patients (43, 46, 47), and increased levels are observed in synovial fluid from arthritis patients (48). In addition, HMGB1 is released by necrotic cells and may act as a natural adjuvant (49, 50).

D. Messmer and colleagues have previously shown that HMGB1 and its B box domain, as well as several HMGB1 peptides, act as potent stimuli for maturation of human dendritic cells (51, 52). Dendritic cells stimulated *in vitro* with Hp91 peptide, an 18 amino acid (aa) peptide that corresponds to amino acids 91-108 of HMGB1 protein, release a cytokine profile including Interleukin-1β (IL-1β), IL-6, IL-2 and IL-12, which biases towards a Th1 immune response (52). Reports have indicated that HMGB1 binds to several receptors, including the receptor for advanced glycation endproducts (RAGE), Toll-like receptor 2 (TLR2), TLR4, and TLR9 (53-55).

Chapters 2 and 4 of this dissertation evaluate several HMGB1-derived peptides and demonstrate that; 1) Hp91 and UC1018 peptides can act as adjuvants *in vivo*, inducing antigen-specific immune responses in mice, 2) Hp91 induces a Th1-type cytokine profile when injected intravenously, and 3) prophylactic antitumor immunization with UC1018 peptide as adjuvant can significantly slow tumor growth and prolong survival in mice.

### 1.2.3 Toll-like receptors

Toll-like receptors (TLRs) are a class of membrane-spanning proteins that sense the invasion of microorganisms and initiate a range of host defense mechanisms (56). In humans, there are at least 10 members of the TLR family (Table 1.3) that recognize specific components of the invading pathogens, such as lipopolysaccaride (LPS) or un-methylated DNA sequences (e.g. CpG). Activation of the TLRs leads to innate immune responses and inflammation as well as antigen-specific adaptive immunity. At least two signaling pathways have been identified, including the MyD88-dependent/TIRAP pathway, which appears to be the main pathway, and the MyD88-independent TRAM/TRIF pathway, which leads to the production of Type-1 interferons (57) (Figure 1.5).

More recently, the TLRs have been implicated as receptors for several endogenous danger signals. Examples of such endogenous TLR ligands include heat shock protein 60 (HSP60), HSP70, fibronectin, hyaluronic acid oligosaccharides, as well as HMGB1 (56-58) (Table 1.3, bold). There has been some controversy over whether these recombinant protein preparations were contaminated with traces of lipoprotein or endotoxin, which would skew the results. M. Bianchi (oral communication) has argued that ultrapure preparations of HMGB1 do not signal through TLR4. This dissertation presents data to show that synthetic, endotoxin-free preparations of Hp91 can cause TLR4-dependent cytokine secretion from dendritic cells.

**Table 1.3.** Toll-like receptors and their identified ligands*

| TLR | Ligand |
|---|---|
| TLR1 | Triacyl lipopeptides (bacteria, mycobacteria) |
| TLR2 | Lipoprotein/lipopeptides (a variety of pathogens)<br>Peptidoglycan (Gram-positive bacteria)<br>Lipoteichoic acid (Gram-positive bacteria)<br>Lipoarabinomannan (mycobacteria)<br>A phenol-soluble modulin (*Staphylococcus epidermidis*)<br>Glycoinositolphospholipids (*Trypanosoma cruzi*)<br>Glycolipids (*Treponema maltophilum*)<br>Porins (Neisseria)<br>Zymosan (fungi)<br>Atypical LPS (*Leptospira interrogans*)<br>Atypical LPS (*Porphyromonas gingivalis*)<br>**HSP70 (host) **** |
| TLR3 (endosomal) | Double stranded RNA<br>Poly(I:C) |
| TLR4 | LPS (Gram-negative bacteria)<br>Taxol (plant)<br>Fusion protein (RSV)<br>Envelope proteins (MMTV)<br>HSP60 (*Chlamydia pneumoniae*)<br>**HSP60 (host)**<br>**HSP70 (host)**<br>**Type III repeat extra domain A of fibronectin (host)**<br>**Oligosaccharides of hyaluronic acid (host)**<br>**Polysaccharide fragments of heparan sulfate (host)**<br>**Fibrinogen (host)**<br>**HMGB1 (host)** |
| TLR5 | Flagellin (bacteria) |
| TLR6 | Diacyl lipopeptides (mycobacteria) |
| TLR7 (endosomal) | Imidazoquinoline (synthetic compounds)<br>Loxoribine (synthetic compounds)<br>Bropirimine (synthetic compounds)<br>Single stranded RNA |
| TLR8 (endosomal) | Small synthetic compounds (e.g. Imiquimod)<br>Single-stranded RNA |
| TLR9 (endosomal) | CpG DNA (bacteria) |
| TLR11 | Profilin (*Toxoplasma gondii*) |

* This table is derived from several texts (56, 58, 59).

** Endogenous (host) ligands are highlighted using bold text.

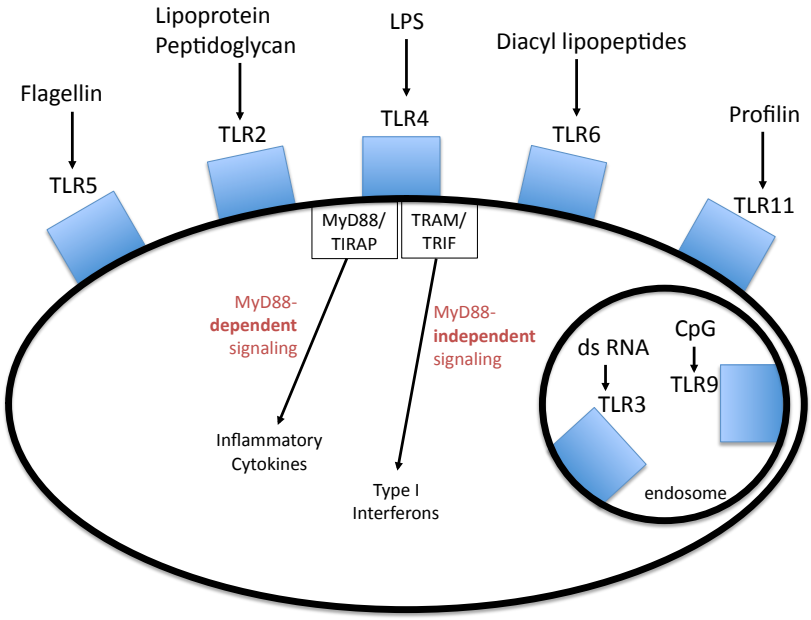


**Figure 1.5.** *Toll-like receptors and downstream signaling pathways within the cell.* The MyD88 adaptor protein is universal for all TLRs except TLR3.

## 1.3 Enhancing the Immune Response

### 1.3.1 Nanotechnology

Nanotechnology offers a long list of benefits for cancer immunotherapeutics including protection of cargo from degradation, sustained release or depot effect, formulation of hydrophobic payloads, and potentially targeted delivery (60-62). Moreover, co-encapsulation of an antigen and adjuvant within a nanoparticle ensures co-delivery of the components to the dendritic cells, and may reduce the tolerance that occurs if a DC encounters antigen only (63-65). Nanoparticles have been shown to be efficient carriers for biomolecules such as protein and peptides. Studies have shown that encapsulation of peptide antigens within biodegradable spheres prolongs MHC Class I peptide presentation, and encapsulation of protein antigen, such as OVA, within PLGA-NPs increases immune responses compared to

dose-matched free protein (66, 67). These data provide strong rationale for the formulation of Hp91 within nanoparticles.

In fact, we have recently shown that delivery of Hp91 peptide via PLGA-NPs enhances its DC-stimulatory capacity (68). This data is included, in part, in Chapter 5 of this dissertation. In addition, newer unpublished data is included to further substantiate the claim that nanotechnology can enhance the effectiveness of immunotherapeutics.

## 1.4 Summary

D. Messmer and colleagues had previously shown that the HMGB1-derived Hp91 peptide induced dendritic cells *in vitro* to secrete a cytokine panel characteristic of a Th1-type immune response (52). Under the guidance of Dr. Messmer and Dr. Sadik Esener, the dissertation author set out to 1) investigate the extent to which Hp91 would act as adjuvant *in vivo* to induce antigen specific, and possibly antitumor, immune responses, 2) determine Hp91's mechanism of action, and 3) investigate methods for enhancing immunotherapies and tumor rejection by utilizing nanoengineering or other technologies. The long-term aim for this project is to develop the endogenous peptide Hp91, or other HMGB1-based peptides, as vaccine adjuvant(s) for cancer immunotherapy.

Chapter 2 of this dissertation shows that Hp91 acts as adjuvant to induce antigen-specific immune responses *in vivo*, and that this response is sequence specific. In addition, we demonstrate that intravenous administration of Hp91 induces secretion of Th1-type cytokines.

Chapter 3 addresses the mechanism of action for Hp91. We demonstrate that dendritic cells and macrophages take up Hp91 in a sequence- and temperature-

dependent manner. Investigation into the uptake mechanism shows it to be clathrin- and dynamin- mediated. TLR4 and MyD88 are demonstrated to be necessary for Hp91-mediated immune activation of bone-marrow derived dendritic cells. Lastly, we show data that suggest in macrophages, Hp91 signals through MyD88-dependent and –independent pathways.

Chapter 4 investigates how structure relates to immunostimulatory activity. In particular, we investigate overlapping peptides and find that it is the C-terminal portion of Hp91, that we call UC1018, which is responsible for the immunostimulatory activity. UC1018 is shown to be a stronger adjuvant *in vivo* than full-length Hp91 peptide. Perhaps most exciting is the prophylactic tumor challenge experiment, wherein UC1018-vaccinated mice show delayed tumor growth and significantly prolonged survival. Additionally, we show that peptide dimerization enhances activity.

Chapter 5 addresses the use of nanoparticles (NPs) and shows that delivery of our immunostimulatory peptides within NPs enhances DC stimulatory capacity and adjuvant potential. Three types of nanoparticles are evaluated, including liposomal NPs (liposomes), PLGA-NPs, and lipid-polymer hybrid NPs. We present preliminary data to demonstrate that delivering UC1018 within NPs delays tumor growth and prolongs survival.

Chapter 6 shows preliminary data to suggest Hp91 can act to modify the local tumor microenvironment. Additionally, we propose future work to combine our HMBG1-based immunotherapy with tumor manipulation to improve clinical response rates.

# 2. HMGB1-Derived Peptide Acts as Adjuvant Inducing Immune Responses to Peptide and Protein Antigen

There is a need for new adjuvants that will induce immune responses to subunit vaccines. We show that a short peptide, named Hp91, whose sequence corresponds to an area within the endogenous molecule High mobility group box (HMGB1) protein potentiates cellular immune responses to peptide antigen and cellular and humoral immune responses to protein antigen *in vivo*. Hp91 promoted the *in vivo* production of the immunomodulatory cytokines, IFN-$\gamma$, TNF-$\alpha$, IL-6, and IL-12 (p70), as well as antigen-specific activation of CD8+ T cells. These results demonstrate the ability of a short immunostimulatory peptide to serve as an adjuvant for subunit vaccines.

## 2.1 Introduction

Vaccines traditionally have, and still consist of whole-inactivated or live-attenuated pathogens or toxins (69, 70). The usage of these modified pathogens is however unattractive for several reasons. Live attenuated pathogens can cause disease by reverting to a more virulent phenotype, especially in the non-developed immune system of newborns or immunodeficient patients, and whole inactivated pathogens contain reactogenic components that can cause undesirable vaccine

side effects. Therefore, there is growing interest and research to develop a new generation of vaccines containing recombinant protein subunits, synthetic peptides, and plasmid DNA (69). While these new modalities promise to be less toxic, many are poorly immunogenic when administered without an immune-stimulating adjuvant. As adjuvants are a crucial component of the new generation of vaccines, there is a great need for safer and more potent adjuvants (69-71).

The development of the appropriate type of immune response is essential for successful immunization. Robust cell-mediated immunity, which is associated with a Th1 type immune response, is thought to be required for the control of intracellular pathogens (18), viruses (72) as well as cancer (9). Humoral immunity, characterized by a Th2 type response is useful for vaccination against extracellular pathogens, such as bacteria. By choosing an appropriate adjuvant, the immune response can be selectively modulated to initiate a Th1 or Th2-type (10). Aluminum salts (alum), which are the only vaccine adjuvants approved for use in most countries (11, 12) are not ideal adjuvants for certain pathogens, since they favor a Th2 response with weak or absent Th1 responses (13-17). Although neutralizing antibodies from a Th2 response can be protective against many pathogens, the generation of Th1 and cytotoxic T lymphocyte (CTL) responses are important, playing crucial roles in the protection and recovery from viruses, intracellular bacteria, and cancer cells.

Pathogen associated molecular patterns (PAMPs) are small molecular sequences commonly associated with pathogens, such as CpG unmethylated bacterial DNA sequences, lipopolysaccharide (LPS), or poly(I:C) (56, 73-75). While many PAMPs have been investigated for their use as vaccine adjuvants, their development has been slowed for several reasons, including reactogenicity, toxicity, and ability to induce or exacerbate autoimmune diseases (4). For instance, CpG

oligodeoxynucleotides, which signal through TLR9, can activate antigen-presenting cells, induce a wide variety of cytokines, and generate a potent cellular Th1 immune response in mice, initially showed strong clinical promise (8, 76-78). However, clinical trials in humans utilizing CpG as a cancer immunotherapy adjuvant failed to produce the potent immune responses that were anticipated, and low TLR9 expression in human plasmacytoid DCs may be implicated (79). Identification of new adjuvants demonstrating low-toxicity and the ability to stimulate a cellular Th1 response in humans would be a great advancement in the development of vaccines for infectious disease and cancer.

In contrast to PAMPs, endogenous molecules and proteins have been proposed and studied as adjuvants. Examples of such endogenous molecules, or danger-associated molecular patterns (DAMPs), include heat stock proteins, cytokines, and high mobility group box 1 (HMGB1) protein (45, 52). Originally identified as a nuclear protein, HMGB1 modulates the innate immune response when released into the extracellular compartment by necrotic and damaged cells (49, 80). HMGB1 is a potent pro-inflammatory cytokine, released by monocytes and macrophages following exposure to LPS, tumor necrosis factor (TNF)-$\alpha$ or IL-1$\beta$ and as a result of tissue damage (49, 81). Extracellular HMGB1 promotes the maturation of myeloid and plasmacytoid DCs (51, 82, 83) and it has been shown to act as immune adjuvant by enhancing immunogenicity of apoptotic lymphoma cells and eliciting antibody responses to soluble ovalbumin protein (50).

We have previously identified a short peptide, named Hp91, within the B box domain of HMGB1 that induces activation of human and mouse DCs (52). Hp91-activated DCs show increased secretion of pro-inflammatory cytokines and chemokines, including the Th1 cytokine, IL-12. In addition, DCs exposed to HMGB1-

derived peptides induced proliferation of antigen-specific syngeneic T cells *in vitro* (52). These immunostimulatory properties of Hp91 and the fact that peptides are easy to manufacture make it an attractive candidate as an adjuvant for vaccine development. Here we show that the immunostimulatory peptide (ISP) Hp91 acts as an adjuvant *in vivo* by enhancing immune responses to peptide and protein antigen.

## 2.2 Materials and Methods

### 2.2.1 Reagents and cell lines

The OVA-transfected EL4 line, E.G7-OVA (ATCC, Manassas, VA, USA), was cultured in RPMI 1640 medium (Invitrogen, Carlsbad, CA, USA) supplemented with 10% (vol/vol) fetal calf serum (FCS) (Omega Scientific, Tarzana, CA, USA), 10 mM HEPES (Invitrogen), and penicillin (100 U $ml^{-1}$) - streptomycin (100 $\mu g$ $ml^{-1}$) - L-glutamine (2 mM) (Invitrogen).

### 2.2.2 Peptides and protein

The peptides, including the ISP Hp91 (DPNAPKRPPSAFFLFCSE), Hp121 (SIGDVAKKLGEMWNNTAA), Scrambled Hp91 (ASLAPPFPNCFDPKSREF), the MHC-Class I (H-$2K^b$)-restricted peptide epitope of ovalbumin (OVA-I: OVA 257-264 aa, SIINFEKL), and the MHC-Class II (I-$A^b$)-restricted peptide epitope of ovalbumin (OVA-II: OVA 323-339 aa, ISQAVHAAHAEINEAGR) were all purchased from GenScript Corp (Piscataway, NJ, USA) and CPC Scientific (San Jose, CA, USA). Hp91, Hp121, and scrambled Hp91 peptides were synthesized with an N-terminal biotin. Additionally, a N-acetylated version of Hp91 was also synthesized. Peptides were routinely synthesized with greater than 95% purity. LPS-free chicken egg white ovalbumin

protein was kindly provided by Dr. Thomas Moran (Department of Microbiology, Mount Sinai School of Medicine, New York, NY, USA). Unless otherwise stated, all peptides and proteins were dissolved in PBS in preparation for immunization.

### 2.2.3 Mice and Immunizations

Female C57BL/6 mice 8-12 weeks of age were used for most experiments. All mice were purchased from Charles River Laboratories (Boston, MA, USA) and housed at the Moores UCSD Cancer Center animal facility. All animal studies were approved by the Institutional Animal Care and Use Committee of UCSD and were performed in accordance with the institutional guidelines. For most experiments, mice were immunized s.c. with 50 μg of SIINFEKL (OVA-I) peptide and 50 μg of ISQAVHAAHAEINEAGR (OVA-II) peptide. The OVA peptide was co-administered with the indicated peptides such as Hp91 (30 to 500 μg), Hp121 (250 μg) or scrambled Hp91 (250 μg), or with PBS (negative control). For some experiments, a protein vaccine group was included, wherein 500 μg of Hp91 was co-administered with 100 μg of LPS-free OVA protein. As positive controls and comparison to Hp91, mice were immunized s.c. with OVA peptide(s) or protein in Alhydrogel "Alum" (500 μg) (Brenntag Biosector, Frederikssund, Denmark), Incomplete Freund's Adjuvant "IFA" (Sigma-Aldrich, St. Louis, MO, USA), CpG 2006 (25 μg; 5' - T*C*G* T*C*G* T*T*T* T*G*T* C*G*T* T*T*T* G*T*C* G*T*T – 3') (Integrated DNA Technologies, San Diego, CA). If not otherwise indicated, mice were primed and boosted two weeks later and spleens and blood were collected 7-14 days after the final immunization.

### 2.2.4 Intravenous administration of ISP

C57BL/6 mice were injected i.v. with 0, 10 or 100 μg Hp91 dissolved in PBS into the tail vein. Blood was collected after 2h and 24h by retroorbital puncture. Blood was allowed to clot and serum was isolated after centrifugation. Serum was diluted and analyzed for systemic cytokine and chemokine release by ELISA (eBioscience, San Diego, CA, USA).

### 2.2.5 Detection of antigen-specific antibody production by ELISA

Serum was obtained by retroorbital puncture or cardiac puncture from mice following immunization. Blood was allowed to clot and serum was isolated after centrifugation. Microtiter plates were coated overnight with OVA protein (Sigma-Aldrich), blocked with BSA, and dilutions of serum were added to the plates for incubation. Plates were washed, incubated with anti-mouse IgG or IgM peroxidase conjugated antibodies (Roche, Basel, Switzerland), developed using Zymed TMB substrate (Invitrogen), and analyzed using a microplate reader at 450 nm.

### 2.2.6 Spleen cell preparation

Single cell suspensions of splenocytes were prepared by mechanical disruption and separation through a 70 mm nylon cell strainer (BD Biosciences, Franklin Lakes, NJ, USA). Red blood cells were lysed using ammonium chloride buffer (Roche Diagnostics, Indianapolis, IN, USA) and the splenocytes were subsequently resuspended in complete medium (RPMI 1640 with 10% FCS, L-glutamine, penicillin, streptomycin, and HEPES). In some experiments, CD4+ and CD8+ cells were depleted from bulk splenocyte populations using anti-CD4 or anti-CD8a conjugated microbeads (Miltenyi-Biotec, Auburn, CA, USA) according to the manufacturer's instructions.

### 2.2.7 Enzyme-linked immunospot assay

Freshly isolated splenocytes were plated in duplicate to wells of an Immobilon-P (PVDF) bottom enzyme-linked immunospot (ELISpot) plate (Millipore, Millerica, MA, USA) that had been previously coated overnight with 5 μg $ml^{-1}$ monoclonal anti-mouse IFN-γ antibody (Mabtech, Stockholm, Sweden). Splenocytes were cultured overnight at 37°C with 2.5 μg $ml^{-1}$ SIINFEKL (OVA-I) peptide, 2.5 μg $ml^{-1}$ ISQAVHAAHAEINEAGR (OVA-II) peptide, 5 μg $ml^{-1}$ concanavalin A positive control (Sigma-Aldrich), or left unstimulated (medium only). After 18 h, culture supernatants were collected for cytokine analysis and ELISpot plates were developed using 1 μg $ml^{-1}$ biotinylated anti-mouse IFN-γ antibody (Mabtech), Streptavidin-HRP (Mabtech), and TMB Substrate (Mabtech). The plate was scanned and the spots were counted using an automated ELISpot Reader System (CTL ImmunoSpot, Shaker Heights, OH, USA).

### 2.2.8 Cytokine Release Assay

Splenocytes were cultured overnight with 2.5 μg $ml^{-1}$ OVA-I peptide, 2.5 μg $ml^{-1}$ OVA-II peptide, 5 μg $ml^{-1}$ concanavalin A positive control (Sigma-Aldrich), or left unstimulated (media only). After 18 h, cell culture supernatants were collected and analyzed for the presence of IL-2 and IL-4 by ELISA (eBioscience).

### 2.2.9 LDH cytotoxicity assay

Splenocytes were expanded in culture at 3 x $10^6$ cells $ml^{-1}$ in complete medium with mitomycin-C (Sigma-Aldrich)-treated E.G7-OVA at a 5:1 ratio in 6 well plates. Four days later, live cells were isolated on a lympholyte gradient (Cedarlane

Laboratories Limited, Burlington, Ontario, Canada) and cultured in complete medium with 25 U $ml^{-1}$ IL-2 (R&D Systems, Minneapolis, MN, USA) for two additional days. Cytotoxicity assays were performed using a CytoTox96 Non-Radioactive Cytotoxicity Assay Kit (Promega, Madison, WI, USA). 1 x $10^4$ E.G7-OVA cells per well were plated as target cells. Expanded splenocyte effector cells were incubated with the target cells at effector to target ratios of 1:1, 3:1, 10:1, and 30:1. Cultures were incubated in phenol-red free RPMI (Invitrogen) with 5% FCS (Omega) for 6h at which point the cell culture supernatants were harvested. The lactate dehydrogenase (LDH) released from lysed cells was proportional to the resulting red formazan product, and was quantified using a microplate reader at 490 nm absorbance. The percentage of cytotoxicity was calculated according to the following equation: % Cytotoxicity = [(E – St – Se)/(M – St)] x 100. Abbreviations are as follow; E = LDH release by effector-target coculture, St = spontaneous release by target cells, Se = spontaneous release by effectors, and M = maximal release by target cells.

#### 2.2.10 Statistical analysis

Data represented are mean ± SEM. Data were analyzed for statistical significance using unpaired Student's *t*-test, 2-way ANOVA, or linear regression. Statistical analysis was performed using GraphPad software version 5.01 for Windows (GraphPad Software, San Diego, CA, USA). A $p$ value $<0.05$ was considered statistically significant.

## 2.3 Results

#### 2.3.1 Hp91 induces cytokine release *in vivo*

We have previously shown that exposure of DCs to an immunostimulatory peptide (ISP) named Hp91 *in vitro* leads to secretion of inflammatory as well as Th1 skewing cytokines (52). To examine the adjuvant properties of Hp91 *in vivo*, serum cytokine responses were measured after intravenous (i.v.) injection of Hp91 into mice. Increased secretion of the Th1 cytokines IFN-γ, IL-12 (p70), as well as TNF-α and IL-6, was observed within 2 h of injection, with levels generally rising further over 24 h (Figure 2.1).

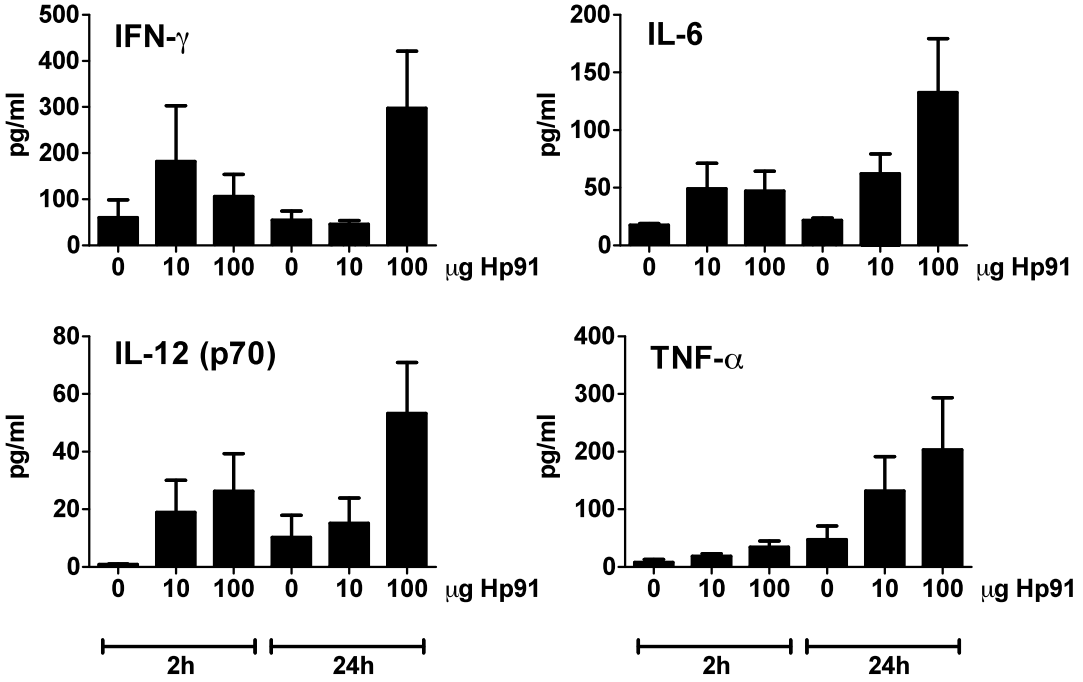


**Figure 2.1.** *Hp91 causes release of cytokines in vivo*. Mice were injected i.v. into the tail vein with Hp91 (10 or 100 μg) or PBS (denoted as 0 μg Hp91). Blood was collected after 2 and 24 h and serum was analyzed for IFN-γ, IL-6, IL-12 (p70), and TNF-α by ELISA. Data shown are mean (±SEM) from 3-4 mice per group.

### 2.3.2 Hp91 enhances CD8 T cell responses to peptide antigen

Since the ISP Hp91 activates DCs and induces antigen-specific T cell responses *in vitro* (52), we tested whether Hp91 acts as a adjuvant to induce antigen-specific immune responses *in vivo*. The ISP Hp91 at both doses tested (250 μg and 500

μg) when co-administered with OVA peptides, caused a significant increase in the number of antigen-specific IFN-γ secreting T cells when splenocytes were restimulated with the CD8 epitope SIINFEKL (Figure 2.2A), but not when restimulated with the CD4 epitope ISQAVHAAHAEINEAGR (Figure 2.2B). Incomplete Freund's Adjuvant (IFA), a known stimulator of cell-mediated immune responses, elicited strong cellular immune responses when splenocytes were restimulated with either the CD8 or CD4 epitope (Figure 2.2A,B).

The OVA-I peptide (SIINFEKL) is recognized in the context of H-2K$^b$ MHC-Class I molecules and is specific for CD8+ T cells. To further confirm that the observed immune response is an OVA-specific CD8+ T cell response, CD4+ or CD8+ cells were depleted from the splenocytes prior to setup up the ELISpot assay. While greater than 95% of CD4+ cells were depleted, CD8+ depletion was not as complete; 20% of CD8+ cells remained in the cultures as observed by flow cytometry (data not shown). As expected, the number of IFN-γ secreting cells was reduced to near background levels (OVA peptides/PBS) in the CD8+ depleted splenocyte populations (Figure 2.2C). In contrast to the CD8+ depletion, the CD4+ depleted splenocytes from the Hp91-OVA immunized groups retained the ability to secrete IFN-γ in response to OVA-I peptide stimulation further supporting the involvement of CD8+ T cells following co-immunization with the ISP Hp91 and OVA peptide, showing that the ISP Hp91 causes activation and proliferation of antigen-specific CD8+ T lymphocytes *in vivo*.

To test whether lower doses of Hp91 would suffice as adjuvant for immunization, titrated doses of Hp91 were co-injected with OVA peptide to determine the minimum injection dose required for a significant increase in antigen-specific IFN-γ secreting T cells. As expected, a dose response was observed (Figure 2.2D). However, with only 5 mice per group, a significant increase in IFN-γ secreting T

cells was observed by ELISpot only in the group receiving an Hp91 dose of 250 μg, suggesting 250 μg is an optimal dose when immunizing small groups of mice. Subsequent experiments showing 500 μg of Hp91 were conducted prior to the titration experiment.

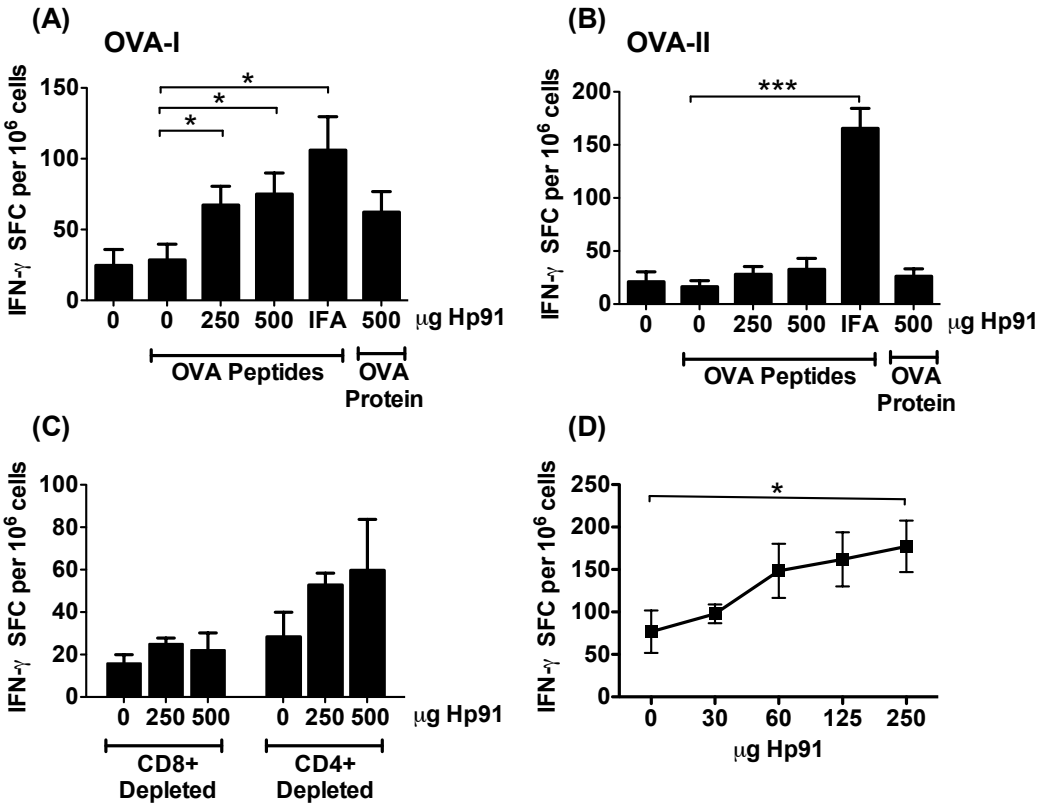


**Figure 2.2.** *Cellular immune response in Hp91 immunized mice.* (**A-B**) Mice were immunized with OVA peptides in PBS (denoted as "0"), Hp91 (250 and 500 μg), or IFA. One group of mice was immunized with OVA protein and Hp91 (500 μg). Freshly-isolated splenocytes from the immunized mice were cultured in the presence of (**A**) OVA-I (SIINFEKL) peptide (2.5 μg $ml^{-1}$) or (**B**) OVA-II (ISQAVHAAHAEINEAGR) (2.5 μg $ml^{-1}$) in an IFN-γ ELISpot assay. The number of IFN-γ-secreting cells was determined 18 hours later. The data shown (IFN-γ spot-forming cells per million cells) are means (±SEM) for 10 mice/group, except the Hp91-OVA protein group which is n=5. Asterisk, $p < 0.05$ between groups; Student's t-test. Data are representative of at least 3 independent experiments. (**C**) Freshly isolated splenocytes from PBS/OVA-peptide and Hp91/OVA-peptide immunized mice were depleted of CD8+ or CD4+ T cells and stimulated overnight in the presence of 2.5 μg $ml^{-1}$ OVA-I (SIINFEKL) peptide in an IFN-γ ELISpot assay as above. Data shown are means (±SEM) for 5 mice per group. (**D**) Mice were immunized twice with OVA-I (SIINFEKL) peptide (50 μg) co-injected with 0, 30, 60, 125, or 250 μg Hp91 dissolved in PBS. Splenocytes from immunized mice were cultured in an OVA-I IFN-γ ELISpot assay as above. Spleens were collected 6 days after the boost. Asterisk, $p < 0.05$ between groups; Student's t-test compared to PBS.

### 2.3.3 The Hp91 adjuvant effect is sequence specific

To test if the *in vivo* adjuvant effect is related to Hp91 or if any peptide will cause similar effects, we used a control peptide named Hp121. Hp121 is also derived from HMGB1 B-box and has the same length, a similar charge, and isoelectric point as Hp91. Hp121 does not cause activation of human DCs (52) or mouse BM-DCs *in vitro* (data not shown). Mice were immunized s.c. with OVA-I peptide co-injected with either Hp91, Hp121 or PBS control. Mice immunized with Hp91 peptide showed a significantly increased number of INF-γ secreting cells as compared to the Hp121 peptide and PBS immunized mice using freshly isolated as well as expanded splenocytes (Figure 2.3A). No significant increase was observed between the Hp121 peptide and PBS immunized groups.

To further investigate if the adjuvant effect is due to the sequence of Hp91 or if a scrambled version of Hp91 would cause similar immune responses, we used a random peptide sequence synthesized with the amino acids found within Hp91. Mice were immunized s.c. with OVA-I peptide co-injected with either Hp91, scrambled Hp91, or PBS control. Mice immunized with Hp91 peptide showed a significantly increased number of INF-γ secreting cells as compared to the scrambled peptide and PBS immunized groups (Figure 2.3B). No significant difference was observed between the scrambled Hp91 group and PBS control group.

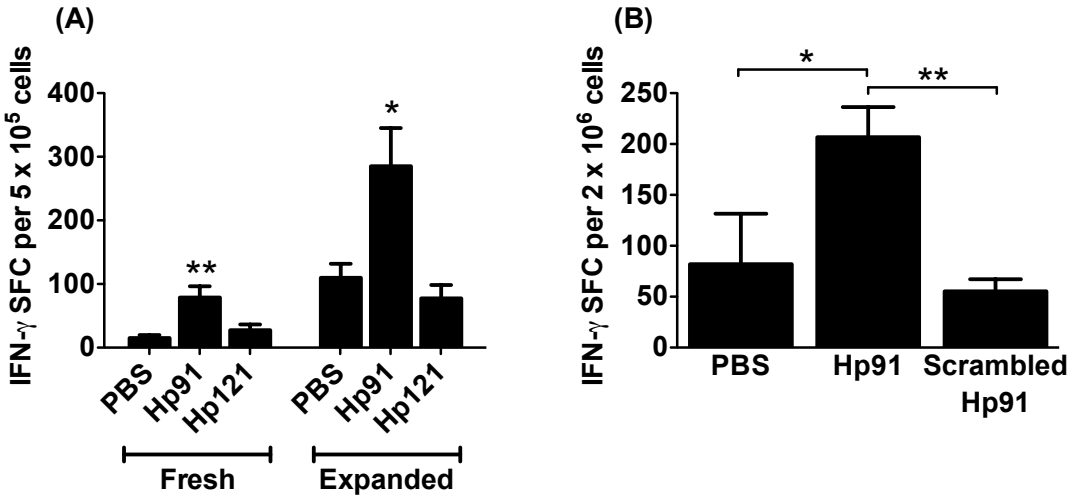


**Figure 2.3.** *Hp91 adjuvant effect is sequence specific.* (**A**) Mice were immunized with OVA peptides in PBS, Hp91 or Hp121 (250 μg). Mice received an additional boost s.c. into the contralateral flank one month after the first boost. Freshly-isolated or OVA-I-expanded splenocytes were cultured in an OVA-I IFN-γ ELISpot assay as above. The number of IFN-γ spot-forming cells are shown as means (±SEM) for 4 mice per group. Asterisks, (*<0.05 and **<0.005); 2-way ANOVA. (**B**) Mice were immunized with OVA-I peptide in PBS with Hp91 or scrambled Hp91 peptide (250 μg). Freshly isolated splenocytes from the immunized mice were cultured in an OVA-I IFN-γ ELISpot assay The data shown is mean (±SEM) for 5-10 mice/group. *p < 0.05 between groups; Student's t-test.

### 2.3.4 Hp91 induces Th1-type immune responses *in vivo*

Since IL-2 is critical for the activation, survival, and proliferation of T lymphocytes, we tested whether IL-2 secretion is increased in Hp91/OVA peptide immunized mice. Freshly isolated splenocytes were cultured overnight in presence of OVA peptide and culture supernatants were analyzed for IL-2 (Figure 2.4) and IL-4, which may indicate the induction of a Th2 type immune response (data not shown) by ELISA. The highest IL-2 secretion was observed in OVA-I restimulated splenocytes from mice immunized with Hp91/OVA peptides (Figure 2.4A), which showed higher IL-2 secretion compared to mice vaccinated with whole OVA protein/Hp91 or OVA peptide/IFA, both of which were also significantly increased as compared to the

PBS/OVA control. After exposure to the MHC-Class II specific OVA-II peptide, splenocytes from Hp91/OVA peptide immunized mice showed a low but significant increase in IL-2 secretion as compared to PBS/OVA immunized mice (Figure 2.4B). IL-4 was not detected in the splenocytes cultures at any of the conditions, though it was detected in the ConA stimulated positive control (data not shown). Additionally, the scrambled version failed to cause IL-2 secretion from OVA-1 restimulated splenocytes, further confirming that the immune response is sequence specific (Figure 2.4C).

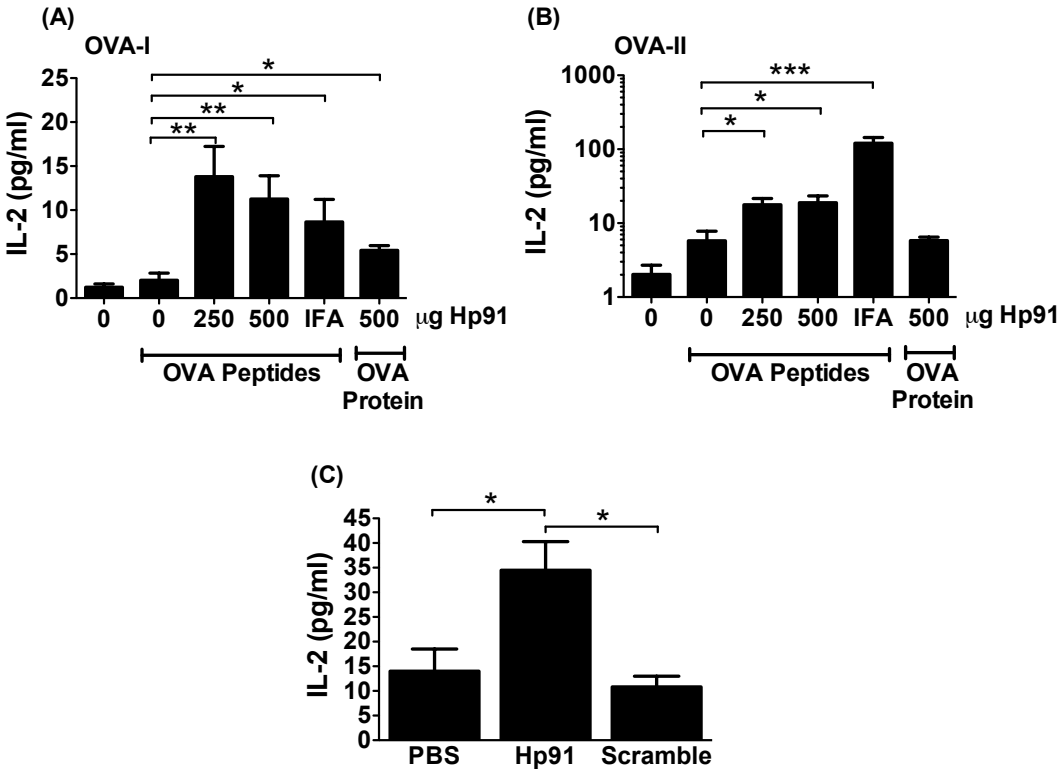


**Figure 2.4.** *Cytokine secretion in Hp91 immunized mice*. Mice were immunized with OVA peptides (50 μg) co-injected with Hp91 (0, 250 or 500 μg dissolved in PBS) or IFA. One group of mice was immunized with OVA protein and Hp91 (500 μg) in PBS. Splenocytes from immunized mice were stimulated overnight with 2.5 μg $ml^{-1}$ of (**A**) OVA-I (SIINFEKL) peptide or (**B**) OVA-II (ISQAVHAAHAEINEAGR). Culture supernatants were collected and analyzed for IL-2 secretion by ELISA. Data shown are mean (±SEM) for 5-10 mice per group. Asterisk, $p < 0.05$; Student's t-test. (**C**) Mice were immunized with OVA-I peptide in PBS with Hp91 or scrambled Hp91 peptide (250 μg). Freshly isolated splenocytes from the immunized mice were cultured overnight in the presence of OVA-I (SIINFEKL) peptide (2.5 μg $ml^{-1}$). Supernatants were collected and analyzed for IL-2 secretion by ELISA. The data shown is mean (±SEM) for 5-10 mice/group. *p < 0.05 between groups; Student's t-test.

### 2.3.5 Hp91 elicits antibody responses to soluble protein

Immunization using OVA protein in context of Hp91 promoted an antibody response to OVA which was dominated by the IgG1 isotype (Figure 2.5A, B). Two-fold serial dilutions of the Hp91/OVA protein group show similar serum titers for the group (Figure 2.5C). Minimal increase in IgG2b and IgM OVA specific antibodies was detected (data not shown). As expected, immunization using OVA peptides (OVA-I and OVA-II) together with Hp91 did not induce antibody responses (Figure 2.5A and data not shown).

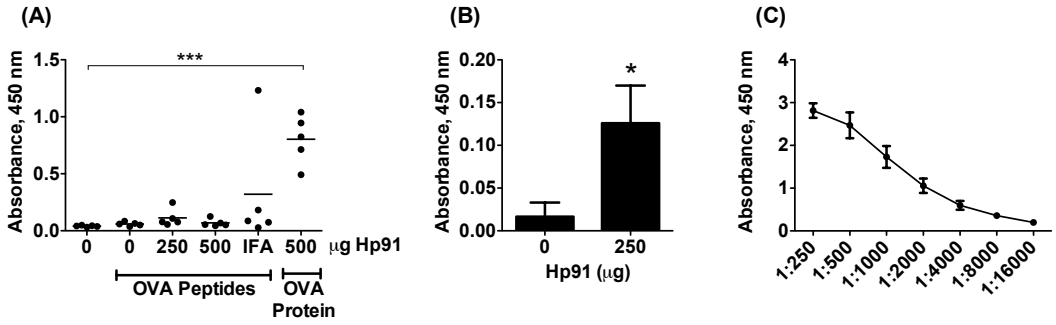


**Figure 2.5.** *Antibody responses in Hp91 immunized mice*. Serum was obtained from immunized mice (5 mice per group) 10 days after the final immunization and analyzed for antibody levels by ELISA. (**A**) A 1:100 dilution of the serum from immunized mice as indicated, (**B**) a 1:100 dilution of serum from mice immunized with OVA protein and Hp91 (0 or 250 μg in PBS) or (**C**) a serial dilution of serum from mice immunized with OVA protein and Hp91 (500 μg) in PBS was added to the plates, followed by a peroxidase-conjugated anti-mouse IgG1 antibody. Plates were developed with TMB substrate and absorbance was analyzed on a microplate reader. Asterisks, $p < 0.001$; Student's t-test.

### 2.3.6 Hp91 induces antigen–specific CTL responses

To further investigate whether OVA-specific cytotoxic T lymphocytes (CTL) responses were induced by immunization with the ISP Hp91, splenocytes from immunized mice were assessed for their ability to lyse OVA-expressing E.G7-OVA cells. The strongest killing was observed using effector splenocytes from mice immunized

with Hp91/OVA peptides (Figure 2.6), which was even higher than of splenocytes from IFA/OVA peptide immunized mice. When data were analyzed by linear regression and slopes were compared, the percent killing of target cells by effectors cells from mice immunized with Hp91/OVA peptides was significantly higher than the PBS control group.

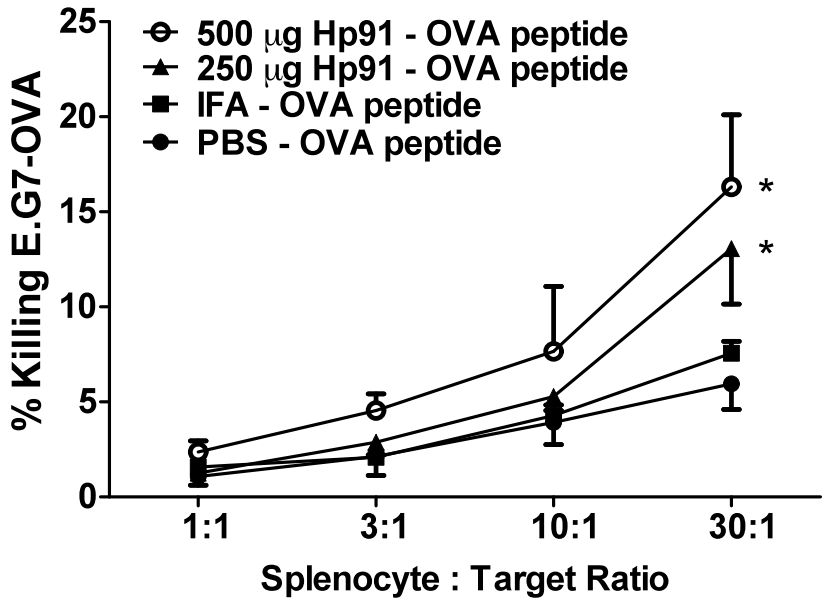


**Figure 2.6.** *CTL Induction in immunized mice*. Expanded splenocytes from immunized mice were cultured with E.G7-OVA cells at the indicated effector to target ratios for 6h. Cell culture supernatants were collected and cytotoxicity was quantified in a CytoTox96 non-radioactive cytotoxicity assay. Data from at least 3 mice per group are shown. Data were analyzed by linear regression and slopes were compared for significance. Asterisk, $p < 0.05$; compared to PBS.

### 2.3.7 Hp91 adjuvant effect strongest in a peptide subunit vaccine

We compared Hp91 to IFA, alum, CpG, and combinations of these adjuvants to investigate how Hp91 compared to the other adjuvants in subunit vaccines containing peptide or protein antigen. When compared to IFA and alum using the MHC-Class I restricted OVA-I (SIINFEKL) peptide as antigen, Hp91 performed well,

inducing a cellular antigen-specific immune response approximately 50% stronger than IFA and 4-fold stronger than alum (Figure 2.7A), as measured by an IFN-γ ELISpot. At the doses used for this experiment, CpG induced a cellular immune response approximately 65% stronger than Hp91. Curiously, the immune response induced by the combined alum/Hp91 adjuvant was slightly synergistic, 15% stronger than a calculated additive affect. From the same immunization, we evaluated IL-2 secretion as an estimate of activation, survival, and proliferation of T lymphocytes. The strongest IL-2 secretion was observed when alum was combined with either Hp91 or CpG (Figure 2.7B).

Using the same panel of adjuvants, we immunized mice using OVA protein as antigen and evaluated cellular immune responses against both OVA-I (MHC Class I) and OVA-II (MHC Class II) peptides. CpG, and adjuvant combinations utilizing CpG, induced significantly stronger cellular responses than any of the other adjuvants, including Hp91 (Figure 2.7C, D). IFA, inducing cellular responses at 10-20% of those of CpG, was the second strongest adjuvant. As our earlier OVA protein immunizations were dominated by IgG1 antibody responses, we evaluated only IgG1 isotype and total IgG. IgG2b and IgM were not measured. Alum, as expected, yielded strong OVA antibody responses (Figure 2.7E, F). Somewhat surprisingly, IFA showed competitive antibody responses. Hp91 did not yield strong IgG1 antibody responses compared to the other adjuvants, however when combined with CpG, Hp91 yielded a very strong total IgG antibody response.

When developing a Th1-type adjuvant, the production of cellular immune responses is more important than the antibody response, therefore the ELISpot and IL-2 ELISA results are of more interest (Figures 2.7 A-D) than the antibody responses (Figures 2.7 E-F). Looking at these cellular immune responses by ELISpot, when

combined into a peptide subunit vaccine, Hp91 is the second strongest cellular adjuvant of those tested (Figure 2.7A). Only CpG was stronger at the doses tested. In the protein context, Hp91 did not compare as well, and was significantly weaker than CpG, as well as weaker than IFA.

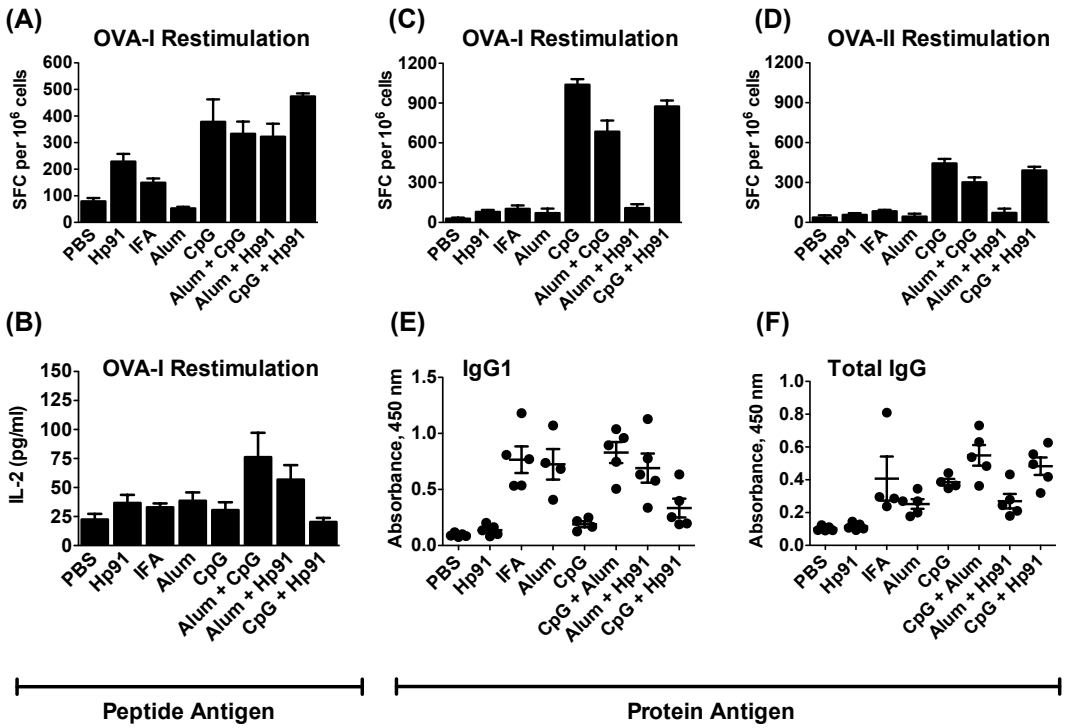


**Figure 2.7.** *Adjuvant comparison*. Mice were primed and boosted two weeks later with (**A-B**) SIINFEKL peptide (50 μg) or (**C-F**) OVA protein (100 μg) co-injected with PBS or 1-2 of the following adjuvants: Hp91 (250 μg), IFA (50% vol/vol), Alum (500 μg), or CpG (25 μg). (**A,C,D**) Splenocytes from immunized mice were stimulated overnight with 2.5 μg $ml^{-1}$ of (**A,C**) OVA-I (SIINFEKL) peptide or (**D**) OVA-II (ISQAVHAAHAEINEAGR) peptide in an IFN-γ ELISpot assay. The number of IFN-γ-secreting cells was determined 18 hours later. (**B**) Splenocytes from immunized mice were stimulated overnight with 2.5 μg $ml^{-1}$ of OVA-I (SIINFEKL) peptide. Culture supernatants were collected and analyzed for IL-2 secretion by ELISA. (**E-F**) Serum was obtained from immunized mice 7 days after the final immunization and analyzed for antibody levels by ELISA. A 1:100 dilution of the serum from immunized mice was added to the plates, followed by a peroxidase-conjugated anti-mouse IgG1 or total IgG antibody, as indicated. Plates were developed with TMB substrate and absorbance was analyzed on a microplate reader. Data shown are mean (+/- SEM) for 4-5 mice per group.

### 2.3.8 Altering Hp91 N-terminal modifications does not affect adjuvant activity

Previous immunizations were conducted with N-terminal biotinylated Hp91 as adjuvant. To evaluate if the N-terminal biotin was necessary and affected immune

responses, we replaced the biotin with an acetyl group and immunized mice with the biotinylated Hp91 and acetylated versions of Hp91. There is no significant difference between the mice receiving biotinylated Hp91 versus the acetylated Hp91 (Figure 2.8), suggesting that the choice of modification does not have an effect on the immune response. Mice immunized with the acetylated Hp91 induced approximately 20% more antigen-specific IFN-γ secreting T lymphocytes (Figure 2.8A), and 10% more IL-2 secretion (Figure 2.8B) than the biotinylated Hp91, though the differences between groups are within error of each other.

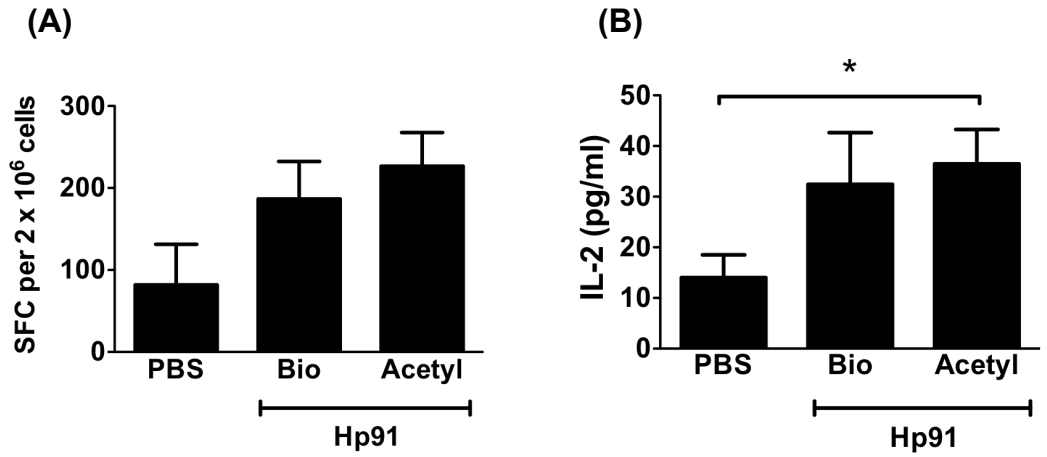


**Figure 2.8.** *Comparing N-terminal biotin to acetyl*. Mice were primed and boosted two weeks later with OVA-I (SIINFEKL) peptide with PBS or Hp91 with an N-terminal biotin (Bio) or acetyl (Acetyl) as indicated. (**A**) Freshly isolated splenocytes from the immunized mice were cultured in the presence of OVA-I peptide (2.5 μg $ml^{-1}$). The number of IFN-γ-secreting cells was determined 18 h later. (**B**) Freshly isolated splenocytes from the immunized mice were cultured in the presence of OVA-I peptide (2.5 μg $ml^{-1}$). Supernatants were collected after 18 hours and analyzed for IL-2 secretion by ELISA. The data shown is mean (±SEM) for 5 mice/group. *$p < 0.05$ between groups; Student's t-test.

### 2.3.9 Hp91 titration and immunization scheme

Previous immunizations were conducted with a prime-boost schedule. To investigate if one Hp91 dose was sufficient, or conversely, if an additional dose further

enhanced the immune response, we immunized mice with 1, 2, or 3 doses of Hp91 peptide, co-injected with OVA-I (SIINFEKL) peptide. We demonstrate that by adding an additional Hp91 injection to our previous schedule, such that there are 3 injections total, we enhance the number IFN-γ secreting cells and improve significance (Figure 2.9).

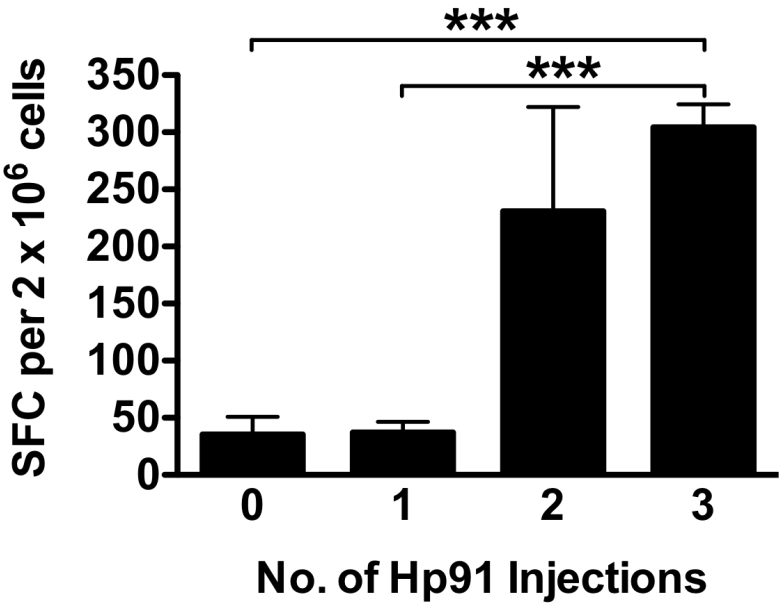


**Figure 2.9.** *Cellular response enhanced with additional Hp91 injection*. Mice were immunized with OVA-I (SIINFEKL) peptide, co-injected with PBS with 0, 1, 2, or 3 doses of Hp91 (250 μg). Hp91 injections were staggered so that the last Hp91 dose was on the same day for each group. Mice were sacrificed one week after the last dose. Freshly isolated splenocytes from the immunized mice were cultured in the presence of OVA-I peptide (2.5 μg $ml^{-1}$). The number of IFN-γ -secreting cells was determined 18 h later. The data shown is mean (±SEM) for 5 mice/group. ***$p < 0.001$ between groups; Student's t-test. (credit: D. Seible).

## 2.4 Discussion

Although subunit vaccines promise to be less toxic, many are poorly immunogenic when administered without adjuvant. Alum, though FDA-approved,

generates a weak Th1 response with a questionable safety profile. Thus, there is a great need for safer and more potent adjuvants (69-71).

We have previously shown that the 18 amino acid long ISP Hp91, is a potent stimulus for human DCs with the ability to generate a Th1-type immune response *in vitro* (52). Here we demonstrate that Hp91 acts as adjuvant *in vivo*; inducing cellular immune responses to peptide and both cellular and humoral immune responses to protein antigen. The CD8 immune response was strong, since no *in vitro* expansion of splenocytes was needed to obtain a significant response as is commonly performed when testing vaccine responses. We show that the ISP Hp91 acts as an immune adjuvant to induce antigen-specific CD8 T cell responses *in vivo*. In addition, the immunostimulatory effects of Hp91 are related to its sequence, as the control peptides, Hp121 and scrambled Hp91, failed to induce cellular immune responses.

The cytokine profile induced by an immune adjuvant plays an important role in the polarization of the immune response. The data show that co-immunization with the ISP Hp91 and OVA peptides as well as OVA protein results in OVA-specific secretion of IL-2, suggesting that immunized mice are able to mount an adaptive immune response that activates T cells to synthesize and secrete IL-2 for *in vivo* proliferation of OVA-specific effector T cells. Interestingly, IL-4 levels were undetectable. Intravenous administration of Hp91 resulted in increased secretion of the Th1 cytokines IFN-γ and IL-12 (p70) associated with cell-mediated immunity. This together with the measured IFN-γ secretion by the T cells along with undetectable IL-4 suggests that Hp91 induces a Th1-type of immune response *in vivo*. We also show that immunization with Hp91/OVA peptide elicited stronger CTL responses than IFA/OVA.

Additionally, when Hp91 was tested side-by-side with the panel of adjuvants, we demonstrate that Hp91 is not just stronger than IFA, but also much stronger than

alum, which is, with few exceptions, the only adjuvant used in FDA-approved vaccines. Hp91 was a weaker adjuvant than CpG here, however we have since developed more potent adjuvant formulations, as shown in Chapters 4 and 5, based on the parent molecule, HMGB1 protein. Additionally, these adjuvant comparison experiments were performed in mice, and clinical trials in humans utilizing CpG as a cancer immunotherapy adjuvant failed to produce the potent immune responses that were anticipated, likely because high TLR9 expression may be lacking in human plasmacytoid DCs (79). In contrast to CpG, Hp91 activates myeloid DCs. Other adjuvants that activate myeloid DCs, such as CD40L (84) and poly(I:C) (85), are being evaluated in clinical and preclinical settings and have shown promising results for tumor immunotherapy (86), emphasizing the importance of activating myeloid DCs. Ultimately, when tested in humans, Hp91, or other more potent HMGB1-based adjuvant formulations, might outperform CpG and would very likely outperform the commonly utilized alum.

We show here that additional boosts enhances cellular immune responses, so we hypothesize that adding boosts to a human vaccination schedule would enhance immune responses. Three or more doses are not uncommon for many currently approved human vaccines, including vaccines for hepatitis B, human papillomavirus (HPV), Diphtheria/Tetanus/Pertussis (DTap), polio, and more.

Although the main objective was to test the potency of Hp91 as adjuvant for peptide vaccines and induction of cellular immune responses, we show that immunization using OVA protein mixed with Hp91 also induced humoral immune responses. This is very promising for future development of this novel adjuvant, as it could be used for prophylactic vaccination against infectious disease, particularly

against diseases caused by intracellular bacteria (18) or viruses (87, 88) which rely on Th1 immune responses.

As a peptide adjuvant, Hp91 has several advantages: it can be made synthetically, is inexpensive, can be produced in high quantities at GMP quality, and it can also be genetically engineered to target DC markers like DEC-205 which promotes strong immune responses when linked to a DC stimulatory molecule (89, 90). Since the tested doses of Hp91 have shown no adverse effects in mice to date, this current data suggest this endogenous peptide should be well-tolerated for use in vaccines.

In conclusion, we show that a short peptide, named Hp91, whose sequence corresponds to an area within the endogenous molecule High mobility group box (HMGB1) protein potentiates cellular immune responses to peptide antigen and cellular and humoral immune responses to protein antigen *in vivo*. Hp91 promoted the *in vivo* production of the immunomodulatory cytokines IFN-γ and IL-12 (p70), among others, as well as antigen-specific activation of CD8+ T cells. These results provided the first evidence that HMGB1-derived peptides can act as adjuvant *in vivo*. Additionally, we demonstrated that the adjuvant effect of Hp91 is sequence specific. We observed Hp91-induced antigen-specific immune responses that were stronger than those induced by Alum. We showed that additional boosts further increase the cellular immune response.

Chapter 2, in part, is a reprint of the material as it appears in Vaccine, 2010. Rebecca Saenz, Cacilda da Silva Souza, Chien-Tze Huang, Marie Larsson, Sadik Esener, and Davorka Messmer (91). The dissertation author was the primary investigator and author of this paper.

# 3. TLR4-Dependent Activation of Dendritic Cells by an HMGB1-Derived Peptide Adjuvant ("Hp91 Characterization")

High mobility group box protein 1 (HMGB1) is released from necrotic cells and acts as an endogenous danger molecule. We have previously shown that a peptide, named Hp91, whose sequence corresponds to an area within the B-Box domain of HMGB1, activates dendritic cells (DCs) and acts as adjuvant *in vivo*. Here we investigated the underlying mechanisms of Hp91-mediated DC activation. We show that Hp91 enters DCs via clathrin-mediated endocytosis. Hp91-induced secretion of IL-6 is MyD88- and TLR4-dependent and is mediated through p38 MAPK and NFκB. Similar to TLR4 activation with LPS, Hp91-induced signaling is dependent on clathrin- and dynamin-mediated endocytosis of Hp91. The MyD88-independent interferon pathway is activated by Hp91 and is mediated through IRF3 phosphorylation. These findings elucidate the mechanisms by which Hp91 acts as immunostimulatory peptide and may serve as a guide for the future development of synthetic Th1-type peptide adjuvants for vaccines.

## 3.1 Introduction

The adaptive immune response is commonly initiated via pathogen-associated molecular patterns (PAMPs). The presence of these microbial structures indicates an infection and their recognition is controlled via a set of receptors, including Toll-like receptors (TLRs) (56). Dendritic cells (DC) are central for the initiation of adaptive immune responses and are activated by exogenous PAMPs such as LPS, CpG, or poly(I:C) (92). Pathogens are not the only cause of inflammation however, and in the absence of infection, endogenous alarmins can signal tissue and cell damage (45). Matzinger described the danger model, wherein antigen presenting cells (APCs), such as dendritic cells, are tuned to endogenous danger/alarm signals from distressed tissues (93). These alarmins can take the form of inflammatory cytokines secreted by cells proximal to the site of injury (31) or, potentially, the normally sequestered internal components of damaged cells. Evidence for the latter includes reports that necrotic cell lysates and, more specifically, heat shock proteins (HSPs) and high mobility group box protein 1 (HMGB1), can induce DC maturation (32-34).

HMGB1 was originally described as a nuclear protein that facilitates DNA bending and stabilizes nucleosome formation (36). HMGB1 contains three domains, including two homologous DNA binding motifs termed A and B boxes, each approximately 80 aa long, and a negatively charged C-terminus (37, 38). In addition to the nuclear functions, HMGB1 is secreted from both macrophages and monocytes after exposure to LPS, TNF-$\alpha$ or IL-1$\beta$ (39) and acts back on monocytes by stimulating the synthesis of additional pro-inflammatory cytokines (40). More recently, HMGB1 was identified as an endogenous alarmin, or damage-associated molecular pattern (DAMP)(44, 45). HMGB1 is released from necrotic cells to trigger inflammation (49) and act as an endogenous adjuvant (50). Several receptors are implicated in

HMGB1 mediated activation of cells, including the receptor for advanced glycation endproducts (RAGE) (83, 94), TLR2 and TLR4 (53, 54, 95-97), TLR9 (98), Mac-1 (99), syndecan-1 (100, 101), receptor-type tyrosine phosphatase-ζ/β (100, 102), and CD24/Siglec-10 (103).

Structure-function studies have revealed that the pro-inflammatory domain maps to the B box domain, which recapitulates the cytokine activity of full-length HMGB1 (41, 42). We have previously shown that the B box domain, and three HMGB1-derived peptides are potent maturation stimuli for mouse and human DCs *in vitro* (104, 105). Of the three peptides, Hp91 was the most potent and induced a cytokine profile typical of a Th1-type response, including IL-12 (52). We recently showed that Hp91 potentiates humoral and cellular immune responses to ovalbumin *in vivo (91)*. Here we explored the mechanism by which Hp91 activates DCs and macrophages by investigating cellular uptake, receptor dependence, and phosphorylation of downstream signaling pathways.

## 3.2 Materials and Methods

### 3.2.1 Animals

C57BL/6 mice were purchased from Charles River Laboratories (Boston, MA, USA). TLR4-/- and IL1R-/- mice were purchased from The Jackson Laboratories (Bar Harbor, ME, USA). IFNαβR-/- mice were purchased from B&K Universal (England, UK). MyD88-/- and TLR7-/- mice were a gift from S. Akira (Osaka University, Osaka, Japan) and backcrossed for 10 generations onto the C57BL/6 background. Mice were bred and maintained at the Moores UCSD Cancer Center animal facility and all animal studies were approved by the Institutional Animal Care and Use Committee of UCSD and were performed in accordance with the institutional guidelines.

### 3.2.2 Reagents

Phenylarsine oxide and chlorpromazine (clathrin-mediated endocytosis inhibitors), sodium azide (energy-dependent endocytosis inhibitor), nystatin (caveolin-mediated endocytosis inhibitor), latrunculin B (phagocytosis inhibitor), amiloride (micropinocytosis inhibitor), and Dynasore (dynamin inhibitor) were purchased from Sigma-Aldrich as endocytosis inhibitors. The p38 MAPK-specific inhibitor, SB203580, and the NFκB inhibitor, *N*-tosyl-L-phenylalanine chloromethyl ketone (TPCK), were purchased from Sigma-Aldrich. The MEK1 inhibitor, PD98059, was purchased from Cell Signaling Technology (Danvers, MA). As many of these inhibitors required solubilization in DMSO, DMSO was used as a negative control.

### 3.2.3 Peptides

The peptides, including Hp91 (DPNAPKRPPSAFFLFCSE), Hp121 (SIGDVAKKLGEMWNNTAA), scrambled Hp91 (ASLAPPFPNCFDPKSREF), and SIINFEKL were all synthesized by GenScript Corp (Piscataway, NJ, USA) and CPC Scientific (San Jose, CA, USA). Peptides were synthesized with an N-terminal biotin, acetyl, or fluorescent tag (Cp488). Peptides were routinely synthesized with greater than 95% purity. Peptides were dissolved in RPMI or PBS for *in vitro* and *in vivo* experiments respectively.

### 3.2.4 Cell lines

The J774 cell line was a gift from Maurizio Zanetti (UCSD) and was cultured in RPMI 1640 medium (Invitrogen), supplemented with 10 mM HEPES (Invitrogen), penicillin (100 U $ml^{-1}$) - streptomycin (100 μg $ml^{-1}$) - L-glutamine (2 mM) (Invitrogen),

and 10% (vol/vol) fetal calf serum (Omega Scientific, Tarzana, CA). The RAW 264.7 cell line was a gift from Dong-Er Zang (UCSD) and was cultured as above, except with 5% (vol/vol) fetal calf serum (Omega).

### 3.2.5 Generation of human monocyte-derived DCs

Peripheral blood mononuclear cells were isolated from the blood of normal volunteers over a Ficoll-Hypaque (Amersham Biosciences, Uppsala, Sweden) density gradient. Anonymous blood was purchased from the San Diego Blood Bank; therefore, no institutional review board approvals were necessary. To generate DCs, peripheral blood mononuclear cells were allowed to adhere to culture plates for 1 hour. The nonadherent cells were washed off, and the adherent cells were cultured in RPMI 1640 medium (Invitrogen) supplemented with 50 mmol 2-mercaptoethanol (Sigma-Aldrich), 10 mM HEPES (Invitrogen), penicillin (100 U $ml^{-1}$) - streptomycin (100 μg $ml^{-1}$) - L-glutamine (2 mM) (Invitrogen), and either 5% (vol/vol) human AB serum (Gemini Bio Products, West Sacramento, CA) or 1% (vol/vol) human plasma (Valley Biomedical, Winchester, VA) and supplemented with GM-CSF (1000 U $mL^{-1}$) (Bayer HealthCare Pharmaceuticals, Wayne, New Jersey), and interleukin-4 (100 U $mL^{-1}$) (IL-4; R&D Systems, Minneapolis, Minnesota) at days 0, 2, and 4. Immature human DCs (iDCs) were harvested on days 5–7.

Alternatively, monocytes can be selected for using CD14 magnetic microbeads beads over a MACS column. $10^7$ peripheral blood mononuclear cells were mixed with 5 μl of washed CD14 microbeads (Miltenyi Biotec, Auburn, CA) in 100 μl MACS buffer (2mM EDTA, 0.5% BSA, PBS) and incubated in the refrigerator for 15 minutes. The cell/bead mixture was diluted with MACS buffer to 10 times the original volume and centrifuged. Cells were resuspended in 0.5 ml MACS buffer per

$10^8$ cells and loaded onto a MACS LS column (Miltenyi) that was pre-equilibrated with 3 ml MACS buffer. The column was washed 3x with 3 ml MACS buffer before eluting the positive fraction with 5 ml MACS buffer. The eluent was centrifuged to wash and 3 millions cells were plated in a Falcon 6 well plate (BD Biosciences, Bedford, MA) with 3 ml/well of supplemented media as above. Cells were supplemented with GM-CSF and IL-4 at days 0, 2, and 4 and immature human DCs (iDCs) were harvested on days 5–7.

### 3.2.6 Generation of mouse bone marrow-derived DCs

Bone marrow-derived DCs (BM-DCs) were prepared from C57BL/6 and knockout mice, as described by Inaba et al (106) with minor modifications. Briefly, single bone marrow cell suspensions were obtained from femurs and tibias and depleted of lymphocytes, granulocytes, and Ia+ cells by incubating with a mixture of monoclonal antibodies (mAbs; anti-CD4, anti-CD8, anti-B220/ CD45R, and anti-Ia) (antibody hybridomas were a gift from Ralph Steinman (Rockefeller)) and low-toxicity rabbit complement (Pel Freez Biologicals, Rogers, AR) for 60 minutes at 37°C. Cells were resuspended at a concentration of $10^6$ cells $mL^{-1}$ in RPMI 1640 medium (Invitrogen) supplemented with 50 mM 2-mercaptoethanol (Sigma-Aldrich), 10 mM HEPES (Invitrogen), penicillin (100 U $ml^{-1}$) - streptomycin (100 μg $ml^{-1}$) - L-glutamine (2 mM) (Invitrogen), and 5% (vol/vol) fetal calf serum (Omega), and 10 ng $mL^{-1}$ recombinant murine granulocyte-macrophage colony-stimulating factor (GM-CSF) (J558L GMCSF-secreting cells were a gift from Ralph Steinman). Fresh complete medium containing GM-CSF was added on days 2 and 4 of culture. Cells were collected for the experiments on days 5-7.

### 3.2.7 Confocal microscopy

$10^5$ immature human DCs, WT BM-DCs, or TLR4 KO BM-DCs were pre-cooled on ice and subsequently incubated for 30 minutes on ice in culture medium with biotinylated Hp91 or Hp121 to allow peptide binding. Cells were washed and then incubated for the indicated time at 37° C. Cells were cytospun (Shandon Cytospin 2 centrifuge) onto glass slides, fixed, permeabilized with acetone, and stained with Streptavidin-Alexa 488 (Invitrogen) to visualize biotinylated peptides and Hoechst 33258 (Invitrogen) to visualize DNA. Cells were imaged on a Zeiss LSM confocal microscope.

### 3.2.8 Binding/uptake studies

For most experiments, iDCs or BM-DCs were pre-cooled on ice for 30 minutes. Cells were subsequently incubated for the indicated times and temperatures in culture medium with biotinylated peptides. Cells were washed, permeabilized with Cytofix/Cytoperm (BD Biosciences, Franklin Lakes, NJ) stained with Streptavidin-Alexa 488 (Invitrogen), and analyzed by flow cytometry. For experiments with endocytosis inhibitors, cells were pre-treated for 30 minutes with the indicated inhibitors prior to incubation with the biotinylated peptides. For experiments with J774 macrophages, cells were pre-cooled on ice, pre-treated with 30 minutes with the indicated inhibitors, and subsequently incubated for 30 minutes with fluorescently-labeled Hp91 (Cp488-Hp91). Cells were immediately analyzed by flow cytometry using the FACSCalibur (Beckon Dickinson, Franklin Lakes, NJ). Data were analyzed using the FlowJo software (Tree Star, Inc., Ashland, OR).

### 3.2.9 Stimulation of iDCs and BM-DCs

At days 5-7 of culture, DCs were either left untreated or were stimulated with indicated doses of peptide. For inhibition experiments, immature human DCs were pre-treated with the indicated doses of SB20358, PD98059, *N*-tosyl-L-phenylalanine chloromethyl ketone (TPCK), or DMSO control for 30 minutes prior to stimulation. For experiments with human DCs, supernatants were analyzed by ELISA (eBioscience, Inc. San Diego, CA), according to the manufacturer's instructions, 48 h after stimulation. For experiments with mouse BM-DCs, supernatants were analyzed by ELISA (eBioscience), 24 h after stimulation.

### 3.2.10 Immunizations and splenocyte preparation

Mice were immunized s.c. with 50 μg of SIINFEKL peptide. The SIINFEKL peptide was co-administered with either PBS, Hp91 (250 μg), or scrambled Hp91 (250 μg). Peptides were dissolved in PBS for all immunizations. Mice were boosted two weeks later and spleens and blood were collected one week after the final immunization. Single cell suspensions of splenocytes were prepared by mechanical disruption and separation through a 70 mm nylon cell strainer (BD Biosciences). Red blood cells were lysed using ammonium chloride buffer (Roche Diagnostics, Indianapolis, IN) and the splenocytes were subsequently resuspended in RPMI 1640 medium (Invitrogen) supplemented with 10 mM HEPES (Invitrogen), penicillin (100 U $ml^{-1}$) - streptomycin (100 μg $ml^{-1}$) - L-glutamine (2 mM) (Invitrogen), and 5% (vol/vol) fetal calf serum (Omega).

### 3.2.11 Enzyme-linked immunospot assay

Freshly isolated splenocytes were cultured overnight with SIINFEKL (OVA-I) peptide in and ELISpot assay as previously described in Chapter 2 Materials and Methods.

### 3.2.12 Cytokine Release Assay

Antigen-specific IL-2 cytokine release from freshly isolated splenocytes was measured as previously described in Chapter 2 Materials and Methods.

### 3.2.13 Immunoblotting

Mouse J774 or RAW 264.7 macrophages stimulated with Hp91 or LPS for 20, 40, or 60 minutes were lysed for 20 minutes on ice in RIPA lysis buffer (10mM Tris pH 7.4, 150mM NaCl, 1% TritonX-100, 0.1% sodium deoxycholate, 0.1% sodium dodecylsulfate (SDS), 5mM EDTA supplemented with 1mM phenylmethylsulfonyl fluoride, Halt phosphatase inhibitor (Thermo Fisher Scientific, Rockford, IL), 1mM sodium vanadate, 1mM sodium fluoride, and complete protease inhibitor cocktail (Roche). Protein concentration was determined with the DC (Detergent Compatible) protein assay (Bio-Rad, Hercules, CA). The lysates were snap-frozen and stored at −80°C. Equal amounts of protein lysates were separated by gel electrophoresis with the use of a NuPAGE Novex 4%-12% Bis-Tris Midi Gel (Invitrogen) and transferred to polyvinylidene fluoride membranes (Bio-Rad). Membranes were washed with 1× TBST (Tris-Buffered Saline Tween-20) and blocked for 1 hour at room temperature in 5% milk/TBST. Membranes were probed overnight for phospho- p38, phospho (p)-interferon regulatory factor 3 (IRF3), p38, IRF3, glyceraldehyde-3-phosphate dehydrogenase (GAPDH), or β-actin (Cell Signaling Technology). The next day, membranes were washed with 1× TBST and incubated with goat anti–rabbit or anti–mouse horseradish

peroxidase–conjugated secondary antibodies (Santa Cruz Biotechnology, Santa Cruz, CA) diluted in 5% milk/TBST for 1 hour at room temperature. Antibodies were detected with the use of either an enhanced chemiluminescence detection kit (GE Healthcare, Piscataway, NJ) or SuperSignal West Femto Maximum Sensitivity Substrate (Thermo Fisher Scientific). In some experiments, cells were pre-treated with the endocytosis inhibitor Dynasore.

### 3.2.14 Qualitative real-time PCR

Qualitative real-time PCR (qPCR) was performed in a Stratagene Mx3005P (Agilent, Santa Clara, CA) for mouse IFN-$\alpha$2 and GAPDH. GAPDH was used as an endogenous standard for normalization of the IFN-$\alpha$2 gene. Briefly, 1.25 x $10^5$ J774 macrophages per well were serum-starved overnight in a 96-well flat bottom plate and stimulated in duplicate with LPS (10 ng/ml), acetylated Hp91 (200 $\mu$g/ml), CpG (5 $\mu$g/ml), or left unstimulated (media) for 6 hours. Cells were harvested and RNA was isolated using TRIzol as follows: the J774 cell pellets were lysed in approximately 1 ml of TRIzol Reagent (Invitrogen) by repetitive pipetting. The cleared homogenate solution was incubated for 5 min at RT, 200 $\mu$l of chloroform was added and samples were shaken for 15 seconds and incubated at RT for an additional 2-3 minutes. Samples were centrifuged at 12000 x g for 15 minutes at 4° C. Pellets were washed with 1 ml 75% RNAse-free ethanol, centrifuged for 7000 x g for 5 min at 4° C, and the RNA pellets were air dried. DNase was removed from samples using a Turbo DNAfree DNase treatment (Applied Biosystems/Ambion, Austin, TX). cDNA was synthesized using Superscript III-RT polymerase (Invitrogen) and related reagents as per the manufacter's instructions. qPCR samples were setup using Brilliant II SYBR Green QPCR Master Mix (Invitrogen) and the following Q-primers: IFN-$\alpha$2 (For. 5'-

ACTCTGTGCTTTCCTCGTGATGCT -3'; Rev. 5'- ATCCAAAGTCCTGCCTGTCCTTCA -3') and GAPDH (For. 5' – TCACCACCATGGAGAAGGC -3'; Rev. 5' – GCTAACCAGTTGGTGGTGCA -3'). Primers were purchased from IDT. qPCR was performed on duplicate samples in a Stratagene Mx3005P. Amplification product lengths were confirmed on a DNA gel. Values are normalized against GAPDH controls.

#### 3.2.15 Statistical analysis

Data represented are mean ± SEM. Data were analyzed for statistical significance using unpaired or paired Student's *t*-tests. Statistical analysis was done using GraphPad software version 5.01 for Windows (GraphPad Software, San Diego, CA, USA). A $p$ value $<0.05$ was considered statistically significant.

## 3.3 Results

#### 3.3.1 Hp91 enters dendritic cells via clathrin-mediated endocytosis

To gain insight into the mechanism of action of the DC stimulatory peptide Hp91, we investigated its interaction with DCs. DCs were exposed to Hp91 or a control peptide, Hp121, which is also derived from HMGB-1 and has the same length, a similar charge and isoelectric point as Hp91. Confocal microscopy showed that Hp91 was detected within DCs within 5 minutes, while the control peptide Hp121 was not detected, even after 30 minutes at 37$^{o}$C (Figure 3.1A). We observed a dose dependent uptake of Hp91 by flow cytometry (Figure 3.1B), which appears to plateau between 10 and 30 minutes (Figure 3.1C). Uptake of Hp91 is sequence specific, as the control peptide Hp121 was not taken up by DCs (Figure 3.1D, 3.1E).

Although a scrambled version of Hp91 was taken up by DCs, it was at a much lesser extent than Hp91 (Figure 3.1D, 3.1E).

**Figure 3.1.** *Hp91 uptake by DCs is dose, time, and sequence dependent*. (**A**) Immature human DCs (iDCs) were pre-cooled, incubated on ice for 30 minutes with biotinylated Hp91 or Hp121 (200 μg $ml^{-1}$) to allow peptide binding, washed, then incubated for 0, 15, or 30 additional minutes at 37°C. Times on figure represent total incubation times (ice and 37°C). Cells were cytospun, fixed, permeabilized, and stained with Streptavidin-Alexa 488 to visualize biotinylated peptides (Green) and Hoechst DNA stain (Blue). Cells were imaged on a Zeiss LSM confocal microscope. Data are representative of 3 independent experiments. (**B**) iDCs were pre-cooled on ice for 30 minutes, then incubated with biotinylated-Hp91 (0, 10, or 100 μg $ml^{-1}$) for 30 minutes at 37° C. Cells were permeabilized with Cytofix/Cytoperm, stained with, and analyzed by flow cytometry. Results shown are representative of 6 independent experiments. (**C**) iDCs were incubated with biotinylated Hp91 for 10 or 30 minutes (at 100 μg $ml^{-1}$) and permeabilized, stained, and analyzed as above. Results shown are mean (±SEM) of 4 independent experiments. (**D-E**) iDCs were pre-cooled on ice for 30 minutes, then incubated with medium only or biotinylated-Hp91, Hp121, or scrambled Hp91 ("Scramble") at 200 μg $ml^{-1}$ for 30 minutes at 37° C. Cells were permeabilized, stained, and analyzed by flow cytometry as above. (**D**) is mean (±SEM) for 3 independent experiments and (**E**) is a representative result. *$p < 0.05$ compared to medium; Student's t-test.

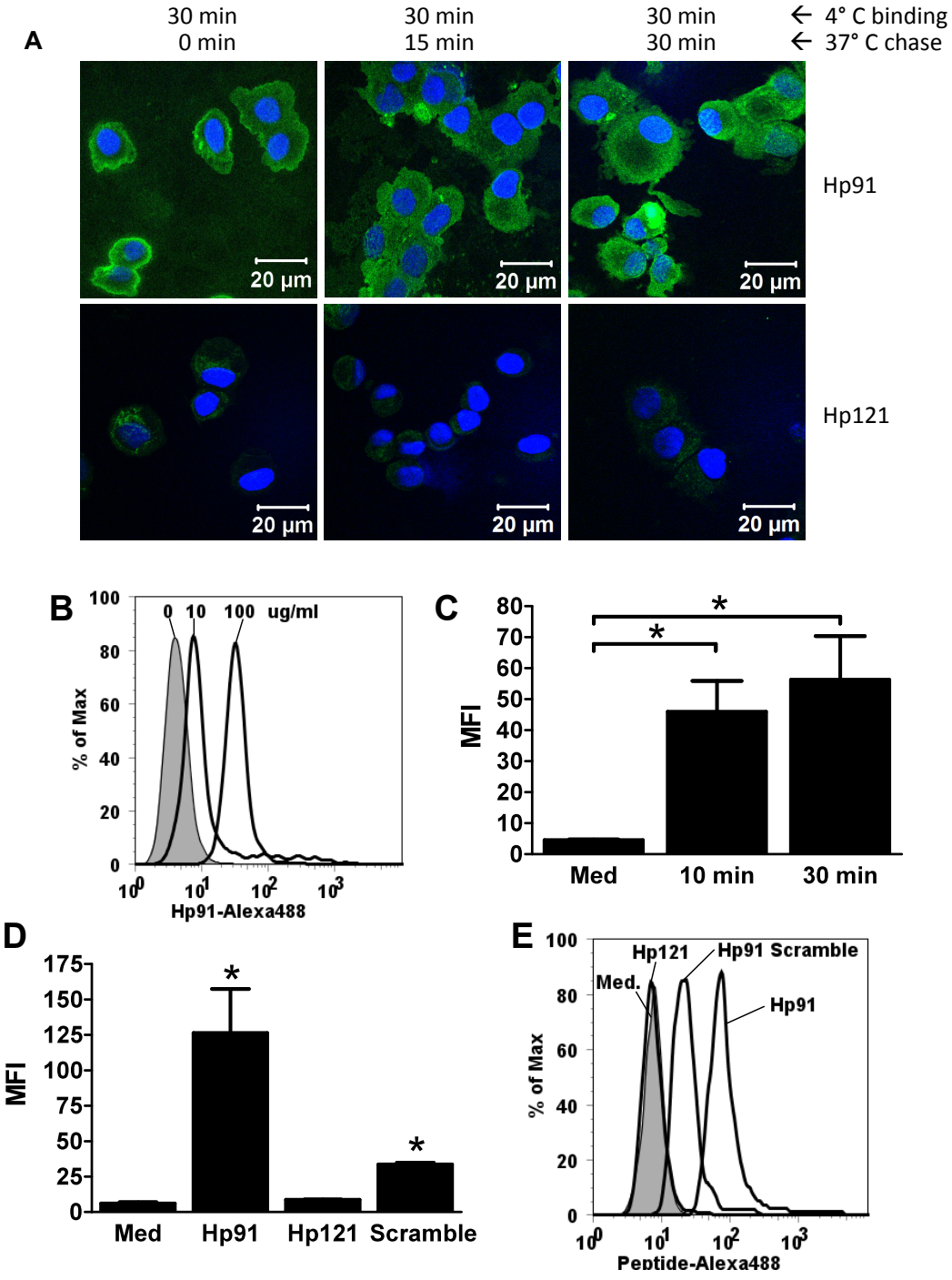
A
30 min
0 min
30 min
15 min
30 min
30 min
← 4° C binding
← 37° C chase
Hp91
Hp121
20 µm
B
0 10 100 ug/ml
% of Max
Hp91-Alexa488
C
MFI
Med
10 min
30 min
D
MFI
Med
Hp91
Hp121
Scramble
E
Hp121
Hp91 Scramble
Med.
Hp91
% of Max
Peptide-Alexa488

Cell penetrating peptides are preferentially taken up via endocytosis, at 37°C, or transcytosis (107), which occurs at 16°C. We tested the temperature at which Hp91 was taken up by DCs to determine the method of uptake. DC uptake of Hp91 occurred at 37°C, but not 16°C, or 4°C (Figure 3.2A, 3.2B), suggesting that uptake occurs via an energy dependent process, such as endocytosis. Endocytosis pathways include phagocytosis, macropinocytosis, clathrin-mediated, or lipid-raft/caveolin-mediated. The mechanism of uptake was determined using specific inhibitors of these endocytosis pathways. Latrunculin B (LatB), a specific phagocytosis inhibitor, while completely abrogating uptake of Dextran FITC (data not shown), did not significantly reduce uptake of Hp91 (Figure 3.2C). Phenylarsine oxide and chlorpromazine, both clathrin-mediated endocytosis inhibitors, significantly reduced the uptake of Hp91, suggesting that uptake occurs via clathrin-mediated endocytosis (Figure 3.2D). Sodium azide, which generally tests for energy-dependent endocytosis, inhibited Hp91 uptake by approximately 40% (Figure 3.2D), though not significantly. When using a fluorescently labeled version of Hp91 (Cp488), sodium azide significantly inhibited Hp91 uptake (data not shown). In contrast, the lipid-raft/caveolin-mediated endocytosis inhibitor, nystatin, and the macropinocytosis inhibitor, amiloride, failed to significantly reduce uptake of Hp91 (Figure 3.2D), suggesting uptake is not via lipid rafts, nor macropinocytosis.

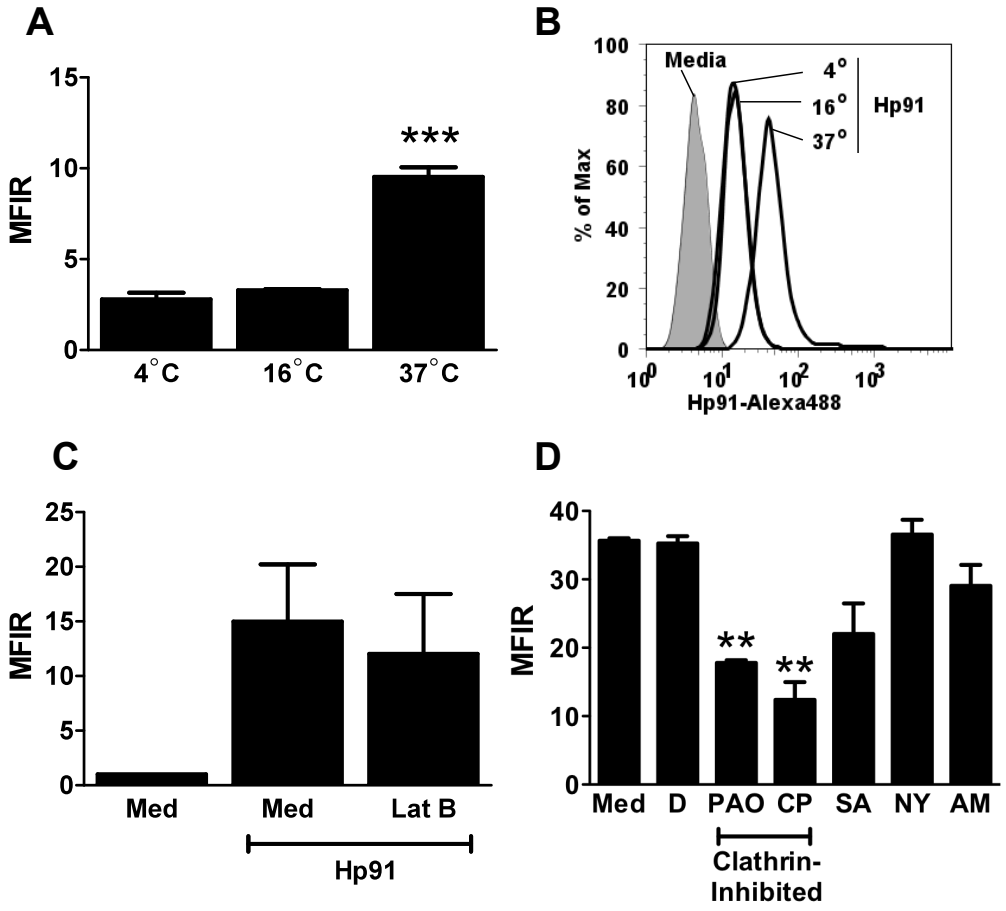


***Figure 3.2.*** *Hp91 is taken up by clathrin-mediated endocytosis.* (**A-B**) Immature human DCs were pre-cooled on ice for 30 minutes, then incubated with biotinylated Hp91 (200 μg ml$^{-1}$) for 30 minutes at 4, 16, or 37° C. Cells were permeabilized with Cytofix/Cytoperm, stained with Streptavidin-Alexa 488, and analyzed by flow cytometry. (**A**) Data are mean (±SEM) of 3 independent experiments and (**B**) is a representative result. ***p < 0.001 compared to 4° C; Student's t-test. (**C**) iDCs were pre-treated with the phagocytosis inhibitor Latrunculin B or medium only for 30 minutes before incubation with biotinylated-Hp91 for 30 minutes. Cells were permeabilized, stained, and analyzed by flow cytometry as above. Data are mean (±SEM) of 5 independent experiments. (**D**) iDCs were pre-treated for 30 minutes with medium only (Med), DMSO control (D), the clathrin-mediated endocytosis inhibitors 1) phenylarsine oxide (PAO) at 2 μM or 2) chlorpromazine (CP) at 100 μM, the energy-dependent endocytosis inhibitor sodium azide (SA) at 10 mM, the caveolin-mediated endocytosis inhibitor nystatin (NY) at 20 μM, or the micropinocytosis inhibitor amiloride (AM) at 2 mM before incubation with biotinylated Hp91 (200 μg ml$^{-1}$) for 30 minutes. Cells were permeabilized, stained, and analyzed by flow cytometry as above. Results are mean (±SEM) of 3 independent experiments. **p < 0.01 compared to DMSO control; Student's t-test.

### 3.3.2 Hp91 induces IL-6 secretion in DCs via p38 MAPK and NF-κB

We have previously shown that the p38 MAPK inhibitor, SB203580, down-regulated HMGB1 B box-induced secretion of IL-6 (51). Pretreatment of human DCs with SB203580, a p38 MAPK inhibitor, and N-p-Tosyl-L-phenylalanine chloromethyl ketone (TPCK), an NF-κB inhibitor, significantly reduced the Hp91-induced IL-6 secretion (Figure 3.3). In contrast, PD98059, a MEK1 inhibitor, failed to significantly reduce IL-6 secretion (Figure 3.3). These results suggest that Hp91 causes DC activation in a p38 and NF-κB dependent manner.

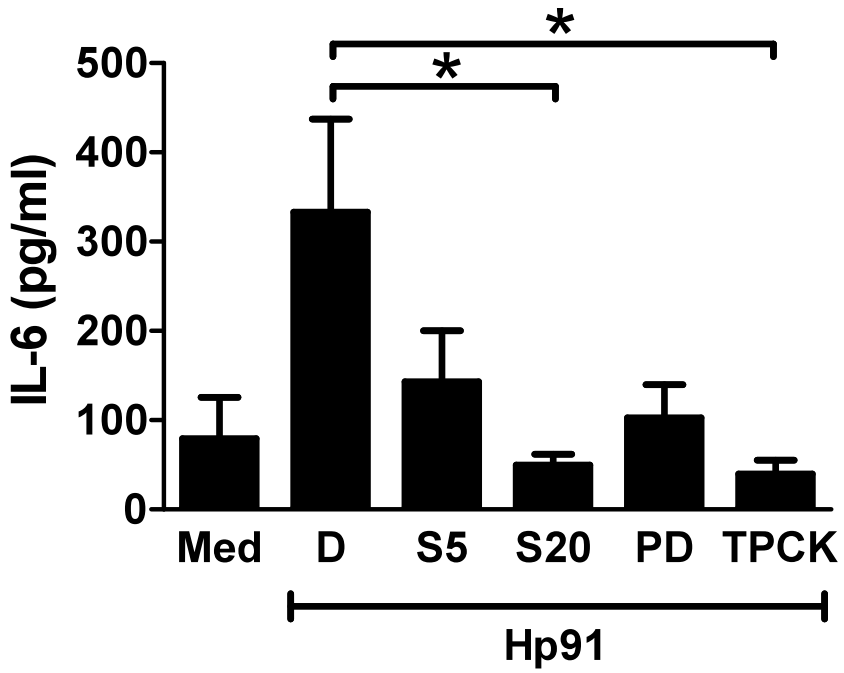


**Figure 3.3.** *p38 MAPK and NF-κB are necessary for Hp91-mediated IL-6 secretion from human dendritic cells.* Immature human DCs were pre-treated for 30 minutes with DMSO control (D), SB203580 at 5 (S5) or 20 (S20) μM, PD98059 (PD) at 20 μM, or TPCK at 20 μM prior to exposure to Hp91. Cell culture supernatants were collected after 48h and analyzed for the presence of IL-6 by ELISA. Results are mean (±SEM) for 5 independent experiments. *$p < 0.05$; Student's t-test.

### 3.3.3 Hp91-mediated activation of DCs is dependent on MyD88, TLR4, and IFNαβR

As clathrin-mediated endocytosis is receptor-mediated, we set out to identify the receptor(s) for Hp91. Several receptors have been implicated in mediating the

responses to the parent molecule HMGB1, including TLR4 (53, 54, 95, 96, 98, 100). To identify the receptor(s) involved in activation of DCs, mouse BM-DCs were generated from wildtype and knockout mice and cells were exposed to Hp91. IL-6 secretion was strongly and significantly reduced in BM-DCs from MyD88 and TLR4 knockout mice (KO) (Figure 3.4A), whereas IL-6 production from BM-DCs generated from TLR7 KO mice was comparable to wild type (Figure 3.4A). In addition, IL-6 secretion in IFN$\alpha\beta$R knockout mice was significantly reduced (Figure 3.4A). No change was observed in IL-6 secretion from IL-1R knockout mice.

Involvement of TLR4 and MyD88 and their downstream pathways was further confirmed by immunoblotting for phospho-p38. Phospho-p38 (p-p38) was upregulated after 40-60 minutes of Hp91 stimulation (Figure 3.4B) in 4 independent experiments. In some, but not all experiments, upregulation of p-p38 was observed as early as 20 minutes after Hp91 stimulation.

### 3.3.4 Hp91-mediated activation of DCs is clathrin- and dynamin-dependent

In LPS signaling within macrophages, TLR4 is endocytosed in a dynamin-dependent manner for downstream signaling (108), so we tested if pre-treatment of macrophages with clathrin- and dynamin- mediated endocytosis inhibitors would reduce Hp91-mediated IL-6 secretion. Similar to with LPS, pre-treatment with the dynamin-dependent endocytosis inhibitor, Dynasore, significantly reduced Hp91-induced IL-6 secretion (Figure 3.4C). In addition, a significant reduction in IL-6 was observed after blocking clathrin-mediated endocytosis with phenylarsine oxide (Figure 3.4C). As we had observed a reduction in Hp91-mediated IL-6 secretion in human DCs following pretreatment with the p38 and NF-$\kappa$B inhibitors, SB203580 and TPCK, in human DCs, we tested if a similar reduction in IL-6 would be observed in

mouse cells. As was seen in human cells, SB203580 and TPCK significantly lowered than the amount of Hp91-stimulated IL-6 secreted from mouse macrophages (Figure 3.4C), further confirming the involvement of p38 and NF-κB in Hp91 signaling. Furthermore, we ensured that the dynamin-dependent endocytosis inhibitor, Dynasore, significantly inhibited uptake of Hp91 (Figure 3.4D) as measured by flow cytometry, as we planned to use Dynasore to investigate additional downstream signaling.

As a decrease in Hp91-induced IL-6 secretion was observed in IFNαβR knockout BM-DCs (Figure 3.4A), we set out to investigate if the MyD88-independent, TRAM/TRIF signaling pathway was activated by probing for phosphorylation of the downstream interferon regulatory factor 3 (IRF3) transcription factor. The phosphorylation of IRF3 (pIRF3) was upregulated after Hp91 stimulation, shown as early as 20 minutes (Figure 3.4E) and at a maximum around 40 minutes after stimulation. In addition, we tested if blocking endocytosis with Dynasore would reduce the phosphorylation of IRF3. As dynasore was solubilized in DMSO, DMSO is used as a control. Dynasore appeared to reduce the phosphorylation of IRF3 at 20, 40 and 60 min (Figure 3.4E), suggesting that Hp91 uptake is required for MyD88-independent interferon regulatory factor 3 signaling.

To further investigate involvement of the MyD88-independent signaling pathway, we evaluated mRNA expression in Hp91-stimulated macrophages. J774 cells were stimulated for 6 hours and, as determined by qPCR, Hp91 was shown to induce IFN-α mRNA expression (Figure 3.4F). A 99-fold increase in mRNA is demonstrated at 6 hours. This is much lower than the increase observed with LPS. CpG did not induce IFN-α mRNA expression in this experiment.

**Figure 3.4.** *TLR4, MyD88, and MyD88-dependent and -independent pathways are necessary for Hp91-mediated activation of mouse cells.* (**A**) Immature BM-DCs from wild type (WT) or knockout mice (as indicated) were incubated with Hp91 (200 μg $ml^{-1}$). Supernatants were collected after 24 hours and analyzed for the presence of IL-6 by ELISA. Results are mean (±SEM) for at least 3 independent experiments. *$p < 0.05$ compared to WT; Student's t-test. (**B**) J774 macrophages were stimulated for 20, 40, or 60 minutes with Hp91 (200 μg $ml^{-1}$) or LPS (10 ng $ml^{-1}$) or left unstimulated (M). Cells were harvested, lysed, and analyzed for p-p38. Immunoblots were probed with anti-p-38, total p38, and GAPDH antibodies. Data shown is representative from 4 separate immunoblots. Non-relevant wells were removed from the blot. (credit: L. Liutenez) (**C**) J774 macrophages were pre-treated for 30 minutes with DMSO control (D), SB203580 at 20 (SB) μM, PD98059 (PD) at 20 μM, TPCK at 20 μM, Dynasore (DYN) at 80 μM, phenylarsine oxide (PAO) at 2 μM, or chlorpromazine (CP) at 100 μM prior to exposure to Hp91. Cell culture supernatants were collected after 24h and analyzed for the presence of IL-6 by ELISA. Data shown are mean (±SEM) for triplicates. SB, PD, and TPCK results are representative of 3 independent experiments. *$p < 0.05$; Student's t-test. (**D**) J774 macrophages were pre-treated for 30 minutes with medium only (Med), DMSO control (D), the dynamin-mediated endocytosis inhibitor Dynasore (DYN) at 80 μM, or the clathrin-mediated endocytosis inhibitors 1) phenylarsine oxide (PAO) at 2 μM or 2) chlorpromazine (CP) at 100 μM before incubation with Cp488-labeled Hp91 (200 μg $ml^{-1}$) for 30 minutes. Cells were washed and immediately analyzed by flow cytometry as above. Results are mean (±SEM) of 4 independent experiments. *$p < 0.05$ compared to DMSO control; Student's t-test. (**E**) RAW 264.7 macrophages were pre-treated for 30 minutes with medium only, DMSO control (DMSO), or Dynasore (DYN) at 80 μM prior to stimulation for 20, 40, or 60 minutes with Hp91 (200 μg $ml^{-1}$) or LPS (10 ng $ml^{-1}$) or medium only (media). Cells were harvested, lysed, and analyzed for p-IRF3. Immunoblots were probed with anti-p-IRF3, total IRF3, and β-actin antibodies. (credit: L. Liutenez, D. Futalan). (**F**) cDNA from stimulated J774 cells were evaluated for IFN-α2 mRNA production by qPCR. Values are normalized against endogenous GAPDH controls and run in duplicate.

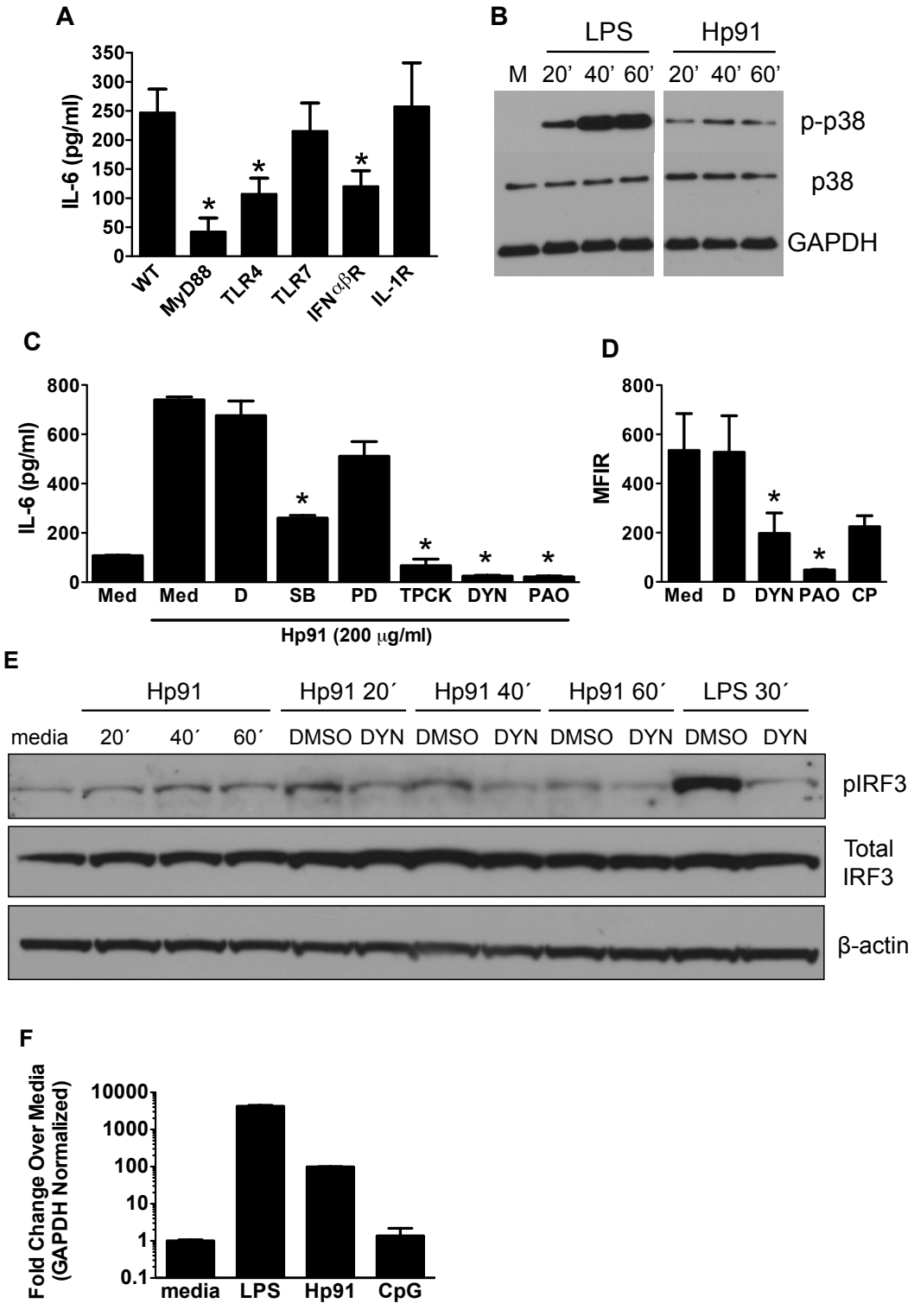
A
IL-6 (pg/ml)
350
300
250
200
150
100
50
0
WT
MyD88
TLR4
TLR7
IFNαβR
IL-1R
B
LPS
Hp91
M 20' 40' 60' 20' 40' 60'
p-p38
p38
GAPDH
C
IL-6 (pg/ml)
800
600
400
200
0
Med
Med
D
SB
PD
TPCK
DYN
PAO
Hp91 (200 μg/ml)
D
MFIR
800
600
400
200
0
Med
D
DYN
PAO
CP
E
Hp91
Hp91 20´
Hp91 40´
Hp91 60´
LPS 30´
media
20´
40´
60´
DMSO
DYN
DMSO
DYN
DMSO
DYN
DMSO
DYN
pIRF3
Total IRF3
β-actin
F
Fold Change Over Media (GAPDH Normalized)
10000
1000
100
10
1
0.1
media
LPS
Hp91
CpG

### 3.3.5 TLR4 is not necessary for Hp91 uptake

As binding and uptake is receptor-mediated via clathrin, and Hp91-mediated activation of DCs is dependent on TLR4, we investigated whether TLR4 was a necessary cell surface receptor for Hp91 binding and uptake. WT and TLR4 KO BM-DCs were stimulated with biotinylated-Hp91 or left unstimulated (media). Cells were stained for Hp91 with Streptavidin-Alexa 488 and examined by confocal microscopy. Surprisingly, knocking out TLR4 did not appear to reduce Hp91 uptake (Figure 3.5A). To quantify uptake in the entire BM-DC population and make it possible to look for small changes in uptake, we stimulated WT and TLR4 KO BM-DCs as above and analyzed the cells by flow cytometry. TLR4 KO BM-DCs showed only a small reduction in Hp91 uptake, within the error of the WT uptake (Figure 3.5B), suggesting that instead of, or in addition to TLR4, alternative receptors are required for uptake.

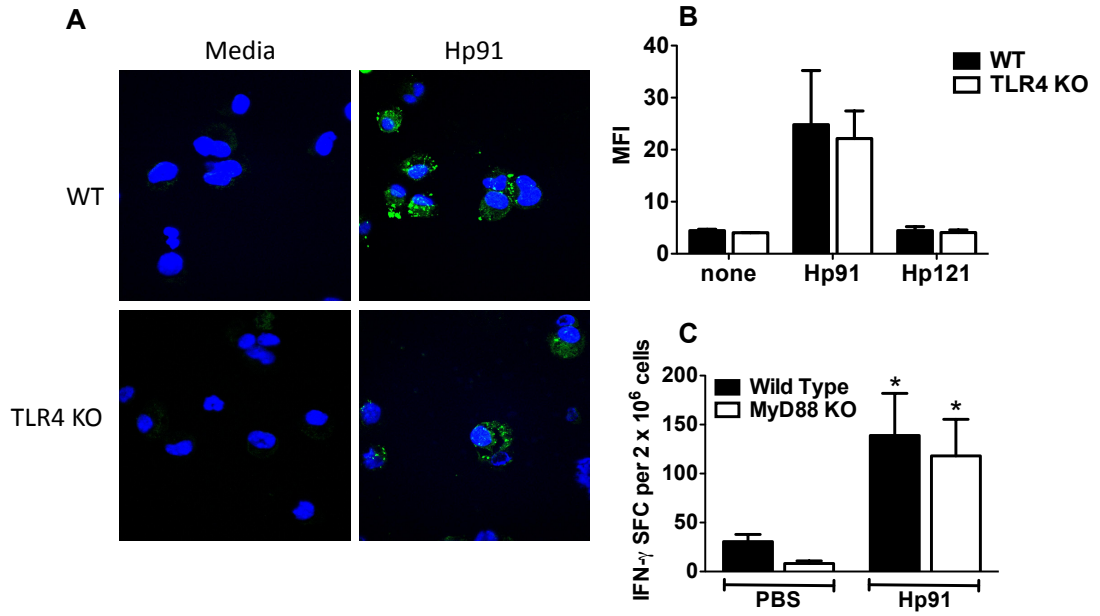


**Figure 3.5.** *Uptake and immune response in knockout mice.* (**A**) Immature BM-DCs from WT or TLR4 knockout mice were pre-cooled, incubated on ice for 30 minutes with biotinylated Hp91 or Hp121 (200 μg/ml) to allow peptide binding, washed, then incubated for 30 additional minutes at 37°C. Cells were cytospun, fixed, permeabilized, and stained with Streptavidin-Alexa 488 to visualize biotinylated peptides (Green) and Hoechst (Blue) to visualize the nucleus. Cells were imaged on a Zeiss LSM confocal microscope. Data are representative of 3 independent experiments. (**B**) Immature BM-DCs from WT or TLR4 knockout mice were precooled on ice for 30 minutes, then incubated with biotinylated Hp91 (200 μg/ml) for 30 minutes at 37° C. Cells were permeabilized with Cytofix/Cytoperm, stained with Streptavidin-Alexa 488, and analyzed by flow cytometry. Data are mean +/- SEM of 3 independent experiments. (**C**) WT or MyD88 knockout mice were immunized with SIINFEKL peptide in PBS with or without Hp91. Freshly isolated splenocytes from the immunized mice were cultured in the presence of SIINFEKL peptide (2.5 μg ml−1). The number of IFN-γ -secreting cells was determined 18 h later. The data shown is mean (±SEM) for 5-10 mice/group. *$p < 0.05$ between groups; Student's t-test.

### 3.3.6 MyD88 not necessary for Hp91-elicited *IFN-γ* immune responses *in vivo*

We demonstrated that the MyD88-dependent signaling pathway is responsible for IL-6 secretion from Hp91-stimulated BM-DCs (Figure 3.4A). Additionally, we suggested that the MyD88-independent interferon pathway is activated by Hp91 (Figure 3.4E). We hypothesized that both pathways would be responsible for the *in*

*vivo* Hp91-induced immune response and that Hp91-immunized MyD88 knockout mice would show a reduced antigen-specific immune response. We immunized age-matched WT and MyD88 KO mice with OVA-I (SIINFEKL) peptide co-injected with PBS only or Hp91. Both WT and MyD88 knockout mice show significant antigen-specific cellular immune responses, as demonstrated by increases in the number of OVA-specific IFN-γ secreting cells (Figure 3.5C). Additionally, the increase in IFN-γ secreting cells over PBS controls is nearly identical in the WT and MyD88 knockout mice, suggesting that this cellular IFN-γ response is not due to MyD88 signaling. Immunizations in mice with MyD88-independent pathway knockouts, such as TRAM and TRIF, have not yet been performed.

### 3.3.7 Serum factors are not required for Hp91 cellular uptake

Though the TLR4 involvement is not entirely understood, we have demonstrated that IL-6 secretion in Hp91-stimualted BM-DCs is dependent on TLR4. TLR4 is known to require the help of serum accessory proteins, such as LPS binding protein (LBP) (109), for downstream signaling. We hypothesized that serum factors may be necessary for Hp91's interaction with DCs, through TLR4 or other receptors. Thus, we investigated if serum factors were involved or required for Hp91's uptake by DCs.

BM-DCs were either left in the original media they were derived in, or the media was replaced with fresh 5% FCS/RPMI or RPMI only. Biotinylated-Hp91 was added to the BM-DCs and cells were incubated for 30 minutes to allow uptake. Cells were permeabilized, stained with Streptavidin-Alexa 488, and cells were analyzed by flow cytometry. Hp91 uptake is enhanced in BM-DCs cultured in fresh 5% FCS/RPMI compared to original media (Figure 3.6). Furthermore, when serum is removed

entirely (RPMI only), Hp91 uptake is further enhanced. These data suggest that Hp91 is not dependent on serum factors for cellular uptake. In contrast, Hp91 uptake may be inhibited by serum factors. Additionally, fresh RPMI, with or without serum, enhances uptake, likely due to the additional sugars, amino acids, vitamins, or other ingredients/conditions that are available in the fresh media.

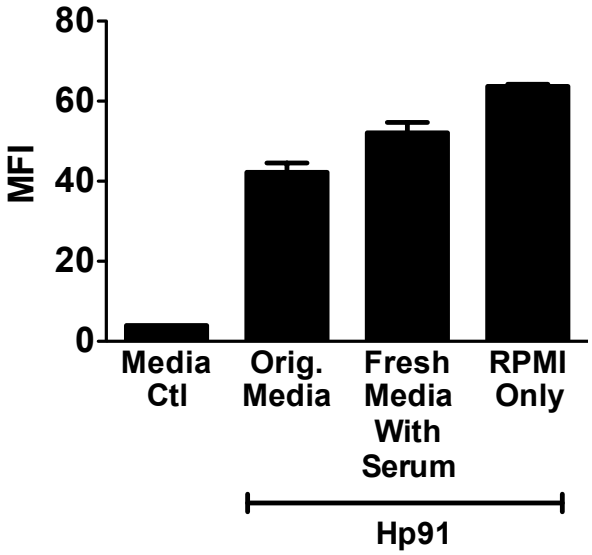


**Figure 3.6.** *Hp91 uptake not dependent on serum factors.* WT BM-DCs were cultured in original media or media was replaced with fresh RPMI with 5% FCS or RPMI only. Cells were incubated with Hp91 peptide (200 μg/ml) for 30 min at 37° C. Cells were permeabilized with Cytofix/Cytoperm, stained with Streptavidin-Alexa 488, and analyzed by flow cytometry. Data are mean (±SEM) of triplicate samples, but data is representative of 3 independent experiments.

## 3.4 Discussion

We wanted to understand how Hp91 was exerting its immunostimulatory effects on DCs, and hypothesized it was signaling through a cell surface receptor.

Based on the knowledge that LPS moves sequentially from the cell surface to endosomes for a full signaling cascade (110), we concluded it might be possible for Hp91 to also be endocytosed by DCs. As shown by confocal microscopy, Hp91 binds cells within 30 minutes on ice, as visible by a rim around the cells, and is taken up into the cells very rapidly in a sequence specific manner, as Hp121 does not enter cells. Scrambling the amino acids of Hp91 results in a great reduction of binding/uptake by cells, indicating that it is neither the total charge nor total hydrophobicity that is important. Rather, we hypothesized that a particular sequence of amino acids is critical for the binding and uptake of peptide into cells, and that the region of the peptide responsible for activity could be investigated by testing shorter, overlapping peptides for their dendritic cell uptake as well as *in vitro* and *in vivo* immunostimulatory activity. Such experiments will be described in Chapter 4, where we identify an Hp91-based short immunostimulatory peptide, UC1018, that activates DCs and acts as adjuvant *in vivo*.

The high proline content of Hp91 initially led us to believe that the uptake may occur via transcytosis, as proline-rich peptides have been found to have cell-penetrating properties (111). Endocytosis is an energy-dependent process, greatly reduced at 16°C, whereas transcytosis is not (112). We felt it was important to establish if this cell penetration was energy-dependent, because energy-dependent endocytosis is often receptor-mediated, and this would help tell us whether Hp91 was binding to a receptor, such as TLR4. Once we ruled out transcytosis by demonstrating that uptake occurs only at 37°C, and not at 4°C or 16°C, we hypothesized that receptor-mediated endocytosis was likely, such as clathrin-mediated endocytosis. For example, LPS binds TLR4, and is subsequently endocytosed (108). The clathrin-dependent endocytosis inhibitors phenylarsine oxide (PAO) and chlorpromazine (CP)

significantly reduce uptake of Hp91 by DCs. As the rest of our panel of inhibitors failed to reduce Hp91's uptake, we conluded endocytosis must be dependent on clathrin. We generated two cartoon based on our results to summarize endocytosis mechanisms and visualize how Hp91 is endocytosed by DCs. Hp91 is designated by the red star in Figure 3.7 and by the green oval in Figure 3.8.

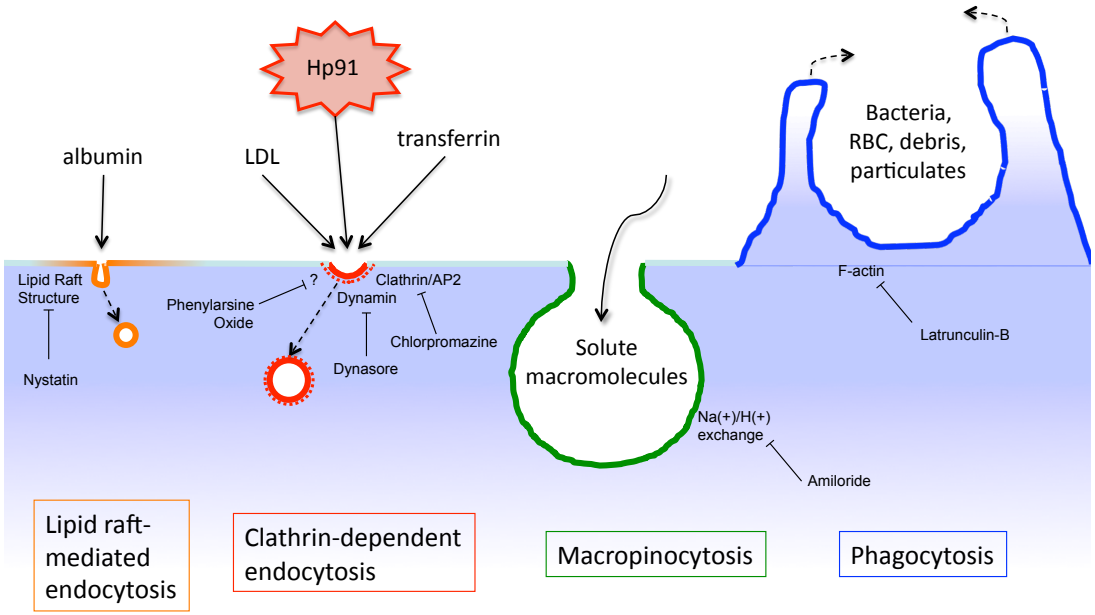


**Figure 3.7.** *Four endocytosis methods – a cartoon.*

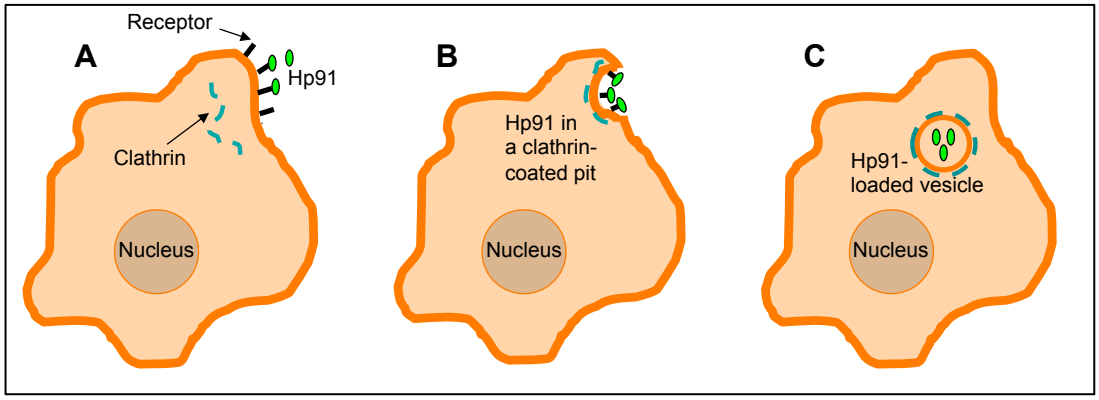


**Figure 3.8.** *A proposed mechanism of Hp91 DC interaction.* (**A**) Hp91 binds a receptor on the cell surface, such as TLR4 or other(s). (**B**) The cell membrane invaginates, and Hp91 and its receptor are opsonized in a clathrin-coated vesicle. (**C**) The clathrin-coated pit buds off into the cell and Hp91 resides in a vesicle within the cell.

As clathrin-mediated endocytosis is receptor mediated, we explored possible receptors for Hp91. TLR2 and TLR4, were particularly interesting receptors to us in that they appear to bind many ligands with a large amount or promiscuity, and it has been difficult to find many structural similarities among the ligands. Matzinger theorizes that it is hydrophobic portions (hyppos) of molecules that interact with receptors such as TLR2 and TLR4 (113). It is not yet precisely understood how the full molecule HMGB1 signals through TLR4, however a recent report published after we conducted our investigation recognized the importance of a cysteine residue in HMGB1 that is critical for TLR4 interaction (97).

By evaluating IL-6 secretion from knockout mice, we show that Hp91-stimulated activation of DCs is dependent on TLR4 and its downstream adaptor protein, MyD88. We further confirm, via phosphorylation of p38 and using p38 inhibitors, that Hp91 activates the MyD88-dependent signaling pathway. In the MyD88 KO immunization, we showed that an Hp91-induced cellular immune response is still possible and comparable to the response seen in WT mice. From this

we conclude that even though MyD88 is required for cytokine signaling in DCs, such as IL-6 secretion, that the *in vivo* response is much more complicated and relies on more than just the MyD88-dependent cell signaling.

We have shown previously (Figure 2.1) that Hp91 induces the *in vivo* production of Th1-type cytokines, such as IL-12, and IFN-γ (91). The Th1 cellular immune response is highly characterized by interferon responses, so we investigated if the MyD88-independent interferon pathway was activated. We show via Hp91-induced phosphorylation of IRF3 that Hp91 signals through the interferon pathway and qPCR results demonstrate that IFN-α mRNA is expressed. Furthermore, in the immunoblot with the inhibitor Dynasore, Dynasore appears to reduce pIRF, demonstrating that Hp91 uptake is required for signaling through this MyD88-independent pathway. This *in vitro* interferon data, combined with the knowledge that MyD88 is not necessary *in vivo* for cellular immune responses, leads to the hypothesis that it is the TRAM/TRIF MyD88-independent pathway that is required for the *in vivo* cellular immune responses. TRAM/TRIF knockouts are available and future immunizations in knockouts such as these are warranted.

Somewhat unexpectedly, even though IL-6 signaling is dependent on TLR4, and two TLR4 signaling pathways are activated, we showed that TLR4 is not necessary for uptake of Hp91. Additional receptors are likely implicated in Hp91 uptake. First, and perhaps most likely, are several more TLRs that should be tested before investigating other alternatives. Additionally, pull-down experiments are being optimized and may yield additional receptors. Another class of receptors, the G-protein coupled receptors (GPCR) were quickly dismissed as likely receptors as we demonstrated that Hp91 fails to induce calcium flux (data not shown), as many or most GPCRs couple to induce calcium ion signaling (114).

Cell signaling involves complicated dynamic processes that are important for cytokine production, cellular maturation or differentiation, migration, etc. We have only just started to understand the mechanisms for Hp91 signaling and immune responses. More experiments are needed, however the data demonstrated in this chapter, including IL-6 secretion in BM-DC knockout mice, small molecule inhibitor results, and immunoblots, is sufficient enough for us to begin fitting together the molecular signaling puzzle pieces. The following cartoon demonstrates some of the implicated mechanisms and pathways of Hp91 signaling (Figure 3.9).

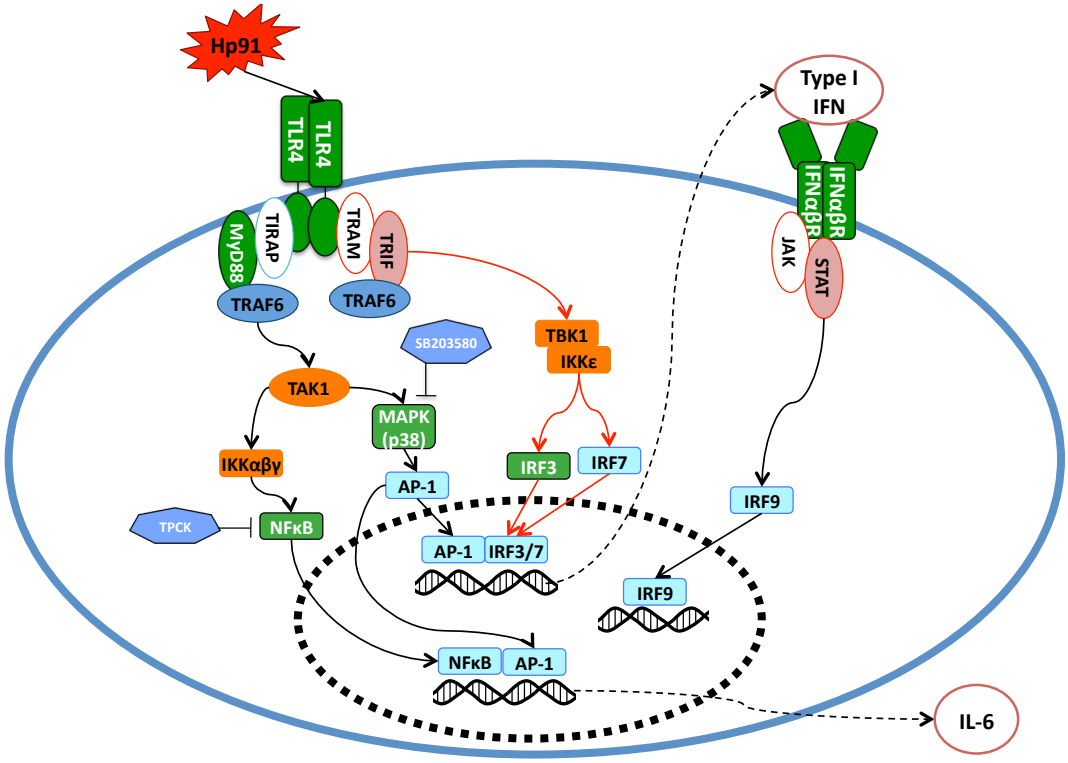


**Figure 3.9.** A proposed mechanism of Hp91 signaling.

In summary, in this chapter we investigated the underlying mechanisms of Hp91-mediated DC activation. Hp91 enters DCs via clathrin-mediated endocytosis. Hp91-induced secretion of IL-6 is MyD88- and TLR4-dependent and is mediated through p38 MAPK and NFκB. Hp91-induced signaling is dependent on clathrin- and

dynamin-mediated endocytosis of Hp91. The MyD88-independent interferon pathway is activated by Hp91 and is mediated through IRF3 phosphorylation.

Chapter 3, in part, is currently being prepared into a manuscript for future submission for publication. Rebecca Saenz, Diahnn Futalan, Lien Leutenez, Fien Eeckhout, Jessie-Farah Fecteau, Simeon Sundelius, Stig Sundqvist, Marie Larsson, Brad Messmer, Tomoko Hayashi, Dennis Carson, Sadik Esener, and Davorka Messmer. The dissertation author is the primary investigator and author of the manuscript.

# 4. Activity of the HMGB1-Derived Immunostimulatory Peptide Hp91 Resides in the Helical C-terminal Portion and is Enhanced by Dimerization ("Structure-Function Relationships")

We have previously shown that an 18 amino acid long peptide, named Hp91, whose sequence corresponds to an area within the endogenous protein HMGB1, activates dendritic cells (DCs) and acts as adjuvant *in vivo* by potentiating Th1-type antigen-specific immune responses. Here we performed structure-function relationship studies on Hp91 peptide to investigate the amino acids and structure responsible for immune responses. We examined oxidation of the cysteine amino acid at position 16 of Hp91 and found that Hp91 spontaneously forms reversible dimers, with over 80% in a dimer form after 96 hours. Using a maleimide conjugation reaction to generate stable capped monomers or cross-linked dimers, we show that the dimer has an enhanced ability to activate DCs compared to the capped control, in addition to an increased ability to bind DCs. Additionally, we show enhanced *in vitro* activation of DCs using Hp91 tetramers. We demonstrate that the C-terminal 9 amino acids of Hp91 are sufficient for DC binding, induction of CTL responses and prophylactic antitumor protection *in vivo*. Utilizing circular dichroism, we show that

the C-terminal 9 amino acids form a true alpha-helical structure. Lastly, we investigate binding and activity of CSE containing peptides and look at Hp91 variations with amino acid modifications. These findings help us understand what structure and amino acid regions of Hp91 are important to promote its function as an immunostimulatory peptide adjuvant and may serve as a guide for the future development of synthetic Th1-type peptide adjuvants for vaccines.

## 4.1 Introduction

Immune adjuvants that enhance the quality and longevity of an immune response are important components of subunit vaccines. Aluminum salts (alum) have been used as vaccine adjuvants for over a century, but in many cases alum is not strong enough or does not induce the desired immune response. Alum induces a primarily humoral, Th2-type immune response, which is undesirable for vaccination against many viruses, intracellular pathogens, and cancer (35).

Rapid advances in vaccine development have recently led to an expanding number of vaccines containing adjuvants other than aluminum salts (alum): 1) the FDA-approved HPV vaccine, Cervarix®, and the European Medicines Agency-approved HBV and seasonal allergy vaccines, Fendrix® and Pollinex Quattro® respectively, are formulated with the bacterial lipoprotein MPL as adjuvant, and 2) several influenza vaccines in Europe are formulated with squalene (e.g. MF59) as adjuvant (2). With the success of these newly approved vaccines comes an intensified search for additional immune adjuvants. Instead of identifying and testing entirely new adjuvants, it may be faster and simpler to engineer new adjuvants by modifying and enhancing current immunostimulatory proteins, peptides, etc. By

understanding the structure-function relationships of current immunostimulatory proteins, scientists may gain the ability to engineer more potent versions based on active regions or important structural elements. Here, we performed structure-function relationship studies to help us understand and enhance the adjuvant activity of HMGB1-derived immunostimulatory peptide, Hp91.

HMGB1 is an endogenous adjuvant (50), originally described as a nuclear binding protein that facilitates DNA bending and nucleosome formation (36). HMGB1 is highly conserved and besides its nuclear functions, it is actively released by monocytes and macrophages following exposure to LPS, TNF$\alpha$, and IL-1$\beta$ and passively released during cell injury and necrosis (49, 80). When released from a cell, HMGB1 acts as an endogenous danger signal, stimulating cytokine release from monocytes, macrophages, and dendritic cells (49, 81). HMGB1 was shown to act as adjuvant to delay tumor growth and increase tumor-free survival in mice (50). The proinflammatory region of HMGB1 has been mapped to the B box domain, and this region is sufficient to cause dendritic cell maturation and Th1 polarization (51).

We have previously identified a short peptide, named Hp91, located within the B box domain of HMGB1, that induces dendritic cell maturation and stimulates secretion of several pro-inflammatory cytokines, including the Th1 cytokine IL-12 (52). Chapter 2 showed that when co-injected with ovalbumin into mice, Hp91 acts as adjuvant, potentiating cellular immune responses to peptide antigen and cellular and humoral responses to protein antigen (91). Hp91 promotes the *in vivo* production of immunomodulatory cytokines such as IFN-$\gamma$, TNF-$\alpha$, IL-6 and IL-12, as well as activation of antigen-specific CD8+ T cells (91). Chapter 3 demonstrated that Hp91 is taken up by dendritic cells by clathrin- and dynamin-dependent endocytosis, and

that Hp91 signals via TLR4, MyD88 and the more traditional p38, NF-κB pathway, as well as the MyD88-independent interferon pathway via phosphorylation of IRF3.

Hp91 contains a cysteine residue at position 16 that corresponds to Cys106 in HMGB1 protein. This Cys106 has been shown to be critical for HMGB1 binding to TLR4 as well as activation of macrophage TNF secretion (97). Other studies have shown that this cysteine is retained in a reduced form *in vivo* and may be responsible for nucleocytoplasmic shuttling of HMGB1 (115). Cysteine residues in synthetic peptides can easily oxidize *in vitro* to form disulphide bonds. Oxidiation of the cysteine at position 16 of Hp91 hypothetically results in the formation of peptide dimers via a disulphide bridge. As mutation of the cysteine residue prevented HMGB1 binding to TLR4 (97), and Hp91 has been shown to also bind TLR4, we hypothesized that the formation of peptide dimers via disulphide bridges at this critical cysteine might affect Hp91 peptide binding and its ability to stimulate dendritic cells. We investigated how both air and maleimide dimer formation affects Hp91 activity in an attempt to design a more potent version of our Hp91 adjuvant.

The structure of the full HMGB1 protein suggests that there may be an alpha helix at the C-terminal portion of the peptide (116). In addition, the N-terminal half of the peptide contains PXXP motifs (Hp91 sequence: D**P**NA**P**KR**PP**SAFFLFCSE) that could break a traditional alpha helix and contribute to a left-handed polyproline II type helix (117-119). Additionally, PXXP motifs can interact with Src homology 3 (SH3) domain containing proteins (120, 121). There are hundreds of human SH3 domains and Hp91 could serve as a ligand for such domains. The significance of these N-terminal and C-terminal domains (NTD and CTD) had not previously been considered, and their predicted secondary structures or signaling potential could contribute to the immune activity of Hp91. In an effort to identify the domains or amino acids

responsible for DC binding and activation, and to evaluate shortened Hp91 variants for their immunostimulatory adjuvant properties, we synthesized and tested overlapping short peptides that spanned the length of Hp91. We performed circular dichroism of the N- and C- terminal domains to evaluate their secondary structure. Circular dichroism spectra of true alpha helices display negative ellipticity bands at 207 and 220 nm and positive ellipticity at 195 nm, while a polyproline type II helix displays a negative ellipticity around 200 nm (117, 118).

To look for amino acids critical for the peptide's immunostimulatory activity, we performed alanine-substitution of the amino acids. Alanine-substitution is commonly used to eliminate side chains off the amino acids without altering the main chain conformation. As adding an alanine meant adding an extra hydrophobic residue to an already hydrophobic peptide, we had some concerns about solubility. Thus, in addition, to reduce hydrophobicity of the parent peptide, lysine-substitution was made for the various hydrophobic phenylalanine residues. We show unexpected results in this chapter to demonstrate that it is not only possible to modify amino acids and maintain activity, but we can modify amino acids to enhance immunostimulatory activity.

In summary, Hp91 is a promising adjuvant for immunotherapy development, particularly due to the cellular, Th1-type of immune responses that are induced following immunization. Structure-function relationships have not previously been considered for Hp91. Here, we evaluate structure-function relationships in an attempt to understand Hp91 function and to design and test more potent immunostimulatory variants of Hp91 for adjuvant development.

## 4.2 Materials and Methods

### 4.2.1 Animals

Female C57BL/6 mice 8-12 weeks of age were used for experiments. All mice were purchased from Charles River Laboratories (Boston, MA, USA) and housed at the Moores UCSD Cancer Center animal facility. All animal studies were approved by the Institutional Animal Care and Use Committee of UCSD and were performed in accordance with the institutional guidelines.

### 4.2.2 Peptides

Peptides, including Hp91 (DPNAPKRPPSAFFLFCSE), UC18 (DPNAPKRP), UC411 (APKRPPSA), UC714 (RPPSAFFL), UC718 (RPPSAFFLFCSE), UC1018 (SAFFLFCSE), UC1018-1A (AAFFLFCSE), UC1018-3A (SAAFLFCSE), UC1018-4A (SAFALFCSE), UC1018-5A (SAFFAFCSE), UC1018-6A (SAFFLACSE), UC1018-7A (SAFFLFASE), UC1018-8A (SAFFLFCAE), UC1018-9A (SAFFLFCSA), UC1018-SS (SASSLFCSE), UC1018-SSS (SASSLSCSE), Hp91-tetramer (linked with a core of three lysines at the C-terminal end of Hp91), CSE, and OVA-I (SIINFEKL) were all synthesized from GenScript Corp (Piscataway, NJ, USA) and CPC Scientific (San Jose, CA, USA). The peptides used for CSE binding experiments, including Hp31 (HPDASVNFSEFSKKCSER), Hp46 (SERWKTMSAKEKGKFEDM), Hp91, Hp106 (CSEYRPKIKGEHPGLSIG), and Hp121, had previously been transported by D. Messmer from her lab at The Feinstein Institute for Medical Research, North Shore. For uptake experiments and immunizations, peptides were synthesized with an N-terminal biotin. For DC stimulation experiments, peptides were synthesized with an N-terminal acetyl group. Peptides were routinely synthesized with greater than 95% purity. Hp91-tetramer was synthesized at 22.8%, as higher purity is difficult to make. Imperfections are almost entirely varied sequence lengths of Hp91

within the tetramer. To enhance solubility of UC1018 peptides, peptides were dissolved in DMSO before dilution in RPMI so that the final concentration was 5% DMSO. Otherwise, unless otherwise stated, all peptides were dissolved in RPMI.

### 4.2.3 Reagents

The p38 MAPK-specific inhibitor, SB203580, and the NFκB inhibitor, *N*-tosyl-L-phenylalanine chloromethyl ketone (TPCK), were purchased from Sigma-Aldrich. The MEK1 inhibitor, PD98059, was purchased from Cell Signaling Technology (Danvers, MA). As these inhibitors required solubilization in DMSO, DMSO was used as a negative control.

### 4.2.4 Cells

The murine melanoma B16.F1 cell line, transduced with a cDNA encoding the chicken ovalbumin gene (B16cOVA), was a gift from Richard Vile (Mayo) and was previously described (122). The cells were cultured in Dulbecco's modification of Eagle's Medium (DMEM) (Mediatech, Manassas, VA), supplemented with 10 mM HEPES (Invitrogen), penicillin (100 U $ml^{-1}$) - streptomycin (100 μg $ml^{-1}$) - L-glutamine (2 mM) (Invitrogen), and 10% (vol/vol) fetal calf serum (FCS) (Omega). To induce apoptosis of B16 cells, the cells were treated with 0.5 mg $ml^{-1}$ mitomycin C (Sigma-Aldrich) in DMEM media for 60 minutes at 37° C. Cells were washed twice in warm DMEM and put back to culture overnight in DMEM supplemented as above.

### 4.2.5 Maleimide Conjugation Reactions

Hp91 peptide monomers, capped at the thiol group of the cysteine, were generated using an N-Ethylmaleimide (NEM) (Thermo Scientific) conjugation reaction.

Briefly, Hp91 was dissolved in PBS and reacted for 2 h at RT in the presence of NEM. Hp91 peptide maleimide dimers, cross-linked at the thiol group of the cysteine, were generated using a Bis-maleimidoethyleneglycol ($BM(PEG)_2$) (Thermo Scientific) conjugation reaction. Briefly, Hp91 was dissolved in PBS/EDTA and reacted for 1 h at RT in the presence of $BM(PEG)_2$. Excess NEM or $BM(PEG)_2$, respectively, was removed by dialysis (2K MWCO cassette, Thermo Scientific). Un-reacted, mock peptide controls were generated under identical reaction and dialysis conditions, while excluding the NEM or $BM(PEG)_2$ reagent. Reagents, glassware, and reaction products were endotoxin-free as determined by the manufacturer or a limulus amoebocyte assay (LAL) (Cambrex Corporation, East Rutherford, NJ) tested according to manufacturer's instructions. Peptides with a biotin at the N-terminal group were used for binding/uptake experiments. Peptides with an acetyl at the N-terminal group were used for DC stimulation experiments.

### 4.2.6 Spontaneous oxidation and dithiothreitol-reduction of Hp91

Hp91 was incubated in PBS at RT for 24 to 96 h to allow spontaneous oxidation of cysteine residues. In some experiments, the peptide was incubated for 30 min +/- 10 mM dithiothreitol (DTT) (Thermo Fisher Scientific) and/or 1% $H_20_2$ (Thermo Fisher Scientific) to reduce or further oxidize the peptide, respectively.

### 4.2.7 Generation of human monocyte-derived DCs

Human iDCs were generated as previously described in Chapter 3, Materials and Methods.

### 4.2.8 Stimulation of DCs

At days 5-7 of culture, iDCs were either left untreated or were stimulated with indicated doses of peptide or LPS (10 ng/ml) (Sigma-Aldrich). For inhibition experiments, immature human DCs were pre-treated with the indicated doses of SB20358, PD98059, *N*-tosyl-L-phenylalanine chloromethyl ketone (TPCK), or DMSO control for 30 minutes prior to stimulation. Supernatants were collected 48 h after stimulation and were analyzed for IL-6 by ELISA (eBioscience), according to the manufacturer's instructions. DC stimulation using the short peptides and the amino-acid substituted peptides was performed in the presence of 200 U $ml^{-1}$ of polymyxin B (Sigma-Aldrich) sufficient to neutralize any endotoxin that could be present in the synthesized peptides. For some experiments, cells were stained to look for phenotypic maturation. After some experiments, DCs were imaged by light microscopy on a Nikon Eclipse TE300 inverted microscope (Nikon Instruments, Melville, NY).

### 4.2.9 Analysis of human DC phenotype

DCs were reacted for at least 20 min at 4°C in 100 ml of PBS/5% FCS/0.1% sodium azide (FACS buffer) with Phycoerythrin-conjugated IgG mAb specific for CD54 (BD Immunocytometry Systems, San Jose, CA) and CD83 (Immunotech-Beckman Coulter, Marseilles, France). Cells were washed four times with FACS buffer, fixed in 3.7% formaldehyde in PBS (pH 7.2–7.4), and examined by flow cytometry using the FACSCalibur (Beckon Dickinson, Franklin Lakes, NJ). Isotype controls were included using irrelevant mAb of the same Ig class conjugated to the same fluorophor. Data were analyzed using the FlowJo software (Tree Star, Inc., Ashland, OR).

### 4.2.10 Peptide binding/uptake studies

Immature DCs were incubated for the indicated times and temperatures in culture medium with biotinylated peptides, biotinylated peptide reaction products or unreacted, mock controls. Cells were washed, permeabilized with Cytofix/Cytoperm, stained with Streptavidin-Alexa 488, and analyzed by flow cytometry using the FACSCalibur (Beckon Dickinson, Franklin Lakes, NJ). Data were analyzed using the FlowJo software (Tree Star, Inc., Ashland, OR).

### 4.2.11 Immunizations

Hp91 tetramer immunization: C57BL/6 mice, approximately 2 months old, were immunized s.c. with 50 μg OVA-I (SIINFEKL) peptide co-administered with PBS, Hp91 (250 μg) (monomer), or matched dose Hp91 tetramer. Mice were boosted after 2 weeks and sacrificed one week post-boost. Single cell suspensions of splenocytes were prepared as previously described in Chapter 2, Materials and Methods. Peptides were dissolved in PBS for all immunizations.

Short peptide immunization: Mice were immunized s.c. with 50 μg of OVA-! (SIINFEKL) peptide co-administered with PBS, Hp91 (250 μg), UC714 (129 μg), or UC1018 (142 μg). Hp91, UC714, and UC1018 peptide doses were equimolar. Mice were boosted two weeks later and spleens and blood were collected one week post-boost. Single cell suspensions of splenocytes were prepared as previously described in Chapter 2, Materials and Methods.

### 4.2.12 Enzyme-linked immunospot assay

IFN-γ ELIspot assay: Freshly isolated splenocytes were cultured overnight with SIINFEKL (OVA-I) peptide in and ELISpot assay as previously described in Chapter 2, Materials and Methods.

Granzyme B ELISpot assay: Splenocytes from naïve syngeneic mice were treated with mitomycin C (Sigma-Aldrich) at 0.5 mg/ml for 60 min at 37°C. Splenocytes from immunized mice were expanded for 5 days at 2 x $10^7$ cells/well, with approximately 1.5 x $10^7$ of the mitomycin C-treated naïve splenocytes, with IL-2 (20 μg $ml^{-1}$) (R&D Systems, Minneapolis, MN), and OVA-1 (SIINFEKL) peptide (10 μg $ml^{-1}$). After 5 days of culture, expanded splenocytes were overlaid onto a Lympholyte M density gradient (Cedarlane Laboratories, Burlington, NC) centrifuged, and the interphase was collected and the cells washed in fresh medium. An Immobilon-P (PVDF) ELISpot plate (Millipore) was coated for 4 hours, without prewetting with ethanol, by diluting the Granzyme B capture antibody (R&D Systems) (1:50) in PBS. After washing the plate with autoclaved water, the plate was blocked with 1% BSA (Sigma-Aldrich) in PBS with 5% sucrose for 2 hours, then washed once with medium. 5 x $10^4$ expanded splenocytes were plated in wells of the ELISpot plate and cultured overnight at 37°C with 2.5 μg $ml^{-1}$ SIINFEKL peptide. ELISpot plates were developed using a 1:50 dilution of Granzyme B detection antibody (R&D Systems) in 1% BSA/PBS, followed by Streptavidin-HRP (Mabtech), and TMB Substrate (Mabtech). The plate was scanned and analyzed as above.

### 4.2.13 Cytokine release assay

Antigen-specific IL-2 cytokine release from freshly isolated splenocytes was measured as previously described in Chapter 2, Materials and Methods.

### 4.2.14 Prophylactic B16 tumor challenge

Mice were immunized s.c. with $2x10^5$ apoptotic mitomycin-C (Sigma-Aldrich)-treated B16 cells co-administered with either PBS or UC1018 (142 μg). Mice were boosted twice, at 4 weeks and 6 weeks post-prime as above, and challenged s.c. into the flank with $2x10^5$ live B16 cells at one week post-boost. Mice were followed for tumor growth and survival. Tumor dimensions were measured using calipers and the tumor volume calculated using the following formula; volume = $4/3\ \pi\ (a^2 \times b)$. Mice were euthanized when tumor volume reached 1.5 $cm^3$. Tumor survival curves were generated, wherein the day of euthanasia was considered as death. Surviving mice were rechallenged with $2x10^5$ live B16 cells at day 75 post-initial challenge.

### 4.2.15 HPLC

Peptides were evaluated by HPLC (Agilent 1100 Series, Software: Chemstation, Agilent, Santa Clara, CA) at 211 nm (column: ZORBAX RP C18, Agilent). Percent dimer was calculated as the area under the curve (AUC) of dimer/(AUC of monomer + AUC of dimer).

### 4.2.16 Circular dichroism

CD spectra of peptides, dissolved in 75%/25% Trifluoroethanol (TFE, Sigma-Aldrich)/$H_20$ (vol/vol), were collected on an AVIV model 202 Circular Dichroism Spectrometer (AVIV Biomedical, Inc., Lakewood, NJ), under nitrogen, using a 1mm pathlength quartz cuvette. These spectra were corrected by subtraction of a "solvent-only" spectrum and smoothed. The spectra are shown in mean residue ellipticity ($\theta_{mrw}$). Peptides were analyzed at 200 μg $ml^{-1}$.

### 4.2.17 Statistical analysis

Data represented are mean ± SEM. Data were analyzed for statistical significance using unpaired or paired Student's *t*-test or the Log Rank test. Statistical analysis was performed using GraphPad software version 5.01 for Windows (GraphPad Software, San Diego, CA, USA). A $p$ value $<0.05$ was considered statistically significant.

## 4.3 Results

### 4.3.1 Hp91 forms spontaneous, reversible dimers

Cysteine residues, with an unprotected sulhydryl group, have a tendency to form disulphide bridges, especially in the presence of oxygen. We hypothesized that the cysteine at position 16 in Hp91 would oxidize under certain conditions to form a peptide dimer with a second Hp91 molecule. Hp91 peptide, dissolved in PBS in the presence of oxygen, was incubated at RT for up to 96 h, and evaluated for the presence of dimers using HPLC. Hp91 dimers, running slower off the HPLC C18 column, were present at approximately 25% of the total peptide within 24 h. Dimers continued to form until measurements were stopped at 96 h, at which point greater than 80% of the peptide was in a dimer formation (Figure 4.1A, B). To determine if this peptide dimer was stable or easily reversible, peptide dimers were allowed to form over 24 hours, and followed with a subsequent reduction in the presence of DTT. After 30 minutes at 10 mM DTT, all Hp91 peptide was found in a monomer state, as demonstrated by the reduction to a single HPLC peak (Figure 4.1C).

As shown in Chapter 3 using confocal microscopy and flow cytomtry, Hp91 binds and is endocytosed by DCs. Here we investigated if reducing or oxidizing the

peptide would result in respective decreases or increases in uptake. DTT was used to reduce peptides, while peroxide ($H_20_2$) was used for oxidation. Theoretically, we could argue reasons for why either the monomer or dimer would preferentially bind DCs, for example: 1) the monomer might bind DCs preferentially because dimerization could alter the structure to lower the affinity for the target protein's binding pocket or 2) the dimer might bind preferentially because dimerization could cross-link a receptor and increase binding affinity.

Compared to untreated peptide controls, uptake of DTT-reduced Hp91 peptide was reduced by approximately 50% (Figure 4.1D). Addition of peroxide alongside the DTT maintained the peptide uptake at levels close to normal, where addition of peroxide to non-reduced peptide enhanced peptide uptake by a small amount. This data suggest that uptake of peptide may be enhanced by dimerization.

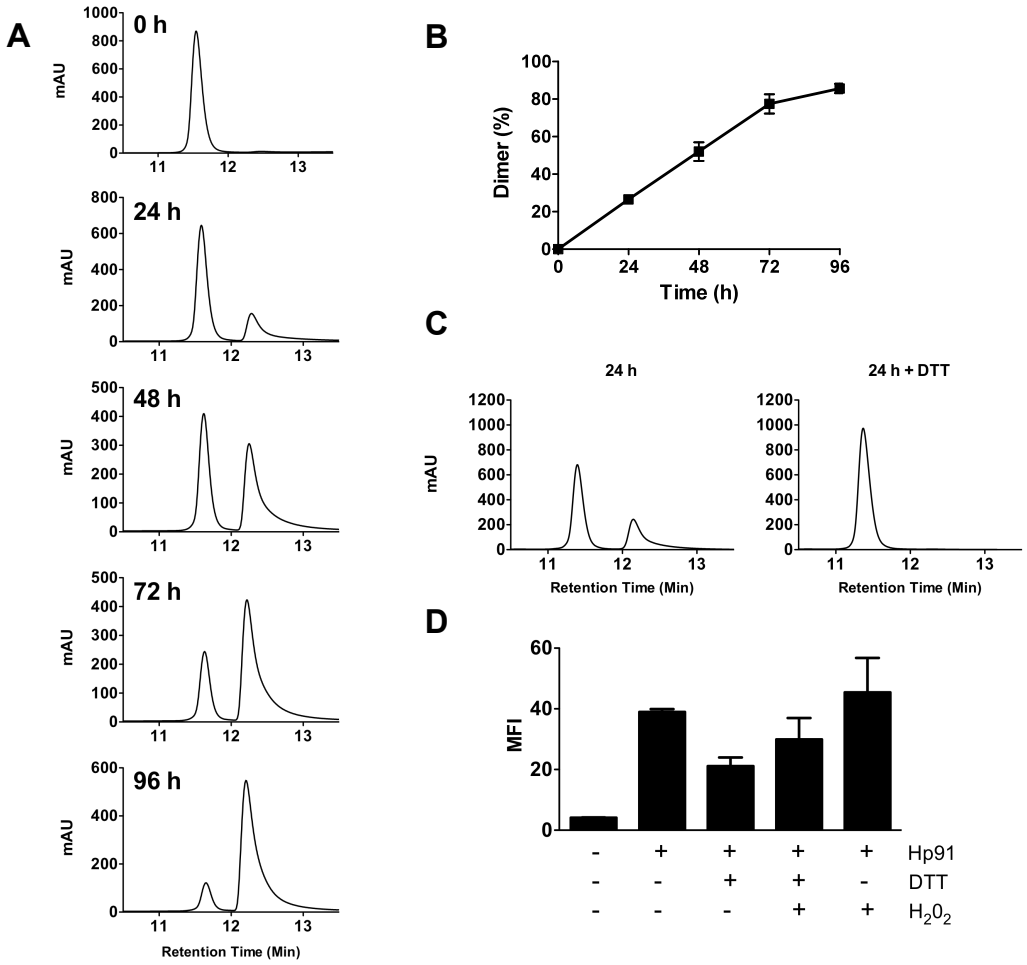


**Figure 4.1.** *Hp91 forms spontaneous, reversible dimers.* (**A-B**) Hp91 peptide was dissolved in PBS and incubated at RT in the presence of oxygen for up to 96 h. Peptides were analyzed by HPLC. Peptide monomers show a peak at an earlier time point than the peptide dimers (12.2 min vs. 12.7 min respectively). Percent dimer was determined by measuring the AUC and calculating the dimer AUC/total AUC. Results shown are (**A**) representative of several independent experiments and (**B**) mean (±SEM) for 3-4 samples. (**C**) Hp91 was allowed to form spontaneous air dimers for 24 h prior to reduction with 10 mM DTT for 30 min. Peptides were analyzed by HPLC. (**D**) Biotinylated Hp91 was incubated for 30 min +/- DTT and/or $H_20_2$. Immature human DCs were incubated with the modified peptides for 30 minutes at 37° C. Cells were permeabilized with Cytofix/Cytoperm, stained with Streptavidin-Alexa 488, and analyzed by flow cytometry. The data shown is mean (±SEM) for 4 independent experiments.

### 4.3.2 Maleimide dimers enhance DC activity

Since the DTT and peroxide appeared to have an affect on the uptake of Hp91, we generated capped peptide monomers and cross-linked peptide dimers

using maleimide conjugation reactions and evaluated the conjugated peptides for DC uptake and activation. Mono- or bis-maleimides contain an imide group that reacts readily with the thiol group of cysteine to form a stable carbon-sulfur bond. We predicted that this stability would enable us to conduct more robust experiments than would be possible with DTT- and peroxide-treated peptides. NEM is a mono-maleimide that generates a capped peptide monomer. $BM(Peg)_2$ is a bis-maleimide that cross-links two peptides to form a dimer.

HPLC of the Hp91 control showed that an estimated 36% of peptide was in a dimer form (Figure 4.2A). HPLC of the maleimide conjugation products showed that the NEM capped monomer forms a single peptide peak, suggestive of close to 100% monomer, where the BM(PEG)2 cross-linked dimer forms two peaks with an estimated 65% dimer (Figure 4.2A). We evaluated the capped monomer for its ability to be taken up by DCs by incubating a biotinylated NEM-capped peptide or control Hp91 peptide with DCs and staining for uptake, as described above. Uptake was evaluated by flow cytometry. The NEM-capped Hp91 monomer decreased Hp91's ability to be taken up by DCs by 27% compared to uncapped controls (Figure 4.2B). To whether the NEM-capped peptide would similarly diminish Hp91's immunostimulatory effects on DCs, we stimulated DC for 48 h with an acetylated NEM-capped Hp91 peptide, as compared to a control. As predicted, the Hp91 monomer exerted a reduced immunostimulatory effect on DC, as determined by a reduction in IL-6 secretion from DCs (Figure 4.2C).

Similar experiments concluded on the bis-maleimide Hp91 dimers show opposite effects. As measured by flow cytometry, the dimer enhanced Hp91 uptake by DCs by 3-fold compared to controls (Figure 4.2D), and enhanced the immunostimulatory effects on DC, as demonstrated by an approximately 10-fold

increase in IL-6 secretion from stimulated DCs compared to controls (Figure 4.2E). These results show that Hp91 dimers enhance uptake and cytokine secretion from DCs.

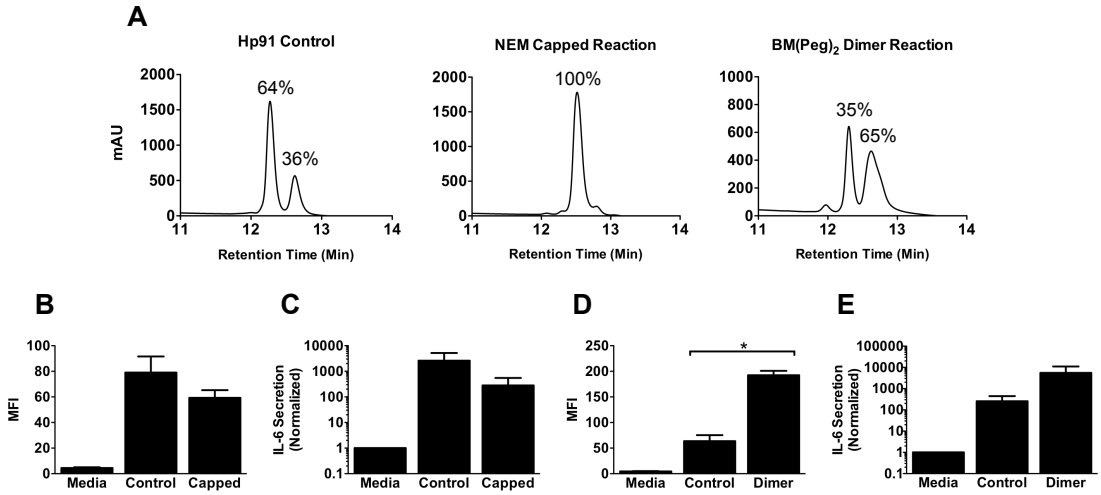


**Figure 4.2.** *HPLC and DC activity of Hp91 maleimide dimers*. (**A**) Hp91 peptide control, NEM capped monomer reaction product, or BM(PEG)$_2$ cross-linked reaction product were analyzed by HPLC. Percent dimer was determined by measuring the AUC and calculating the dimer AUC/total AUC. (**B**) Immature human DCs were pre-cooled on ice for 30 minutes, then incubated with media only, biotinylated-Hp91 ("Control") or the biotinylated Hp91 NEM monomer reaction product ("Capped") (100 mg ml$^{-1}$) for 60 minutes at 37° C. Cells were permeabilized with Cytofix/Cytoperm, stained with Streptavidin-Alexa 488, and analyzed by flow cytometry. Results shown are mean (±SEM) for 3 independent experiments. (**C**) Immature DCs were incubated with media only, un-reacted acetylated Hp91 ("Control"), or an acetylated Hp91 NEM monomer reaction product ("Capped") (100 mg ml$^{-1}$). Supernatants were collected after 48 hours and analyzed for the presence of IL-6 by ELISA. Data are normalized with respect to media controls. Results are mean (±SEM) for 3 independent experiments. (**D**) Immature human DCs were pre-cooled on ice for 30 minutes, then incubated with media only, biotinylated-Hp91 ("Control") or a biotinylated Hp91 BM(PEG)$_2$ cross-linked reaction product ("Dimer") (100 mg ml$^{-1}$) for 60 minutes at 37° C. Cells were permeabilized and stained as above and analyzed by flow cytometry. Results shown are mean (±SEM) for 3 independent experiments. *$p < 0.05$; Student's t-test. (**E**) Immature DCs were incubated with media only, un-reacted acetylated Hp91 ("Control"), or an acetylated Hp91 BM(PEG)$_2$ cross-linked reaction product ("Dimer") (56 mg ml$^{-1}$). Supernatants were collected after 48 hours and analyzed for the presence of IL-6 by ELISA. Data are normalized with respect to media controls. Results are mean (±SEM) for 3 independent experiments.

### 4.3.3 Tetramer enhances Hp91 *in vitro* but not *in vivo* responses

As dimers enhance the immunostimulatory activity of Hp91, we tested if Hp91 tetramers, linked by a core of three lysines at the N-terminal end of the Hp91 peptides (Figure 4.3A), would similarly enhance Hp91 activity. DCs were stimulated for 48 hours with monomeric (free) Hp91 peptide or Hp91 tetramer at a matched concentration. Supernatants were collected and measured for IL-6 secretion. Hp91 tetramer increased IL-6 secretion from DCs by 10- to 21-fold, depending on concentration tested, with an average fold increase of 15 (Figure 4.3B).

Free Hp91 does not normally induce phenotypic changes in DCs, but as there was such an increase in IL-6 secretion using tetrameric Hp91, we tested if DCs also showed an upregulation of CD markers that occurs with DC maturation. DCs stimulated with Hp91 tetramer showed an increase in CD83 surface expression that is equivalent to the increase observed in DCs stimulated with 10 ng/ml LPS (Figure 4.3C). Additionally, when observing DC stimulated with Hp91 tetramer under the microscope, there is an obvious phenotypic change in the tetramer-matured DCs. Immature DCs, as well as most Hp91-stimulated DCs, appear fairly round, with occasional dendrites at the poles of the cell (Figure 4.3D). In contrast, DCs stimulated with Hp91 tetramer take on a characteristic mature appearance, with dendrites waving from all sides of the cell (Figure 4.3E).

In Chapter 3, we demonstrated that Hp91 signals through p38 MAPK and NFκB. Tetrameric Hp91 was shown to signal in a similar manner (Figure 4.3F). DCs that were pretreated with small molecule inhibitors specific to the p38 and NFκB pathways (SB203580 and TPCK respectively), showed significant decreases in IL-6 secretion. The MEK1 inhibitor (PD98059), failed to reduce IL-6 secretion significantly.

As tetrameric Hp91 demonstrated a great enhancement of DC stimulation *in vitro*, we immunized mice with PBS, monomeric Hp91, or tetrameric Hp91, co-injected

with OVA-I peptide to evaluate antigen-specific cellular immune responses of the Hp91 tetramer. *In vivo*, there was no significant advantage to using a tetrameric form of Hp91. OVA-specific cellular immune responses were no better with the Hp91 tetramer compared to monomer, as measured by both IFN-γ and Granzyme B ELISpot (Figure 4.3G, H). IL-2 secretion from OVA-restimulated splenocytes, which is a measure of T cell activation and differentiation, is nearly 40% lower in the tetramer-immunized group (Figure 4.3I). These *in vivo* data were surprising and led us to abandon further *in vivo* immunizations with the Hp91 tetramer.

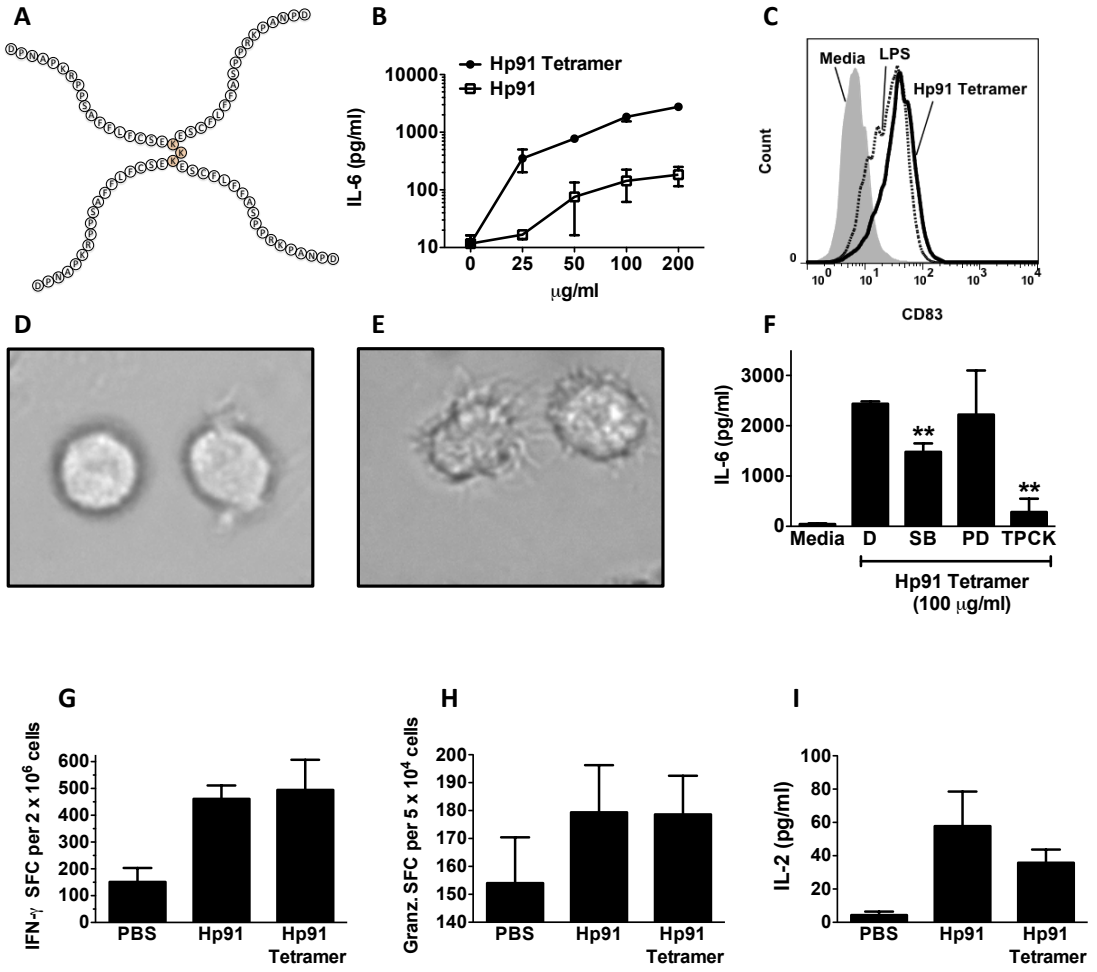


**Figure 4.3.** *Immunostimulatory effects of tetrameric Hp91.* (**A**) Representation of tetrameric Hp91. (**B**) Immature DCs were exposed to increasing concentrations of free Hp91 and matching amounts of Hp91 tetramer. Cell culture supernatants were collected after 48h and analyzed for the presence of IL-6 by ELISA. Data are mean (±SEM) for 3 independent experiments. (**C**) Cells were collected 48h after exposure to media only, LPS (10 ng/ml) or Hp91 tetramer (100 μg/ml) and analyzed for the expression of CD83 by surface membrane immunofluorescence techniques using fluorophor conjugated mAbs. (**D**) Immature human DCs. (**E**) Hp91-tetramer matured DCs. (**F**) Immature DCs were pre-treated with the SB203580 (SB), PD98059 (PD), TPCK, or DMSO control (D) for 30 min prior to exposure to tetrameric Hp91. Cell culture supernatants were collected after 48h and analyzed for the presence of IL-6 by ELISA. Data are mean (±SEM) for 3 independent experiments. **p<0.01 compared to DMSO; Student's t test.

### 4.3.4 Activity of Hp91 resides in C-terminal amino acids

In an effort to identify the region of Hp91 required for DC binding and activation, overlapping 8-12 aa long peptides that span the length of Hp91 were

synthesized and evaluated (Figure 4.4A). These short peptides are named with UC (University of California) followed by the starting and ending aa residues in the Hp91 peptide sequence, e.g. amino acids 10-18 of Hp91 are called UC1018.

Human iDCs were incubated with the indicated short peptides and supernatants were tested after 48 hours for the presence of IL-6. While peptides UC714 and UC718 from the C-terminal half of Hp91induced IL-6 at levels comparable to the full-length peptide, the N-terminal half failed to induce cytokine secretion from DCs (Figure 4.4B). Similar secretion profiles were observed with other chemokines and cytokines, such as AP-10 and IL-8 (data not shown). Using mouse BM-DCs, IL-6 secretion was similarly observed in conditions stimulated with the N-terminal UC714 and UC718 peptides (data not shown). UC1018 peptide was not tested in these preliminary DC activation experiments because of problem with peptide synthesis at the manufacturer's facility.

To test uptake of the short peptides by DCs compared to Hp91, DCs were incubated with biotinylated versions of the short peptides (equivalent molarity) for 30 minutes at 37°C to allow uptake. Cells were fixed, permeabilized, stained with streptavidin-Alexa 488, and evaluated by flow cytometry. The 9 aa acid long peptide UC1018, which corresponds to the C-terminal half of Hp91, enhanced uptake by DCs over 3-fold compared to Hp91 controls (Figure 4.4C, D). In contrast, UC18, UC411, and UC714, containing varying portions of the N-terminal 14 aa of Hp91, failed to be endocytosed by DCs (Figure 4.4C, D).

As measured by cytokine secretion, the C-terminal half of Hp91 peptide had appeared responsible for *in vitro* activity of Hp91, thus we set out to verify if the C-terminal peptides were similarly responsible for *in vivo* activity of Hp91. We have previously shown in Chapter 2 that full-length Hp91 peptide acts as adjuvant *in vivo*

to induce antigen-specific immune responses. We hypothesized that either one or both of the C-terminal short peptides, UC714 and UC1018, would act as adjuvant to induce antigen-specific immune responses *in vivo*. Mice were co-immunized with OVA-I (SIINFEKL) peptide as antigen and equimolar amounts of UC714, UC1018, or Hp91. The C-terminal domain (CTD) UC1018 induced a significant increase in the number of antigen-specific IFNγ-secreting T cells compared to PBS controls as measured by ELISpot (Figure 4.4E). These UC1018-induced immune responses were 4-fold stronger than even our Hp91 positive control. UC714, though showing moderate increases in IFNγ-secreting T cells compared to PBS, showed only 50% of the IFNγ-secreting T cells observed with full-length Hp91 peptide (Figure 4.4E). We further show that IL-2, which is critical for the activation, survival, and proliferation of T lymphocytes, was significantly enhanced in mice immunized with UC1018, at levels 4-fold higher than Hp91 controls (Figure 4.4F).

In cancer treatment, an antigen-specific immune response becomes more meaningful if it translates into a survival advantage. As UC1018 peptide induced a significant antigen-specific immune response *in vivo*, we tested whether UC1018 could act as adjuvant in a prophylactic tumor challenge to induce antitumor immunity. Mice were co-immunized with apoptotic B16 melanoma cells and either PBS or UC1018 peptide. Mice were boosted twice and challenged one week post-boost with live B16 melanoma cells. The melanoma model used in this study is highly lethal, such that within 7-10 days, the PBS control mice demonstrated tumor formation and rapid tumor growth, with the first mouse being sacrificed by day 16 post-challenge due to a substantial tumor burden (Figure 4.4G). In marked contrast to the PBS group, the UC1018 peptide immunized mice demonstrated a delay in tumor formation and slowing of tumor growth, significant as early as 11 days post

challenge (Figure 4.4G), indicating an induction of significant protective antitumor immunity in the UC1018 immunized mice. The mice were monitored for survival, and mice that received the UC1018 prophylactic treatment demonstrated a striking and significant enhancement of survival, with 60% of mice tumor-free and alive at 75 days post-tumor challenge (Figure 4.4H). In contrast, all mice in the control group developed tumor with 100% of mice succumbing to tumor burden by 49 days post-challenge (Figure 4.4H).

At 75 days post-tumor challenge, the surviving mice were re-challenged with B16 to evaluate if long-term immunological memory was obtained. Mice immunized with UC1018 peptide developed tumor and subsequently were euthanized due to tumor burden at levels comparable to the survival of the PBS group at original challenge (Figure 4.4I).

**Figure 4.4.** *Immunostimulatory activity of Hp91 short peptides.* (**A**) Full length Hp91 (18 aa) is broken into 5 smaller, truncated peptides (8-12 aa). (**B**) Immature DCs were stimulated with the indicated peptides for 48 hours. Supernatants were analyzed for the presence of IL-6 by ELISA. Data are mean (±SEM) for 3 independent experiments. (**C, D**) Immature DCs were pre-cooled on ice for 30 minutes, then incubated with medium only, Hp91, or truncated Hp91 short peptides (90 μM) for 30 minutes at 37° C. Cells were permeabilized with Cytofix/Cytoperm, stained with Streptavidin-Alexa 488, and analyzed by flow cytometry. (**C**) is mean (±SEM) of 4 independent experiments and (**D**) is a representative result. (**E-F**) Mice were immunized with OVA-I (SIINFEKL) peptide in PBS with PBS (negative), UC714, UC1018, or Hp91. Freshly isolated splenocytes from the immunized mice were cultured in the presence of SIINFEKL peptide (2.5 μg ml−1) in an (**E**) IFN-γ ELISpot assay, wherein the number of IFN-γ-secreting cells was determined 18 h later, or (**F**) culture supernatants were collected and analyzed for IL-2 secretion by ELISA. The data shown is mean (±SEM) for at least 5 mice/group. *$p < 0.05$ compared to PBS; Student's t-test. (**G-I**) Mice were immunized s.c. with apoptotic mitomycin-C treated B16 cells co-injected with PBS (negative) or UC1018 peptide (142 μg) and boosted twice. One week post boost, mice were inoculated s.c. on the flank with $5x10^5$ live B16 cells. (**G**) Tumor dimensions were measured using calipers and the tumor volume calculated using the following formula; volume = $4/3\ \pi\ (a^2 \times b)$. The data shown is mean (±SEM) for at least 14 mice/group. *$p < 0.01$ compared to PBS; Student's t-test at each time point. (**H**) Mice were euthanized when tumor volume reached 1.5 $cm^3$. Tumor survival curves were generated, wherein the day of euthanasia was considered as death. ***$p < 0.001$ compared to PBS; Log rank test. (**I**) Surviving mice in the UC1018 group were re-challenged with $5x10^5$ live B16 cells and monitored for tumor growth. Mice were euthanized as above. The PBS curve represents the death of the PBS group from the original challenge as no mice remained alive for re-challenge.

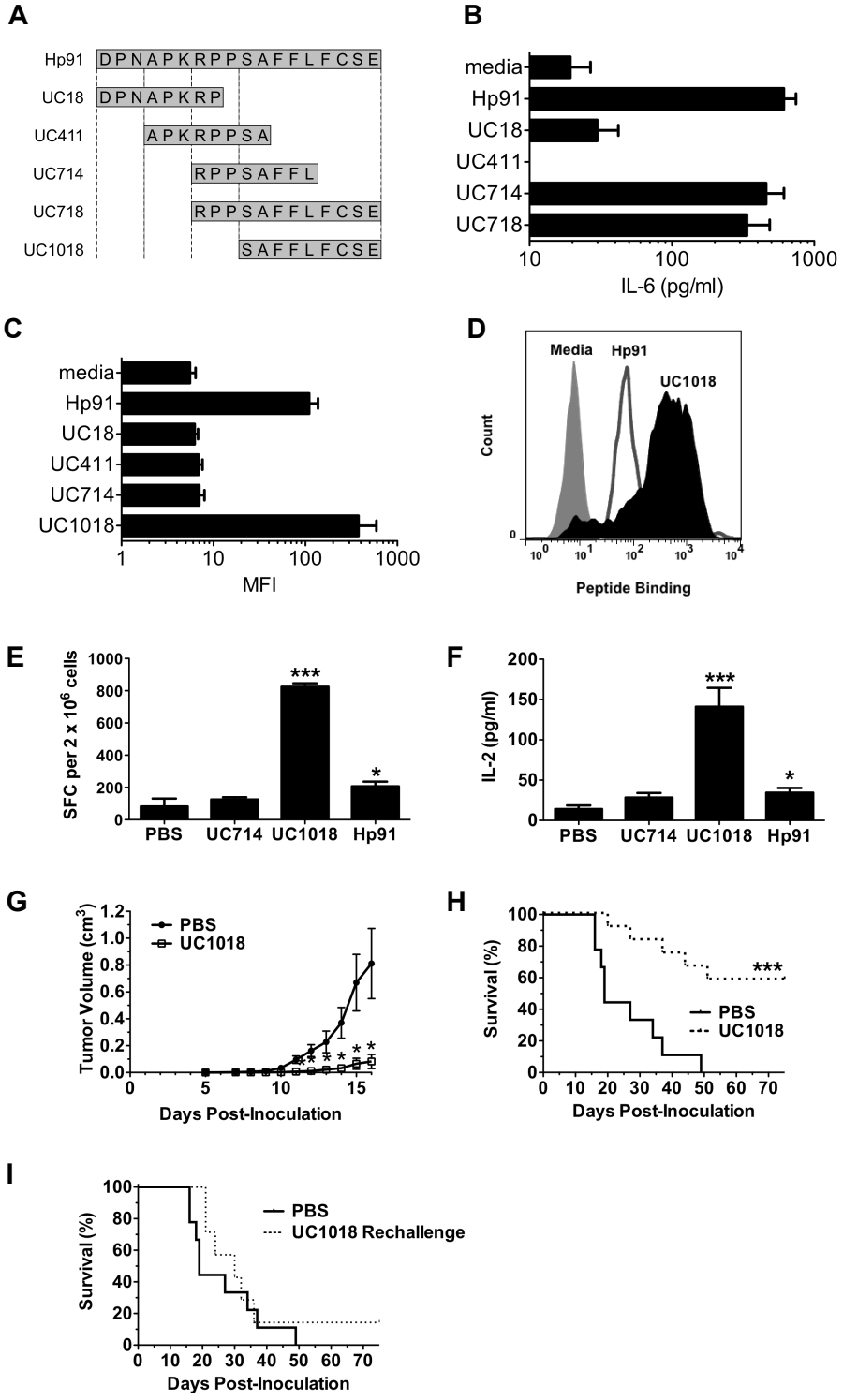
A
Hp91 DPNAPKRPPSAFFLFCSE
UC18 DPNAPKRP
UC411 APKRPPSA
UC714 RPPSAFFL
UC718 RPPSAFFLFCSE
UC1018 SAFFLFCSE
B
media
Hp91
UC18
UC411
UC714
UC718
10
100
1000
IL-6 (pg/ml)
C
media
Hp91
UC18
UC411
UC714
UC1018
1
10
100
1000
MFI
D
Media
Hp91
UC1018
Count
0
Peptide Binding
E
SFC per 2 x 10^6 cells
1000
800
600
400
200
0
***
*
PBS
UC714
UC1018
Hp91
F
IL-2 (pg/ml)
200
150
100
50
0
***
*
PBS
UC714
UC1018
Hp91
G
Tumor Volume (cm^3)
1.2
1.0
0.8
0.6
0.4
0.2
0.0
PBS
UC1018
0
5
10
15
Days Post-Inoculation
H
Survival (%)
100
80
60
40
20
0
***
PBS
UC1018
0 10 20 30 40 50 60 70
Days Post-Inoculation
I
Survival (%)
100
80
60
40
20
0
PBS
UC1018 Rechallenge
0 10 20 30 40 50 60 70
Days Post-Inoculation

### 4.3.5 C-terminal portion of Hp91 is helical

As the CTD of Hp91, UC1018, is important for DC uptake and for exerting the immunostimulatory effects of Hp91, we set out to evaluate the secondary structure of this peptide. Studies of HMGB1 protein suggested that the secondary structure at the UC1018 position within HMGB1 would contain an alpha helix (116). Circular dichroism (CD) measures the difference in absorbance of right- and left-circularly polarized light. The phenomenon of CD is sensitive to the secondary structure of polypeptides and can be used between wavelengths of 190-250 nm to analyze a peptide for different structural types such as alpha helix, beta sheet, polyproline II helix, random coil, and more.

To perform the CD experiment, we dissolved peptides in a trifluoroethanol (TFE) buffer (75%/25% TFE/$H_20$ by volume), which enhances polypeptide folding (123). The CD spectrum of the CTD UC1018 showed negative ellipticity bands at 207 and 222 nm, with a positive ellipticity at 198 nm (Figure 4.5). Such a spectra is characteristic of an alpha helix, matching our prediction for the sequence. The CD spectrum for the NTD UC18 showed a negative maximum at 202 nm (Figure 4.5), which is close to the negative peak expected at 200 nm for a prolyproline II helix. A spectra with a negative peak around 200 nm is relatively ambiguous however, as random coils also display similar spectra. With some uncertainty, we conclude that the N-terminal domain (NTD) UC18 is a polyproline II helix, rather than random coil. This conclusion is made because the NTD contains two PXXP motifs, which are known to form polyproline II helices (120). The CD spectrum for the entire length of Hp91 remains more difficult to interpret. The negative peak near 205 for Hp91 (Figure 4.5) may be an additive effect of the NTD and CTD spectra negative maximums.

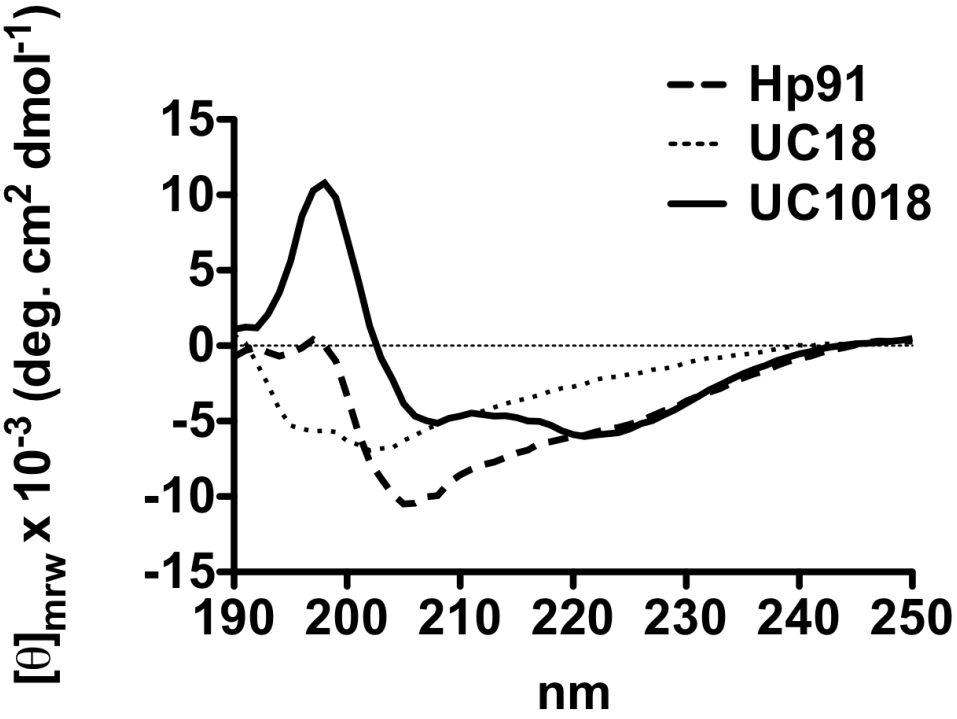


**Figure 4.5.** *Circular dichoism suggests alpha helical shape of UC1018.* Hp91, UC18, and UC1018 were dissolved in 75%/25% TFE/$H_20$ (vol/vol) at 200 μg $ml^{-1}$ and CD spectra were collected on an AVIV Circular Dichroism Spectrometer using a 1mm pathlength quartz cuvette. These spectra were corrected by subtraction of a "solvent-only" spectrum and smoothed. The spectra are shown in mean residue ellipticity ($\theta_{mrw}$). The Hp91 curve is representative of two independent experiments.

### 4.3.6 CSE motif is important for peptide uptake by DCs

UC714 and UC1018 short peptides are overlapping peptides that differ by 3-4 aa on each end. As UC1018, but not UC714, is taken up by DCs, we hypothesized that the 4 aa sequence, FCSE, was important for uptake. Upon further investigation of the sequence of UC1018, Hp91, and the HMGB1 protein, we observed that the 3 aa sequence, CSE, is also present at positions 45-47 in HMGB1 protein as well as in the previously analyzed Hp31 and Hp106 HMGB1-derived peptides (Table 4.1). Surprisingly, Hp31 and Hp106 also had immunostimulatory activity and matured DCs, as demonstrated by ELISpot and cytokine secretion (52). We hypothesized that these CSE-containing peptides might also be taken up by DCs. Hp46, which did not have a

CSE peptide, was added as an additional negative control. As hypothesized, Hp31 and Hp106 bind or were taken up by DCs, though not to the same extent as Hp91 (Figure 4.6A, B). Confocal data has not yet been performed to verify that the peptides are inside the DCs.

**Table 4.1.** A sampling of HMGB1-derived peptides ± CSE motifs.

| **Name** | **Sequence** | **Immunostimulatory Activity (52)** | **CSE motif** |
|---|---|---|---|
| Hp31 | HPDASVNFSEFSKK**CSE**R | Yes | Yes |
| Hp46 | SERWKTMSAKEKGKFEDM | No | No |
| Hp91 | DPNAPKRPPSAFFLF**CSE** | Yes | Yes |
| Hp106 | **CSE**YRPKIKGEHPGLSIG | Yes | Yes |
| Hp121 | SIGDVAKKLGEMWNNTAA | No | No |

For the next step, we tested if a short CSE tripeptide would also bind or be taken up by dendritic cells. We demonstrate the CSE peptide binds DCs in a dose response, though 3-fold as much CSE peptide only yields approximately 40% of the MFI (Figure 4.6C). We then evaluated if the CSE motif was sufficient for stimulating cytokine secretion from DCs. Preliminary experiments show that DCs require 3-fold more CSE peptide than full-length Hp91 peptide (molarity matched) to get an equivalent amount of IL-6 secretion (Figure 4.6D). It is not yet clear if similarly high concentrations of other tripeptides would also stimulate cytokine release from DCs. Additional studies are warranted.

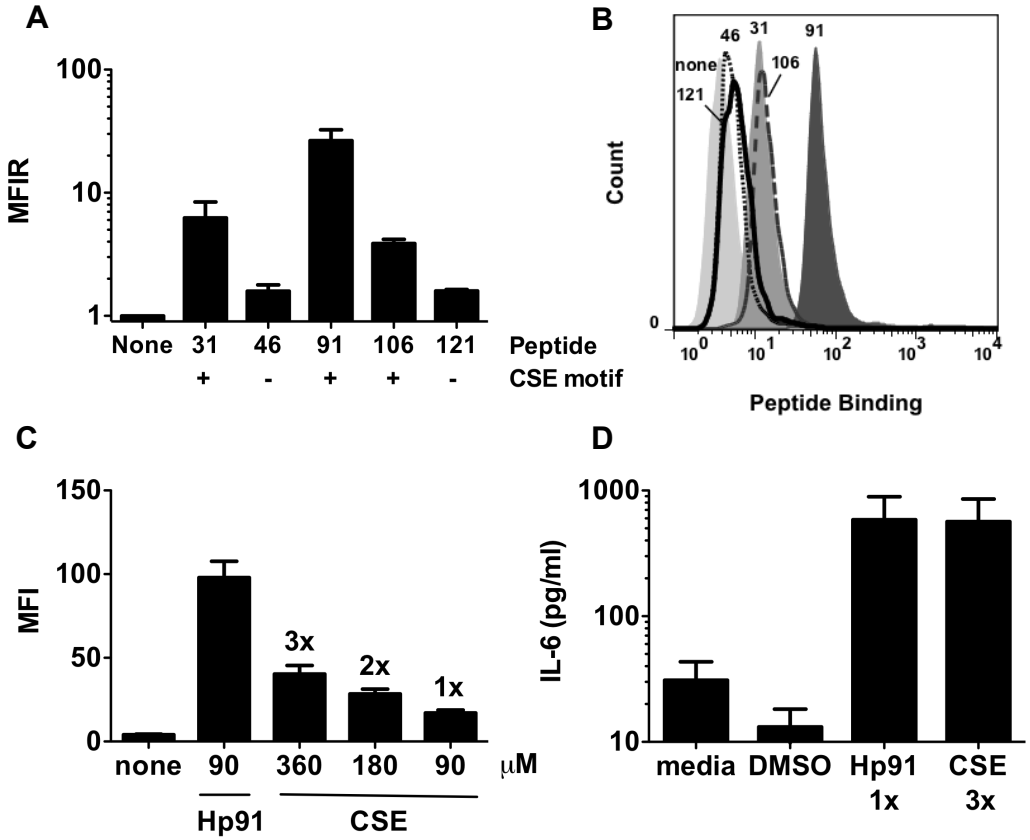


**Figure 4.6.** *DC binding and activation with CSE-containing peptides.* (**A-B**) Immature DCs were precooled on ice for 30 minutes, then incubated with medium only (none) or the indicated "Hp" peptides (90 μM) for 30 minutes at 37° C. Cells were permeabilized with Cytofix/Cytoperm, stained with Streptavidin-Alexa 488, and analyzed by flow cytometry. (**A**) is mean (±SEM) of 3 independent experiments and (**B**) is a representative result. (**C**) Immature DCs were precooled on ice for 30 minutes, then incubated with medium only (none), Hp91, or CSE at the indicated doses for 30 minutes at 37° C. Cells were permeabilized, stained, and analyzed as above. Data is mean (±SEM) of 3 independent experiments. (**D**) Peptides were dissolved in 10% DMSO/RPMI (vol/vol). Immature DCs were stimulated with media, DMSO control, or the indicated peptides for 48 hours. Supernatants were analyzed for the presence of IL-6 by ELISA. Data are mean (±SEM) for 3 independent experiments.

### 4.3.7 C-terminal alanine-substitutions enhance DC stimulatory capacity

We performed amino acid substitutions in an attempt to find critical amino acids that when mutated would kill the immunostimulatory activity of UC1018. Instead we demonstrate several surprising mutations that appear to enhance UC1018's immunostimulatory activity. Alanine-substitution was performed at each residue of

the UC1018 peptide sequence. Four mutations at the most C-terminal end of UC1018 (UC1018-6A through -9A) appeared to enhance IL-6 secretion from DCs (Figure 4.7).

One might hypothesize that these C-terminal mutations enhance IL-6 secretion by increasing hydrophobicity, which Matzinger theorizes interact with receptors such as TLR2 and TLR4 (113). If this was the case, our serine-substitutions which reduce overall hydrophobicity by removing hydrophobic phenylalanines, would show decreased IL-6 secretion. There is a very small decrease in IL-6 secretion for the serine mutations (UC1018-SS and UC1018-SSS) (Figure 4.7), but not likely not enough that would make us conclude the IL-6 secretion is due to hydrophobicity. To confirm that the enhanced IL-6 secretion seen in the mutated C-terminal peptides was real and not due to error in weighing peptides for solubilization, we weighed and solubilized the peptide panel three independent times. In each peptide set, IL-6 was highest for the C-terminally mutated peptides (data not shown). More work is warranted with these mutated peptides.

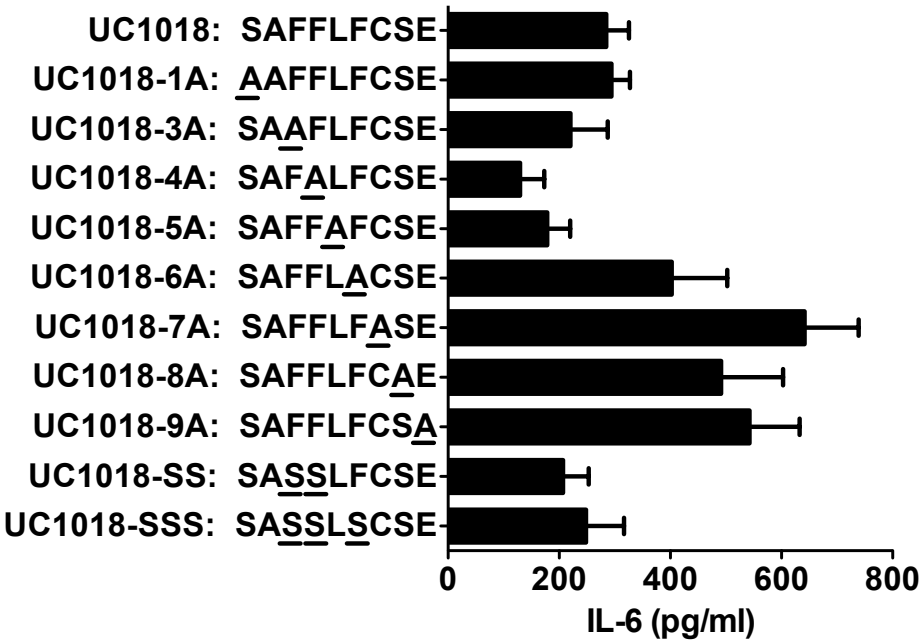


**Figure 4.7.** *C-terminal alanine-substitution enhances DC stimulatory capacity.* Immature DCs were stimulated with the indicated peptides (90 μM) in the presence of polymyxin B for 48 hours. Supernatants were analyzed for the presence of IL-6 by ELISA. Data are mean (±SEM) for 4 independent experiments.

## 4.4 Discussion

There is a great need for safer and more potent adjuvants (69, 70). D. Messmer and colleagues have previously shown that the 18 amino acid long immunostimulatory peptide (ISP) Hp91 is a potent stimulus for human DCs with the ability to generate a Th1-type immune response *in vitro* (52). We demonstrated in Chapter 1 that Hp91 acts as adjuvant *in vivo;* inducing cellular immune responses to peptide and both cellular and humoral immune responses to protein antigen (91). The results presented here characterize the structural basis for Hp91 activity, identifying a new ISP, UC1018, that acts as adjuvant *in vivo* and demonstrating that Hp91 dimerization enhances activity.

We set out to investigate what structures and amino acid domains were responsible for the activity of the Hp91 immunostimulatory peptide and adjuvant. After determining that Hp91 formed spontaneous dimers in the presence of air, we tested whether these dimers would affect Hp91's activity. While we hypothesized that Hp91 dimerization at the cysteine might prevent proper binding and uptake into dendritic cells, somewhat surprisingly we discovered that dimers actually enhanced peptide uptake.

We showed in Chapter 3 that activity of Hp91 is dependent on TLR4 for cytokine secretion from DCs. Toll-like receptors, such as TLR4, form homo- or hetero-dimers with other members of their protein family (124). Such TLR4 homodimers are thought to be necessary for recruitment of adaptor proteins and subsequent signaling. For example, the Mal and TRAM adaptor proteins are predicted to bind at the TLR4 homodimer interface (125). It is possible that dimerization of Hp91 peptide promotes TLR4 cross-linking, adaptor recruitment, and downstream signaling leading to activation of NF-κB and IRF3. While the cross-linking of the TLR4 receptor was not tested in this work, this may be investigated in the future, as the results might be useful for the engineering of future synthetic adjuvants. Additionally, preliminary experiments suggest that air dimerization of Hp91 peptide enhances phosphorylation of IRF3 (immunoblots not shown).

It is somewhat surprising to us that the dimers would enhance Hp91 activity. Hp91 is a short peptide, only 18 aa long. We could imagine it binding to a groove in a single protein or receptor. It is hard to picture that a small peptide, even in dimer form, would be large enough to simultaneously bind both subunits of the TLR4 homodimer.

In Chapter 3, we showed that the scrambled version of Hp91 is not taken up by DCs, suggesting that it is neither the total charge nor hydrophobicity of the

peptide that is important for Hp91 activity. Rather, it is a particular sequence of amino acids that leads to the immunostimulatory activity and binding of peptide to cells. In this chapter we determine the region of the peptide responsible for activity by testing shorter, overlapping peptides for their binding. Hp91 contains two PXXP motifs at the N-terminal half, present in short peptides UC18 and UC411, that we originally hypothesized may be responsible for the cell permeability and perhaps activity as cell permeable peptides often contain proline-rich regions (111, 126). To our surprise, it was the C-terminal end, not the N-terminal end of the peptide with activity. We demonstrate here that the C-terminal domain of Hp91 induces cytokine release from DCs (UC718 peptide) and binds or is taken up by dendritic cells (UC1018). In addition, we show that the CTD, UC1018, is sufficient to act as adjuvant *in vivo*, inducing cellular, antigen-specific immune responses. Somewhat surprisingly, we demonstrate that UC1018, despite being only half the length of Hp91, is taken up by DCs to a greater extent and is a 3-fold stronger adjuvant *in vivo*, as measured by IFN -γ ELISpot and IL-2 cytokine release.

UC1018 is a unique peptide, with an extremely hydrophobic N-terminal half, and a C-terminal CSE motif. Hydrophobicity has been shown to enhance cell penetrating properties of peptides (111) and based on this, one might predict that it is this hydrophobic region of UC1018 that is responsible for uptake by DCs. As this hydrophobic patch is also present in the UC714 peptide however, which has no ability to bind DCs, we hypothesized that it must be the CSE motif that is the critical sequence for DC binding and uptake. We confirmed that by showing the strong uptake of UC1018 peptide. Interestingly, the cysteine residue in this CSE motif is the same cysteine that has previously been hypothesized to be critical for TLR4 interaction (97).

It was at this point in our experimenting that we realized, to our surprise, that the Hp31 and Hp106 HMGB1-derived peptides also contain this CSE motif. Thus we tested if Hp31 and Hp106 also were taken up by DCs. We discovered that flow cytometry indicated these CSE-containing peptides are binding, and presumably being taken up by DCs. At some point in the future, confocal microscopy should be used to confirm that these CSE-containing peptides are inside the cells.

Up to this point, all peptides tested were at least 8 aa long. Next, we evaluated the short tripeptide, CSE, for binding and cytokine secretion from DCs. These results show minimal DC binding and IL-6 secretion, at levels approximately 3 times lower than for full-length Hp91. Thus, while the CSE motif appears necessary for DC binding, and perhaps *in vivo* adjuvant activity, the motif is not sufficient to act alone. Additional amino acids appear necessary, and we hypothesize that the next sequence of amino acids to test for potent immunostimulatory activity may be FCSE, LFCSE, FLFCSE, etc.

We show here that the structure of UC1018 peptide takes the form of an alpha helix. Perhaps this alpha helix plays a role in the adjuvanticity potential of peptides and could be designed into new synthetic adjuvants. Also, while the hydrophobic patch of UC1018 peptide did not appear to be responsible for uptake, it was also present in UC714 peptide, which had the ability to induce cytokine secretion from DCs. Hydrophobic peptides have been shown to act as danger signals to the immune system (113). Perhaps introducing hydrophobic regions into synthetically designed adjuvants may enhance their activity, especially with regard to cytokine secretion. The increased cytokine secretion seen with the hydrophobic alanine-substitutions does suggest that increasing the hydrophobicity enhances immunostimulatory activity.

We have spent most of our research and discussion on the C-terminal domains, as that is where we observed experimental activity. The N-terminal half of Hp91 appeared to have no activity, however we only performed uptake studies and looked at cytokine secretion from DCs. This region, which contains two PXXP motifs, may have as yet unidentified activities that are important for HMGB1 or Hp91 activity. This region may be responsible for intracellular activities that occur after Hp91 has entered a cell. The polyproline II helix conformation of PXXP motifs, such as those in the CTD, is necessary for binding to Src homology-3 (SH3) domains (120).

These SH3 domains play critical roles in a wide variety of biological processes ranging from regulation of enzymes by intramolecular interactions, increasing the local concentration or altering the subcellular localization of components of signaling pathways, and mediating the assembly of large multiprotein complexes (127). Interestingly, several previously identified PXXP motifs bind proteins that are responsible for cellular budding or endocytosis. The PKRPP motif of synaptojanin protein, also present in HMGB1 and Hp91, has been shown to bind the SH3-containing endophilin-2, which is involved in inward budding of the cell membrane (128). A mutated P**N**AP motif of HIV's GAG protein, also present in HMGB1 and Hp91, as well as the naturally occurring P**T**AP motif of GAG, bind the human Tsg101 protein, which is responsible for viral budding (129, 130). One could hypothesize that these PXXP motifs in Hp91 and HMGB1 are important for cellular endocytosis or budding. Interestingly, and directly upon this line of research, we present data in Chapter 7 that suggests Hp91 does promote endocytosis of foreign cargo, in this case microbeads, into HeLa cells. The significance of the PXXP motifs in HMGB1 and possible binding to SH3 domains has not been previously studied and may be an interesting and open area for future research related to Hp91 and HMGB1.

In summary, in this chapter we have investigated the activity of Hp91 immunostimulatory peptide, whose structure-function relationships had not been clear before now. We show that Hp91 dimerization enhances activity and that the CSE-containing, helical C-terminus, UC1018, has DC binding and adjuvant activity that is stronger than full-length Hp91. We demonstrated exciting tumor challenge results in which 60% of UC1018-immunized mice remained tumor-free after a highly lethal B16 challenge. These surviving mice did succumb to tumor burden at the re-challenge, but we hypothesize that additional boosts would strengthen immunological memory.

In addition, in this discussion, we put forward ideas about new peptide sequences to evaluate for potent immunostimulatory activity We hypothesize about a possible role for the PXXP-containing N-terminal region of Hp91, related to SH3 binding and possible cellular budding. This research improves our understanding of Hp91 peptide, may help us further enhance its adjuvant activity in subunit vaccines, and may assist us in the engineering of new adjuvants.

In conclusion, in this chapter we performed structure-function relationship studies on Hp91 peptide to investigate the amino acids and structure responsible for immune responses. We examined oxidation of the cysteine amino acid at position 16 of Hp91 and found that Hp91 spontaneously forms reversible dimers. Using maleimide cross-linked dimers dimers, we showed that the Hp91 dimer, compared to monomer controls, has an enhanced ability to activate DCs and an increased ability to bind DCs. We demonstrate that the C-terminal 9 amino acids of Hp91, named UC1018, are sufficient for DC binding, induction of CTL responses and significant prophylactic antitumor protection *in vivo*. 60% of UC1018 immunized mice remained tumor-free after 75 days.

Chapter 4, in part, is currently being prepared into a manuscript for future submission for publication. Rebecca Saenz, Diahnn Futalan, Brad Messmer, Yitzhak Tor, Sadik Esener and Davorka Messmer. The dissertation author is the primary investigator and author of the manuscript.

# 5. Nanoparticles Enhance DC Stimulatory Capacity and Adjuvant Potential of HMGB1-Derived Peptides

Nanoparticles (NPs) are attractive carriers for vaccines. We have previously shown that a short peptide (Hp91) activates dendritic cells (DCs), which are critical for initiation of immune responses. In an effort to develop Hp91 as a vaccine adjuvant with NP carriers, we evaluated its activity when encapsulated in or conjugated to the surface of 3 types of NPs: **1**) liposomal NPs (liposomes), **2**) poly(D,L-lactic-co-glycolic) acid (PLGA) NPs, and **3**) PLGA- Lecithin- 1,2-distearoyl- *sn*-glycero-3- phosphoethanolamine- N- [carboxy (polyethylene glycol)- 2000] (DSPE-PEG-Carboxy) ("Lipid-polymer hybrid") NPs. We found that Hp91, when encapsulated in or conjugated to the surface of NPs, not only maintained its ability to activate both human and mouse DCs, but was in fact more potent than free Hp91. Hp91 packaged within NPs was about 4-5 fold more potent than the free peptide, and Hp91 conjugated to the surface of NPs was ~20-fold more potent than free Hp91. Delivering Hp91 *in vivo* within lipid-polymer hybrid NPs enhanced the adjuvant activity of Hp91. IFN-γ cellular immune responses were stronger when Hp91 was delivered in NPs, and mice receiving prophylactic immunization with Hp91-nanoparticle-based vaccines showed delayed tumor growth and prolonged survival. Because of their capacity to enhance activation of DCs and act as adjuvant, such

Hp91-NP systems are promising as delivery vehicles for subunit vaccines against cancer.

## 5.1 Introduction

Nanoparticles (NPs) are being evaluated as carriers for vaccine antigens. Vaccination remains the most successful prophylaxis for infectious disease and in the past decades it has also been explored as an approach to prevent or cure cancer (6, 131). Since peptides tend to be unstable *in vivo*, NPs can protect them from degradation and potentially increase the immune response to peptide and possibly protein vaccines. Encapsulation of antigen peptides into biodegradable spheres has been shown to increase MHC-class-I presentation (66). Delivery of OVA protein as antigen in Poly-g-Glutamic acid nanoparticles (gPGA-NPs) lead to increased immune responses in comparison to vaccinations using the same amount of free OVA protein (67). Additionally, enhanced immune responses were observed when the cancer associated antigen MUC-1 (132, 133) as well as Tetanus Toxoid (134) was delivered using Poly-lactic-glycolic acid nanoparticles (PLGA-NPs).

Dendritic cells (DCs) are the most potent antigen-presenting cells and central for the initiation of adaptive immune responses (92). DCs need to receive a maturation signal in order to present antigen, upregulate co-stimulatory and adhesion molecules, and become potent activators of T cells. Antigen-displaying mature DCs can then activate T cells to act as CTLs. We have previously identified several immunostimulatory peptides (ISPs), derived from the endogenous protein HMGB1, that can activate both mouse and human DCs. We have shown that the 18 aa long ISP named Hp91, when used to activate DCs, can induce potent antigen-

specific CTL responses (104). Due to their immuno-activating properties, ISPs are attractive candidates for vaccine adjuvants. In an effort to develop ISPs for vaccine adjuvant usage we evaluated whether Hp91 could be incorporated into nanoparticles and still maintain its activity. PLGA was chosen as a core material for our NPs, since it is a biodegradable and biocompatible polymer (135-138) that has been employed for numerous *in vivo* applications (139-141). In addition, polymeric NPs are more stable on the gastrointestinal tract as compared to other carriers like liposomes and can be used for oral vaccine development (142). Different composition polymers allow for controlled and prolonged release of cargo, allowing for antigen depot formation at the injection site, again another major advantage for vaccine development.

The third type of nanoparticles we use are nicknamed "lipid-polymer hybrid" NPs. These particles are made by a stable nanoprecipitation synthesis process wherein the lipids self assemble around the polymer core. PLGA forms the core, which is surrounded with phospholipids common to cell membranes as well as DSPE, which is a synthetic phosphatidylethanolamine (PE) derivate that helps stabilize the particles.

## 5.2 Materials and Methods

### 5.2.1 Reagents

Peptides, including Hp91 (DPNAPKRPPSAFFLFCSE), Hp121 (SIGDVAKKLGEMWNNTAA), OVA-1 (SIINFEKL), UC1018 (SAFFLFCSE), and mouse HER2 (PDSLRDLSVF), were synthesized by Genscript Corporation (Piscatway, NJ). For some experiments, peptides had an N-terminal biotin. When used *in vitro* as free peptide,

the peptides were dissolved at 2 mg/ml in 5% DMSO/RPMI. Poly(lactic-co-glycolic acid) (PLGA, 50:50) was purchased from Birmingham Polymers (Birmingham, AL) or Lactel Absorbable Polymers (Pelham, AL). Lecithin (avg. MW – 330) was purchased from Alfa Aesar (Ward Hill, MA). 1,2-distearoyl- sn- glycero- 3- phosphoethanolamine-N-[carboxy (polyethylene glycol)-2000] (DSPE-PEG carboxylic acid), 1,2-dioleoyl-sn-glycero-3-phosphoethanolamine (DOPE), 1,2-dioleoyl-sn-glycero-3-phospho-choline (DOPC), Cholesterol, and DOPE-PEG were purchased from Avanti Polar Lipids (Alabaster, AL). Denacol EX-521 was courtesy of Nagase America (New York NY). Bovine serum albumin (BSA-Fraction V), zinc tetrafluoroborate hydrate, acetonitrile and DMF were purchased from Fisher Scientific (Pittsburg, PA). Polyvinyl alcohol was purchased from Sigma-Aldrich. Chloroform was purchased from EMD Chemicals (San Diego, CA) or Sigma-Aldrich.

### 5.2.2 Liposome Synthesis

Hp91 peptide was diluted in methanol to 10 mM (30 μl volume per ml liposomes). Adding extra peptide interfered with spontaneous reassembly of liposomes, therefore peptide concentration was limited to 30 μl at 10 mM. To make 1 ml of liposomes, the following solutions were given a quick vortex and were added to a small glass vial: a) 200 μl DOPE (10 mM in chloroform), b) 200 μl DOPC (10 mM in chloroform), c) 200 μl Cholesterol (10 mM in chloroform), d) 30 μl DOPE-PEG (8.9 mM in chloroform) e) 30 μl Peptide (10 mM) Contents were mixed together and rotavaporated at 40°C for 15 minutes at low vacuum to dry the lipids. Alternatively, contents could be dried into a lipid film using an argon stream. 1ml of endotoxin-free water (Hyclone) was added to the vial to hydrate the lipid film, and vortexed for 1 min to remove any adhering dry lipid film. Contents were then bath sonicated for 2-3

minutes to produce multilamellar vesicles (MLVs), then sonicated with a PMB-cleaned probe sonicator for 1 minute (25w as output power) to produce small unilamellar vesicles (SUVs). In some experiments, lipids were allowed to sit in biosafety cabinet (BSC) overnight to "swell." An extruder (Avanti) was cleaned with ethanol, then endotoxin-free water for use in the next step. To reduce the size of the SUVs, step-wise filtration was performed with the final step being extrusion through a Nucleopore Track-Etch polycarbonate filter with 100 nm pore size (Whatman, GE Healthcare). A Sephadex G75 (GE Life Sciences, GE Healthcare) column was prepared by swelling Sephadex with sterile, endotoxin-free water (15 mL per g), packing swelled-Sephadex over fiberglass in the bottom of a syringe and washing the column 10x with endotoxin-free water. The extruded liposome solution was loaded onto the Sephadex column and centrifuged at 50 x g for 10 min, then 1000 x g for 3 min. Eluent was transferred to a syringe and filtered over 0.2 μm filter. Liposomes were aliquoted into glass vials and stored at 4°C. To prepare empty liposomes, peptide was omitted from the synthesis protocol. The size distribution of liposomes was measured by Zetasizer Nano ZS (Malvern Instruments). Early batches of liposomes assumed 45 μM concentration of incorporated peptide. Later experiments used liposomes, quantified by HPLC after dissolving in >1% Triton X-100 (RICCA Chemical Co., Arlington TX).

### 5.2.3 Synthesis of Hp91-Encapsulated PLGA Nanoparticles

Poly(lactic-*co*-glycolic acid)) nanoparticles (PLGA-NPs) that encapsulated the immunostimulatory peptide Hp91 peptide were synthesized. The particles were made using the water-in-oil-in-water (w-o-w) double emulsion method. The PLGA co-polymer (polymer ratio 50:50) was dissolved at 25 mg $mL^{-1}$ in chloroform and vortexed for 1h. To make a 30 mg batch of PLGA-NP loaded with Hp91, Hp91 was dissolved in

DMSO at 20 mg $mL^{-1}$ and 30 μl was added to 270 μl of an aqueous BSA solution (10 mg $mL^{-1}$). As a control, 300 μl BSA solution was used to make empty NPs. The Hp91/BSA solution was added to the PLGA dissolved in chloroform, and then vortexed and sonicated. This created the first emulsion (water in oil). Subsequently this mixture was slowly added to about 10x the volume of 2% (w/v) polyvinyl alcohol and the emulsion was vortexed and sonicated to create the double emulsion. The double emulsion was stirred overnight at RT to evaporate off the chloroform, solidifying the particles. The next day the emulsion was stirred under a dessicator in vacuum to remove the remaining chloroform. The particles were washed 3 times with endotoxin-free water (HyClone Laboratories, Thermo Scientific, Inc., Logan, UT) by ultracentrifugation for 30 min at 30,000 rpm (Beckman Coulter Optima L-90K Ultracentrifuge) and the PLGA-NP were lyophilized for storage at -20°C. PLGA-NPs were dissolved in PBS at 1 mg $mL^{-1}$ before addition to the cells. Empty PLGA-NPs were synthesized to serve as "carrier" control or for conjugation of Hp91 to the outside (see next method) by excluding peptide from the DMSO during preparation.

### 5.2.4 Conjugation of Hp91 to the surface of PLGA-NPs

Hp91 was conjugated to the surface of empty PLGA-NPs using the linker molecule Denacol EX-521 (Figure 5.1). NPs were suspended in borate buffer (pH5) containing Denacol EX-521 (linker) and zinctetrafluroborate hydrate (catalyst). The sample was mixed by vortexing and sonication. For activation of the NPs, the sample was stirred for 30 min at 37°C. To remove un-reacted Denacol, the activated NPs were washed with water by ultracentrifugation and resuspended in borate buffer. To couple the Hp91 peptide, the peptide was dissolved in DMSO and borate buffer and added to the activated NPs. The reaction was carried out for 2h at 37°C under

constant stirring. Excess unbound peptide was removed by ultracentrifugation and the samples were lyophilized for storage. The amount of Hp91 on the surface of NPs was quantified by HPLC. PLGA-NPs were dissolved in PBS at 1 mg $mL^{-1}$ before addition to the cells.

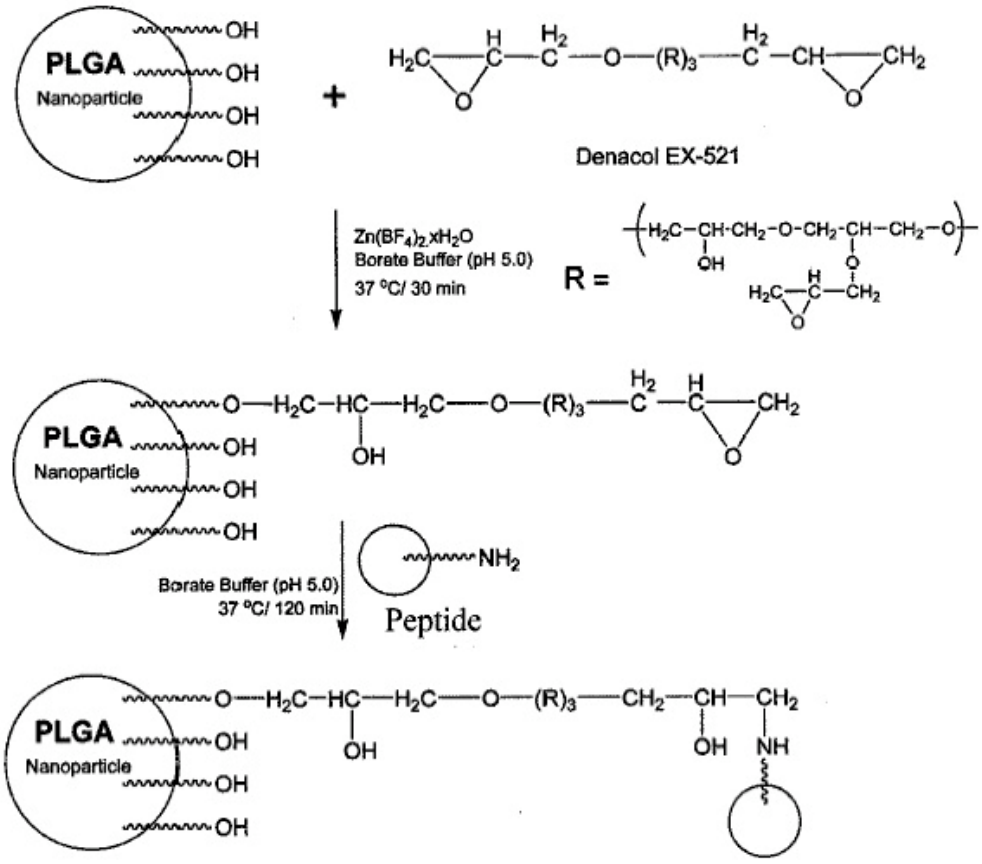


**Figure 5.1.** Synthesis scheme for conjugation of Hp91 to the surface of PLGA-NPs.

### 5.2.5 Nanoprecipitation Synthesis of Lipid-Polymer Hybrid NPs

Poly(lactic-co-glycolic acid)- lecithin- 1,2-distearoyl- *sn*-glycero- 3-phosphoethanolamine- N- [carboxy (polyethylene glycol)- 2000] nanoparticles (Lipid-polymer hybrid NPs) were synthesized via nanoprecipitation (Figure 5.2). A nanoprecipitation method Briefly, a lipid mixture of lecithin and DSPE-PEG carboxylic acid (40% molar ratio of DSPE-PEG carboxylic acid) was prepared in 4% ethanol

(endotoxin-free water). The PEG group stabilizes the particles. In addition, the ratio of lecithin to DSPE was selected based on previous stability and optimization studies and to make particles more uniform than if using lecithin alone. A PLGA mixture was prepared by dissolving peptide (when applicable) and PLGA (1 mg $mL^{-1}$) in dimethylformamide (DMF). The lipids were heated to 68°C and the peptide-PLGA mixture was nanoprecipitated within the lipid solution by dropwise addition to the stirring hot lipids. NPs in solution were vortexed at max speed for 3 minutes and ethanol was subsequently evaporated off for 2 h in a biosafety cabinet while stirring. To remove DMF, NPs were washed 3 times with endotoxin-free water (Hyclone) in 10K MW Amicon centrifugal filtration devices (Millipore, Billerica, MA,). Finally, lipid-polymer hybrid NPs were resuspended in a 10% sucrose solution, flash frozen, and stored at -80°C until use.

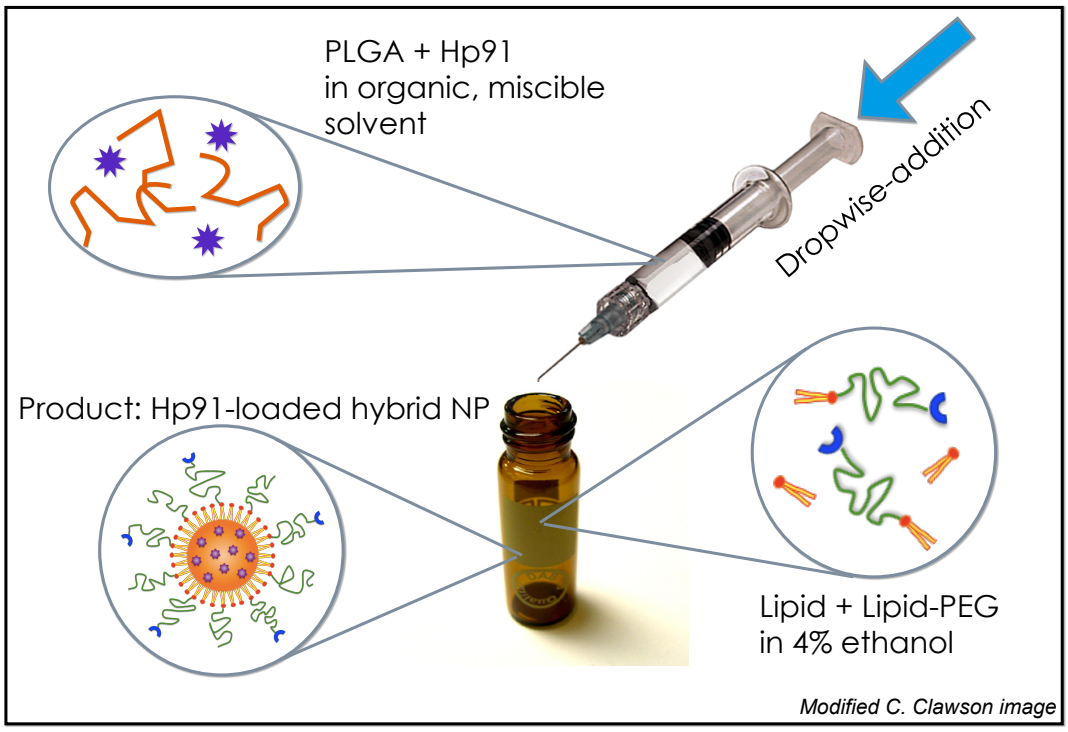


**Figure 5.2.** Synthesis of Hp91-loaded lipid-polymer hybrid nanoparticles.

### 5.2.6 Dynamic Light Scattering

The NPs were analyzed for particle size by dynamic light scattering (DLS) using a Zetasizer (Malvern Zetasizer Nano ZS, Worcestershire, UK). Z-average size (diameter) by intensity was determined in nanometers.

### 5.2.7 Peptide Quantification by HPLC

A spectral scan of the peptides was performed and the peptides, but not the polymer, were detected at 211 nm. To quantify the amount of peptide present inside or on the surface of the NPs, NPs were dissolved in acetonitrile or DMF for 30 min (if loaded inside) or overnight (if conjugated to the outside) under constant shaking at room temperature and peptide content was quantified by HPLC at 211 nm in comparison to a standard curve (HPLC: Agilent 1100 Series, Agilent, Santa Clara, CA. Software: Chemstation, Agilent. Column for PLGA-NPs: WATERS DELTA PAKC18 5 microns, Waters Corporation, Milford, MA. Column for lipid-polymer hybrid NPs: ZORBAX RP C18, Agilent.).

### 5.2.8 Nanoparticle Release Kinetics

To measure stability and peptide release kinetics of the NPs, 100 μL of particle solution was added to multiple 10,000 MW cutoff micro dialysis cassettes (Pierce, Thermo Scientific) and dialyzed against 1 L of PBS buffer at pH 7.4 or potassium hydrogen phthalate buffer at pH 5. At each time point, two-three samples were recovered from the micro dialysis cassettes for each buffer condition and the volumes were brought up to 125 μL to keep all volumes constant. To each sample, 125 μL of DMF was added to dissolve the PLGA-NPs and release the remaining peptide. The samples were shaken for 1 hour and then the total amount of peptide in

each sample was quantified using HPLC. The amounts were normalized against the starting concentration of peptide before dialysis, which was set at 100% to calculate the percent release.

### 5.2.9 Evaluating Peptide Adsorption onto NPs

In order demonstrate that the Hp91 peptide was covalently linked to the PLGA-NPs and not only adsorbed to the surface, 100 μL of Hp91 conjugated PLGA-NPs were sonicated for 3 min and the supernatant was removed using a 10k Amicon spin column (Millipore, Billerica, MA). As control, 10 μL of Hp91 conjugated PLGA particles were filtered using the spin column without the sonication step. Both the filtrate and the retentate were analyzed for peptide content by HPLC.

### 5.2.10 Atomic force microscopy

Atomic force microscopy (AFM) experiments were performed with a Multimode V SPM system (Veeco Instruments Inc.). Height, amplitude, and phase images were obtained in tapping mode in ambient environment with Tapping Mode Etched Silicon Probes (TESP, Veeco Instruments Inc.). Only phase images are shown unless specified. The scan rate is 0.5Hz. Here, AFM phase imaging is used to provide nanometer-scale information about surface structure. During the topographic tapping mode scan, the AFM phase lag of the cantilever oscillation is simultaneously monitored, which is very sensitive to variations in material properties.

### 5.2.11 Scanning transmission electron microscopy

Nanoparticles were diluted 50 times in water. Formvar/carbon film copper grids (Electron Microscopy Sciences, Hatfield, PA) were glow discharged (EMITECH

K950X evaporator with K350 glow discharge unit, EMITECH Ltd., Ashford, UK) to render them more hydrophilic. 3.5 μL of diluted NP sample was transferred onto the grid and excess water was removed using blotting paper and allowing the sample to dry. After drying, a layer of carbon was deposited onto the sample, approximately 8 Å thick (EMITECH). Scanning transmission electron microscopy (STEM) was performed with a Hitachi HD-2000 ultra-thin film evaluation system (Hitachi, Ltd., Tokyo, Japan). Both transmission and scanning modes were utilized.

### 5.2.12 Generation of human monocyte-derived DCs

Human iDCs were generated as previously described in Chapter 3, Materials and Methods.

### 5.2.13 Stimulation of DCs

$10^5$ immature DCs were incubated in culture media with the indicated amounts of empty or peptide carrying NPs, free peptide and for some experiments a cocktail of inflammatory cytokines (CyC) consisting of IL-1β at 10 ng $ml^{-1}$, TNF-α at 10 ng $ml^{-1}$ (R&D Systems), and PGE2 at 1 mg $ml^{-1}$ (Sigma-Aldrich), or 10 ng $ml^{-1}$ LPS (from *E. coli* 026:B6) (Sigma-Aldrich). 48h after activation the cell culture supernatants were collected and analyzed for cytokines by ELISA (eBioscience, Inc. San Diego, CA) according to the manufacturer's instructions.

### 5.2.14 Analysis of Human DC phenotype

DCs were tested for phenotypic maturation as per Chapter 4, Materials and Methods.

### 5.2.15 Animals and Cell Lines

C57BL/6 mice were purchased from Charles River Laboratories (Boston, MA, USA). FVB.N*neu*-tg (HER2 transgenic) mice were derived from in-house breeding stocks. TLR4 knockout mice were purchased from Jackson Laboratories. TLR7 and TLR9 knockout mice were a gift from S. Akira (Osaka University) and backcrossed for 10 generations onto the C57BL/6 background. Animals were housed at the Moores UCSD Cancer Center animal facility. All animal studies were performed with human care of animals and approved by the Institutional Animal Care and Use Committee of UCSD and were performed in accordance with the institutional guidelines.

The murine melanoma B16 cell line and apoptosis method were previously described in Chapter 4, Materials and Methods.

### 5.2.17 Generation of mouse BM-DCs

Bone marrow-derived dendritic cells (BM-DC) were prepared from C57BL/6 mice, HER-2/*neu* transgenic mice (H-2$^q$), and knockout mice as previously described in Chapter 3, Materials and Methods.

### 5.2.18 Analysis of BM-DC phenotype

BM-DCs were incubated for 20 min at 4$^o$C in 100 μl of PBS/5% FCS/0.1% sodium azide (FACS buffer) with Phycoerythrin-conjugated IgG mAb specific for CD80 and CD40, and APC-conjugated IgG mAb specific for CD11c (eBioscience). Cells were washed four times with FACS buffer, fixed in 3.7% formaldehyde in PBS (pH 7.2–7.4), and examined by flow cytometry using the FACSCalibur (Beckon Dickinson, Franklin Lakes, NJ). In all experiments, isotype controls were included using irrelevant mAb of the same Ig class conjugated to the same fluorophor. Data were analyzed using the

FlowJo software (Tree Star, Inc., Ashland, OR). Data are shown as mean fluorescence intensity gated on CD11c+ cells.

### 5.2.19 Immunizations and Tumor Monitoring

OVA: C57BL/6 mice, approximately 2 months old, were immunized subcutaneously (s.c.) with OVA peptide (SIINFEKL) in PBS or with empty NP, Hp91-loaded lipid-polymer hybrid NPs (174 μg), or free Hp91 (174 μg). Mice were boosted after 2 weeks and sacrificed one week post-boost. Single cell suspensions of splenocytes were prepared by mechanical disruption and separation through a 70 mm nylon cell strainer (BD Biosciences, Franklin Lakes, NJ, USA). Red blood cells were lysed using ammonium chloride buffer (Roche Diagnostics, Indianapolis, IN, USA) and the splenocytes were subsequently resuspended in complete medium (RPMI 1640 with 10% FCS, L-glutamine, penicillin, streptomycin, and HEPES). One group received a multiple antigenic peptide system (MAP) (250 μg) (Genscript) at immunization to serve as a positive control in the Hp91 ELISA.

B16: C57BL/6 mice, approximately 2 months old, were immunized s.c. with $2x10^5$ apoptotic mitomycin-C (Sigma-Aldrich)-treated B16 cells co-administered with either PBS or UC1018-NP (24 μg UC1018 peptide/mouse). Due to a manufacturing/solubility problem, UC1018 peptide was not available for boosts. Thus, all mice were boosted twice, at 4 weeks and 6 weeks with $2x10^5$ apoptotic mitomycin-C-treated B16 cells in PBS. Mice were challenged s.c. into the flank with $2x10^5$ live B16 cells at one week post-boost. Mice were followed for tumor growth and survival. Tumor dimensions were measured using calipers and the tumor volume calculated using the following formula; volume = $4/3\ \pi\ (a^2 \times b)$. Mice were euthanized

when tumor volume reached 1.5 $cm^3$. Tumor survival curves were generated, wherein the day of euthanasia was considered as death.

HER2: HER-2/neu-transgenic mice at 2 months of age were immunized s.c. with 5 μg HER2 peptide in PBS, or co-injected with 25 μg Hp91 free peptide or the same amount of Hp91 packaged within lipid-polymer hybrid NPs. Mice were boosted at 2 weeks and again one month later. Spleens were collected 8 days after the final immunization. Single cell suspensions of splenocytes were prepared as above. The splenocytes were expanded for 5 days in RPMI 1640 medium (Invitrogen) with 50 mM 2-mercaptoethanol (Sigma-Aldrich), 10 mM HEPES (Invitrogen), penicillin (100 U $ml^{-1}$) - streptomycin (100 μg $ml^{-1}$) - L-glutamine (2 mM) (Invitrogen), and supplemented with 20 U/mL of recombinant mouse IL-2 (R&D Systems) and HER2 peptide (10 μg/mL). 5-day expanded splenocytes from were collected and washed twice before plating in an IFN-γ ELISpot assay.

HER2 tumor monitoring: Female HER-2/neu mice, 8 weeks of age, were immunized with either PBS only, 25 μg of Hp91 free peptide or 25 μg of Hp91 delivered in PLGA-NPs. The 5 μg HER2 antigen was delivered in its free peptide form or encapsulated in PLGA-NPs. Mice received their first boost 2 weeks post-prime, and a second boost 1 month thereafter. All injections were performed subcutaneously on the right flanks of mice. The incidence and growth of tumors were evaluated twice a week by measuring palpable tumors, defined as tumors with diameters that exceed 3mm with calipers in two perpendicular diameters. Calipers were used to measure tumors in two perpendicular diameters and volume was calculated as volume ($mm^3$) = $(width)^2$ x length/2. All mice bearing tumor masses exceeding 1.5cm mean diameter were killed for humane reasons.

### 5.2.20 Enzyme-linked immunospot assay

IFN-γ assay: An Immobilon-P (PVDF) bottom enzyme-linked immunospot (ELISpot) plate (Millipore, Millerica, MA, USA) was prewet with 30% ethanol, washed 4 times with autoclaved water, and coated overnight with 5 μg $ml^{-1}$ monoclonal anti-mouse IFN-γ antibody (Mabtech, Stockholm, Sweden). After washing with autoclaved water, the coated plate was blocked with medium containing FCS. Freshly isolated splenocytes (OVA immunization) or 5-day expanded splenocytes (HER2 immunization) were plated in duplicate to wells of the ELISpot plate and cultured overnight at 37°C with 2.5 μg $ml^{-1}$ OVA-I (SIINFEKL) peptide, 5 μg $ml^{-1}$ concanavalin A positive control (Sigma-Aldrich), or left unstimulated (medium only). ELISpot plates were developed using 1 μg $ml^{-1}$ biotinylated anti-mouse IFN-γ antibody (Mabtech), Streptavidin-HRP (Mabtech), and TMB Substrate (Mabtech). The plate was scanned and the spots were counted using an automated ELISpot Reader System (CTL ImmunoSpot, Shaker Heights, OH, USA).

Granzyme B ELISpot assay: Performed as described in Chapter 4, Materials and Methods.

### 5.2.21 Cytokine Release Assay

Antigen-specific IL-2 cytokine release from freshly isolated splenocytes was measured as previously described in Chapter 2 Materials and Methods.

### 5.2.22 Detection of Hp91 antibody production by ELISA

Serum was obtained by cardiac puncture from mice at sacrifice. Blood was allowed to clot and serum was isolated after centrifugation. Microtiter plates were coated overnight with 5 μg/ml Hp91 peptide or multiple antigenic peptide (MAP),

washed 4x with TBST, blocked with 1% BSA/TBS (BSA - Sigma-Aldrich), and 1:25 dilutions of serum were added to the plates and incubated at RT for 1-2 hours. Plates were washed 4x with TBST, incubated with anti-mouse total IgG peroxidase conjugated antibody (Roche) at RT for 1 hour. Plates were washes 4x with TBST, developed using Zymed TMB substrate (Invitrogen), stopped with 1M sulfuric acid, and analyzed using a microplate reader at 450 nm.

#### 5.2.23 Statistical analysis

Data are represented as mean (±SEM) if not otherwise indicated. Data were analyzed for statistical significance using Student's t-test. p-values $< 0.05$ were considered statistically significant.

## 5.3 Results

#### 5.3.1 Hp91-loaded liposomes enhance DC stimulatory capacity

Preliminary work with Hp91-nanoparticles (Hp91-NPs) included the synthesis of Hp91-loaded liposomes and tests for DC activation and maturation. Liposomes were synthesized as described above in Materials and Methods (Figure 5.3A). Hp91 encapsulation within liposomes was estimated, as advised by W. Wrasidlo, based on average peptide loading efficiency into liposomes using the described synthesis method.

Immature human DCs were stimulated with free Hp91 peptide, empty liposomes, or Hp91-loaded liposomes at the doses indicated. Culture supernatants were collected after 48 hours and analyzed for the presence of IL-6 by ELISA. DC stimulated with Hp91-liposomes showed an estimated 27-fold increase in IL-6

secretion compared to free Hp91 peptide controls (Figure 5.1B). Unfortunately, fold-changes varied greatly from batch to batch. Empty liposome controls did not induce IL-6 expression (Figure 5.3B).

Free Hp91 does not normally induce phenotypic changes in DCs. To determine whether Hp91-liposomes could induce phenotypic maturation of DCs, immature DCs were left unstimulated (media) or were exposed to empty liposomes, liposomes loaded with Hp91, free Hp91 peptide, or bacterial lipopolysaccharide (LPS), which served as positive control. After 48h cells were harvested and analyzed for surface expression of CD83, CD54, CD86, or CD40 by flow cytometry (Figure 5.3C). Empty liposomes did not cause any changes in phenotypic markers as compared to media control. Free Hp91, as has been previously observed, did not induce changes in phenotypic markers. Interestingly, when Hp91 was encapsulated within liposomes, we observed a strong increase in surface expression of CD83 and CD54, comparable to LPS. The changes in CD86 and CD40 were minimal.

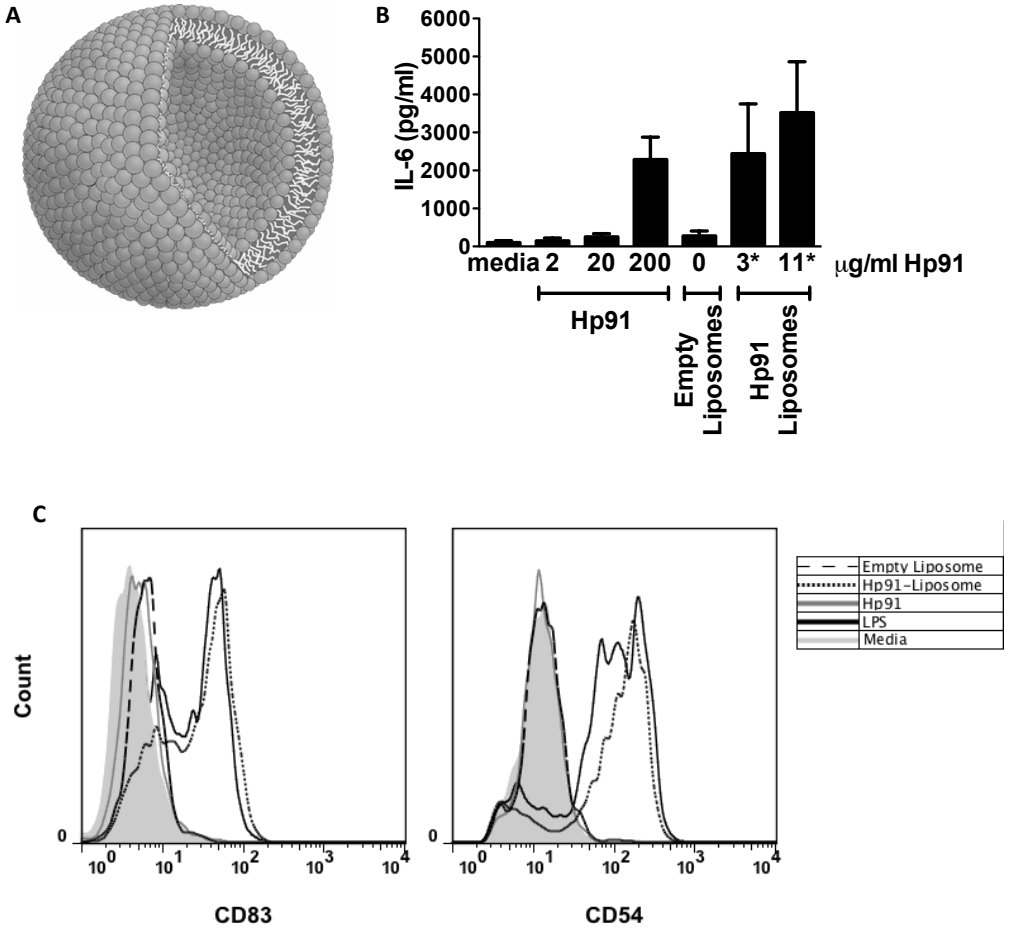


**Figure 5.3.** *Hp91-loaded liposomes enhance DC stimulatory capacity and maturation.* (**A**) Representation of a liposome. (**B**) Immature DCs were stimulated with the indicated peptides/liposomes for 48 hours. Supernatants were analyzed for the presence of IL-6 by ELISA. Data are mean (±SEM) for 3 independent liposomes batches and experiments. *Hp91 encapsulation is estimated. (**C**) Immature human DCs were exposed to media, empty liposomes, free Hp91 (20 μg), Hp91* (0.5 μg) loaded into liposomes, or LPS for 48h. Cells were collected and analyzed for CD83 expression by flow cytometry. Data is representative of 3 independent experiments. *Hp91 encapsulation is estimated.

Encapsulating Hp91 within liposomes appeared to enhance the immunostimulatory capacity of Hp91. However, high batch variability combined with our inability to synthesize liposomes without equipment previously exposed to large

amounts of endotoxin led us to quickly abandon the liposomal NPs. The liposomal work demonstrated a proof of principle to us and led us to synthesize alternative types of NPs for our experiments.

### 5.3.2 Characterization of PLGA-NPs

PLGA-NPs were synthesized by a double emulsion method and Hp91 was conjugated onto the surface of the NPs as described above in Materials and Methods. To demonstrate the presence of Hp91 on the surface of the PLGA-NPs, we applied atomic force microscopy comparing empty PLGA-NPs to PLGA-NPs that have been conjugated with Hp91 (NP-Hp91). PLGA-NPs with peptide show a rough surface, note arrows (Figure 5.4A right image) compared to empty PLGA-NPs generated in the absence of peptide (Figure 5.4A left image). Although AFM only indicates the presence of protein on the PLGA-NP surface, since the difference in synthesis was presence or absence of Hp91, we conclude that the detected protein on the surface is Hp91. The presence of Hp91 on the PLGA-NP surface was confirmed and quantified by HPLC at 211 nm, which detected peptide in the preparation with Hp91 on the PLGA-NP surface, but not on empty NPs. As measured by HPLC, 112 μg Hp91 were conjugated per milligram of PLGA-NP. These data indicate that we successfully conjugated Hp91 to the outside of the PLGA-NPs.

In order to test whether or not the peptide was covalently linked to the PLGA particles or only adsorbed to the surface, the peptide-conjugated PLGA-NPs were sonicated to release loosely bound peptide, spun down using a using a 10k Microcon Amicon spin column, and the supernatants were analyzed for the presence of peptide by HPLC. After sonication for 3 min, approximately 4.4% of the total Hp91 was measured in the supernatant, while the majority of the peptide, 95.6% was still associated with the

particles. Peptide-conjugated PLGA-NPs that were not sonicated, but simply filtered in the same manner, only 0.06% of the Hp91 was measured in the filtrate and 99.9% of the Hp91 remained associated with the particles.

We noted that the PLGA-NPs showed some level of aggregation when observed under the light microscope. In order to improve on the synthesis scheme we investigated at what stage of the synthesis process the aggregation occurred. The size distribution of the PLGA-NPs was measured by DLS after each of the three ultracentrifugation spins which were used to remove un-incorporated peptide from the NPs. Only a slight increase in size was observed. The average size of the PLGA-NPs was 201, 235, and 243 nm after the first to third wash respectively (Table 5.1). Since the NPs were lyophilized for long-term storage, the NP size was measured before lyophilization and after resuspension of the lyophilized NPs. After resuspension of the lyophilized NPs their average size was 1365 nm (Figure 5.4B), which indicates formation of small aggregates/quadruplets.

**Figure 5.4.** *Characterization of PLGA-NPs.* (**A**) Atomic force microscopy phase images of empty PLGA-NPs and PLGA-NPs conjugated with Hp91. Arrows point to the areas where peptide was detected on the NP surface. (**B**) The size distribution of PLGA-NPs was analyzed before and after lyophilization by dynamic light scattering. (**C**) Human immature DCs were exposed to media, empty NPs (300 μg/ml), lyophilized PLGA-NPs containing Hp91 (300 μg/ml), and non-lyophilized PLGA-NPs containing Hp91 (240 μg/ml) for 48h. Cell culture supernatants were collected and analyzed for IL-6 by ELISA. Depicted is a representative result showing fold-increase in IL-6 secretion as compared to the empty NP control, which was set as 1. (**D-E**) The graphs show release kinetic profiles of Hp91 peptide from PLGA -NPs at pH 7.4 and pH 5 over 36 h. The peptide input at time 0 is set as 100%. Samples were taken at the indicated time points and the amount of peptide in PLGA-NPs was quantified by HPLC. Data shown are mean +/-SEM of triplicate measurements. (**D**) Hp91 conjugated to the surface of PLGA-NPs. (**E**) PLGA-NPs with Hp91 encapsulated inside the NPs (credit: C. Clawson).

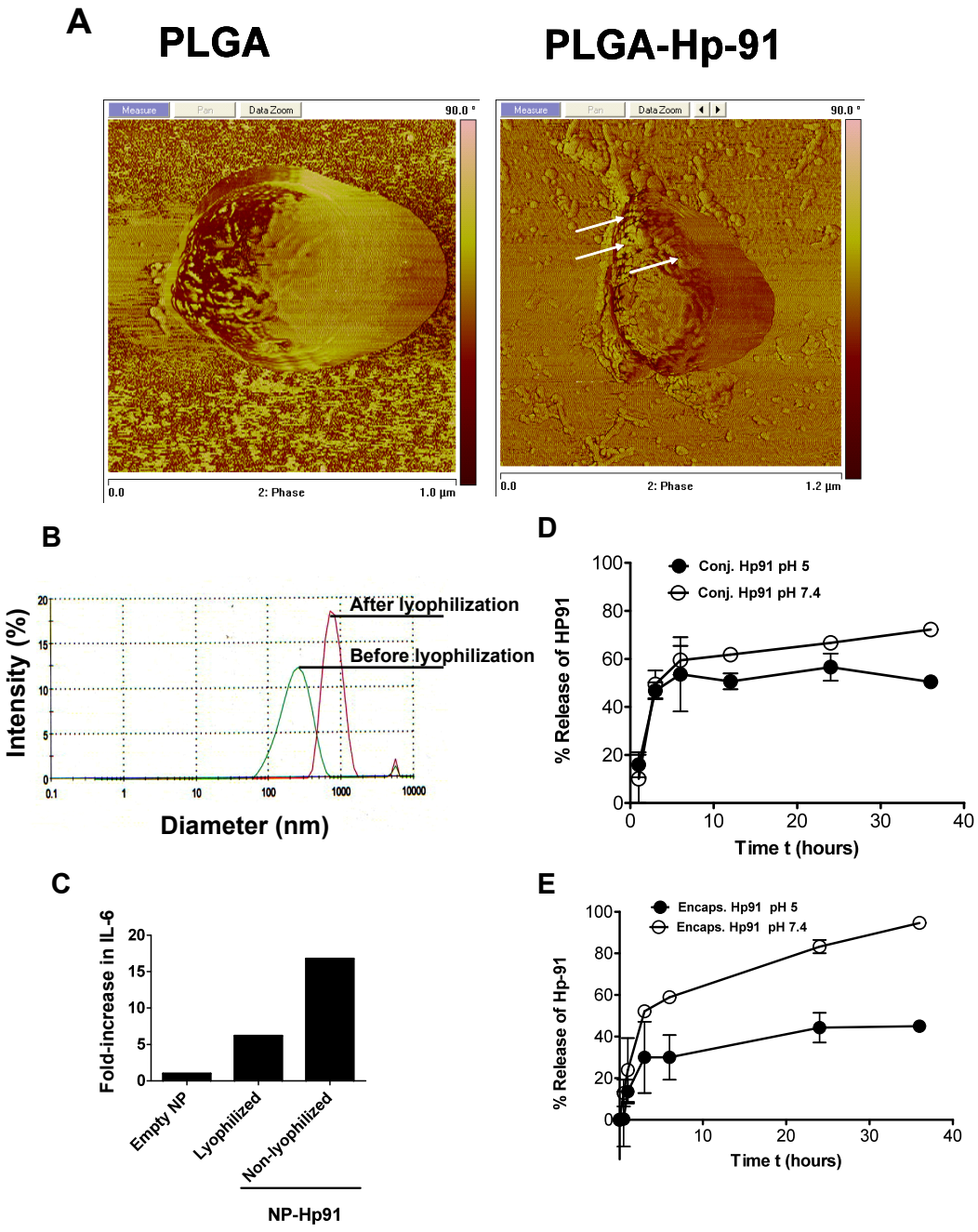
A
PLGA
PLGA-Hp-91
Measure
Pan
Data Zoom
90.0 °
0.0
2: Phase
1.0 µm
1.2 µm
B
Intensity (%)
Diameter (nm)
After lyophilization
Before lyophilization
C
Fold-increase in IL-6
Empty NP
Lyophilized
Non-lyophilized
NP-Hp91
D
% Release of HP91
Time t (hours)
Conj. Hp91 pH 5
Conj. Hp91 pH 7.4
E
% Release of Hp-91
Time t (hours)
Encaps. Hp91 pH 5
Encaps. Hp91 pH 7.4

**Table 5.1.** PLGA nanoparticles size distribution during preparation.

| Number of washes | Size of PLGA-NPs (nm)* |
|---|---|
| One | 201 |
| Two | 235 |
| Three | 243 |

*The size distribution of poly(D,L-lactic-co-glycolic) acid nanoparticles (PLGA-NPs) was measured by Zetasizer Nano ZS (Malvern Instruments) after each of the three washes of ultracentrifugation (credit: C. Clawson).

Next, we tested whether sonication for prolonged periods for time would dissolve the aggregates. NPs were measured after different sonication times (1 to 30 min). After 30 min of sonication their size was reduced from 1365+/- 906 to 648+/- 254 nm (Table 5.2). This decrease in size after sonication indicates that although the big aggregates were disrupted, some small aggregates, most likely duplets, were still present. Since the aggregation occurred in the lyophilization step, for all subsequent experiments, the NPs were not lyophilized, but instead stored in a mixture of water/10% sucrose at -20°C to avoid aggregation.

**Table 5.2.** PLGA nanoparticles size distribution after sonication.

| [a] PLGA-NP sonication time (min) | [b] Size of PLGA-NP (nm) |
|---|---|
| 1 min | 1365 +/- 906 |
| 15 min | 791 +/- 111 |
| 30 min | 648 +/- 255 |

[a] PLGA nanoparticles were lyophilized after the final wash and resuspended in PBS. The suspension was then sonicated for 1, 15, or 30 min at 40 kHz in an iced sonicator waterbath (Brandon; Model 2510).
[b] The NP size distribution (+/- SD) was measured by dynamic light scattering using three different batches of NPs after the different sonication times: 1, 15, and 30 min (credit: C. Clawson).

We hypothesized that non-aggregated PLGA nanoparticles are more potent than aggregated particles due to the increased surface area. To test this hypothesis lyophilized NPs that were conjugated with Hp91 on the surface were resuspended in PBS and compared to NPs that had never been lyophilized, but were instead frozen

in PBS/10%sucrose solution immediately after synthesis. Immature human DCs were exposed to empty PLGA-NPs, previously lyophilized PLGA-NPs containing Hp91, and non-lyophilized PLGA-NPs containing Hp91 (Figure 5.4C). As expected the particles that were stored in solution (non-lyophilized) and had very few aggregates if any, caused increased activation of DCs even at the lower amount tested.

We next measured the stability of the Hp91 conjugated to the surface of PLGA-NPs (Figure 5.4D). After approximately 3 h, 50% of the conjugated peptide is released from the PLGA-NPs at pH 7.4 and pH5. Although the lower pH results in a slower release of the conjugated peptide over prolonger periods of time than at neutral pH, the difference is not as significant as that for the encapsulated peptide at different pH (Figure 5.4E). After 3 hours, the release rate begins to flatten out for both pH conditions. After 36 h, PLGA-NPs at pH 7.4 have released approximately 72% of the conjugated peptide, while at pH 5, approximately 50% of the peptide is released.

A similar trend was observed with Hp91 loaded PLGA-NPs with stronger peptide release at higher pH (Figure 5.4E). After approximately 3h 50% of the peptide is released from within the PLGA-NPs at pH7.4 and after 36 h, 95% of the peptide is released from the PLGA particles in pH 7.4, while only 45% is released from the PLGA-NPs at pH 5. Both conditions produce an initial burst release with a large proportion of the released peptide being released within the first 3 hours. After 3h, both curves flatten out and the release rate is reduced; however, the PLGA-NPs at pH 7.4 continue to release at a higher rate than at pH 5 throughout the time course (Figure 5.4E).

### 5.3.3 Hp91 conjugated to the surface of PLGA-NPs induces cytokine secretion in human DCs

DC activation is characterized by the secretion of inflammatory cytokines such as IL-6 (143). We have previously shown IL-6 secretion in human monocyte-derived DCs (104). To test whether Hp91 when conjugated to the surface of PLGA-NPs maintains its DC stimulatory capacity, immature human monocyte-derived DCs were exposed to empty PLGA-NPs (NP), PLGA-NPs with Hp91 conjugated to the surface (NP-Hp91), free Hp91 peptide, or a cocktail of inflammatory cytokines (CyC) known to activate DCs. Two days later the cell culture supernatants were collected and analyzed for the presence of IL-6 by ELISA. A highly significant increased in IL-6 secretion was observed when NP-Hp91 with a final Hp91 concentration of 11.2 μg/ml was added to DCs as compared to the same amount of empty PLGA-NPs ($p<0.0001$) and as compared to 200 μg/ml of free Hp91 peptide ($p<0.0001$) (Figure 5.5). At 11.2 μg/ml, Hp91 when conjugated to the surface of PLGA-NPs induced 3,923 (+/- 410) pg/ml IL-6, whereas 200 μg/ml free Hp91 induced only 1,485 (+/- 376) pg/ml IL-6. This is a 47-fold increased in IL-6 secretion when normalized for the same amount of Hp91. In addition Hp91 conjugated to the PLGA-NP surface induced higher IL-6 secretion as compared to a cocktail of inflammatory cytokines CyC known to mature DCs (144). When lower amounts of Hp91 (1.12 μg/ml) conjugated to the PLGA-NP surface were used, although an increase in IL-6 was observed, the differences as compared to the controls were not significant (Figure 5.5).

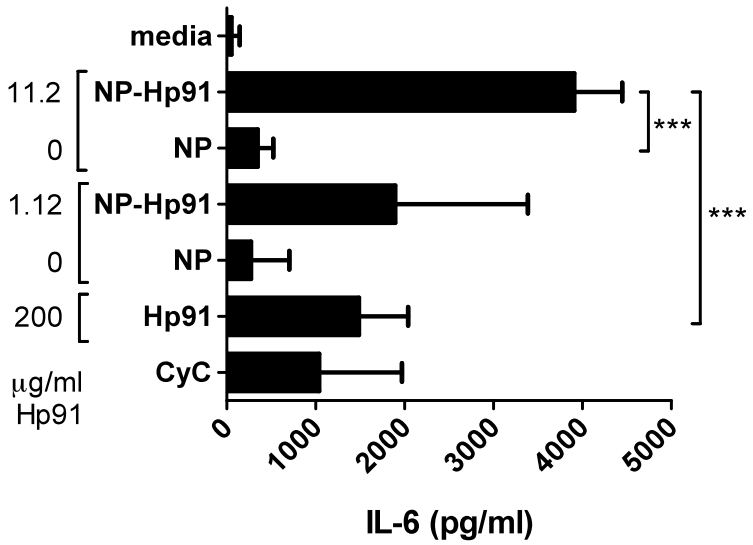


**Figure 5.5.** *Hp91 conjugated to the outside of PLGA-NPs causes stronger activation of human DCs as compared to free peptide.* $10^5$ immature human DCs were exposed to media, PLGA-NPs carrying Hp91 on the surface (Np-Hp91) with 2 concentrations of Hp91: 11.2 and 1.12 μg/ml, empty NPs matching the amount of PLGA-NPs used with peptides (as NP control), 200 μg/ml of free Hp91 peptide, or a cytokine cocktail CyC (see methods for composition). Cell culture supernatants were collected after 48h and analyzed for IL-6 by ELISA. Data shown is mean +/-SD of three independent experiments using DCs from different donors. * indicates a statistically significant increase (credit: C. Clawson).

### 5.3.4 Hp91 conjugated to the surface of PLGA-NPs causes cytokine secretion in mouse BM-DCs

To determine whether PLGA-NPs carrying Hp91 on the surface also elicit cytokine secretion in mouse DCs, immature mouse bone marrow-derived DCs (BM-DCs), were generated as previously described (104), and exposed to media only, indicated doses of empty PLGA-NPs (NP) (as particle control; matching the amount of PLGA-NP in peptide carrying PLGA-NP), 3 dilutions of PLGA-NPs that have been conjugated with Hp91 on the surface (NP-Hp91), free Hp91 peptide (200 μg/ml), or LPS (10 ng/ml) as positive control. Two days later the cell culture supernatants were collected and analyzed for the presence of IL-6 by ELISA. As observed with human DC, we found that the peptide Hp91 when conjugated to the surface of the PLGA-

NPs induced high levels of IL-6 secretion. NP-Hp91 with a final peptide concentration of 34 μg/ml Hp91 induced an average of 5050 +/- 277 pg/ml IL-6, which was significantly higher than empty NPs at the same dose (p=0.008) and than 200 μg/ml free Hp91, which induced an average of 1446 +/- 559 pg/ml IL-6 (p=0.01) (Figure 5.6A). When normalized to the amount of Hp91, Hp91 is ~20-fold more potent when delivered on the surface of PLGA-NPs as compared to free Hp91. NP-Hp91 with a final peptide concentration of 3.4 μg/ml Hp91 elicited significant IL-6 expression as compared to empty NPs at the same dose (p=0.03), but it was not significantly different from 200 μg/ml of free Hp91 (Figure 5.6A).

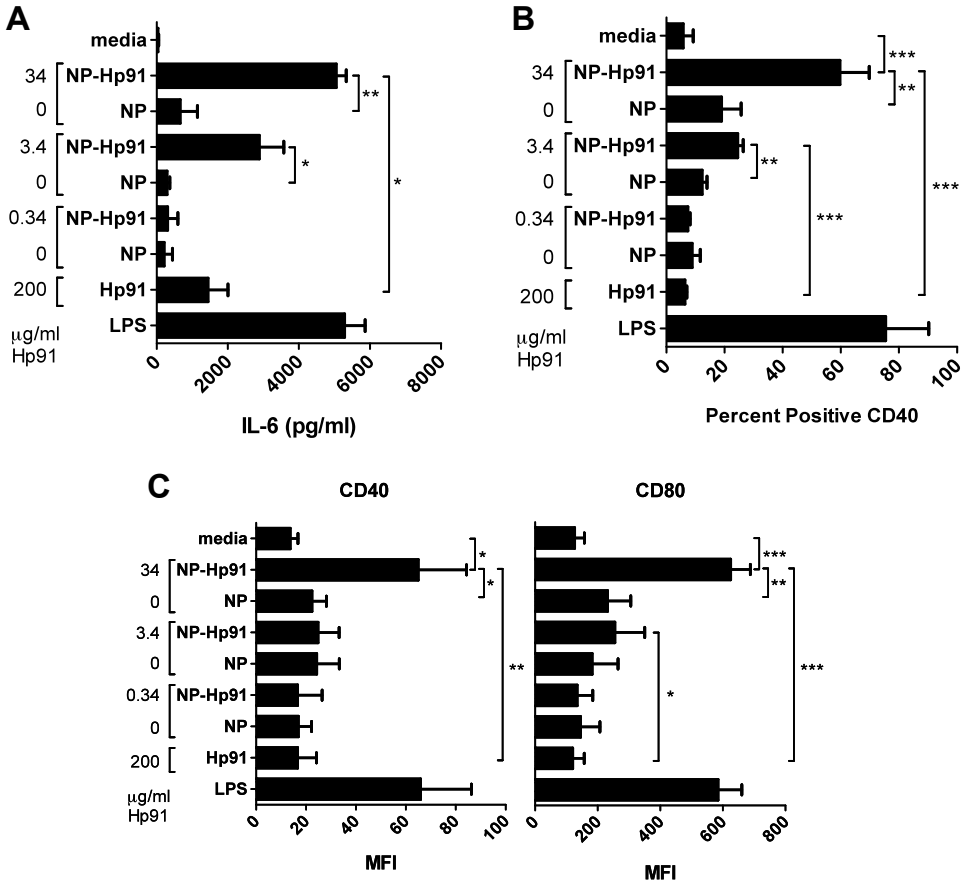


**Figure 5.6.** *Hp91 conjugated to the outside of PLGA-NPs causes stronger activation of mouse DCs as compared to free peptide.* $10^5$ immature mouse BM-DCs were exposed to media only, PLGA-NPs carrying Hp91 on the surface (Np-Hp91) with 3 concentrations of Hp91: 34, 3.4, and 0.34 μg/ml, empty NPs matching the amount of PLGA-NPs used with peptides (as NP control), 200 μg/ml of free Hp91 peptide, or LPS (10 ng/ml). (**A**) Cell culture supernatants were collected after 48h and analyzed for the presence of IL-6 by ELISA. Data shown is mean +/-SD of two independent experiments using DCs from different donors. (**B, C**) Cells were collected 48h after exposure to the different NP conditions and analyzed for the expression of CD40 and CD80 by surface membrane immunofluorescence techniques using fluorophor conjugated mAbs. DCs were gated on CD11c+ cells and analyzed for expression of the indicated markers. B) depicts percent positive cells and C) depicts mean fluorescence intensity (MFI). Data shown is mean +/-SD of three independent experiments using DCs from different donors. * indicates a statistically significant increase (credit: C. Clawson).

### 5.3.5 Hp91 conjugated to the surface of PLGA-NPs induces phenotypic maturation of mouse BM-DCs.

To determine whether Hp91 when conjugated to the surface of PLGA-NPs can induce phenotypic maturation of mouse BM-DCs, immature BM-DCs were exposed to empty PLGA-NPs (NP), PLGA-NPs with Hp91 conjugated to the surface (NP-Hp91), free Hp91 peptide, or bacterial lipopolysaccharide (LPS), which served as positive control. After 48h cells were harvested and analyzed for surface expression of CD40, CD80, and MHC class II by flow cytometry (Figure 5.6B, C). Empty PLGA-NPs did not cause any changes in CD40 and CD80 expression, but they increased MHC II expression in immature DCs by 2-fold as compared to media control. However, no additional changes in MHC II expression were observed with peptide loaded NPs (data not shown). Interestingly, although free Hp91 peptide did not increase expression of CD40 or CD80, Hp91 conjugated to the surface of PLGA-NPs caused a significant increase in CD40 and CD80 expression levels comparable to those induced by LPS (Figure 5.56B, C). During the process of DC maturation some surface molecules are weakly expressed on immature DCs and are upregulated upon activation. This manifests as an increase in mean fluorescence intensity (MFI) when measuring expression levels by flow cytometry. Other surface molecules are not or barely expressed on immature DCs and the percentage of cells positive for those molecules can increase upon activation.

On immature DCs (=media control) only a small percentage of DCs in the population expressed CD40 (Figure 5.6B) and on those the expression was very low (Figure 5.6C). After exposure to NP-Hp91 with a final Hp91 concentration of 34 μg/ml, the number of CD40 positive DCs significantly increased in comparison to media control ($p=0.0009$) and to empty NPs at the same concentration ($p=0.004$) (Figure

5.6B). Furthermore, NP-Hp91 with 34 μg/ml of Hp91 elicited a highly significant increase in the percentage of CD40 positive cells as compared to 200 μg/ml of free Hp91 ($p=0.0008$). The same was true for the lower concentration of NP-Hp91 with 3.4 μg/ml of Hp91. Even the low dose of peptide (3.4 μg/ml), NP-Hp91 elicited a significant increase in the percentage of CD40 positive DCs as compared to media control ($p=0.04$), the same dose of empty NPs ($p=0.001$), and 200 μg/ml of free Hp91 ($p<0.0001$) (Figure 5.6B).

In addition to the increase in the number of CD40-positive DCs, NP-Hp91 with 34 μg/ml of Hp91 elicited a significant increase in CD40 cell surface expression levels as compared to media ($p=0.01$), empty NPs at the same concentration ($p=0.02$), and as compared to 200 mg/ml of free Hp91 ($p=0.005$) (Figure 5.6C). Although lower amounts NP-Hp91 with a final concentration of 3.4 μg/ml of Hp91 significantly increasing the number of CD40 positive DCs (Figure 5.6B), no significant increase in CD40 expression were observe additionally (Figure 5.6C).

In the case of CD80, the majority of the immature DCs (~80%) within the population were already positive for CD80, although the expression levels were very low (Figure 5.6C), there was no further increase in the number of positive cells (data not shown). However, NP-Hp91 with 34 μg/ml of Hp91 elicited a highly significant increase in CD80 cell surface expression levels as compared to media ($p=0.0002$), empty PLGA-NPs at the same concentration ($p=0.002$), and as compared to 200 μg/ml of free Hp91 ($p<0.0001$) (Figure 5.6C). Lower amounts NP-Hp91 with a final concentration of 3.4 μg/ml of Hp91 did not significantly increase the CD80 expression levels as compared to empty PLGA-NPs at the same concentration, but did cause a significant increase as compared to 200 μg/ml of free Hp91 ($p=0.04$) (Figure 5.6C). Hence Hp91 when delivered on the surface of PLGA-NPs not only maintains its ability

to activate DCs, but the peptide is much more potent as a result and gained additional functions like induction of surface molecule expression on DCs, which is very favorable for vaccine adjuvants.

**5.3.6 Delivery of Hp91 inside of PLGA-NPs leads to increased activation of human DCs.**

We next tested whether Hp91 when packaged inside PLGA-NPs would maintain its ability to activate human DCs. Immature human DCs were exposed to media only, empty-NPs, PLGA-NPs that contained Hp91 inside the nanoparticles NP-(Hp91), and the same amount of free Hp91 peptide as present in the PLGA-NPs. Two days later the cell culture supernatants were collected and analyzed for the presence of IL-6 by ELISA (Figure 5.7A). Hp91 loaded inside of PLGA-NPs at 9 μg/ml ($p=0.01$) and 18 μg/ml ($p=0.03$) significantly increased secretion of IL-6 by DC as compared to media control. In contrast, free Hp91 peptide at 9 or 18 μg/ml did not induce significant increase in IL-6 as compared to media control, indicating that PLGA-NP delivered Hp91 is more potent. Empty NPs did not induce significant changes in IL-6 expression. At 9 μg/ml Hp91 loaded inside of PLGA-NPs a significant increase (5-fold; ($p=0.02$) in IL-6 secretion was observed as compared to free Hp91 peptide (Figure 5.7A). Since Hp91 was dissolved in DMSO for the synthesis of the PLGA-NPs and empty PLGA-NPs carry BSA, we also tested the effect of BSA/DMSO added at the same dose as present in the added PLGA-NPs to DCs. No increase in IL-6 was observed under these control conditions (Figure 5.7B). To further test whether the observed effects are due to Hp91 or simply caused by the presence of any peptide packaged inside of PLGA-NPs, we incorporated Hp121 as control peptide into PLGA-NPs. Hp121 is derived from the same molecule as Hp91, HMGB1, and we have previously shown has no activity on DCs as free peptide [9]. Here we show that

the control peptide Hp121, neither as free peptide, nor packages inside of PLGA-NPs induces secretion of IL-6 by human DCs (Figure 5.7B).

We also evaluated whether PLGA-NPs exert toxic effects on DCs by comparing empty and Hp91 loaded PLGA-NPs. We did not observe any toxicity with either empty or peptide loaded PLGA-NPs in comparison to media control at doses used in these experiments even after 4 days of culture (data not shown).

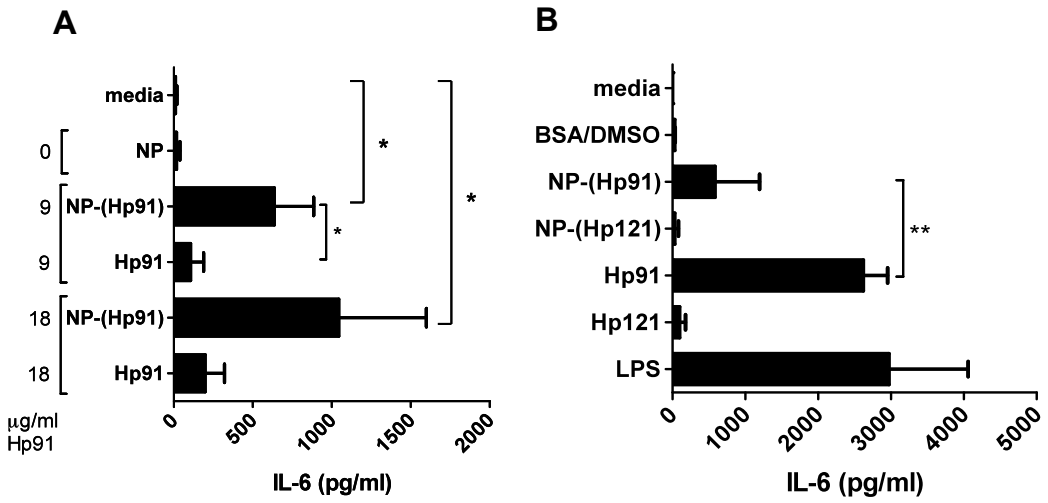


**Figure 5.7.** *Packaging of the immunostimulatory peptide Hp91 inside of PLGA-NPs increases its potential to activate human DCs.* (**A**) Immature human DCs were exposed to media, empty PLGA-NPs, PLGA-NPs containing Hp91 encapsulated (Np-Hp91) at 2 doses of Hp91 (9 and 18 μg/ml), or the same amount of free Hp91 peptide was added to the cells. Cell culture supernatants were collected after 48h and analyzed for IL-6 by ELISA. Data shown is mean +/-SD of three independent experiments using DCs from different donors. * indicates a statistically significant increase. (**B**) Immature mouse BM-DCs were exposed to media only, BSA/DMSO control matching the amount present in the NP preparations, PLGA-NPs that have been filled with Hp91 (NP-Hp91) added at a final concentration of 9 μg/ml of Hp91, PLGA-NPs that have been filled with Hp121 (NP-Hp121) added at a final concentration of 4 μg/ml of Hp121, free Hp91 peptide (200 μg/ml), free Hp121 peptide (200 μg/ml), or LPS (10 ng/ml). 48h later the cell culture supernatants were collected and analyzed for the presence of IL-6 by ELISA. Data shown is mean +/-SD of three independent experiments using DCs from different donors. * indicates a statistically significant increase (credit: C. Clawson).

### 5.3.7 Hp91 packaged inside of PLGA-NPs activate mouse BM-DCs

Since increased biological activity using Hp91 loaded PLGA-NPs as compared to free peptide was observed in human DCs, we next evaluated whether the same was true for mouse BM-DCs. Immature mouse BM-DCs were exposed to media only, empty PLGA-NPs (NP), PLGA-NPs that have been filled with Hp91 (NP-(Hp91)) with the final peptide concentration being (13 μg/ml), or 200 μg/ml free Hp91 peptide. Two days later the cell culture supernatants were collected and analyzed for the presence of IL-6 by ELISA (Figure 5.8). As observed with human DCs, when Hp91 was packaged inside the PLGA-NPs the peptide maintained its ability to induce IL-6 secretion. Hp91 was delivered inside of the PLGA-NPs cause a significant increased in IL-6 expression as compared to media control ($p=0.03$) and as compared to empty NPs ($p=0.04$). At only 13 μg/ml when packaged inside the PLGA-NPs Hp91 induced in average 707 pg/ml IL-6 whereas free Hp91 at 200 μg/ml induced similar levels of 545 pg/ml of IL-6. Thus a 15-fold lower amount of Hp91 was sufficient to elicit a similar level of IL-6.

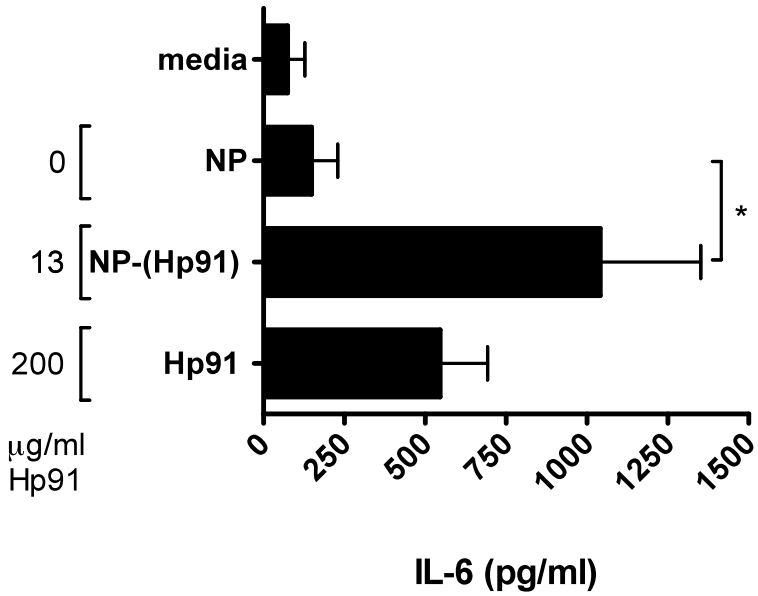


**Figure 5.8.** *Packaging of the immunostimulatory peptide Hp91 inside of PLGA-NPs increases its potential to activate mouse DCs.* Immature mouse BM-DCs were exposed to media only, empty-PLGA NPs, PLGA-NPs that have been filled with 13 μg/ml of Hp91 (Np-Hp91), or, free Hp91 peptide (200 μg/ml). 48h later the cell culture supernatants were collected and analyzed for the presence of IL-6 by ELISA. Data shown is mean +/-SD of three independent experiments using DCs from different donors (credit: C. Clawson).

### 5.3.8 Nanoprecipitation synthesis generates smaller nanoparticles that are easily scalable to large batch production

While the Hp91 PLGA-NPs described above proved to be immunostimulatory and warranted future studies to develop them as vaccine adjuvants, the particles had disadvantages. Lyophilization of the PLGA-NPs resulted in aggregation. Even without lyophilization, the PLGA-NPs were measured at 243 nm after washes (Table 5.1), which is considered large by nano-standards. Additionally, the synthesis of PLGA-NPs was time consuming and difficult and eventually led us to engineer a new nanoparticle design. With the help of Dr. Liangfang Zhang's lab (UCSD Nanoengineering), we switched to a new synthesis method following a previously

described method that takes advantage of nanoprecipitation and lipid self-assembly in order to create a simple and scalable manufacturing process (145-147). We call these particles lipid-polymer hybrid NPs.

Briefly, these lipid-polymer hybrid NPs combine the FDA-approved PLGA with phospholipids common to cell membranes (lecithin mix); in this case the particles mostly contain DSPE, which is a synthetic phosphatidylethanolamine (PE) derivate. PLGA forms the core of the particle, and the lipids self assemble to form a shell around the polymer core. As determined by DLS, the diameter of an empty polymer-lipid hybrid NP is mean of 64 nm, compared to 243 nm for the old method (Figure 5.9A, B and Table 5.1). This is almost a 4-fold reduction in diameter. Loading peptide into the lipid-polymer hybrid NPs results in an increase in size. By adding relatively short peptides, OVA-1 and UC1018 for example at 8-9 aa, the diameter of the particle increases to 92.5 nm (Figure 5.9A). This is a significant 44% increase in size for the OVA-1 NPs compared to the empty NPs. Adding the 18aa Hp91 peptide leads to NPs of 106 nm in diameter, which is a 65% increase in size; a significant increase compared to empty NPs (Figure 5.9A). Additionally, the NPs were evaluated for size after a freeze/thaw and were measured at approximately the same diameter compared to pre-freeze (data not shown) suggesting these particles lack the tendency to aggregate.

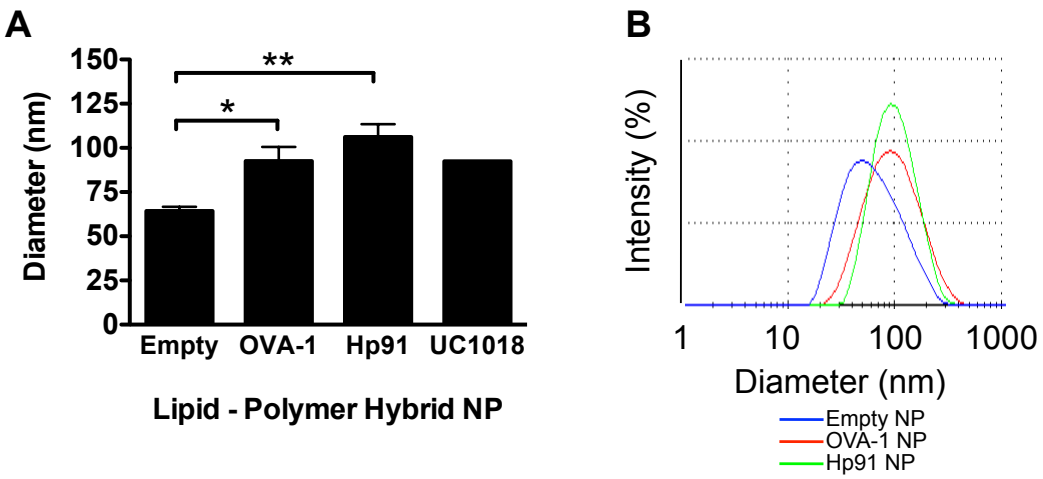


**Figure 5.9.** *Dynamic light scattering of lipid-polymer hybrid NPs.* (A-B) Batches of lipid-polymer hybrid NPs were characterized on a Malvern Nano ZS. Z-average size (diameter) by intensity was determined by DLS. (**A**) Batch diameters are shown as mean (±SEM) for each type of NP. *$p < 0.05$, **$p < 0.01$ between groups; Student's *t*-test. (**B**) are representative results.

### 5.3.9 Lipid-polymer hybrid NPs are uniformly round and without aggregation

In addition to characterizing the NPs by DLS, the lipid-polymer hybrid NPs were imaged by electron microscopy to evaluate shape, uniformity, and aggregation. Empty and Hp91-encapsulated NP batches, both after a freeze/thaw, were imaged. The Hp91-NPs were found to be single particles, without signs of aggregation (Figure 5.10A, B). Scanning electron microscopy (SEM) showed uniformly round Hp91-NPs with a dark core and light rim (Figure 5.10A). Size estimates of nanoparticles using the Hitachi STEM software, showed the Hp91-NPs to be a mean size of 109 nm (as measured by SEM), almost identical to the 106 nm diameter mean size determined by DLS. Interestingly, when observing the same particles by transmission electron microscopy (TEM), the particles appeared smaller, lacked a contrasting rim, and had a mean diameter of 84 nm (Figure 8.10B), attributed either to the lipid layer not being visible by TEM, or due to a melting artifact, as TEM uses a strong electron beam. Additionally, Hp91-NPs appeared "easier" to image than the empty NPs, as the

electron beam appeared to quickly melt the empty NPs in both SEM and TEM modes, suggesting that the Hp91 peptide stabilizes the particle for EM.

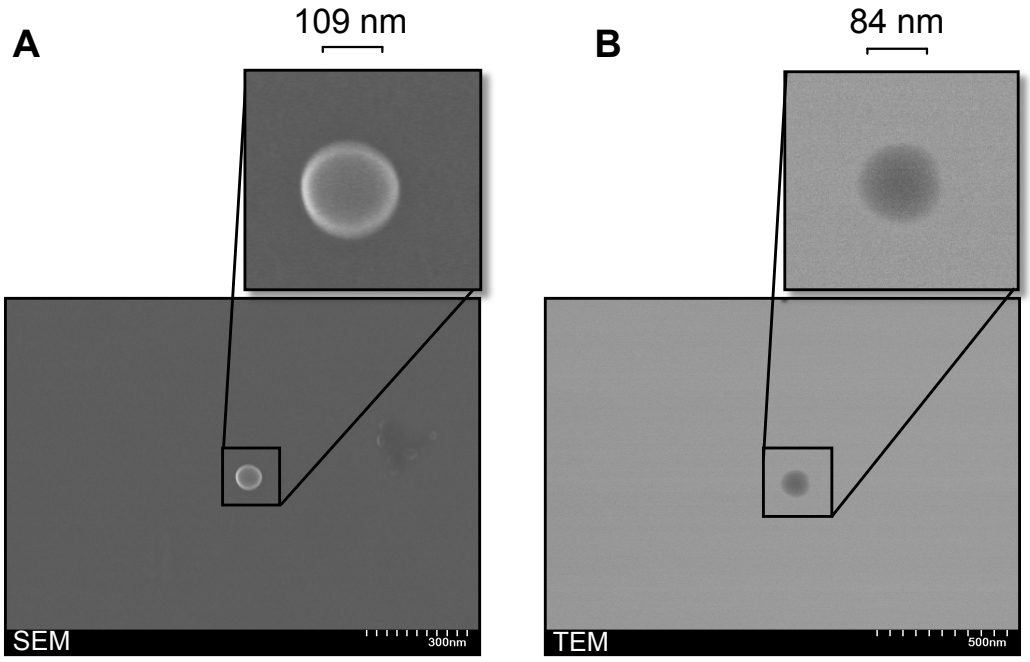


**Figure 5.10.** *Electron microscopy of lipid-polymer hybrid NPs.* Hp91-loaded lipid-polymer hybrid nanoparticles were deposited onto mesh copper grids, carbon-coated, and imaged with a Hitachi STEM. (**A**) Scanning electron microscopy of a representative nanoparticle. (**B**) Transmission electron microscopy of the same nanoparticle. Diameters of 3-4 NPs were measured by Hitachi STEM software and values shown above represent mean diameters for each microscopy method (SEM vs TEM).

### 5.3.10 Characterizing release profile of Hp91 lipid-polymer hybrid NPs

We next measured the stability of the Hp91 lipid-polymer hybrid NPs by performing release kinetics. After approximately 1 hour, 30% of the peptide is released from the hybrid-NPs at pH 7.4, compared to less than 10% at pH 5 (Figure 5.11A). By 4 hours, approximately 40% and 20% has been released respectively. Similar to with the old method PLGA-NPs, the lower pH results in a slower release of Hp91 over prolonger periods of time than at neutral pH (Figure 5.11A). After 10 hours, the release rate begins to flatten out for both pH conditions. After 24 hours, lipid-polymer hybrid NPs at

pH 7.4 have released approximately 45% of the Hp91 peptide, while at pH 5, approximately 30% of the peptide is released.

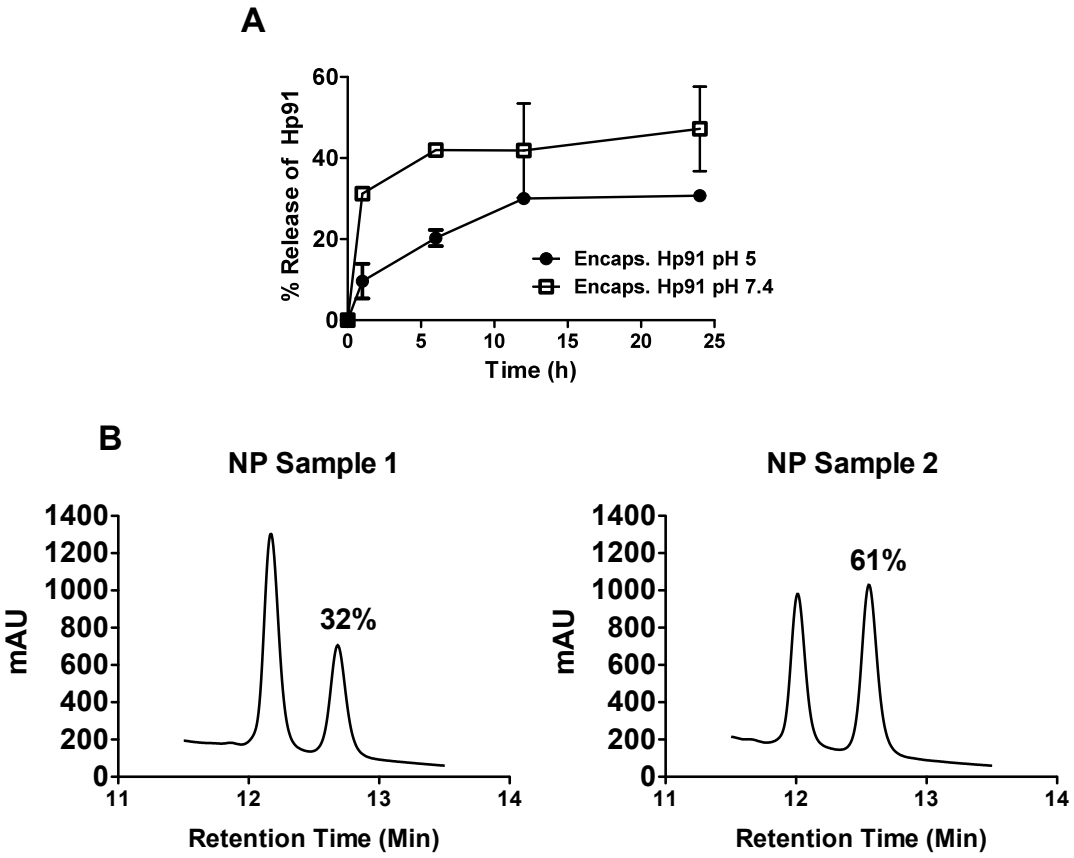


**Figure 5.11.** *HPLC: Release kinetics and dimer formation in Hp91-loaded lipid-polymer hybrid NPs.* (**A**) Normalized peptide release kinetics from Hp91 loaded lipid-polymer hybrid NPs at pH 7.4 and pH 5 over 24 hours. The peptide encapsulation quantity at time 0 was set as 100%. Samples were taken at indicated time points, and the amount of peptide was quantified by HPLC. Data shown are mean ± SEM of triplicate measurements (credit: C. Clawson). (**B**) Hp91 was loaded into lipid-polymer hybrid NP. NP were dissolved and Hp91 was analyzed by HPLC for formation for dimers. Percent dimer was determined by measuring the AUC and calculating the dimer AUC/total AUC. Samples are representative of the range of dimer observed with greater than 10 batches.

### 5.3.11 Nanoparticle synthesis promotes Hp91-dimer formation

As Hp91 encapsulation is determined by HPLC against a standard curve, we were consistently evaluating and quantifying lipid-polymer hybrid NP batches by HPLC. Freshly prepared Hp91 standards showed a predominantly single peptide peak

running off the column near 12 minutes with 0-10% of peptide in the dimer configuration (data not shown and Figure 4.1A). In contrast, Hp91 lipid-polymer hybrid NP batches consistently showed two peaks, representative of a Hp91-monomer near 12 minutes and a Hp91-dimer running off the column between 12.5 and 13 minutes (Figure 5.11B). The AUCs were calculated and Hp91 dimer formation within the NPs ranged from 30-60%. Representative NP batches are shown in Figure 5.11B. Nanoparticle synthesis and subsequent dissolving for Hp91-NPs takes up to 7 hours total, and according to the air oxidation dimerization curve (Figure 4.1B), the total dimerization during this time should be under 10%. This is in stark contrast to the observed 30-60% dimerization, suggesting that nanoprecipitation synthesis promotes dimerization of Hp91 peptide. In addition, as we have previously demonstrated that freeze/thaw of free Hp91 peptide does not result in dimer formation (data not shown), the dimer peak observed with these NPs is not due to a freeze/thaw.

### 5.3.12 Delivery of Hp91 inside of lipid-polymer hybrid NPs leads to increased activation of human DCs.

We have shown that delivery of Hp91 inside of old method PLGA-NPs leads to increased activation of human DCs (Figure 5.6A). We next tested whether Hp91, when packaged inside of the newer nanoprecipitated lipid-polymer hybrid NPs, would similarly activate human DCs. Immature human DCs were exposed to free Hp91 peptide or lipid-polymer hybrid NPs with an equivalent amount of Hp91 peptide. Culture supernatants were collected after 48 hours and analyzed for the presence of IL-6 by ELISA (Figure 5.12). Hp91-lipid-polymer hybrid NPs at 0.9 μg/ml, 1.8 μg/ml, and 3.6 μg/ml significantly increased secretion of IL-6 by DC as compared to free Hp91 peptide controls. On average, encapsulating Hp91 within lipid-polymer hybrid NPs

increased IL-6 secretion by greater than 7-fold (Figure 5.12). A 7-fold increase in IL-6 seen with the lipid-polymer hybrid NPs is very comparable to the 5-fold increase in IL-6 secretion seen with Hp91 loaded inside of the old method PLGA-NPs. Empty lipid-polymer NPs did not induce significant IL-6 expression (data not shown).

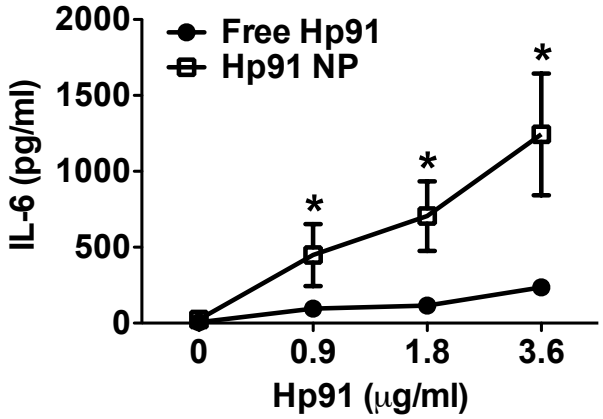


**Figure 5.12.** *Packaging Hp91 inside of lipid-polymer hybrid NPs increases its potential to activate human DCs*. Immature human DCs were exposed to increasing doses of free Hp91 or the same amount of Hp91 delivered inside of lipid-polymer NPs and incubated for 48 hours. Supernatants were analyzed for the presence of IL-6 by ELISA. Data shown are mean (±SEM) of three independent experiments using DCs from different donors. Asterisks, $p < 0.05$; Student's *t*-test (credit: D. Futalan).

### 5.3.13 Delivery of Hp91 inside of lipid-polymer hybrid NPs leads to increased adjuvant potential *in vivo*

We demonstrated in Chapter 2 that Hp91 acts as adjuvant *in vivo* to induce antigen-specific cellular immune responses to peptide antigen. Next we tested if immunization with Hp91 encapsulated within lipid-polymer hybrid NPs (174 μg) resulted in an increased cellular immune response to co-injected OVA-1 (SIINFEKL) peptide as compared to free Hp91 peptide. Though empty lipid-polymer hybrid NPs had not induced IL-6 secretion from DCs, we included a group where mice received empty lipid-polymer hybrid NPs, co-injected with OVA-1 peptide to confirm that the empty NPs, similar to *in vitro*, did not exert immunostimulatory adjuvant effects.

Mice were primed and boosted once, using a schedule identical to the schedule used for the early of immunizations in Chapter 2. The free Hp91 dose used in this immunization (174 μg) was selected to match the highest dose that could be injected into mice using the Hp91-loaded NPs. This dose (174 μg) is lower than the 250 μg dose determined necessary for significance using this prime/boost schedule (Figure 2.2D).

As expected, this reduced dose (174 μg) of free Hp91 peptide did not induce a significant increase in the number of antigen-specific IFN-γ secreting T cells compared to the PBS group when splenocytes were restimulated with the OVA-1 peptide in an ELISpot assay (Figure 5.12A). When a matched dose of Hp91 was delivered in the lipid-polymer hybrid NPs however, there was a significant increase in the number of OVA-specific IFN-γ secreting T cells compared to both PBS ($p < 0.05$) and empty NP groups ($p < 0.01$) (Figure 5.13A), suggesting that delivering Hp91 within NPs increases its adjuvant potential.

To further evaluate the OVA-specific cellular immune response in mice immunized with lipid-polymer hybrid NPs, we cultured expanded splenocytes overnight with OVA-1 peptide and measured the number of Granzyme B spot forming cells. Granzyme B is a serine protease stored in granules and released by cytotoxic T cells and NK cells during cellular responses, thus its release is another measure of the antigen-specific CTL response. Mice receiving Hp91 delivered within the lipid-polymer hybrid NPs showed a significant increase in the number of OVA-specific Granzyme B secreting T cells compared to PBS ($p < 0.05$) (Figure 5.13B). Though not significant, the cellular Granzyme B response in the Hp91-NP group was also higher than in the empty NP group and matched dose free Hp91 group. The matched dose free Hp91 group, while increasing the number of Granzyme B

secreting cells by approximately 25 spots, failed to achieve significant increase over the PBS group. This was likely a result of: 1) the reduced Hp91 dose of 174 μg versus the usual 250 μg or 2) because the background of the PBS group was quite high. The high background number of Granzyme B-secreting cells in the PBS group (mean 154) was possibly due to the 5-day splenocyte expansion with OVA antigen prior to the ELISpot assay.

IL-2 secretion from the freshly-isolated splenocytes of immunized mice was evaluated as a measure of the activation, survival, and proliferation of T lymphocytes. Similar to what was observed in the IFN-γ and Granzyme B assays, delivering the Hp91 adjuvant within the lipid-polymer hybrid NPs resulted in a significant increase in IL-2 secretion as compared to the PBS control (Figure 5.13C). IL-2 secretion from the Hp91-NP group was 5-fold higher than the PBS group, and nearly 4-fold higher than the empty NP group. The free peptide Hp91 group also showed a 5-fold increase in IL-2 secretion compared to PBS controls, however this increase was not significant.

We next tested the serum of immunized mice in an anti-Hp91 ELISA to determine if mice developed antibodies against the Hp91 peptide. We wanted to ensure that antibodies were not developed toward Hp91 as it is derived from an endogenous protein, HMGB1, and we believed that encapsulating Hp91 within NPs might increase the potential for a humoral response. As we desired, no mice in this immunization mounted an anti-Hp91 IgG response (Figure 5.13D), suggesting: 1) that mice receiving free Hp91 immunostimulatory peptide do not mount an antibody response against Hp91 and 2) that mice receiving Hp91 delivered within lipid-polymer hybrid NPs do not mount a humoral response against the Hp91. In contrast, the multiple antigenic peptide system (MAP), a known stimulator of humoral immune responses and positive control in this anti-Hp91 assay, elicited strong anti-MAP

immune responses when mice were immunized with the MAP in place of Hp91 peptide (Figure 5.13D).

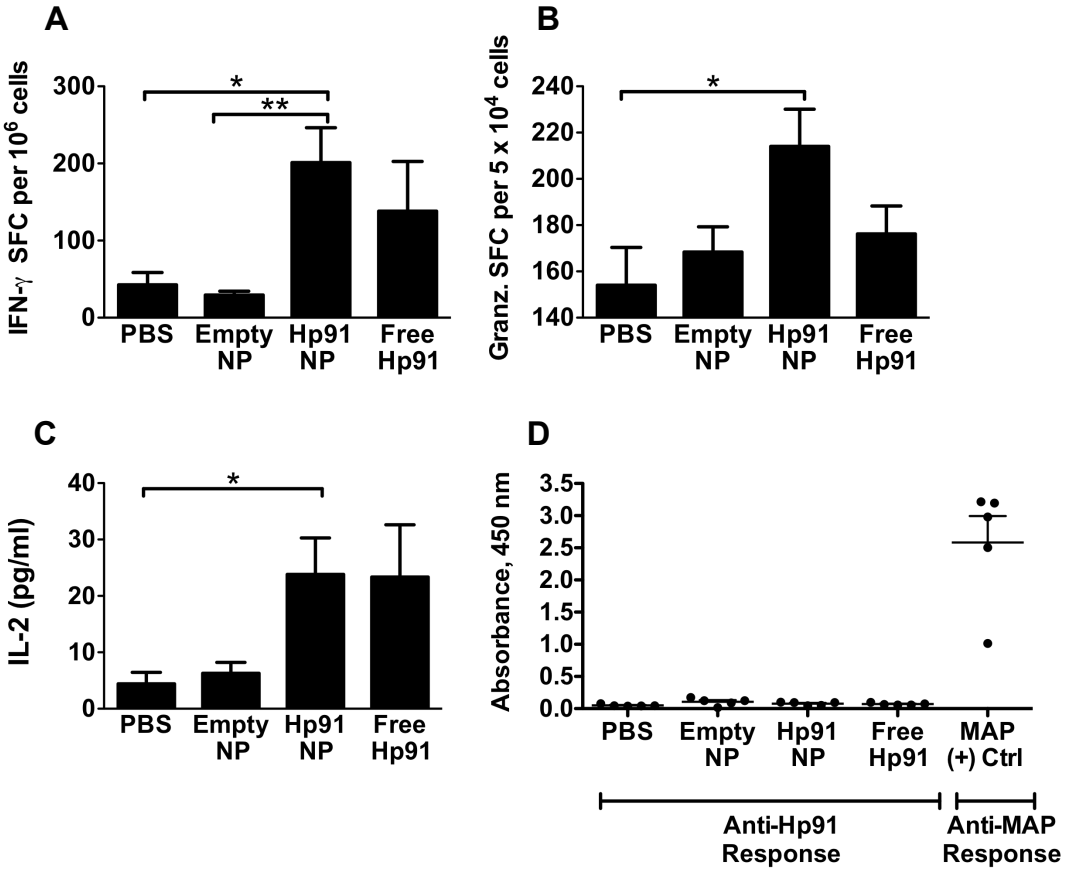


**Figure 5.13.** *Packaging Hp91 Inside of Lipid-Polymer Hybrid NPs Increases Adjuvant Potential in vivo*. (**A-D**) Mice were immunized with OVA peptide (SIINFEKL) in PBS or with empty NP, Hp91-loaded lipid-polymer hybrid NPs (174 μg), or free Hp91 (174 μg). Mice were boosted once and were sacrificed one week post-boost. Splenocytes were cultured in the presence of OVA-I (SIINFEKL) peptide (2.5 μg $ml^{-1}$) (**A**) overnight in an IFN-γ ELISpot assay, (**B**) overnight in a Granzyme B ELISpot assay, or (**C**) overnight in a cytokine release assay wherein supernatants were analyzed by ELISA for IL-2. (**D**) Serum was obtained from immunized mice at sacrifice and analyzed for Hp91 antibody levels by ELISA as follows. A 1:25 dilution of the serum from immunized mice was added to the pre-coated plates, followed by a peroxidase-conjugated anti-mouse IgG antibody. Plates were developed with TMB substrate and absorbance was analyzed on a microplate reader. Asterisks, *$p < 0.05$, **$p < 0.01$; Student's t-test. 4-5 mice/group.

### 5.3.14 Immunization with UC1018 Lipid-Polymer Hybrid NPs Delays Tumor Growth and Prolongs Survival

We demonstrated that mice mounted significant CTL responses against OVA antigen when co-delivered with Hp91-NPs. Next, we aimed to incorporate such adjuvant-loaded NPs into a prophylactic cancer vaccine in an attempt to delay tumor formation and prolong survival, as antigen-specific immune responses are more meaningful if they translate into a survival advantage. Instead of using Hp91 peptide, the short peptide UC1018 was delivered within lipid-polymer hybrid NPs. Mice in the treatment group received a single injection of UC1018-NPs co-injected with apoptotic B16 cells, followed by two boosts of apoptotic B16 cells in PBS.

Mice were challenged one week post-boost with highly lethal live B16 melanoma cells. This NP immunization was performed concurrent with the B16 challenge in Chapter 2, thus the PBS tumor growth and survival curves are the same as those shown previously. Briefly again, the PBS control mice demonstrated tumor formation within 7-10 days, rapid tumor growth, with the first death at day 16 post challenge (Figure 4.4G and Figure 5.14A). In contrast to the PBS group, the UC1018-NP immunized group demonstrated a delay in tumor formation and slowing of tumor growth, significant as early as 10 days post challenge (Figure 5.14A), indicating an induction of significant protective antitumor immunity in the UC1018-NP immunized mice. The mice were monitored for survival, and mice that received the UC1018-NP prophylactic treatment demonstrated a significantly prolonged survival. Median survival in the UC1018-NP group was 32 days post challenge, compared to only 19 days in the PBS group (Figure 5.14B). This data, combined with the prior research showing additional boosts increases cellular immune responses (Figure 2.9), suggests that additional boosts with UC1018-NPs would more significantly prolong survival.

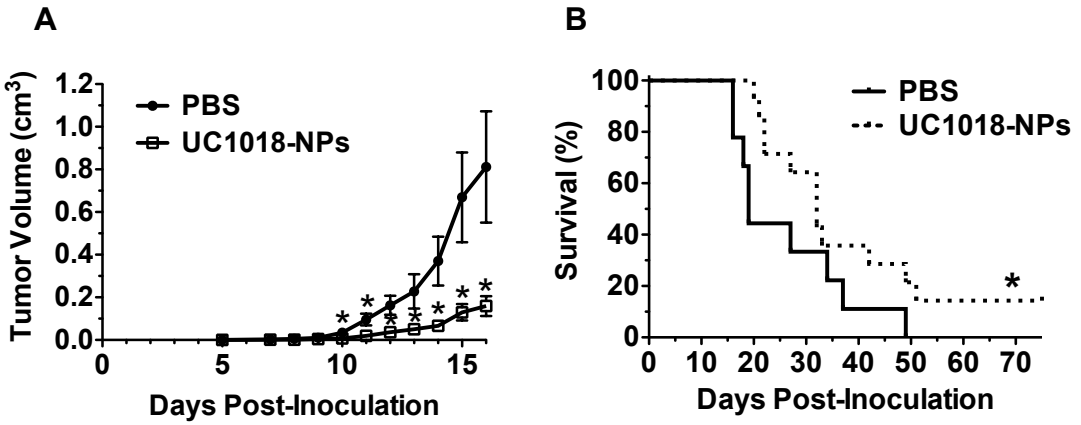


**Figure 5.14.** *Immunization with Hp91 lipid-polymer hybrid NPs retards tumor growth and prolongs survival.* Mice were immunized s.c. with apoptotic mitomycin-C treated B16 cells co-injected with PBS (negative) or UC1018 peptide delivered in lipid-polymer hybrid NPs (24 μg UC1018) and boosted twice with apoptotic B16 cells in PBS. One week post-boost, mice were inoculated s.c. on the flank with $5x10^5$ live B16 cells. (**A**) Tumor dimensions were measured using calipers and the tumor volume calculated using the following formula; volume = $4/3\ \pi\ (a^2 \times b)$. The data shown is mean (±SEM) for at least 14 mice/group. *$p < 0.05$ compared to PBS; Student's *t*-test at each time point. (**B**) Mice were euthanized when tumor volume reached 1.5 $cm^3$. Tumor survival curves were generated, wherein the day of euthanasia was considered as death. *$p < 0.05$ compared to PBS; Gehan-Breslow-Wilcoxon test.

The B16 melanoma model has flaws: 1) the tumor is inoculated into the mouse instead of forming spontaneously and 2) the tumor inoculation can be timed to the peak of the immune response when antitumor responses are likely strongest. In contrast, FVB.N*neu* (HER2) transgenic mice spontaneously form breast tumors, and immunized mice must rely on immunological memory to prevent tumor growth and prolong survival. In our first HER2 experiment, we immunized mice and cultured fresh splenocytes in an ELISpot assay to ensure we could develop an HER2 specific IFN-γ cellular immune response in immunized mice. Mice receiving Hp91-NPs demonstrated a significant increase in IFN-γ secreting cells compared to PBS and dose-matched free Hp91 groups (Figure 5.15A). The significant cellular response observed in the Hp91-NP group was encouraging and we hypothesized that FVB.N*neu* mice

receiving Hp91-NPs in a prophylactic HER2 vaccine might mount a cellular response strong enough to prolong survival.

We immunized FVB.N/*neu* mice at 2 months of age with HER2 peptide antigen, co-delivered with PBS, low-dose Hp91, or a matched dose of Hp91 delivered in lipid-polymer hybrid NPs. Mice were followed for tumor growth and survival. Mice in the PBS and free Hp91 groups started developing tumors considerably sooner than mice in the Hp91-NP group (159 -166 days, compared to 200 days in the NP group) (Figure 5.15B). 100% of PBS mice developed tumors by 160 days, and by 310 days no PBS mice remained alive (Figure 5.15B, C). The low-dose free Hp91 group performed slightly better, but the real improvement was seen with the NP group. 20% of the mice in the NP group remained tumor-free until 450 days, though this is not a significant increase over controls (Figure 5.15B). A similar trend is observed for the survival curve (Figure 5.15C).

**Figure 5.15.** *Immunization with Hp91 Lipid-Polymer Hybrid NPs Enhances CTL Response and Retards Tumor Development.* (**A**) HER-2/neu-transgenic mice at 2 months of age were immunized and boosted twice with 5 μg HER2 peptide in PBS, or with 25 μg Hp91 free peptide or the same amount of Hp91 packaged within lipid-polymer hybrid NPs. One week post-boost, mice were sacrificed. Expanded splenocytes were cultured overnight in the presence of HER2 peptide in an IFN-γ ELISpot assay. Data shown represents the means (±SEM) for 5 mice per group. Asterisks, $*p < 0.05$, $***p < 0.001$; Student's *t*-test. (**B**) At 2 months of age, mice were immunized with 5 μg HER2 peptide in PBS only or with 25 μg of Hp91 free peptide or the same amount of Hp91 delivered in lipid-polymer hybrid NPs. After final immunization, mice were monitored twice a week for tumor growth and survival. Percentages of tumor-free mice were calculated as (total mice without tumor)/(number of mice at the start of the experiment). (**C**) Mice were sacrificed once tumor masses exceeded 1.5 cm mean diameter and survival was analyzed considering day of sacrifice as death (credit: D. Futalan).

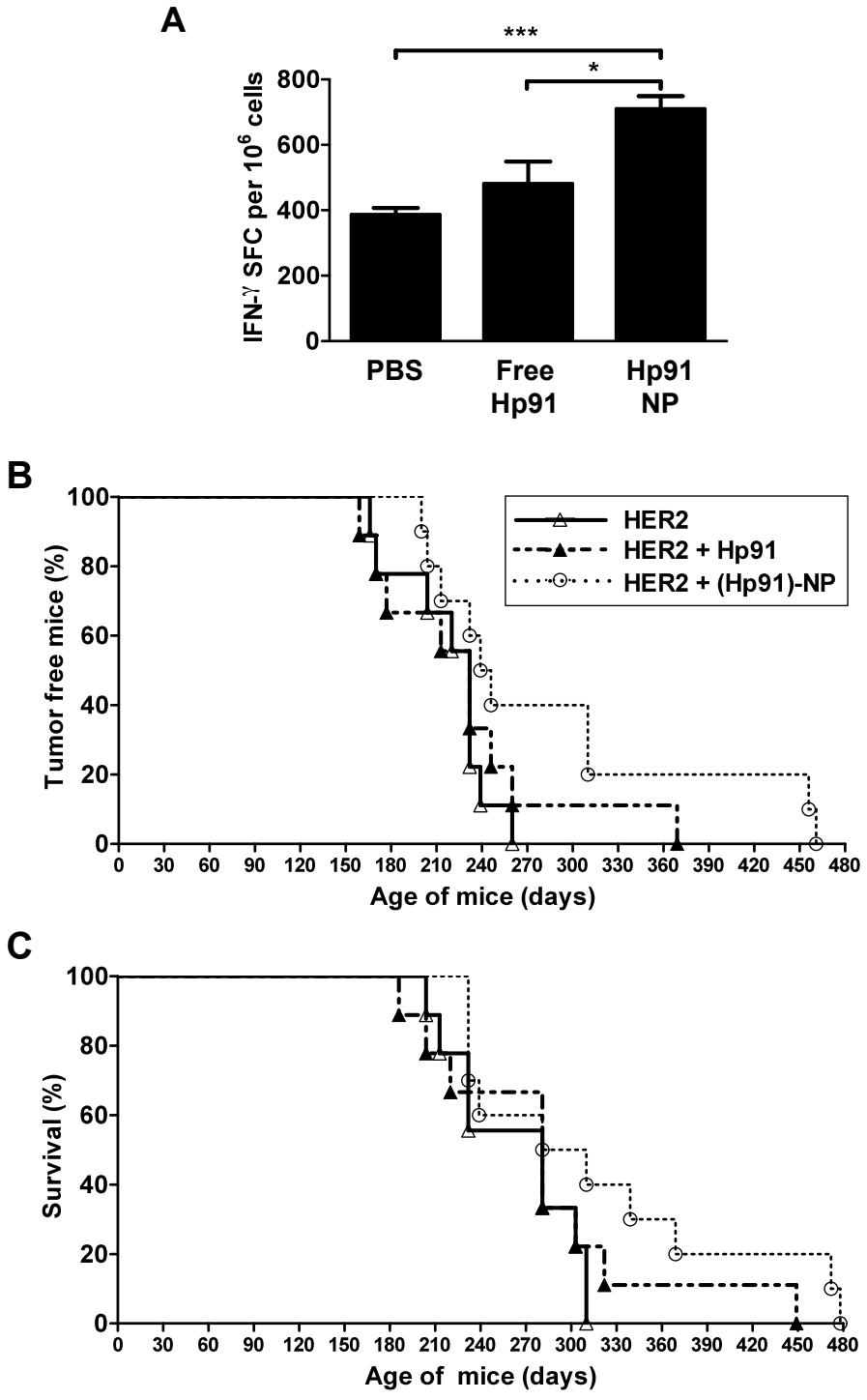
A
***
*
IFN-γ SFC per 10^6 cells
800
600
400
200
0
PBS
Free Hp91
Hp91 NP
B
HER2
HER2 + Hp91
HER2 + (Hp91)-NP
Tumor free mice (%)
100
80
60
40
20
0
0 30 60 90 120 150 180 210 240 270 300 330 360 390 420 450 480
Age of mice (days)
C
Survival (%)
100
80
60
40
20
0
0 30 60 90 120 150 180 210 240 270 300 330 360 390 420 450 480
Age of mice (days)

### 5.3.15 Hp91-induced IL-6 secretion is dependent on the endosomal receptor, TLR9

Release kinetic profiles show that in a low pH buffer (pH 5), Hp91 is released from within NPs over a prolonged period of time (Figure 5.4, 5.11A). NPs enter dendritic cells and macrophages via endocytosis and are subjected to a similarly low pH within the endosomes. We theorized that when Hp91-NPs enter endosomes, such a prolonged release of Hp91 occurs, and this prolonged Hp91 release and subsequent signaling explains the enhanced immunostimulatory effects observed by delivering Hp91 within nanoparticles both *in vitro* and *in vivo*. We had a clear problem with this theory however. In Chapter 3, we demonstrated Hp91 dependence on the cell surface receptor TLR4. If Hp91 is released directly into endosomes however, it has missed the opportunity to signal at the cell surface via TLR4.

Reports have indicated that the parent molecule HMGB1, in addition to binding TLR4, also binds to TLR9 (53-55), which is located within endosomes. We used TLR knockouts to investigate whether Hp91 is also dependent on TLR9. BM-DCs were generated from wildtype and knockout mice. Cells were exposed to Hp91 and supernatants were collected for IL-6 secretion. IL-6 secretion was significantly reduced in BM-DCs from TLR9 knockout mice (Figure 5.16), though not to the same extent as was observed with TLR4 knockout mice. This data suggests that Hp91 activity is dependent on several receptors, including TLR4 at the cell surface in addition to TLR9 within endosomes where NPs likely reside.

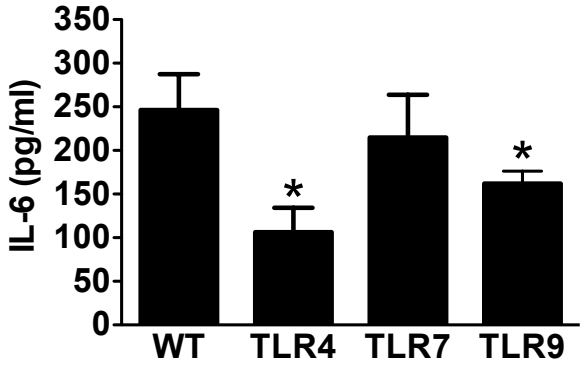


**Figure 5.16.** *Hp91-mediated activation of mouse cells is dependent on TLR9.* Immature BM-DCs from wild type (WT) or knockout mice (as indicated) were incubated with Hp91 (200 μg $ml^{-1}$). Supernatants were collected after 24 hours and analyzed for the presence of IL-6 by ELISA. Results are mean (±SEM) for at least 3 independent experiments. *$p < 0.05$ compared to WT; Student's *t*-test.

## 5.4 Discussion

Nano- and microparticles are being evaluated as vaccine carriers. They are very attractive platforms for vaccine delivery since antigen and adjuvant can be co-delivered to antigen presenting cells such as DCs. It has been shown that the generation of CD4 T cell epitopes requires antigen and TLR agonist (adjuvant) to co-translocate to the endosomes (63) and co-delivery of CpG-ODN together with antigen in PLGA microparticles lead to effective cross-presentation and antigen-specific CD8 T cell responses *in vivo* (148). Another advantage of using micro- or nanoparticles (NPs) is that the cargo can be protected from degradation by serum or tissue proteases and the co-delivery of antigen and adjuvant ensures that a DC will always encounter both. This is very critical as the uptake of antigen in the absence of adjuvant can lead to generation of tolerance (149), which has to be avoided/minimized to achieve activation of effective immune responses. This is

particularly important when trying to break tolerance in the context of a self antigen for cancer immunotherapy.

Although some materials carry intrinsic adjuvant properties like pluronic-stabilized polypropylene sulfide which activates the immune system via the complement cascade (150) or poly(g-glutamic acid) (67, 151), addition of adjuvants into NPs should further increase immune responses. In some situations inert materials might be preferable as one can control the type of immune response by selecting appropriate adjuvants for incorporation or attachment. Adjuvants like monophosphoryl lipid A (133), as well TLR agonists: CpG (134, 148, 152), and poly(I:C) (153, 154) have been packaged inside micro- and nanoparticles. Although microparticles show efficacy, depending on the route of application, nanoparticles could be of further advantage. Different size NPs are preferably taken up by different cell types. For example 40-50 nm NPs are predominantly taken up by DCs, 20 nm NPs by B cells, and 1 mm NPs by monocytes/ macrophages (155). Furthermore, it has been shown that 40 nm, but not 750 nm or larger NPs enter epidermal CD1a+ cells after transcutaneous application on human skin (156).

We have previously shown that the 18 aa long ISP Hp91 is a potent stimulus for mouse and human DCs (104) and acts as adjuvant *in vivo* to induce cellular and humoral antigen-specific immune responses to peptide and protein antigen (91). In an effort to further develop Hp91 as vaccine adjuvant we tested whether it could be incorporated into or conjugated to the surface of NPs. PLGA was chosen as a material for our NPs, since it is a biodegradable and biocompatible polymer (135-138) that has been employed for numerous *in vivo* applications (139-141). In addition to PLGA, we synthesized our lipid-polymer hybrid NPs with lecithin and a synthetic phosphatidylethanolamine (DSPE). Lecithin is a mixture of phospholipids that more

closely resemble the make up of a real cell membrane. The synthetic DSPE was added after optimization studies to stabilize the NPs.

We synthesized PLGA-NPs that were loaded with Hp91 peptide or that carried it on the surface via conjugation. We measured the amount of peptide loosely attached to the surface in the process of synthesized PLGA-NPs with peptide conjugated to the surface and found that approximately 4.4% of the Hp91 peptide dissociated from the PLGA particles after sonication, suggesting that it was not conjugated but loosely attached. Although sonication increased the amount of peptide released from the particles, the overall amount was still very low, indicating that the Hp91 is in fact covalently attached to the PLGA particles and not just loosely adsorbed to the surface. In addition to releasing any peptide loosely associated with the PLGA particles, sonication of the particles is likely to break up some particles, thus releasing a small amount of peptide. Therefore, we cannot firmly conclude that the 4.4% are truly loosely attached. However, the percentage released is small compared to the amount retained.

We found that Hp91, when packaged inside or outside of PLGA-NPs activates both mouse and human DCs. In both cases the DC stimulatory capacity was higher when the peptide was delivered via NPs as compared to free peptide. One possible explanation is that the delivery is more efficient, since the NPs are readily taken up by DCs and each NP will deliver many peptides, whereas free peptide will diffuse around the cells and the uptake is much less effective. In addition packaging of Hp91 inside of PLGA-NPs or conjugation to the surface most likely protects the peptide from degradation. The increase in Hp91 potency when delivered via NPs could be due to enhanced delivery into intracellular compartments that contain TLR9, which Hp91 is dependent upon.

The peptide release characteristics show that at pH 5 the peptide is released slower than at pH 7.4. One possible reason for this is due to the protonation of carboxyl groups on the peptide at lower pH values, which would make the peptide less polar and therefore more likely to remain encapsulated in the hydrophobic polymer core. The slow release at pH 5, which is present in endosomes could also contribute to the increased activity of the peptide, as a DC might carry a reservoir that is slowly released and can exert the effect on DCs over a prolonged period of time within the cell. The peptide conjugated to the surface of the PLGA spheres is released slower than the peptide only encapsulated by the PLGA. This is expected as the peptide is covalently linked to the PLGA and must either be cleaved off the PLGA or the PLGA must be sufficiently degraded to be released from the particle.

Furthermore, Hp91 peptides conjugated to the surface of NPs could potentially cross-link a receptor to increase binding affinity, lead to adaptor recruitment, and ultimately to stronger DC activation (125). Cross-linking would explain the increased IL-6 secretion and enhanced immune responses observed with not just NPs, but also peptide dimers and tetramers described in Chapter 4. It is more difficult to explain how NPs delivering Hp91 in the core are able to activate DCs. When Hp91 is packaged inside of NPs, the NPs not only maintain Hp91's ability to activate DCs, but show increased potency as compared to free peptide. Our NPs are taken up by dendritic cells (data not shown), suggesting that the receptor, or at least one receptor, is not on the cell surface, but most likely in an intracellular compartment, possibly endosomes. Several adjuvant binding receptors are located within endosomes, including TLR 3, 7/8 and 9 (157). While we have previously shown that activity is dependent on TLR4, uptake studies in TLR4 KO mice suggested that TLR4 is not the only receptor that Hp91 interacts with. We demonstrate here that Hp91

is additionally dependent on the endosomal receptor TLR9, possibly explaining why NPs loaded with Hp91 can maintain activity when endocytosed by DCs.

A 30-60% of Hp91 peptide was observed in the lipid-polymer hybrid NPs, as observed by HPLC. In Chapter 4, Hp91 dimers were shown to enhance the activity of Hp91. It is plausible that an element of the enhanced immune response observed with NP delivery of Hp91 may be due to the dimer population of Hp91 peptide. To test this theory, maleimide-capped Hp91 monomers or the alanine for cysteine substituted UC1018 (UC1018-6A) could be incorporated within NPs and tested for enhanced activity compared to free peptide controls of the same modified peptide.

Though *in vitro* assays are informative, ultimately, antitumor protection is what is most important. We show here that NP delivery of Hp91 delays tumor growth and increases survival in both melanoma and breast cancer mice models. The results are very promising. Especially exciting are the results from UC1018-NP immunized mice challenged with B16 melanoma. Mice received a single dose of UC1018-NPs, encapsulating 24 μg of UC1018 per mouse, which is 14% of the dose used for free UC1018 peptide immunizations (174 μg). After the one NP dose, mice had a significant survival advantage over PBS-immunized control mice. These data demonstrate a real potential for the development and formulation of HMGB1-based nanoparticle immunotherapies for cancer. Additionally, the lipid-polymer hybrid NPs are synthesized via a simple, scalable nanoprecipitation method that should make commercial manufacturing easily obtainable.

In conclusion, we show that HMGB1-derived peptide adjuvants, when delivered via three distinct types of NPs, not only maintain their ability to activate DCs, but NPs carrying these peptide adjuvants are stronger than free peptide in activating DCs *in vitro*. Additionally, hybrid NP formulations enhance the *in vivo* immune

responses. These data clearly warrant further exploration and formulation in vaccine settings.

Chapter 5, in part, is a reprint of the material as it appears in Nanomedicine, 2010, Corbin Clawson, Chien-Tze Huang, Diahnn Futalan, Daniel Martin Seible, Rebecca Saenz, Marie Larsson, Wenxue Ma, Boris Minev, Fiona Zhang, Mihri Ozkan, Cengiz Ozkan, Sadik Esener, and Davorka Messmer. The dissertation author was a major contributor to the synthesis of PLGA-NPs and dendritic cell activation experiments with PLGA-NPs. The dissertation was a co-author of this paper and helped with preparation of the manuscript, particularly methods and legends.

Chapter 5, in part, is currently being prepared into a manuscript for submission for publication. This manuscript includes the experiments with lipid-polymer hybrid NPs as related to the HER2 model. Diahnn Futalan, Rebecca Saenz, Ila Bharati, Daniel Seible, Marie Larsson, Liangfang Zhang, Davorka Messmer. The dissertation author was a major contributor to both the *in vitro* and *in vivo* experiments; helping with experimental design, training, execution, and manuscript preparation.

# 6. Manipulation of the Local Tumor Microenvironment ("Arm II")

## 6.1 Introduction

Researchers are increasingly understanding how to mount tumor-specific systemic immune responses, but the immune response does not always correlate with clinical responses (5, 6). The immunosuppressive tumor microenvironment interferes, on many levels, with the tumor infiltrating immune cells.

To eliminate a tumor, the immune system must "see" the cancer, activate tumor-specific CTLs, and the tumor must be susceptible to killing. This is often not achieved because of tumor evasion strategies wherein tumors evolve mechanisms to evade detection and killing, including the following: down-regulation of adhesion molecules; shedding of antigens into serum leading to tolerance; antigenic modulation or immunoselection; downregulation of MHC molecules; and perhaps most detrimentally, release of immunosuppressive cytokines such as TGFβ, IL-10, and VEGF (158-160). TGFβ, for example, suppresses many T cell functions such as differentiation, proliferation, and cytokine secretion. In addition, TGFβ polarizes tumor-associated neutrophils toward a pro-tumor phenotype, is released from pro-tumor macrophages to induce tissue remodeling and fibrosis, and it shifts the Th1-Th2 balance towards Th2 (158, 161).

Just as these tumor evasion strategies favor tumor escape from the natural immune surveillance, they also interfere with the antitumor immune response generated from cancer immunotherapy. Thus, many methods are being developed to counteract the immunosuppressive tumor environment, including systemic blockade of TGFβ, which has been demonstrated to slow tumor growth (158). Immune manipulation of the local tumor microenvironment may allow for a more potent, fully mediated immune response.

This chapter presents early research to demonstrate that Hp91 may be used locally to manipulate the tumor microenvironment. The data shown here is unique because tumor manipulation at a local level is in contrast to the immune-modulation currently underdevelopment which commonly uses TGFβ blockade, IL-2, IL-12, and/or interferons at a systemic level (160, 162, 163).

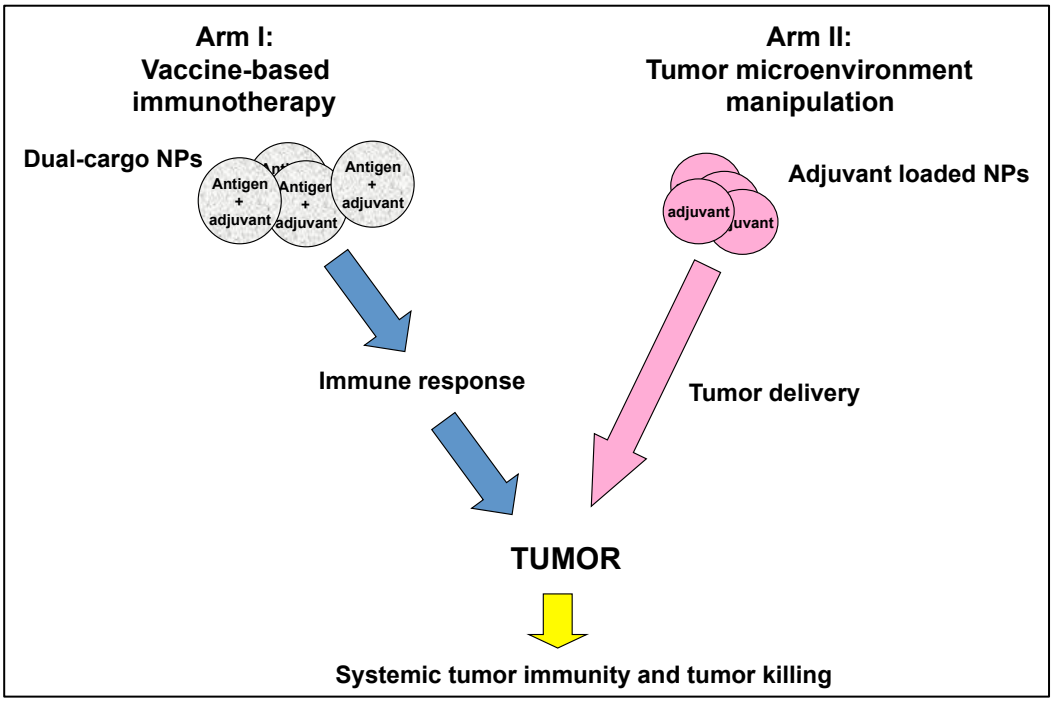


**Figure 6.1.** *Proposed anti-cancer therapeutic combining a vaccine-based immunotherapy (Arm I) with tumor microenvironment manipulation (Arm II).*

Ultimately, we theorize that to achieve significant antitumor protection over a large population, cancer immunotherapies must be combined with manipulation of the immunosuppressive tumor microenvironment. Our long-term goal is to develop a two-armed therapeutic anti-cancer regimen by merging an HMGB1-peptide adjuvant-based immunotherapy ("Arm I") with local tumor manipulation ("Arm II"). We anticipate NP formulations and tumor targeting will enable us to locally deliver this two-armed immunotherapy via the vasculature for effective treatment of metastatic malignancies with potential for long-term remission (Figure 6.1).

## 6.2 Materials and Methods

### 6.2.1 Peptides

Hp91 was synthesized from GenScript Corp (Piscataway, NJ, USA) and CPC Scientific (San Jose, CA, USA). Peptides were synthesized with an N-terminal biotin. Peptides were routinely synthesized with greater than 95% purity.

### 6.2.2 Animals and Cell Lines

C57BL/6 mice were purchased from Charles River Laboratories (Boston, MA, USA). Animals were housed at the Moores UCSD Cancer Center animal facility. All animal studies were performed with human care of animals and approved by the Institutional Animal Care and Use Committee of UCSD and were performed in accordance with the institutional guidelines.

The murine melanoma B16 cell line was previously described in Chapter 4, Materials and Methods.

### 6.2.3 Intratumoral injection with tumor monitoring

C57BL/6 mice were inoculated 2.5 x $10^5$ B16 melanoma cells on the flank. Mice were monitored for tumor growth daily and injections were started when mice had palpable tumors. Mice were injected intra-tumorally near the boundary with 2-3 sticks per tumor; 100 μl volume. The agents, including PBS, free Hp91 (100 μg), Hp91-NPs (hybrids) (Hp91 dose not quantified), and empty NPs (hybrids), were injected daily for 10 days and tumor volume was monitored over the indicated time period. Calipers were used to measure tumors in two perpendicular diameters and volume was calculated as volume ($mm^3$) = $(width)^2$ x length/2.

### 6.2.4 Intratumoral Injection with immunohistochemistry

C57BL/6 mice were inoculated with $10^6$ B16 cells. When tumors were approximately 1/3 inch in diameter, tumors were injected with PBS, poly(I:C) (10 μg) (InvivoGen, San Diego, CA), Hp91 (270 μg), Hp91-PLGA NPs (100 μg Hp91) or Hp91-liposomes (100ul; unknown quantity Hp91). Mice were sacrificed after 48 hours and tumors were removed, embedded in Tissue-Tek O.C.T. Compound (Sakura Finetek, Torrance, CA) and flash frozen in 2-methyl butane (Electron Microscopy Sciences, Hatfield, PA). Frozen tumors were cryosectioned with a cryostat-microtome onto glass slides. After 30 minutes of air drying, sections were fixed in acetone for 10 minutes, washed with PBS, and endogenous peroxidase was blocked with 0.03% $H_20_2$ (Fisher) in PBS for 30 minutes. The remaining steps were performed in a humid chamber. Endogenous biotin was subsequently blocked with an avidin/biotin blocking kit (Vector Laboratories, Burlingame, CA): sections were incubated in Avidin-D for 15 minutes, washed in PBS, then incubated in 0.1% biotin, followed by additional washes.

To reduce non-specific binding, sections were blocked in 1% BSA (Sigma-Aldrich) in PBS for 30 minutes. Sections were incubated for 30 min with biotinylated antibodies specific for Mac-1/CD11b, CD3, or CD11c (BD Pharmingen, BD Biosciences). After 3 PBS washes, sections were incubated with horseradish peroxidase-streptavidin (Jackson ImmunoResearch, West Grove, PA) for 30 min and then washed. Sections were developed with an AEC peroxidase substrate kit (Vector Laboratories) as per the manufacturer's instructions. Slides were counterstained in Mayer's Hematoxylin Solution (Sigma-Aldrich), washed in water, and gel mounted (Electron Microscopy Sciences). Slides were imaged on a Nikon Eclipse TE300 inverted microscope (Nikon Instruments).

### 6.2.5 Actin Polymerization Assay

Cell culture plates containing at least 5 x $10^5$ DCs/well were rested at 37° C in low serum medium for 1 hour. A staining solution with phalloidin-FITC (18% formaldehyde in PBS, 4x$10^{-7}$ M FITC-labelled phalloidin (Sigma-Aldrich, for staining actin polymers), and 0.5mg/mL 1-α-lysophosphatidylcholine (Sigma-Aldrich, for cell permeabilization)) was aliquoted into FACS tubes (40 μl per tube). DC plates (1 ml/well) were transferred to a heat block set at 37°C. 200 μl was removed from the well and pipetted into a FACS tube with staining solution for a 0 s time point. Hp91 (200 μg/ml) was added while rotating the culture plate. The reaction was stopped at the indicated time points by removing 200 μl of cells and pipetting into the FACS tube with staining solution. FACS tubes were incubated in the dark for 15 min at 37°C. Fixed cells were immediately analyzed by flow cytometry using the FACSCalibur (Beckon Dickinson, Franklin Lakes, NJ). Data were analyzed using the FlowJo software (Tree Star, Inc., Ashland, OR).

### 6.2.6 Statistical analysis

Data are represented as mean (±SEM) if not otherwise indicated. Data were analyzed for statistical significance using Student's t-test. p-values $< 0.05$ were considered statistically significant.

## 6.3 Results

### 6.3.1 Intratumoral Hp91 slows tumor growth

As Hp91 has been shown to be immunostimulatory and induce cytokines from a several of cell types, including DCs and macrophages, we aimed to determine if Hp91 had any *in vivo* immune effects when injected directly into the tumor. We theorized that Hp91 could act upon the tumor in several capacities, including acting directly on the tumor cells to promote growth or conversely to promote cytotoxicity, or Hp91 could act upon the tumor microenvironment, including infiltrating immune cells to either slow growth or enhance growth. Because of the large number of possible compounding effects, we did not know what to expect.

Mice were inoculated with B16 tumors and injected daily into the tumor with PBS or 100 μg of Hp91 for 10 days. Mice receiving daily intratumoral Hp91 peptide injections showed significant slowing of tumor growth after 8 days compared to mice receiving intratumoral PBS injections (Figure 6.2A). A similar delay in tumor growth was observed when Hp91 was delivered intratumorally within lipid-polymer hybrid NPs compared to empty NP control mice (Figure 6.2B).

### 6.3.2 Intratumoral Hp91 recruits immune cells

To begin to characterize the local effects of Hp91 on tumor microenvironment, we injected Hp91 intratumorally and removed tumors after 48 hours for immunohistochemistry staining. Tumors were sectioned and stained for macrophages (Mac-1), T cells (CD3), and DCs (CD11c). Positive cells are shown in red while the B16 tumor is counterstained to appear yellow/blue in color.

Mice injected with PBS as a negative control showed no infiltration of immune cells (Figure 6.3A,B). Poly(I:C), which served as a positive control for this experiment, recruited a large number of macrophages (Mac-1) to the tumor, but no T cells or dendritic cells (CD3 and CDIIc respectively) (Figure 6.3A). In contrast, free Hp91 peptide delivered in PBS to the tumor showed recruitment of macrophages, as well as T cells and pockets of DCs. This was surprising as the poly(I:C) positive control was not able to recruit all these cell types.

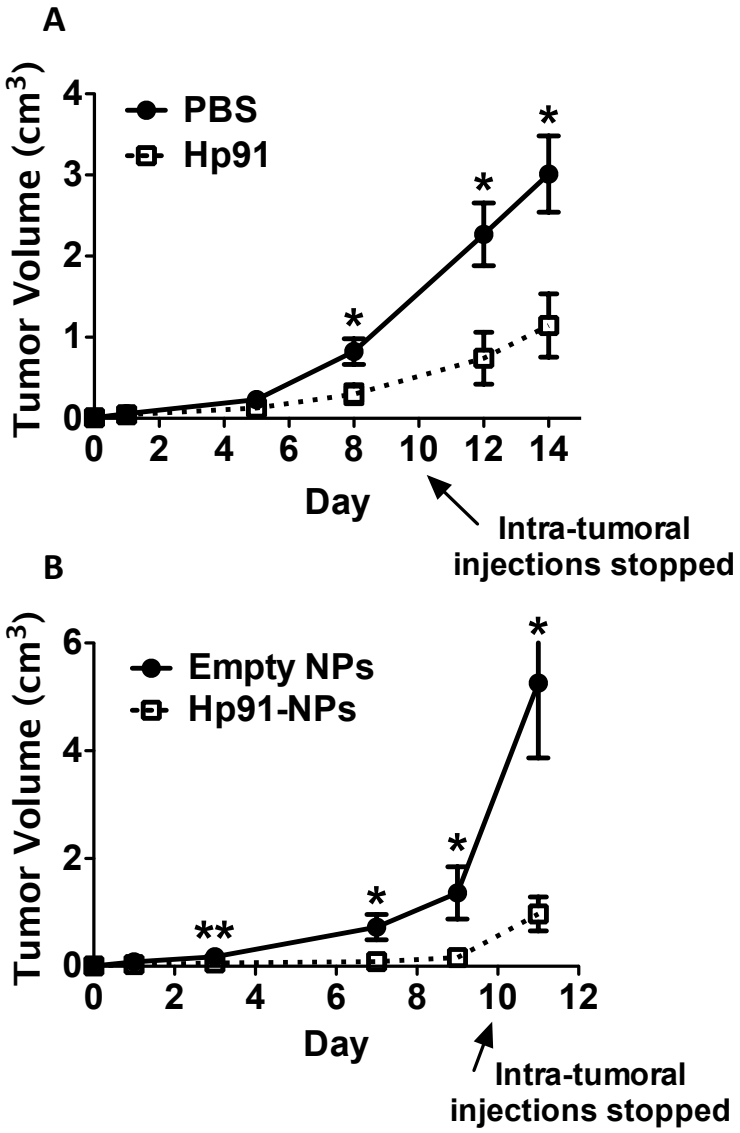


**Figure 6.2.** *Intratumoral injection of Hp91.* (**A**) Mice were injected intra-tumorally into B16 tumors with PBS or Hp91 peptide for 10 days. Growth was measured with calipers over the indicated time period. 5 mice/group. (**B**) Mice were injected intra-tumorally with empty or Hp91-loaded lipid-polymer hybrid NPs for 10 days. Growth was measured with calipers over the indicated time period. 5 mice/group. *$p < 0.05$, **$p < 0.01$; Student's t test compared to other group. (credit: C. da Silva Souza).

The experiment was repeated with Hp91 encapsulated in lipid-polymer hybrid NPs or liposomes to confirm that this immune cell recruitment was maintained with Hp91 in NPs. We show that intratumoral injection of both Hp91-loaded lipid-polymer

hybrid NPs and liposomes recruits macrophages to the tumor (Figure 6.3B). Staining for other cell types has not been completed.

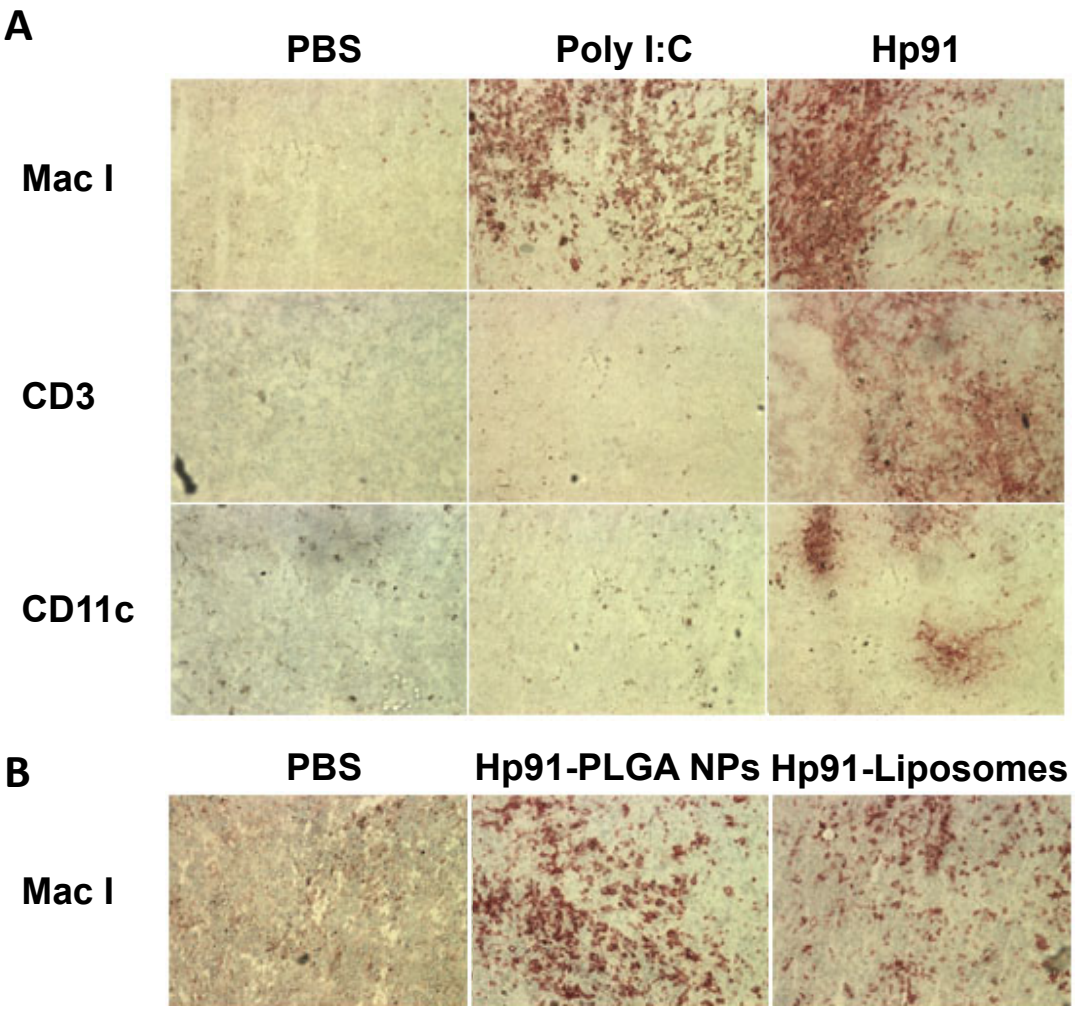


**Figure 6.3.** *Intratumoral Hp91 recruits immune cells.* (**A**) B16 tumors were injected intratumorally with PBS, poly(I:C), or Hp91. Tumors were removed 24 hours later, frozen, sectioned, and stained using biotinylated-antibodies specific to Mac-1, CD3, and CD11c. Positive cells were developed (red) using an AEC kit. Sections were counterstained with Mayer's Hematoxylin. Sections are representative of at least 2 mice/group. (**B**) B16 tumors were injected intratumorally with PBS, Hp91-NPs (100 μg Hp91), or Hp91-liposomes (Hp91 dose not determined) and stained as above for Mac-1.

### 6.3.3 Hp91 induces reorganization of the actin cytoskeleton

The Hp91-mediated recruitment of dendritic cells into the tumor microenvironment was encouraging. The parent molecule, HMGB1, is a chemokine and behaves as a trigger of inflammation, actively recruiting lymphocytes to the site of injury. Additionally, HMGB1 has been shown to recruit stem cells to sites of tissue repair (164). The recruitment of lymphocytes after intratumoral Hp91 injection suggests that the HMGB1-derived short peptide Hp91 additionally acts as a chemokine.

Reorganization of the actin cytoskeleton is an early event in the migratory response to chemokines. Thus, to observe if Hp91 has chemokine-type effects on DCs, we stimulated DCs with Hp91 and looked for transient changes in the actin cytoskeleton. Typically, a transient increase in f-actin polymerization can occur within seconds of exposure to a chemokine, followed by subsequent depolymerization. Phalloidin conjugated to FITC was used to detect actin polymerization by flow cytometry, since this molecule binds only to polymeric and oligomeric forms of actin and not to monomeric actin. 1-α-lysophosphatidylcholine was used at low concentration to permeabilize the cell surface membranes without complete lysis of the cells. DCs were exposed to Hp91, and within 15 seconds of exposure, approximately 30% of DCs showed f-actin polymerization, demonstrated by a right-shift in flow cytometry (Figure 6.4A). By 30 seconds, actin-polymerization appeared to peak and was observed in 100% of the DCs. By 60 seconds, the transient increase in polymerization was waning and within 4 minutes had returned to near normal levels. Calculated relative f-actin polymerization showed that at 30 seconds, there was over a 4-fold increase in f-actin polymerization.

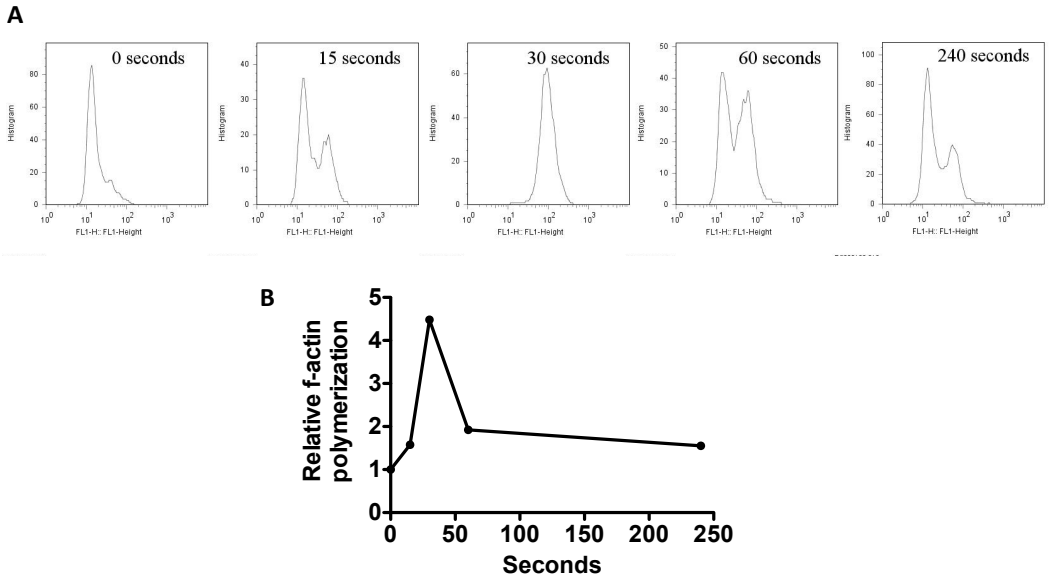


**Figure 6.4.** *Hp91-induced transient f-actin polymerization.* (**A**) DCs were exposed to Hp91 and cell samples were taken at 0 s, 15 s, 30 s, 60 s, and 260 s. Cells were stained immediately with FITC-phalloidin. (**B**) f-actin polymerization was normalized to the signal at time 0. Data are representative of at least 2 experiments.

## 6.4 Discussion

These data provide the first evidence that Hp91 may induce local manipulation of the tumor microenvironment. When injected intratumorally, Hp91, either free or delivered within NPs, delayed growth of B16 tumors. This effect could be due to a direct effect of Hp91 on tumor cells or due to an indirect effect such as recruitment of lymphocytes and possibly polarization of lymphocytes to an antitumor phenotype.

When tumor sections were stained 48 hours after intratumoral injection of Hp91, we observed recruitment of at least macrophages, T cells, and dendritic cells. This would suggest that the delay in tumor growth is likely due to recruitment of immune cells. It is not clear if these cells are pro-tumor or polarized to an antitumor

phenotype, thus additional experiments are warranted. For example, the infiltrating immune cells could be evaluated to look for antitumor polarization markers, such as Ly6G on Mac-1+ cells or downregulation of CCR2 on macrophages (158, 161). Additionally, we could use qPCR to measure cytokines and chemokines in the tumor, or flow cytometry to evaluate cell adhesion molecules in tumors.

The actin-polymerization experiment showed preliminary evidence that Hp91 acts directly on dendritic cells. Polymerization could additionally be evaluated in other immune cells, such as macrophages, T cells, neutrophils, and NK cells. This actin-polymerization only suggests there might be a migratory response to the ligand. Additional migration assays using transwell systems are needed to prove Hp91 directly mediates migration.

Additionally, the experiments performed in Chapter 6 did not test for a direct antitumor effect. To evaluate if a direct antitumor effect exists, cytotoxicity tests are needed.

In summary, the data here demonstrate proof of principle for Hp91-mediated local tumor modification. Long-term follow-up experiments, beyond the scope of this dissertation, include incorporation of tumor-targeting molecules for vascular delivery of Hp91-NPs, such as RGD or LyP-1 in development by collaborators at the UCSD Cancer Center (61, 165). We anticipate that the eventual combination regimen of tumor-modifying or tumor-conditioning nanoparticles with vaccine-based immunotherapy will help achieve protective immune responses in patients.

# 7. Conclusions and Future Work

Vaccine-based active immunotherapy holds promise as an effective treatment of metastatic malignancies with potential for long-term remission. It is clear that a Th1-type of immune response is preferred for tumor protection. Unfortunately, the most commonly used vaccine adjuvants are ineffective for cancer because they induce a mostly humoral Th2-type immune response with few or no tumor-specific cytotoxic T lymphocytes (4). Adjuvant research and development is critical for the advancement of cancer immunotherapy.

This dissertation introduces several new Th1-type peptide adjuvants derived from, or based upon, HMGB1 protein. Data are presented to demonstrate the following:

1. The basic principle: The HMGB1-derived Hp91 peptide acts as an adjuvant *in vivo* to induce Th1-type immune responses.

2. Hp91 characterization and mechanism of action:
   a. Hp91 is dependent on TLR4 and its downstream signaling pathways for activation of dendritic cells.
   b. Hp91 is taken up into dendritic cells via clathrin-mediated endocytosis.

3. Structure-function relationships:
   a. Peptide multimers enhance the activity of Hp91.
   b. The C-terminal domain of Hp91 is responsible for cellular uptake and immunostimulatory activity.

4. Nanoparticles enhance the DC stimulatory capacity and adjuvant potential of Hp91 and UC1018 peptides.

The work presented in this dissertation has proven that HMGB1-based peptide adjuvants can be formulated into vaccine immunotherapies that significantly delay tumor growth and prolong survival in mice. Future work is warranted to further develop these newly identified peptide adjuvants. The following sections summarize the data presented in this dissertation and discuss future work and additional applications, outside of the realm of cancer immunotherapy, for these HMGB1-based peptides.

## 7.1 Hp91 acts as adjuvant *in vivo*

We show that a short peptide, named Hp91, whose sequence corresponds to an area within the endogenous molecule High mobility group box (HMGB1) protein potentiates cellular immune responses to peptide antigen and cellular and humoral immune responses to protein antigen *in vivo*. Hp91 promoted the *in vivo* production of the immunomodulatory cytokines IFN-$\gamma$ and IL-12 (p70), among others, as well as antigen-specific activation of CD8+ T cells. These results provided the first evidence that HMGB1-derived peptides can act as adjuvant *in vivo*.

Additionally, we demonstrated that the adjuvant effect of Hp91 is sequence specific. We observed Hp91-induced antigen-specific immune responses that were stronger than those induced by Alum. We showed that additional boosts further increase the cellular immune response.

## 7.2 Characterizing Hp91

We investigated the underlying mechanisms of Hp91-mediated DC activation. Hp91 enters DCs via clathrin-mediated endocytosis. Hp91-induced secretion of IL-6 is

MyD88- and TLR4-dependent and is mediated through p38 MAPK and NFκB. Hp91-induced signaling is dependent on clathrin- and dynamin-mediated endocytosis of Hp91. The MyD88-independent interferon pathway is activated by Hp91 and is mediated through IRF3 phosphorylation. These signaling findings, summarized in Figures 7.1, elucidate the mechanisms by which Hp91 acts as immunostimulatory peptide. To date, the proteins shown in green have been investigated and implicated in Hp91's mechanism of action.

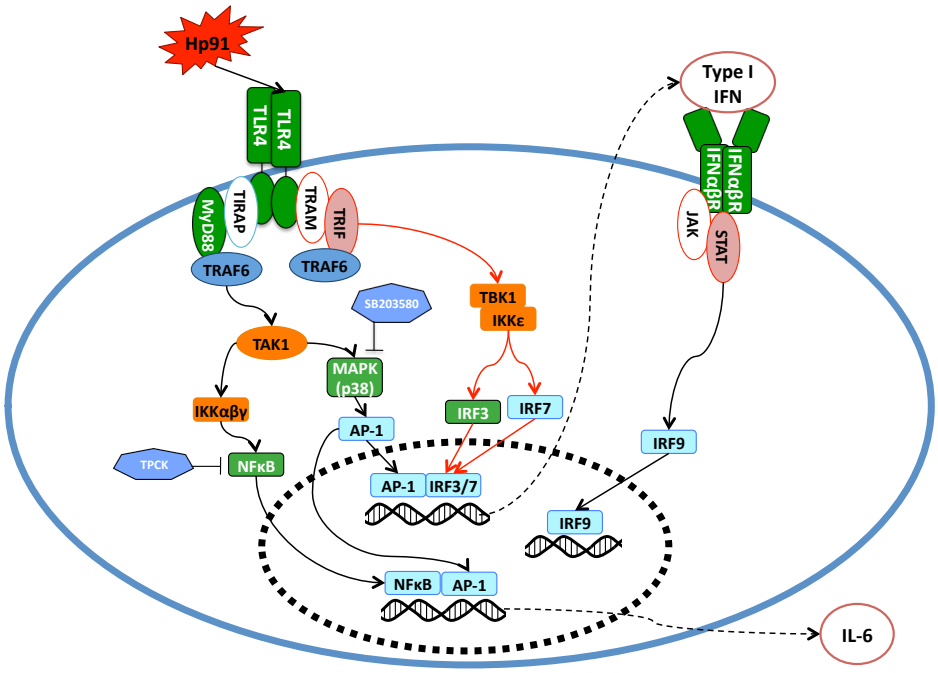


**Figure 7.1.** *Hp91 signaling summary.* Proteins in green have been implicated in Hp91-mediated activation of dendritic cells.

## 7.3 Structure-Function Relationships

We performed structure-function relationship studies on Hp91 peptide to investigate the amino acids and structure responsible for immune responses. We examined oxidation of the cysteine amino acid at position 16 of Hp91 and found that Hp91 spontaneously forms reversible dimers. Using maleimide cross-linked dimers

dimers, we showed that the Hp91 dimer, compared to monomer controls, has an enhanced ability to activate DCs and an increased ability to bind DCs. We demonstrate that the C-terminal 9 amino acids of Hp91, named UC1018, are sufficient for DC binding, induction of CTL responses and significant prophylactic antitumor protection *in vivo*. Perhaps the most impressive experimental findings were those of the melanoma challenge, wherein 60% of UC1018 immunized mice remained tumor-free after 75 days.

These findings help us understand what regions of Hp91 are important to promote its function as an immunostimulatory peptide adjuvant and may serve as a guide for the future development of synthetic Th1-type peptide adjuvants for vaccines.

## 7.4 Nanoparticle formulations enhance immunostimulatory activity

Nanoparticles (NPs) are attractive carriers for vaccines. We evaluated Hp91's activity when encapsulated in or conjugated to the surface of 3 types of NPs: **1**) liposomal NPs (liposomes), **2**) PLGA-NPs, and **3**) lipid-polymer hybrid NPs. Hp91, when encapsulated in or conjugated to the surface of NPs, not only maintained its ability to activate both human and mouse DCs, but was in fact more potent than free Hp91. *In vivo* IFN-γ cellular immune responses were stronger when Hp91 was delivered in NPs. As shown with two different mouse models, mice receiving prophylactic immunization with Hp91-NP vaccines showed delayed tumor growth and prolonged survival. Because of their capacity to enhance activation of DCs and act as adjuvant, such Hp91-NP systems are promising as delivery vehicles for vaccines against cancer.

## 7.5 Two-arm immunotherapy approach

The immunosuppressive tumor microenvironment presents a challenge that currently inhibits cancer immunotherapy and must be overcome to see improved antitumor responses (166). Hp91 injected intra-dermally induces the production of Th1-type cytokines (data not shown), thus is capable of exerting local immunostimulatory activity. More importantly, we have shown that intra-tumoral injection of Hp91 slows the growth of B16 tumors (Figure 6.2). Additionally, Hp91 injected locally induces infiltration of immune cells, such as macrophages, T cells, and dendritic cells, into the tumor.

Ultimately, we theorize that to achieve significant antitumor protection over a large population, cancer immunotherapies must be combined with manipulation of the immunosuppressive tumor microenvironment. Our long-term goal is to develop a two-armed therapeutic anti-cancer regimen by merging an HMGB1-peptide adjuvant-based immunotherapy ("Arm I") with tumor manipulation ("Arm II"). We anticipate NP formulations and tumor targeting will enable us to deliver this two-armed immunotherapy via the vasculature for effective treatment of metastatic malignancies with potential for long-term remission (Figure 7.2).

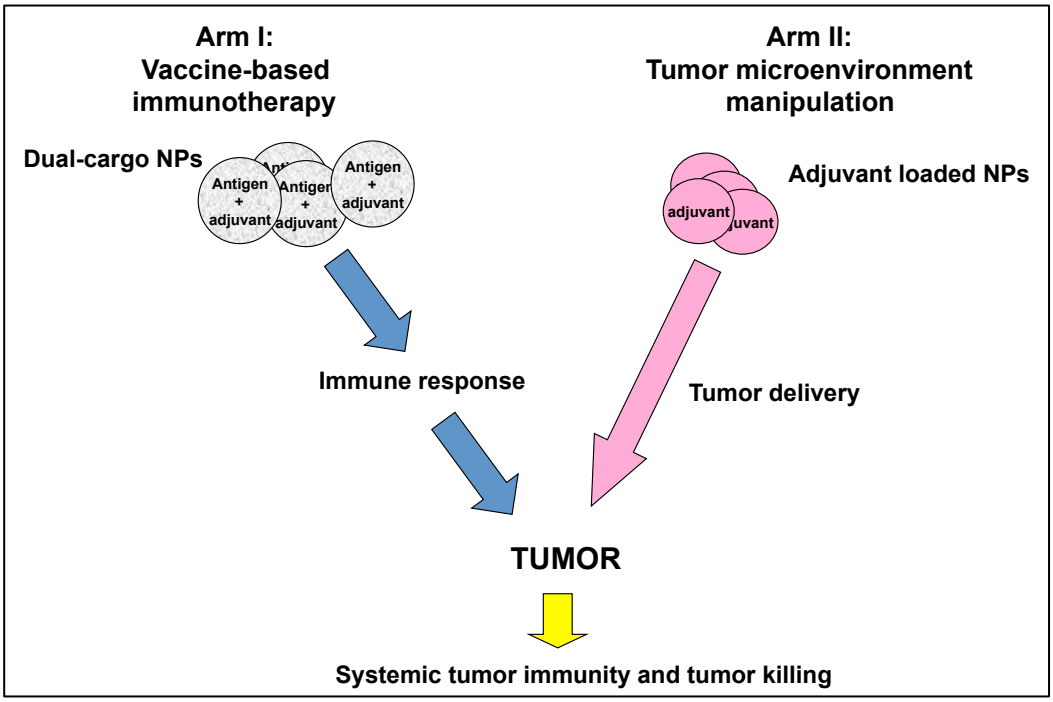


**Figure 7.2.** *Proposed anti-cancer therapeutic combining a vaccine-based immunotherapy (Arm I) with tumor microenvironment manipulation (Arm II).*

## 7.6 Future Work

While no toxicity, adverse effects, or anti-peptide antibody immune responses have been observed with Hp91 injection, before Hp91 or other HMGB1-based adjuvants can be taken into the clinic, additional toxicity testing needs to be performed. In addition to monitoring mice for necrotic areas at the site of injection, weight loss, anti-peptide antibody responses, and signs of distress and death over the immunization period, analysis of hematology and development of anti-Hp91 antibody responses should be performed at least 6 months after the final injection. Organs from immunized mice should be examined, both at the end of the immunization period and after 6 months, for pathological abnormalities and autoimmune symptoms such as deposition of immune complexes. Additionally, before going to clinic, future work to optimize dose, formulation, and scheduling

should be performed. Memory responses should be tested using ELISpot or MHC/Tetramer technology to determine how often boosts are required for long-term protection.

Hp91 showed a moderate synergistic effect when combined with alum. Additional preparations and formulations could be tested wherein HMBG1-based adjuvants are combined with alum/MPL, for example, as such formulations have recently gained FDA approval. Additionally, the HMGB1-based adjuvants could be conjugated to phospholipids and/or polyethylene glycol (PEG) chains. Considerable increases in adjuvant activity have been observed by conjugating other TLR agonists to phospholipids and PEG (167, 168).

The signaling and mechanism of action for Hp91 is not completely understood. Work needs to be performed to complete the signaling map and more completely understand the mechanism of action. Additional receptors are implicated and should be investigated. Pull-down assays using Hp91 as bait are being optimized and may be used to probe for such receptors or interacting proteins. N-terminally biotinylated Hp91, will be immobilized on streptavidin-conjugated magnetic beads and incubated with DC lysates. Alternatively, Hp91 will be preincubated with DCs, the cells lysed, and lysates incubated with the streptavidin beads. The bound proteins will be resolved by polyacrylamide gel electrophoresis and the excised bands will be subjected to mass spectroscopy to identify the candidate peptide binding proteins. Involvement of the identified proteins in DC activation will be confirmed using knockout mice if available or siRNA knockdown.

Future experiments can be designed based on results from the structure-function relationship studies. For example, dimers showed enhanced immunostimulatory activity, as did the shortened peptide, UC1018. The next step is to

dimerize the UC1018 peptide and look for further enhancement of the immune response. There are several ways to synthesize dimers: in addition to cysteine crosslinked, we will prepare other forms of dimers, capable of forming unique intra- and inter-molecular disulphide linked structures. N-terminal and C-terminal linked dimers will be formed by click chemistry using reagents available from Life Technologies.

Additionally, we propose to synthesize fusion peptides that link together the HMGB1-based peptide adjuvant with the peptide antigen. By combining the antigen together with adjuvant, we hypothesize that administering such fusions may reduce the tolerance that occurs if a DC encounters antigen only (63-65).

Future work should include evaluation of the mechanism by which NPs enhance immune immunization. Additionally, to commercialize such NP formulations, scalability and reproducibility of manufacturing are important. Experiments should be initiated to scale the production of the lipid-polymer hybrid NPs. Alternatively, additional methods to conjugate Hp91 onto the surface of NPs should be investigated as PLGA-NPs conjugated to Hp91 increased IL-6 secretion from DCs by 47-fold over free Hp91 peptide controls.

Future work for the development of our proposed two-arm cancer therapeutic includes additional work on the vaccine-based immunotherapy and formulation within NPs, as described previously. With regard to "Arm II," future work could include evaluating the infiltrating immune cells to look for antitumor polarization markers, such as Ly6G on Mac-1+ cells or downregulation of CCR2 on macrophages (158, 161). Additionally, we could use qPCR to measure cytokines and chemokines in the tumor, or flow cytometry to evaluate cell adhesion molecules in tumors. In addition, in lieu of Hp91, other immune factors, such as anti-TGFβ or anti-IL-

10 may delivered locally to the tumor. Systemic blockage of TGFβ has shown delayed tumor growth and we hypothesize that a similar delayed growth may be observed with local delivery of TGFβ antibodies or small molecule inhibitors, or antibodies against IL-10 (158).

## 7.7 Additional Applications

### 7.7.1 Infectious disease applications

Infectious diseases are a major public health concern worldwide. Well-known pathogens (e.g. *P. falciparum,* HIV, *M. tuberculosis*, and influenza) as well as pathogens that have recently come to receive attention (*Borrelia burgdorferi*, West Nile virus, SARS virus, *Bacillus anthraxis*, etc) represent great challenges to the health care system and society. Vaccination remains the single most effective tool to prevent infectious diseases.

Traditionally, vaccines consist of whole inactivated organisms, live attenuated pathogens, or inactivated toxins (69, 70). However, safety concerns make those vaccines unattractive and there is growing interest and research to develop a new generation of vaccines including recombinant protein subunits, synthetic peptides, and plasmid DNA (69). Though these new modalities promise to be less toxic, many are poorly immunogenic when administered without adjuvant. As explained in Chapter 1, nearly all adjuvanted-vaccines contain aluminum salts (alum) as adjuvant. Only recently have additional adjuvant formulations started to get market approval, including squalene and MPL, but historical data is lacking to determine efficacy for these new adjuvants for a broad spectrum of antigens. Additionally, although a large variety of adjuvants has been developed, most of them exhibit excess toxicity,

making them unsuitable for routine clinical use (18). Thus, there is a great need for safer and more potent adjuvants for infectious diseases vaccines (69, 70).

Th1-type responses, important for tumor protection, are also particularly valuable for protection intracellular bacteria and viruses (18, 35, 72). Hp91, as a Th1-type adjuvant, may be a model adjuvant for such pathogens. Thus, while our inspiration lies in the prophylactic and therapeutic treatment of cancer, we would be unwise to pass up the infectious disease vaccine market. Preliminary results suggest that Hp91 can act as adjuvant to induce antiviral cellular immune responses, as demonstrated with a Vaccinia virus (VACV) peptide immunization.

#### 7.7.1.1 UC1018 induces a significant antiviral immune response

C57BL/6 mice were immunized twice s.c. with B8R (VACV) peptide s.c. co-injected with PBS or UC1018 immunostimulatory peptide. Splenocytes from immunized mice were restimulated with B8R peptide in an IFN-γ ELISpot assay. The UC1018 peptide group experienced a significant increase in IFN-γ secreting cells ($p<0.01$) (Figure 7.3). Compared to PBS controls, these UC1018-immunized mice saw a 5-fold increase in the number of IFN-γ secreting cells, suggesting that UC1018 peptide can act as a Th1-type adjuvant for formulation into vaccines which will induce immune responses against infectious diseases. A significant increase in antigen-specific CD8+ T cells was also observed using an MHC/tetramer assay (data not shown).

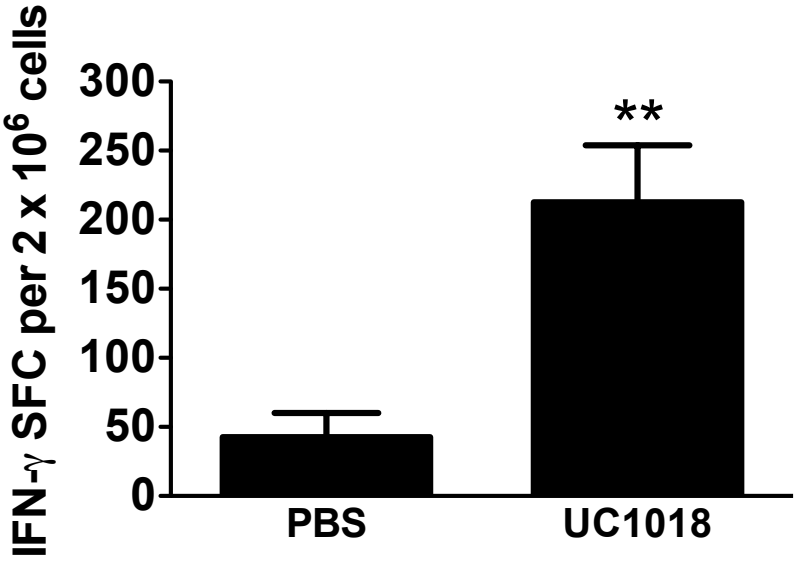


**Figure 7.3.** *UC1018 induces cellular immune responses against viral peptide antigen.* Mice were immunized with B8R (VACV) peptide antigen, co-injected with PBS or UC1018 peptide (142 μg). Splenocytes were restimulated with B8R peptide and cultured in an IFN-γ ELISpot assay to identify B8R specific T lymphocytes. **p<0.01 compared to PBS; Student's t test. 5 mice/group. Detailed materials and methods may be found in the Appendix.

The preliminary results show an anti-viral response, but do not show if this immune response is protective. Thus, protective viral challenges are warranted.

### 7.7.2 Veterinary Applications

There is a high level of species homology in Hp91 and UC1018's parent molecule, HMGB1 protein. HMGB1, shown in the region of Hp91 (Table 7.1), was analyzed by Pubmed's GenRef comparison. Amino acid changes are highlighted in red. The HMGB1 gene is conserved in (at least) human, chimp, dog, cow, horse, mouse, rat, and chicken. Such species homology means the Hp91 peptide adjuvant is likely to work similarly as an adjuvant in at least all the mentioned species, suggesting that Hp91 and UC1018 are competitive candidates for animal health and veterinary vaccine development.

**Table 7.1.** *Species homology of HMGB1 protein*.*

| | | | |
|---|---|---|---|
| | | |_____Hp121_____| | |
| | | |_____Hp91_____| | |
| Homo sapiens | 83 | GETKKKFKDPNAPKRPPSAFFLFCSEYRPKIKGEHPGLSIGDVAKKLGEMWNNTAADDKQP | 143 |
| Pan troglodytes | 83 | GETKKKFKDPNAPKRPPSAFFLFCSEYRPKIKGEHPGLSIGDVAKKLGEMWNNTAADDKQP | 143 |
| Canis lupus familiaris | 83 | GETKKKFKDPNAPKRPPSAFFLFCSEYRPKIKGEHPGLSIGDVAKKLGEMWNNTAADDKQP | 143 |
| Bos taurus | 83 | GETKKKFKDPNAPKRPPSAFFLFCSEYRPKIKGEHPGLSIGDVAKKLGEMWNNTAADDKQP | 143 |
| Equus caballus | 83 | GETKKKFKDPNAPKRPPSAFFLFCSEYRPKIKGEHPGLSIGDVAKKLGEMWNNTAADDKQP | 143 |
| Mus musculus | 83 | GETKKKFKDPNAPKRPPSAFFLFCSEYRPKIKGEHPGLSIGDVAKKLGEMWNNTAADDKQP | 143 |
| Rattus norvegicus | 83 | GETKKKFKDPNAPKRPPSAFFLFCSEYRPKIKGEHPGLSIGDVAKKLGEMWNNTAADDKQP | 143 |
| Gallus gallus | 83 | GETKKKFKDPNAPKRPPSAFFLFCSEFRPKIKGEHPGLSIGDVAKKLGEMWNNTAADDKQP | 143 |
| Drosophila melanogaster | 259 | GKKRKQIKDPNAPKRSLSAFFWFCNDERNKVKALNPEFGVGDIAKELGRKWSDVDPEVKQK | 319 |
| Anopheles gambiae | 197 | GKKRKQFKDPNAPKRSLSAFFWFCHDERNKVKALNPEYGVGDIAKELGRKWSDMDAEIKQK | 257 |
| Caenorhabditis elegans | 123 | RKRKRAKKDPHAPKRALSAFFFYSQDKRPEIQAGHPDWKVGQVAQELGKMWKLVPQETKDM | 183 |

* Amino acid changes are highlighted in red.

In July of 2011, The University of California filed an international patent to protect much of the work described in this dissertation. During Fall 2011, a well-known pharmaceutical company (to remain un-named here) will be evaluating a UC1018 dimer as adjuvant in a veterinary infectious disease model.

### 7.7.3 Cellular Delivery Applications

Peptides are emerging as attractive tools for drug delivery. The HIV Tat-derived protein transduction domain (PTD), for example, is a small basic peptide that delivers a large variety of cargo to cells, including nucleic acids, peptides, proteins, and small particles such as liposomes (169-172). CPPs have been shown to have varying amino acid compositions, however an amphipathic type of CPPs typically contains an alternating pattern of polar/charged amino acids and non-polar, hydrophobic amino acids. Proline-rich amphipathic peptides, often containing PXXP motifs as seen in Hp91, are particularly effective cell penetrating peptides, demonstrating efficient cellular uptake and non-cytotoxicity (111). CPPs hold great potential as delivery vectors *in vitro* and *in vivo*. Their use is limited however due to a

lack of cell specificity for many CPPs and there is an insufficient understanding of the modes of uptake for more CPPs.

We have preliminary data that suggest Hp91 acts as a cell-penetrating peptide to drag cargo into cells. We also suggest that uptake of Hp91 has some cell specificity (data not shown). This exciting and unexpected preliminary data lays the foundation for future experiments utilizing Hp91 as a CPP.

#### 7.7.3.1 Hp91 facilitates cellular uptake of microbeads

Similar to what was demonstrated in DCs, Hp91, but not Hp121, is taken up by HeLa cells by clathrin-mediated endocytosis at 37° C (data not shown). To test if Hp91 or Hp121 could be carried into cells, magnetic 3 μm beads were coated with Hp91, Hp121, or left uncoated and the beads were cultured overnight with HeLa cells. Cells were washed vigorously to remove excess beads.

Hp91 acts as a cell penetrating peptide to drag cargo into cells, as demonstrated by the Hp91-conjugated beads that have entered HeLa cells (Figure 7.4A, B-right). The HeLa cell membrane is clearly visible and the beads are packed inside the cells, not at the edges. In contrast, the Hp121-conjugated beads and un-conjugated control beads were visible at the boundaries between cells and at the cell free spaces of the plate (Figure 7.4A, B). This data demonstrate that Hp91 can facilitate cellular uptake of cargo as large as 2.8 μm.

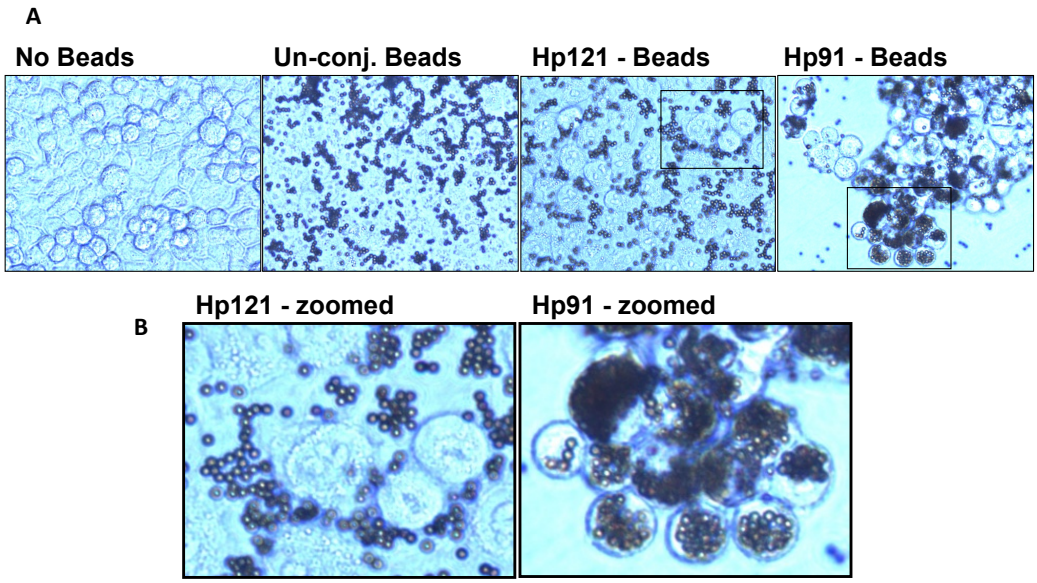


**Figure 7.4.** *Hp91 facilitates cellular uptake of microbeads.* (**A**) M280-Streptavidin-coated Dynabeads (2.8 μm) were conjugated to biotinylated Hp91, Hp121, or left uncoated. After washing off excess peptide, beads were incubated overnight with HeLa cells. Cells were washed and imaged in PBS on a Nikon Eclipse TE300 inverted microscope. (**B**) Images were cropped/zoomed to more clearly show cellular boundaries. Detailed materials and methods may be found in the Appendix.

The light microscopy used to evaluate microbead uptake suggests that the Hp91-conjugated beads were taken into the HeLa cells. Confocal microscopy is necessary to confirm the uptake. Fluorescent cargo, such as Q-dots could be conjugated to Hp91 and evaluated for uptake by confocal microscopy. Other cargo to be linked to Hp91 and tested for uptake may include siRNA for gene silencing or DNA for transfection of target cells.

# 8. Appendix

## 8.1 Supplemental Materials and Methods

### 8.8.1 Peptides for "Additional Applications"

The peptides, including Hp91 (DPNAPKRPPSAFFLFCSE), UC1018 (SAFFLFCSE), and Hp121 (SIGDVAKKLGEMWNNTAA) were all synthesized from GenScript Corp (Piscataway, NJ, USA) and CPC Scientific (San Jose, CA, USA). Peptides were synthesized with an N-terminal biotin. Peptides were routinely synthesized with greater than 95% purity. VACV CD8 T cell peptide epitope B8R (20-27; TSYKFESV) and Hepatitis B virus core peptide (128-140; TPPAYRPPNAPIL) helper epitope were gifts from Shahram Salek-Ardakani (LIAI).

### 8.8.1 Animals and Cell Lines for "Additional Applications"

C57BL/6 mice were purchased from Charles River Laboratories (Boston, MA, USA). Animals were housed at the Moores UCSD Cancer Center animal facility. All animal studies were performed with human care of animals and approved by the Institutional Animal Care and Use Committee of UCSD and were performed in accordance with the institutional guidelines.

The HeLa cell line was passed on to our lab from the Carson lab (UCSD), and hence shared in the same manner that HeLa cells have been shared for decades. The cells were cultured in Dulbecco's modification of Eagle's Medium (DMEM)

(Mediatech), supplemented with 10 mM HEPES (Invitrogen), penicillin (100 U $ml^{-1}$) - streptomycin (100 μg $ml^{-1}$) - L-glutamine (2 mM) (Invitrogen), and 10% (vol/vol) fetal calf serum (FCS) (Omega).

### 8.1.3 B8R Immunization and ELISpot

C57BL/6 mice, approximately 2 months old, were immunized subcutaneously (s.c.) with VACV B8R peptide (TSYKFESV) (10 μg) co-injected with PBS or UC1018 peptide (142 μg). The quantity of UC1018 peptide matches that used in earlier UC1018 immunizations. A Hepatitis B virus core peptide (128-140; TPPAYRPPNAPIL) (140 μg) was included in immunizations as a helper epitope. Mice were boosted after 2 weeks and sacrificed one week post-boost. Single cell suspensions of splenocytes were prepared as described in Chapter 2, Materials and Methods. Freshly isolated splenocytes were plated in an IFN-γ ELISpot, as previously described in Chapter 2, however instead of OVA-I (SIINFEKL) peptide, splenocytes were restimulated with 2.5 μg $ml^{-1}$ B8R peptide (TSYKFESV).

### 8.1.4 Microbead conjugation and uptake by HeLa

Biotinylated Hp91 or Hp121 was immobilized Streptavidin-coated microbeads (M-280 Dynabeads, Invitrogen) as follows. Beads were placed in a magnet for 1-2 minutes and then supernatant was removed. Beads were resuspended in an equivalent volume of working buffer (0.5% BSA in PBS). Beads were washed twice more and then resuspended in a suitable volume of working buffer. Hp91 or Hp121 (1000 pmol/mg) was added to the beads. Beads were rotated in a MACS rotator for 30-45 minutes to coat. After removing from the magnet, remaining beads stuck to the walls of the tube were washed down with working buffer. Coated beads were then

washed 3-4 times more (2-3 minutes per wash) to remove non-bound Hp91 or Hp121 and finally resuspended in working buffer. Un-conjugated beads were treated with the same conditions, but no peptide was added. Beads were added to cultures of growing HeLa cells and allowed to incubate overnight. After incubation, cells were vigorously washed with PBS to remove as many beads as possible. Cells were imaged in PBS on a Nikon Eclipse TE300 inverted microscope (Nikon Instruments, Melville, NY).

## REFERENCES


1. Blattman JN, Greenberg PD. Cancer immunotherapy: a treatment for the masses. Science. 2004;305(5681):200-5.

2. Dubensky TW, Jr., Reed SG. Adjuvants for cancer vaccines. Semin Immunol. 2010.

3. Li J, Song W, Czerwinski DK, Varghese B, Uematsu S, Akira S, Krieg AM, Levy R. Lymphoma immunotherapy with CpG oligodeoxynucleotides requires TLR9 either in the host or in the tumor itself. J Immunol. 2007;179(4):2493-500.

4. Petrovsky N, Aguilar JC. Vaccine adjuvants: current state and future trends. Immunology and Cell Biology. 2004;82(5):488-96.

5. Rosenberg SA, Yang JC, Restifo NP. Cancer immunotherapy: moving beyond current vaccines. Nat Med. 2004;10(9):909-15. PMCID: 1435696.

6. Gattinoni L, Powell DJ, Jr., Rosenberg SA, Restifo NP. Adoptive immunotherapy for cancer: building on success. Nat Rev Immunol. 2006;6(5):383-93.

7. Janeway C. Immunobiology : the immune system in health and disease. 6th ed. New York: Garland Science; 2005.

8. Weiner GJ, Liu HM, Wooldridge JE, Dahle CE, Krieg AM. Immunostimulatory oligodeoxynucleotides containing the CpG motif are effective as immune adjuvants in tumor antigen immunization. Proc Natl Acad Sci U S A. 1997;94(20):10833-7. PMCID: 23500.

9. Dredge K, Marriott JB, Todryk SM, Dalgleish AG. Adjuvants and the promotion of Th1-type cytokines in tumour immunotherapy. Cancer Immunology, Immunotherapy. 2002;51(10):521-31.

10. Xu-Amano J, Kiyono H, Jackson RJ, Staats HF, Fujihashi K, Burrows PD, Elson CO, Pillai S, McGhee JR. Helper T cell subsets for immunoglobulin A responses: oral immunization with tetanus toxoid and cholera toxin as adjuvant selectively induces Th2 cells in mucosa associated tissues. J Exp Med. 1993;178(4):1309-20.

11. Engers H, Kieny MP, Malhotra P, Pink JR. Third Meeting on novel adjuvants curently in or close to clinical testing world health organization-Organization mondiale de la sante, Fondation Merieux, Annecy France, 7-9 January 2002. Vaccine. 2003;21:3503-24.

12. De Gregorio E, Tritto E, Rappuoli R. Alum adjuvanticity: unraveling a century old mystery. European Journal of Immunology. 2008;38(8):2068-71.

13. Gupta RK. Aluminum compounds as vaccine adjuvants. Adv Drug Deliv Rev. 1998;32(3):155-72.

14. Audibert FM, Lise LD. Adjuvants: current status, clinical perspectives and future prospects. Immunol Today. 1993;14(6):281-4.

15. Gupta RK, Siber GR. Adjuvants for human vaccines--current status, problems and future prospects. Vaccine. 1995;13(14):1263-76.

16. Bomford R. Will adjuvants be needed for vaccines of the future? Dev Biol Stand. 1998;92:13-7.

17. Brewer JM, Conacher M, Satoskar A, Bluethmann H, Alexander J. In interleukin-4-deficient mice, alum not only generates T helper 1 responses equivalent to freund's complete adjuvant, but continues to induce T helper 2 cytokine production. European Journal of Immunology. 1996;26(9):2062-6.

18. Kovarik J, Siegrist CA. The search for novel adjuvants for early life vaccinations: can "danger" motifs show us the way? 2001;49(3):209-15.

19. Dubensky TW, Jr., Reed SG. Adjuvants for cancer vaccines. Semin Immunol. 2010;22(3):155-61.

20. Eisenbarth SC, Colegio OR, O'Connor W, Sutterwala FS, Flavell RA. Crucial role for the Nalp3 inflammasome in the immunostimulatory properties of aluminium adjuvants. Nature. 2008;453(7198):1122-6.

21. Duthie MS, Windish HP, Fox CB, Reed SG. Use of defined TLR ligands as adjuvants within human vaccines. Immunol Rev. 2011;239(1):178-96.

22. Granadillo M, Vallespi MG, Batte A, Mendoza O, Soria Y, Lugo VM, Torrens I. A novel fusion protein-based vaccine comprising a cell penetrating and immunostimulatory peptide linked to human papillomavirus (HPV) type 16 E7 antigen generates potent immunologic and anti-tumor responses in mice. Vaccine. 2011;29(5):920-30.

23. Lillard JW, Jr., Boyaka PN, Chertov O, Oppenheim JJ, McGhee JR. Mechanisms for induction of acquired host immunity by neutrophil peptide defensins. Proc Natl Acad Sci U S A. 1999;96(2):651-6. PMCID: 15191.

24. Tani K, Murphy WJ, Chertov O, Salcedo R, Koh CY, Utsunomiya I, Funakoshi S, Asai O, Herrmann SH, Wang JM, Kwak LW, Oppenheim JJ. Defensins act as potent adjuvants that promote cellular and humoral immune responses in mice to a lymphoma idiotype and carrier antigens. Int Immunol. 2000;12(5):691-700.

25. An LL, Yang YH, Ma XT, Lin YM, Li G, Song YH, Wu KF. LL-37 enhances adaptive antitumor immune response in a murine model when genetically fused with M-CSFR (J6-1) DNA vaccine. Leuk Res. 2005;29(5):535-43.

26. Scott MG, Dullaghan E, Mookherjee N, Glavas N, Waldbrook M, Thompson A, Wang A, Lee K, Doria S, Hamill P, Yu JJ, Li Y, Donini O, Guarna MM, Finlay BB, North JR, Hancock RE. An anti-infective peptide that selectively modulates the innate immune response. Nat Biotechnol. 2007;25(4):465-72.

27. Kindrachuk J, Jenssen H, Elliott M, Townsend R, Nijnik A, Lee SF, Gerdts V, Babiuk LA, Halperin SA, Hancock RE. A novel vaccine adjuvant comprised of a synthetic innate defence regulator peptide and CpG oligonucleotide links innate and adaptive immunity. Vaccine. 2009;27(34):4662-71.

28. Banchereau J, Steinman RM. Dendritic cells and the control of immunity. Nature. 1998;392(6673):245-52.

29. De Smedt T, Pajak B, Muraille E, Lespagnard L, Heinen E, De Baetselier P, Urbain J, Leo O, Moser M. Regulation of dendritic cell numbers and maturation by lipopolysaccharide in vivo. J Exp Med. 1996;184(4):1413-24.

30. Hartmann G, Weiner GJ, Krieg AM. CpG DNA: a potent signal for growth, activation, and maturation of human dendritic cells. Proceedings of the National Academy of Sciences of the United States of America. 1999;96(16):9305-10.

31. Gallucci S, Matzinger P. Danger signals: SOS to the immune system. Current Opinion in Immunology. 2001;13(1):114-9.

32. Gallucci S, Lolkema M, Matzinger P. Natural adjuvants: endogenous activators of dendritic cells. Nature Medicine. 1999;5(11):1249-55.

33. Sauter B, Albert ML, Francisco L, Larsson M, Somersan S, Bhardwaj N. Consequences of cell death: exposure to necrotic tumor cells, but not primary tissue cells or apoptotic cells, induces the maturation of immunostimulatory dendritic cells. The Journal of Experimental Medicine. 2000;191(3):423-34.

34. Basu S, Binder RJ, Suto R, Anderson KM, Srivastava PK. Necrotic but not apoptotic cell death releases heat shock proteins, which deliver a partial maturation signal to dendritic cells and activate the NF-kappa B pathway. Int Immunol. 2000;12(11):1539-46.

35. Steinman RM, Banchereau J. Taking dendritic cells into medicine. Nature. 2007;449(7161):419-26.

36. Agresti A, Bianchi ME. HMGB proteins and gene expression. Curr Opin Genet Dev. 2003;13(2):170-8.

37. Bustin M, Lehn DA, Landsman D. Structural features of the HMG chromosomal proteins and their genes. Biochimica Et Biophysica Acta. 1990;1049(3):231-43.

38. Bustin M, Reeves R. High-mobility-group chromosomal proteins: architectural components that facilitate chromatin function. Progress in Nucleic Acid Research and Molecular Biology. 1996;54:35-100.

39. Wang H, Vishnubhakat JM, Bloom O, Zhang M, Ombrellino M, Sama A, Tracey KJ. Proinflammatory cytokines (tumor necrosis factor and interleukin 1) stimulate release of high mobility group protein-1 by pituicytes. Surgery. 1999;126(2):389-92.

40. Andersson U, Wang H, Palmblad K, Aveberger AC, Bloom O, Erlandsson_Harris H, Janson A, Kokkola R, Zhang M, Yang H, Tracey KJ. High mobility group 1 protein (HMG-1) stimulates proinflammatory cytokine synthesis in human monocytes. The Journal of Experimental Medicine. 2000;192(4):565-70.

41. Li J, Kokkola R, Tabibzadeh S, Yang R, Ochani M, Qiang X, Harris HE, Czura CJ, Wang H, Ulloa L, Warren HS, Moldawer LL, Fink MP, Andersson U, Tracey KJ, Yang H.

Structural basis for the proinflammatory cytokine activity of high mobility group box 1. Mol Med. 2003;9(1-2):37-45.

42. Yang H, Wang H, Czura CJ, Tracey KJ. HMGB1 as a cytokine and therapeutic target. 2002;8(6):469-72.

43. Yang H, Ochani M, Li J, Qiang X, Tanovic M, Harris HE, Susarla SM, Ulloa L, Wang H, DiRaimo R, Czura CJ, Roth J, Warren HS, Fink MP, Fenton MJ, Andersson U, Tracey KJ. Reversing established sepsis with antagonists of endogenous high-mobility group box 1. Proc Natl Acad Sci U S A. 2004;101(1):296-301.

44. Hreggvidsdottir HS, Ostberg T, Wahamaa H, Schierbeck H, Aveberger AC, Klevenvall L, Palmblad K, Ottosson L, Andersson U, Harris HE. The alarmin HMGB1 acts in synergy with endogenous and exogenous danger signals to promote inflammation. J Leukoc Biol. 2009;86(3):655-62.

45. Bianchi ME. DAMPs, PAMPs and alarmins: all we need to know about danger. Journal of Leukocyte Biology. 2007;81(1):1-5.

46. Wang H, Yang H, Tracey KJ. Extracellular role of HMGB1 in inflammation and sepsis. J Intern Med. 2004;255(3):320-31.

47. Popovic K, Ek M, Espinosa A, Padyukov L, Harris HE, Wahren-Herlenius M, Nyberg F. Increased expression of the novel proinflammatory cytokine high mobility group box chromosomal protein 1 in skin lesions of patients with lupus erythematosus. Arthritis Rheum. 2005;52(11):3639-45.

48. Andersson U, Erlandsson-Harris H. HMGB1 is a potent trigger of arthritis. J Intern Med. 2004;255(3):344-50.

49. Scaffidi P, Misteli T, Bianchi ME. Release of chromatin protein HMGB1 by necrotic cells triggers inflammation. Nature. 2002;418(6894):191-5.

50. Rovere-Querini P, Capobianco A, Scaffidi P, Valentinis B, Catalanotti F, Giazzon M, Dumitriu IE, Muller S, Iannacone M, Traversari C, Bianchi ME, Manfredi AA. HMGB1 is an endogenous immune adjuvant released by necrotic cells. EMBO Rep. 2004;5(8):825-30.

51. Messmer D, Yang H, Telusma G, Knoll F, Li J, Messmer B, Tracey KJ, Chiorazzi N. High mobility group box protein 1: an endogenous signal for dendritic cell maturation and Th1 polarization. J Immunol. 2004;173(1):307-13.

52. Telusma G, Datta S, Mihajlov I, Ma W, Li J, Yang H, Newman W, Messmer BT, Minev B, Schmidt-Wolf IG, Tracey KJ, Chiorazzi N, Messmer D. Dendritic cell activating peptides induce distinct cytokine profiles. Int Immunol. 2006;18(11):1563-73.

53. Park JS, Svetkauskaite D, He Q, Kim JY, Strassheim D, Ishizaka A, Abraham E. Involvement of toll-like receptors 2 and 4 in cellular activation by high mobility group box 1 protein. J Biol Chem. 2004;279(9):7370-7.

54. van Zoelen MA, Yang H, Florquin S, Meijers JC, Akira S, Arnold B, Nawroth PP, Bierhaus A, Tracey KJ, van der Poll T. Role of Toll-Like Receptors 2 and 4, and the

Receptor for Advanced Glycation End Products (Rage) in Hmgb1 Induced Inflammation in Vivo. Shock. 2008.

55. Kawai T, Akira S. The role of pattern-recognition receptors in innate immunity: update on Toll-like receptors. Nat Immunol. 2010;11(5):373-84.

56. Takeda K, Kaisho T, Akira S. Toll-like receptors. Annual Review of Immunology. 2003;21:335-76.

57. Netea MG, Van der Meer JW, Kullberg BJ. Toll-like receptors as an escape mechanism from the host defense. Trends in Microbiology. 2004;12(11):484-8.

58. Park JS, Svetkauskaite D, He Q, Kim JY, Strassheim D, Ishizaka A, Abraham E. Involvement of toll-like receptors 2 and 4 in cellular activation by high mobility group box 1 protein. The Journal of Biological Chemistry. 2004;279(9):7370-7.

59. Warshakoon HJ, Hood JD, Kimbrell MR, Malladi S, Wu WY, Shukla NM, Agnihotri G, Sil D, David SA. Potential adjuvantic properties of innate immune stimuli. Hum Vaccin. 2009;5(6):381-94.

60. Brigger I, Dubernet C, Couvreur P. Nanoparticles in cancer therapy and diagnosis. Adv Drug Deliv Rev. 2002;54(5):631-51.

61. Murphy EA, Majeti BK, Barnes LA, Makale M, Weis SM, Lutu-Fuga K, Wrasidlo W, Cheresh DA. Nanoparticle-mediated drug delivery to tumor vasculature suppresses metastasis. Proc Natl Acad Sci U S A. 2008;105(27):9343-8. PMCID: 2453735.

62. Tang BC, Dawson M, Lai SK, Wang YY, Suk JS, Yang M, Zeitlin P, Boyle MP, Fu J, Hanes J. Biodegradable polymer nanoparticles that rapidly penetrate the human mucus barrier. Proc Natl Acad Sci U S A. 2009;106(46):19268-73. PMCID: 2780804.

63. Blander JM, Medzhitov R. Toll-dependent selection of microbial antigens for presentation by dendritic cells. Nature. 2006;440(7085):808-12.

64. Kaiser-Schulz G, Heit A, Quintanilla-Martinez L, Hammerschmidt F, Hess S, Jennen L, Rezaei H, Wagner H, Schatzl HM. Polylactide-coglycolide microspheres co-encapsulating recombinant tandem prion protein with CpG-oligonucleotide break self-tolerance to prion protein in wild-type mice and induce CD4 and CD8 T cell responses. J Immunol. 2007;179(5):2797-807.

65. Schlosser E, Mueller M, Fischer S, Basta S, Busch DH, Gander B, Groettrup M. TLR ligands and antigen need to be coencapsulated into the same biodegradable microsphere for the generation of potent cytotoxic T lymphocyte responses. Vaccine. 2008;26(13):1626-37.

66. Audran R, Peter K, Dannull J, Men Y, Scandella E, Groettrup M, Gander B, Corradin G. Encapsulation of peptides in biodegradable microspheres prolongs their MHC class-I presentation by dendritic cells and macrophages in vitro. Vaccine. 2003;21(11-12):1250-5.

67. Uto T, Wang X, Sato K, Haraguchi M, Akagi T, Akashi M, Baba M. Targeting of antigen to dendritic cells with poly(gamma-glutamic acid) nanoparticles induces antigen-specific humoral and cellular immunity. J Immunol. 2007;178(5):2979-86.

68. Clawson C, Huang CT, Futalan D, Martin Seible D, Saenz R, Larsson M, Ma W, Minev B, Zhang F, Ozkan M, Ozkan C, Esener S, Messmer D. Delivery of a peptide via poly(d,l-lactic-co-glycolic) acid nanoparticles enhances its dendritic cell-stimulatory capacity. Nanomedicine. 2010.

69. Singh M, O_Hagan D. Advances in vaccine adjuvants. Nature Biotechnology. 1999;17(11):1075-81.

70. McCluskie MJ, Weeratna RD. Novel adjuvant systems. 2001;1(3):263-71.

71. Singh M, O'Hagan DT. Recent advances in vaccine adjuvants. Pharm Res. 2002;19(6):715-28.

72. Chisari FV, Ferrari C. Hepatitis B virus immunopathogenesis. Annual Review of Immunology. 1995;13:29-60.

73. Krieg AM. CpG motifs in bacterial DNA and their immune effects. Annu Rev Immunol. 2002;20:709-60.

74. Alexopoulou L, Holt AC, Medzhitov R, Flavell RA. Recognition of double-stranded RNA and activation of NF-kappaB by Toll- like receptor 3. Nature. 2001;413(6857):732-8.

75. Netea MG, van der Graaf C, Van der Meer JW, Kullberg BJ. Toll-like receptors and the host defense against microbial pathogens: bringing specificity to the innate-immune system. J Leukoc Biol. 2004;75(5):749-55.

76. Chu RS, Targoni OS, Krieg AM, Lehmann PV, Harding CV. CpG oligodeoxynucleotides act as adjuvants that switch on T helper 1 (Th1) immunity. Journal of Experimental Medicine. 1997;186(10):1623-31. PMCID: 2199137.

77. Krug A, Towarowski A, Britsch S, Rothenfusser S, Hornung V, Bals R, Giese T, Engelmann H, Endres S, Krieg AM, Hartmann G. Toll-like receptor expression reveals CpG DNA as a unique microbial stimulus for plasmacytoid dendritic cells which synergizes with CD40 ligand to induce high amounts of IL-12. European Journal of Immunology. 2001;31(10):3026-37.

78. Krieg AM. Therapeutic potential of Toll-like receptor 9 activation. Nat Rev Drug Discov. 2006;5(6):471-84.

79. Schmidt C. Clinical setbacks for toll-like receptor 9 agonists in cancer. Nature Biotechnology. 2007;25(8):825-6.

80. Ulloa L, Messmer D. High-mobility group box 1 (HMGB1) protein: friend and foe. Cytokine Growth Factor Rev. 2006;17(3):189-201.

81. Wang H, Vishnubhakat JM, Bloom O, Zhang M, Ombrellino M, Sama A, Tracey KJ. Proinflammatory cytokines (tumor necrosis factor and interleukin 1) stimulate release of high mobility group protein-1 by pituicytes. Surgery. 1999;126(2):389-92.

82. Siegal FP, Kadowaki N, Shodell M, Fitzgerald-Bocarsly PA, Shah K, Ho S, Antonenko S, Liu YJ. The nature of the principal type 1 interferon-producing cells in human blood. Science. 1999;284(5421):1835-7.

83. Dumitriu IE, Baruah P, Bianchi ME, Manfredi AA, Rovere-Querini P. Requirement of HMGB1 and RAGE for the maturation of human plasmacytoid dendritic cells. Eur J Immunol. 2005;35(7):2184-90.

84. Loskog A, Totterman TH. CD40L - a multipotent molecule for tumor therapy. Endocr Metab Immune Disord Drug Targets. 2007;7(1):23-8.

85. Kadowaki N, Ho S, Antonenko S, Malefyt RW, Kastelein RA, Bazan F, Liu YJ. Subsets of human dendritic cell precursors express different toll-like receptors and respond to different microbial antigens. J Exp Med. 2001;194(6):863-9.

86. Jasani B, Navabi H, Adams M. Ampligen: A potential toll-like 3 receptor adjuvant for immunotherapy of cancer. Vaccine. 2009.

87. Brazolot Millan CL, Weeratna R, Krieg AM, Siegrist CA, Davis HL. CpG DNA can induce strong Th1 humoral and cell-mediated immune responses against hepatitis B surface antigen in young mice. Proc Natl Acad Sci U S A. 1998;95(26):15553-8.

88. Wong BR, Josien R, Lee SY, Sauter B, Li HL, Steinman RM, Choi Y. TRANCE (tumor necrosis factor [TNF]-related activation-induced cytokine), a new TNF family member predominantly expressed in T cells, is a dendritic cell-specific survival factor. J Exp Med. 1997;186(12):2075-80.

89. Gurer C, Strowig T, Brilot F, Pack M, Trumpfheller C, Arrey F, Park CG, Steinman RM, Munz C. Targeting the nuclear antigen 1 of Epstein-Barr virus to the human endocytic receptor DEC-205 stimulates protective T-cell responses. Blood. 2008;112(4):1231-9.

90. Trumpfheller C, Caskey M, Nchinda G, Longhi MP, Mizenina O, Huang Y, Schlesinger SJ, Colonna M, Steinman RM. The microbial mimic poly IC induces durable and protective CD4+ T cell immunity together with a dendritic cell targeted vaccine. Proc Natl Acad Sci U S A. 2008;105(7):2574-9.

91. Saenz R, Souza Cda S, Huang CT, Larsson M, Esener S, Messmer D. HMGB1-derived peptide acts as adjuvant inducing immune responses to peptide and protein antigen. Vaccine. 2010;28(47):7556-62. PMCID: 2963688.

92. Banchereau J, Steinman RM. Dendritic cells and the control of immunity. Nature. 1998;392(6673):245-52.

93. Matzinger P. Tolerance, danger, and the extended family. Annual Review Of Immunology. 1994;12:991-1045.

94. Hori O, Brett J, Slattery T, Cao R, Zhang J, Chen JX, Nagashima M, Lundh ER, Vijay S, Nitecki D, et al. The receptor for advanced glycation end products (RAGE) is a cellular binding site for amphoterin. Mediation of neurite outgrowth and co-expression of rage and amphoterin in the developing nervous system. J Biol Chem. 1995;270(43):25752-61.

95. Yu M, Wang H, Ding A, Golenbock DT, Latz E, Czura CJ, Fenton MJ, Tracey KJ, Yang H. HMGB1 signals through toll-like receptor (TLR) 4 and TLR2. Shock. 2006;26(2):174-9.

96. Park JS, Gamboni-Robertson F, He Q, Svetkauskaite D, Kim JY, Strassheim D, Sohn JW, Yamada S, Maruyama I, Banerjee A, Ishizaka A, Abraham E. High mobility group box 1 protein interacts with multiple Toll-like receptors. Am J Physiol Cell Physiol. 2006;290(3):C917-24.

97. Yang H, Hreggvidsdottir HS, Palmblad K, Wang H, Ochani M, Li J, Lu B, Chavan S, Rosas-Ballina M, Al-Abed Y, Akira S, Bierhaus A, Erlandsson-Harris H, Andersson U, Tracey KJ. A critical cysteine is required for HMGB1 binding to Toll-like receptor 4 and activation of macrophage cytokine release. Proc Natl Acad Sci U S A. 2010;107(26):11942-7. PMCID: 2900689.

98. Ivanov S, Dragoi AM, Wang X, Dallacosta C, Louten J, Musco G, Sitia G, Yap GS, Wan Y, Biron CA, Bianchi ME, Wang H, Chu WM. A novel role for HMGB1 in TLR9-mediated inflammatory responses to CpG-DNA. Blood. 2007;110(6):1970-81. PMCID: 1976374.

99. Orlova VV, Choi EY, Xie C, Chavakis E, Bierhaus A, Ihanus E, Ballantyne CM, Gahmberg CG, Bianchi ME, Nawroth PP, Chavakis T. A novel pathway of HMGB1-mediated inflammatory cell recruitment that requires Mac-1-integrin. EMBO J. 2007;26(4):1129-39. PMCID: 1852832.

100. Rauvala H, Rouhiainen A. Physiological and pathophysiological outcomes of the interactions of HMGB1 with cell surface receptors. Biochim Biophys Acta. 2010;1799(1-2):164-70.

101. Salmivirta M, Rauvala H, Elenius K, Jalkanen M. Neurite growth-promoting protein (amphoterin, p30) binds syndecan. Exp Cell Res. 1992;200(2):444-51.

102. Milev P, Chiba A, Haring M, Rauvala H, Schachner M, Ranscht B, Margolis RK, Margolis RU. High affinity binding and overlapping localization of neurocan and phosphacan/protein-tyrosine phosphatase-zeta/beta with tenascin-R, amphoterin, and the heparin-binding growth-associated molecule. J Biol Chem. 1998;273(12):6998-7005.

103. Chen GY, Tang J, Zheng P, Liu Y. CD24 and Siglec-10 selectively repress tissue damage-induced immune responses. Science. 2009;323(5922):1722-5. PMCID: 2765686.

104. Telusma G, Datta S, Mihajlov I, Ma W, Li J, Yang H, Newman W, Messmer BT, Minev B, Schmidt-Wolf IG, Tracey KJ, Chiorazzi N, Messmer D. Dendritic cell activating peptides induce distinct cytokine profiles. Int Immunol. 2006;18(11):1563-73.

105. Messmer D, Yang H, Telusma G, Knoll F, Li J, Messmer B, Tracey KJ, Chiorazzi N. High mobility group box protein 1: an endogenous signal for dendritic cell maturation and Th1 polarization. Journal of Immunology. 2004;173(1):307-13.

106. Inaba K, Inaba M, Romani N, Aya H, Deguchi M, Ikehara S, Muramatsu S, Steinman RM. Generation of large numbers of dendritic cells from mouse bone marrow cultures supplemented with granulocyte/macrophage colony-stimulating factor. The Journal of Experimental Medicine. 1992;176(6):1693-702.

107. Zaro JL, Shen WC. Quantitative comparison of membrane transduction and endocytosis of oligopeptides. Biochemical and Biophysical Research Communications. 2003;307(2):241-7.

108. Kagan JC, Su T, Horng T, Chow A, Akira S, Medzhitov R. TRAM couples endocytosis of Toll-like receptor 4 to the induction of interferon-beta. Nat Immunol. 2008;9(4):361-8.

109. Medzhitov R. Toll-like receptors and innate immunity. Nat Rev Immunol. 2001;1(2):135-45.

110. Watts C. Location, location, location: identifying the neighborhoods of LPS signaling. Nat Immunol. 2008;9(4):343-5.

111. Pujals S, Giralt E. Proline-rich, amphipathic cell-penetrating peptides. Adv Drug Deliv Rev. 2008;60(4-5):473-84.

112. Barroso M, Sztul ES. Basolateral to apical transcytosis in polarized cells is indirect and involves BFA and trimeric G protein sensitive passage through the apical endosome. J Cell Biol. 1994;124(1-2):83-100. PMCID: 2119901.

113. Seong SY, Matzinger P. Hydrophobicity: an ancient damage-associated molecular pattern that initiates innate immune responses. Nat Rev Immunol. 2004;4(6):469-78.

114. Bucci G, Mochida S, Stephens GJ. Inhibition of synaptic transmission and G protein modulation by synthetic CaV2.2 Ca2+ channel peptides. J Physiol. 2011;589(Pt 13):3085-101. PMCID: 3145926.

115. Hoppe G, Talcott KE, Bhattacharya SK, Crabb JW, Sears JE. Molecular basis for the redox control of nuclear transport of the structural chromatin protein Hmgb1. Exp Cell Res. 2006;312(18):3526-38.

116. Thomas JO, Travers AA. HMG1 and 2, and related 'architectural' DNA-binding proteins. Trends Biochem Sci. 2001;26(3):167-74.

117. Bienkiewicz EA, Moon Woody A, Woody RW. Conformation of the RNA polymerase II C-terminal domain: circular dichroism of long and short fragments. J Mol Biol. 2000;297(1):119-33.

118. van Holst GJ, Fincher GB. Polyproline II Confirmation in the Protein Component of Arabinogalactan-Protein from Lolium multiflorum. Plant Physiol. 1984;75(4):1163-4. PMCID: 1067069.

119. Li SC, Goto NK, Williams KA, Deber CM. Alpha-helical, but not beta-sheet, propensity of proline is determined by peptide environment. Proc Natl Acad Sci U S A. 1996;93(13):6676-81. PMCID: 39085.

120. Yu H, Chen JK, Feng S, Dalgarno DC, Brauer AW, Schreiber SL. Structural basis for the binding of proline-rich peptides to SH3 domains. Cell. 1994;76(5):933-45.

121. Li SS. Specificity and versatility of SH3 and other proline-recognition domains: structural basis and implications for cellular signal transduction. Biochem J. 2005;390(Pt 3):641-53. PMCID: 1199657.

122. Linardakis E, Bateman A, Phan V, Ahmed A, Gough M, Olivier K, Kennedy R, Errington F, Harrington KJ, Melcher A, Vile R. Enhancing the efficacy of a weak allogeneic melanoma vaccine by viral fusogenic membrane glycoprotein-mediated tumor cell-tumor cell fusion. Cancer Res. 2002;62(19):5495-504.

123. Sonnichsen FD, Van Eyk JE, Hodges RS, Sykes BD. Effect of trifluoroethanol on protein secondary structure: an NMR and CD study using a synthetic actin peptide. Biochemistry. 1992;31(37):8790-8.

124. Jin MS, Lee JO. Structures of the toll-like receptor family and its ligand complexes. Immunity. 2008;29(2):182-91.

125. Nunez Miguel R, Wong J, Westoll JF, Brooks HJ, O'Neill LA, Gay NJ, Bryant CE, Monie TP. A dimer of the Toll-like receptor 4 cytoplasmic domain provides a specific scaffold for the recruitment of signalling adaptor proteins. PLoS One. 2007;2(8):e788. PMCID: 1945083.

126. Fernandez-Carneado J, Kogan MJ, Van Mau N, Pujals S, Lopez-Iglesias C, Heitz F, Giralt E. Fatty acyl moieties: improving Pro-rich peptide uptake inside HeLa cells. J Pept Res. 2005;65(6):580-90.

127. Mayer BJ. SH3 domains: complexity in moderation. J Cell Sci. 2001;114(Pt 7):1253-63.

128. Cestra G, Castagnoli L, Dente L, Minenkova O, Petrelli A, Migone N, Hoffmuller U, Schneider-Mergener J, Cesareni G. The SH3 domains of endophilin and amphiphysin bind to the proline-rich region of synaptojanin 1 at distinct sites that display an unconventional binding specificity. J Biol Chem. 1999;274(45):32001-7.

129. Morales I. Functional Analysis of Potential Phosphorylation Sites in the HIV-1 p6Gag Domain. Doctoral Dissertation, Ruperto-Carola University of Heidelberg, Germany. 2011.

130. Pornillos O, Alam SL, Davis DR, Sundquist WI. Structure of the Tsg101 UEV domain in complex with the PTAP motif of the HIV-1 p6 protein. Nat Struct Biol. 2002;9(11):812-7.

131. Fournier P, Schirrmacher V. Randomized clinical studies of anti-tumor vaccination: state of the art in 2008. Expert Rev Vaccines. 2009;8(1):51-66.

132. Diwan M, Elamanchili P, Lane H, Gainer A, Samuel J. Biodegradable nanoparticle mediated antigen delivery to human cord blood derived dendritic cells for induction of primary T cell responses. J Drug Target. 2003;11(8-10):495-507.

133. Elamanchili P, Diwan M, Cao M, Samuel J. Characterization of poly(D,L-lactic-co-glycolic acid) based nanoparticulate system for enhanced delivery of antigens to dendritic cells. Vaccine. 2004;22(19):2406-12.

134. Diwan M, Tafaghodi M, Samuel J. Enhancement of immune responses by co-delivery of a CpG oligodeoxynucleotide and tetanus toxoid in biodegradable nanospheres. J Control Release. 2002;85(1-3):247-62.

135. Dillen K, Vandervoort J, Van den Mooter G, Verheyden L, Ludwig A. Factorial design, physicochemical characterisation and activity of ciprofloxacin-PLGA nanoparticles. Int J Pharm. 2004;275(1-2):171-87.

136. Fonseca C, Simoes S, Gaspar R. Paclitaxel-loaded PLGA nanoparticles: preparation, physicochemical characterization and in vitro anti-tumoral activity. J Control Release. 2002;83(2):273-86.

137. Govender T, Stolnik S, Garnett MC, Illum L, Davis SS. PLGA nanoparticles prepared by nanoprecipitation: drug loading and release studies of a water soluble drug. J Control Release. 1999;57(2):171-85.

138. Lemoine D, Preat V. Polymeric nanoparticles as delivery system for influenza virus glycoproteins. J Control Release. 1998;54(1):15-27.

139. Ayalasomayajula SP, Kompella UB. Subconjunctivally administered celecoxib-PLGA microparticles sustain retinal drug levels and alleviate diabetes-induced oxidative stress in a rat model. Eur J Pharmacol. 2005;511(2-3):191-8.

140. Lee SY, Oh JH, Kim JC, Kim YH, Kim SH, Choi JW. In vivo conjunctival reconstruction using modified PLGA grafts for decreased scar formation and contraction. Biomaterials. 2003;24(27):5049-59.

141. Zhou T, Lewis H, Foster RE, Schwendeman SP. Development of a multiple-drug delivery implant for intraocular management of proliferative vitreoretinopathy. J Control Release. 1998;55(2-3):281-95.

142. des Rieux A, Fievez V, Garinot M, Schneider YJ, Preat V. Nanoparticles as potential oral delivery systems of proteins and vaccines: a mechanistic approach. J Control Release. 2006;116(1):1-27.

143. Morelli AE, Zahorchak AF, Larregina AT, Colvin BL, Logar AJ, Takayama T, Falo LD, Thomson AW. Cytokine production by mouse myeloid dendritic cells in relation to differentiation and terminal maturation induced by lipopolysaccharide or CD40 ligation. Blood. 2001;98(5):1512-23.

144. Jonuleit H, Kuhn U, Muller G, Steinbrink K, Paragnik L, Schmitt E, Knop J, Enk AH. Pro-inflammatory cytokines and prostaglandins induce maturation of potent immunostimulatory dendritic cells under fetal calf serum-free conditions. European Journal of Immunology. 1997;27(12):3135-42.

145. Fang RH, Aryal S, Hu C-MJ, Zhang L. Quick Synthesis of Lipid-Polymer Hybrid Nanoparticles with Low Polydispersity Using a Single-Step Sonication Method. Langmuir. 2010;26(22):16958-62.

146. Valencia PM, Basto PA, Zhang L, Rhee M, Langer R, Farokhzad OC, Karnik R. Single-step assembly of homogenous lipid-polymeric and lipid-quantum dot nanoparticles enabled by microfluidic rapid mixing. ACS Nano. 2010;4(3):1671-9.

147. Zhang L, Chan JM, Gu FX, Rhee J-W, Wang AZ, Radovic-Moreno AF, Alexis F, Langer R, Farokhzad OC. Self-Assembled Lipid,àíPolymer Hybrid Nanoparticles: A Robust Drug Delivery Platform. ACS Nano. 2008;2(8):1696-702.

148. Heit A, Schmitz F, Haas T, Busch DH, Wagner H. Antigen co-encapsulated with adjuvants efficiently drive protective T cell immunity. Eur J Immunol. 2007;37(8):2063-74.

149. Steinman RM. The control of immunity and tolerance by dendritic cell. Pathol Biol (Paris). 2003;51(2):59-60.

150. Reddy ST, van der Vlies AJ, Simeoni E, Angeli V, Randolph GJ, O'Neil CP, Lee LK, Swartz MA, Hubbell JA. Exploiting lymphatic transport and complement activation in nanoparticle vaccines. Nat Biotechnol. 2007;25(10):1159-64.

151. Yoshikawa T, Okada N, Oda A, Matsuo K, Matsuo K, Mukai Y, Yoshioka Y, Akagi T, Akashi M, Nakagawa S. Development of amphiphilic gamma-PGA-nanoparticle based tumor vaccine: potential of the nanoparticulate cytosolic protein delivery carrier. Biochem Biophys Res Commun. 2008;366(2):408-13.

152. de Jong S, Chikh G, Sekirov L, Raney S, Semple S, Klimuk S, Yuan N, Hope M, Cullis P, Tam Y. Encapsulation in liposomal nanoparticles enhances the immunostimulatory, adjuvant and anti-tumor activity of subcutaneously administered CpG ODN. Cancer Immunol Immunother. 2007;56(8):1251-64.

153. Fujimura T, Nakagawa S, Ohtani T, Ito Y, Aiba S. Inhibitory effect of the polyinosinic-polycytidylic acid/cationic liposome on the progression of murine B16F10 melanoma. Eur J Immunol. 2006;36(12):3371-80.

154. Zaks K, Jordan M, Guth A, Sellins K, Kedl R, Izzo A, Bosio C, Dow S. Efficient immunization and cross-priming by vaccine adjuvants containing TLR3 or TLR9 agonists complexed to cationic liposomes. J Immunol. 2006;176(12):7335-45.

155. Fifis T, Gamvrellis A, Crimeen-Irwin B, Pietersz GA, Li J, Mottram PL, McKenzie IF, Plebanski M. Size-dependent immunogenicity: therapeutic and protective properties of nano-vaccines against tumors. J Immunol. 2004;173(5):3148-54.

156. Vogt A, Combadiere B, Hadam S, Stieler KM, Lademann J, Schaefer H, Autran B, Sterry W, Blume-Peytavi U. 40 nm, but not 750 or 1,500 nm, nanoparticles enter epidermal CD1a+ cells after transcutaneous application on human skin. J Invest Dermatol. 2006;126(6):1316-22.

157. Kaisho T, Akira S. Toll-like receptor function and signaling. J Allergy Clin Immunol. 2006;117(5):979-87; quiz 88.

158. Fridlender ZG, Sun J, Kim S, Kapoor V, Cheng G, Ling L, Worthen GS, Albelda SM. Polarization of tumor-associated neutrophil phenotype by TGF-beta: "N1" versus "N2" TAN. Cancer Cell. 2009;16(3):183-94. PMCID: 2754404.

159. Bierie B, Moses HL. Transforming growth factor beta (TGF-beta) and inflammation in cancer. Cytokine Growth Factor Rev. 2010;21(1):49-59. PMCID: 2834863.

160. Chouaib S, Asselin-Paturel C, Mami-Chouaib F, Caignard A, Blay JY. The host-tumor immune conflict: from immunosuppression to resistance and destruction. Immunol Today. 1997;18(10):493-7.

161. Mantovani A, Sozzani S, Locati M, Allavena P, Sica A. Macrophage polarization: tumor-associated macrophages as a paradigm for polarized M2 mononuclear phagocytes. Trends Immunol. 2002;23(11):549-55.

162. Muraoka RS, Dumont N, Ritter CA, Dugger TC, Brantley DM, Chen J, Easterly E, Roebuck LR, Ryan S, Gotwals PJ, Koteliansky V, Arteaga CL. Blockade of TGF-beta inhibits mammary tumor cell viability, migration, and metastases. J Clin Invest. 2002;109(12):1551-9. PMCID: 151012.

163. Wigginton JM, Wiltrout RH. IL-12/IL-2 combination cytokine therapy for solid tumours: translation from bench to bedside. Expert Opin Biol Ther. 2002;2(5):513-24.

164. Bianchi ME, Manfredi AA. High-mobility group box 1 (HMGB1) protein at the crossroads between innate and adaptive immunity. Immunol Rev. 2007;220:35-46.

165. Laakkonen P, Akerman ME, Biliran H, Yang M, Ferrer F, Karpanen T, Hoffman RM, Ruoslahti E. Antitumor activity of a homing peptide that targets tumor lymphatics and tumor cells. Proc Natl Acad Sci U S A. 2004;101(25):9381-6. PMCID: 438985.

166. Pardoll DM. Spinning molecular immunology into successful immunotherapy. Nat Rev Immunol. 2002;2(4):227-38.

167. Chan M, Hayashi T, Kuy CS, Gray CS, Wu CC, Corr M, Wrasidlo W, Cottam HB, Carson DA. Synthesis and immunological characterization of toll-like receptor 7 agonistic conjugates. Bioconjug Chem. 2009;20(6):1194-200. PMCID: 2976567.

168. Hayashi T, Chan M, Norton JT, Wu CC, Yao S, Cottam HB, Tawatao RI, Corr M, Carson DA, Daniels GA. Additive melanoma suppression with intralesional phospholipid-conjugated TLR7 agonists and systemic IL-2. Melanoma Res. 2010.

169. Tseng YL, Liu JJ, Hong RL. Translocation of liposomes into cancer cells by cell-penetrating peptides penetratin and tat: a kinetic and efficacy study. Mol Pharmacol. 2002;62(4):864-72.

170. Wadia JS, Stan RV, Dowdy SF. Transducible TAT-HA fusogenic peptide enhances escape of TAT-fusion proteins after lipid raft macropinocytosis. Nat Med. 2004;10(3):310-5.

171. Brooks H, Lebleu B, Vives E. Tat peptide-mediated cellular delivery: back to basics. Adv Drug Deliv Rev. 2005;57(4):559-77.

172. Patel LN, Wang J, Kim KJ, Borok Z, Crandall ED, Shen WC. Conjugation with cationic cell-penetrating peptide increases pulmonary absorption of insulin. Mol Pharm. 2009;6(2):492-503. PMCID: 2798810.